Dynamic behaviour of jackets exposed to wave-in-deck forces

by

Katrine van Raaij (née Hansen)

Dissertation submitted in partial fulfillment
of the requirements for the degree of

DOCTOR OF PHILOSOPHY
(DR. ING.)

Department of Mechanical and Structural Engineering and Materials Science
Faculty of Science and Technology
University of Stavanger
Norway
2005

University of Stavanger
N-4036 STAVANGER
Norway
http://www.uis.no/

ISBN: 82-7644-274-9
ISSN: 1502-3877

Til onkel Manfred

Abstract

During the last decade, wave-in-deck loading on fixed offshore structures has increasingly been acknowledged as an issue of concern to the offshore oil and gas industry. Being mainly an issue for existing structures, the reason is partly that some offshore fields experience seabed subsidence due to reservoir compaction and partly that the data we possess on environmental conditions indicate that certain extreme events are not as rare as previously estimated.

This work deals with the dynamic effects of wave-in-deck loading on jacket platforms. Focus has been on the underlying mechanisms of the global structural response and on dynamic versus static response in the elastic as well as the plastic response domain. The evaluation of different methods for the calculation of wave-in-deck loading, comprising both magnitude and time variation, came naturally as a part of the work.

Dynamic and static response to external loading has been studied by carrying out analyses of jacket models using a simplified model as well as a full finite element model. The simplified model is a single degree of freedom (SDOF) type of model that utilises results, i.e. load-displacement or resistance curves, from nonlinear static pushover analysis to calculate dynamic response. The SDOF model used herein is not to be confused with e.g. commonly used generalised SDOF models. The applicability of the simplified model to predict dynamic response of complex structural systems is particularly investigated.

The application of the SDOF model and development of a modified model has contributed to important understanding of the nature of jacket response to wave-in-deck loading. The type of SDOF model used in this work is found unsuited for use as an analysis tool in case of loading involving a distribution which varies with time, however, it is believed to have a potential for (nonlinear) problems of non-varying load distribution.

The examination of the inherent differences in dynamic and static behaviour by use of the different analysis methods has made it clear that improved performance detected by dynamic analysis compared to static can mainly be attributed to 1) ductility reserves of the structure beyond ultimate capacity — as opposed to response reduction caused by inertia of the mass — and 2) the change in load distribution immediately prior to deck impact. With respect to

the former, the author will recommend explicit attention to be paid to ductile design for new structures.

Although existing jackets are not explicitly designed to resist the loads generated by wave impact on deck, this work has shown that ductile North Sea jackets may be able to resist considerable wave-in-deck loading.

Further, the levels of acceleration detected during the analyses identifies acceleration response as an important indicator of dynamic performance for jackets exposed to wave-in-deck loading.

Preface

This doctoral work has been carried out under the supervision of Adjoint Professor Ove Tobias Gudmestad, Professor Jasna Bogunović Jakobsen and Professor Ivar Langen in the period from May 1999 to September 2005. Most of the work, including one semester of compulsory courses, was carried out at the University of Stavanger. Integral to the work was a 4 1/2 months study period spent at Delft University of Technology, under the supervision of Professor dr. ir. Jan H. Vugts.

I would like to thank the University of Stavanger, and in particular the Faculty of Science and Technology, for financing this work and for for its accommodating support throughout this period. I would also like to thank The Norwegian Research Council (NFR), who provided funding for my study visit in Delft (project no. 142455/432).

In short, these years can be characterised as having been *challenging*. In addition to carrying out the largest continuous piece of work so far in my life, this period has involved starting a family, giving birth to our little boy, Viljan, and setting about the long-term task of raising him. Looking back, it has truly been a period of both frustration and worry but, most of all, joy.

Several persons have contributed to this work in various ways. Firstly, I would like to express my profound gratitude to my principal supervisor Adjoint Professor Ove Tobias Gudmestad, who has guided and inspired me throughout, in such a way that I feel that I have gained greater understanding, not only of my subject, but also of myself. I am grateful to Professor Jasna Bogunović Jakobsen, who has been a great inspiration to me. Our discussions have been 'fruitful' ones in a very real sense. I would also like to thank Rector and Professor Ivar Langen for his support and advice on matters relating to my research.

I very much appreciated my study visit in Delft in 2001, Professor Jan H. Vugts deserves acknowledgement for supervising me and for making the stay possible.

I am furthermore grateful to Structural Safety Specialist Sverre Haver of Statoil ASA for his freely given interest and participation in this doctoral work, and for the encouragement he has given me.

Special thanks are also due to Tore Holmås of USFOS Reality Engineering / USFOS Support for all the help — regardless of time or day of the week — on the use of the finite element program USFOS.

Statoil ASA and SINTEF are acknowledged for providing finite element models of jackets, and Tor Vinje of Marine Technology Consulting AS for his contribution to Chapter 4. The Statfjord Late Life project carried out by the Statfjord Licence is acknowledged for permission to refer to the MTC report, reference Statoil (2002).

I also want to thank my colleague and dear friend Kjersti Engan for having supported me on more general academic and personal matters.

My parents Sieglinde and Torbjørn deserve acknowledgement for their love and their encouragement in my academic efforts. And to my sister Siri, simply thanks for being there.

Above all; thank you, Eelco, for believing in me; for all your steadfast and unwavering support during good and difficult times these years. Thank you for being a wonderful husband and father, and a constant source of inspiration.

Table of contents

Notation and abbreviations

Parentheses and operators:

$[\,]$	Matrix
$\{\,\}$	Vector
f	Function
δ	Variation
Δ	Increment

Abbreviations:

ALS	Accidental limit state
API	American Petroleum Institute
BS	Base shear
CFD	Computational fluid dynamics
DAF	Dynamic amplification factor
DHI	Danish Hydraulic Institute
DMF	Dynamic magnification factor
EPP	Elastic-perfectly-plastic
FLS	Fatigue limit state
GBS	Gravity base structure
HSE	Health & Safety Executive
IR	Interaction ratio
JIP	Joint industry project
LRFD	Load and resistance factor design
MDOF	Multi degree of freedom
NNS	Northern North Sea
NPD	Norwegian Petroleum Directorate
PSA	Petroleum Safety Authority
QRA	Quantitative reliability analysis
RSR	Reserve strength ratio
SDOF	Single degree of freedom
SNS	Southern North Sea

SRA	Structural reliability analysis
SWL	Still water level
ULS	Ultimate limit state
VOF	Volume of fluid
WHI	Wave height incrementation
WLI	Wave load incrementation
WSD	Working stress design

Arabic letters:

A	Area
b	Width of deck normal to wave heading direction
c	Damping coefficient, celerity
C_{d}	Drag coefficient
C_{m}	Mass coefficient
C_{s}	Slamming coefficient
d	Water depth
D	Diameter (outer diameter of pipe)
E	Modulus of elasticity
f	Distributed force
F	Load
$F_{\mathrm{c}}()$	Current load
F_{cm}	'Inertia load' arising from concentrated mass
$F_{\mathrm{d}}()$	Wave load on deck
F_{dm}	'Inertia load' arising from distributed mass
$F_{\mathrm{e}}()$, $\mathbf{F}_{\mathrm{e}}$	External loads, vector of external loads
$F_{\mathrm{e,max}}$	Maximum external load
$F_{\mathrm{j}}()$	Wave load on jacket
F_{k}	Force at kink of time history
F_{v}	Vertical force
$F_{\mathrm{w}}()$	Wind load
g	Acceleration due to gravity, equal to 9.81 m/s^2
h	Wave height
h_n	n-year wave height
h_{100}	100 year wave height
h_{10000}	10000 year wave height
h_{s}	Significant wave height
H	Heaviside function, potential of external loads
I	Moment of inertia
k	Wave number ($k = 2\pi/L$)
k , $\mathbf{k}$	Stiffness, stiffness matrix
k_{f}	Elastic stiffness to resist external loading
k_{i}	Elastic stiffness to resist inertia loading
k_s	Static stiffness

$\mathbf{K}_{\mathrm{T}}$	Elastic tangent stiffness matrix
L	Wave length
m , $\mathbf{m}$	(Distributed) mass, mass matrix
m_{c}	Concentrated mass
m_{f}	Mass associated with 'external load stiffness' k_{f}
m_{i}	Mass associated with 'free vibration stiffness' k_{i}
M	Moment
M_{p}	Plastic moment capacity
N	Axial force
N_{p}	Plastic axial capacity
P_{f}	Probability of failure
q	Distributed load
r_{r}	Residual resistance ratio
r_{ν}	Dynamic overload ratio
$R_{\mathrm{d}}()$, $\mathbf{R}_{\mathrm{d}}$	Damping forces, vector of damping forces
R	Resistance / capacity
R_{el}	Static capacity at first global yield of system as determined from pushover analysis
$R_{\mathrm{f}}()$	Resistance curve referred to external load
$R_{\mathrm{i}}()$	Resistance curve referred to inertia forces
$R_{\mathrm{m}}()$, $\mathbf{R}_{\mathrm{m}}$	Inertia forces, vector of inertia forces
$R_{\mathrm{r}}()$, $\mathbf{R}_{\mathrm{r}}$	Restoring forces, vector of restoring forces
$R_{\mathrm{r,max}}$	Maximum attainable restoring force
R_{res}	Static residual strength as determined from pushover analysis
R_{ult}	Static capacity as determined from pushover analysis
s	Crest front steepness
s_{d}	Subsided height of deck
S	Local element forces, load effect
t	Time
t_{w}	Wall thickness
T	Period (e.g. wave)
T_{100}	100 year wave period
T_{10000}	10000 year wave period
T_{n}	Natural period
T_{p}	Peak wave period
u , $\mathbf{u}$	Displacement, displacement vector
$\dot{u}$	Velocity
$\ddot{u}$, $\ddot{\mathbf{u}}$	Acceleration, acceleration vector
u_{cap}	Maximum allowable displacement (displacement capacity)
u_{ce}	Current velocity
u_{cm}	Displacement caused by 'inertia force' from concentrated mass
u_{cs}	Water particle velocity at the top of the wave crest
u_{dm}	Displacement caused by 'inertia force' from distributed mass
u_{el}	Displacement corresponding to first yield

u_{m}	Maximum displacement
u_{p}	Permanent displacement
u_{ref}	A reference value of water particle velocity, equal to 9.80 m/s
u_{res}	Displacement corresponding to initiation of residual capacity R_{res}, see Fig. 6.2
u_{ult}	Displacement at ultimate static capacity R_{ult}
u_{w}	Horisontal water particle velocity
U	Strain energy
v , $\mathbf{v}$	Displacement of material point, vector of displacements of material point
$\mathbf{v}_{\mathrm{N}}$	Local displacement of element nodes
v_{w}	Vertical water particle velocity
V	Shear force, reaction shear force
V_{f}	Reaction shear force caused by external loading
V_{i}	Reaction shear force caused by 'inertia loading'
V_{p}	Plastic shear capacity
z_{b}	Size of bounding surface, equal to 1
z_{d}	Height coordinate at the lower edge of the deck
z_{y}	Size of yield surface relative to bounding surface
Z	Safety margin

Greek symbols:

α	Translation of bounding surface, integration parameter
α_{m}	Mass modifier, see section 6.5
β	Reliability index, frequency ratio T_{n}/T, translation of yield surface, integration parameter
γ	Integration parameter
ε	Strain
η	Sea surface elevation
η_{max}	Crest height
θ	Phase angle (wave)
λ	Uncertainty parameter, size of plastic increment
μ	Ductility ratio, statistic mean value
ξ	Damping ratio (relative to critical damping)
Π	Total potential
ρ	Sea water density
σ	Stress, standard deviation
ϕ	Deflected shape, shape function
$\mathbf{\Phi}$	Shape function matrix, cumulative standard normal distribution
ω	Circular frequency

Chapter 1

Introduction

1.1 General

There are more than 9000 fixed offshore platforms around the world related to hydrocarbon production, the largest numbers of platforms are located in South East Asia, Gulf of Mexico and the North Sea followed by the coast of India, Nigeria, Venezuela and the Mediterranean Sea. The majority of the worlds platforms have been designed according to the different editions of Recommended Practice by The American Petroleum Institute (API), which until 1993 have been in Working Stress Design (WSD) format. The 20th edition (1993) was also issued in Load and Resistance Factor Design (LRFD) format, and was in 1997 supplemented with a section on requalification of offshore structures. However, from the mid seventies, Norwegian Petroleum Directorate (NPD) and Det Norske Veritas (DNV) in Norway and Health and Safety Executive (HSE) in Great Britain developed their own set of rules, which replaced the API recommendations relating to design of structures for petroleum exploitation in the North Sea. Pemex / IMP issued their own rules for Mexican Waters in 1997 / 1998 (Pemex / IMP, 1998), including requirements for requalification of structures.

Approximately one third of existing platforms are reaching the end of their design life. Desired extension of service life may create a need for requalification of a structure. Other circumstances can also necessitate a requalification process on an earlier stage in the design life, be it seabed subsidence caused by reservoir compaction, increased topside weight or operational loads, revised environmental criteria[1], reduced capacity due to damage, corrosion or deterioration, increased knowledge about material behaviour or new information on soil properties achieved during driving of piles. A requalification process may also be needed as a consequence of structural damage caused by, for instance, extreme weather or boat impact.

'Requalification' can be explained as approving a structure for its (new) purpose and conditions, including smaller or larger modifications if needed. The process of requalification

[1] Following Hurricane Katrina in August 2005, updating of criteria is again a topic for discussion amongst experts (Mouawad, 2005)

of the marine structures in an area often starts with a very simplified evaluation of a larger number of structures, proceeding to more detailed analyses for those structures that do not fulfill relevant code requirements when being subject to simplified evaluation methods.

If a structure fails to fulfill the requirements during the reassessment process, there are several alternatives for mitigation, such as removal of weight from topside or removal of conductors, marine growth etc. to reduce environmental loads. The most obvious methods are maybe those aiming to strengthen the most exposed parts of the structure, e.g. strengthening of joints by grouting or use of clamps or repair of fatigue cracks in joints. Raising of deck level to an appropriate height, where wave loads onto the deck are unlikely, is another measure that can be considered as the outcome of a requalification process (Gudmestad, 2000). This was done for several platforms on the Ekofisk field in 1987. To control propagation of fatigue cracks that are not yet critical, or to detect new ones, one can implement inspection and monitoring as part of the requalification. Complete demanning of platforms in order to reduce failure consequences as well as weather dependent demanning related to extreme weather hazards that can be predicted or observed in advance are methods that are in use in for instance Gulf of Mexico.

1.2 Extreme weather hazards

The extreme weather environment may have major implications for exposed marine structures.

Local and global damage as well as toppling of fixed structures in the Gulf of Mexico have been reported after e.g. hurricanes Hilda in 1964, Camille in 1969, Carmen in 1974, Andrew in 1992, Roxanne in 1995 (Bea et al., 2001) and hurricane Ivan in 2004 (e.g. Sgouros et al., 2005; Wisch et al., 2005). A number of these incidents can most probable be attributed to wave impact on the topside structure.

In late August 2005, Hurricane Katrina made landfall near New Orleans with disastrous consequences. On it's way through the Gulf of Mexico prior to landfall it passed through areas with high density of pipelines and fixed and floating installations related to hydrocarbon exploitation. More than 700 platforms and rigs were evacuated prior to the hurricane. At the time of writing, exact assessments of the consequences are not yet carried out. However, visual assessments have indicated that 58 installations have been displaced, damaged or lost (http://www.rigzone.com). Substantial topside damage is explicitly reported for one deep water tension leg platform (TLP). Based on the preliminary assessments of consequences to the hydrocarbon industry, Hurricane Katrina is expected to be the most expensive hurricane for this industry in the American history.

There also exists observations of structural damage caused by large waves to floating and fixed installations in the North Sea (Kvitrud and Leonhardsen, 2001). In January 1995, the deck of the semisubmersible platform Veslefrikk B was hit by a large wave from underneath, resulting in local damage. In the Ekofisk area, of which the seafloor now has subsided considerably (in the range of 10 m), there has been several damage incidents since the beginning of the 1980's that are known or presumed to have been caused by wave hitting topside structures.

When Hurricane Ivan in mid September 2004 travelled across the Gulf of Mexico and generated the largest waves ever recorded in that area, it caused extensive seafloor mudflows (Hooper and Suhayda, 2005). They were initiated at the Mississippi delta front, to which many of the Gulf of Mexico pipelines are directed. The size of mudslides implied a major (temporary) disruption of a significant part of the United States' hydrocarbon supplies. As of early September 2005, it is not yet clear if Hurricane Katrina has caused similar mudslides, but it will not be surprising if that is the case.

1.3 The wave-in-deck problem

Reservoir compaction and consequently subsidence of the seafloor is seen at e.g. the Ekofisk and Valhall fields (chalk reservoirs) in the Southern North Sea. The subsidence of the Ekofisk field was slightly less than 40 cm / year until 1999 and has since then been some 15 cm / year, adding up to almost 10 meters (Madland, 2005), whereas the Valhall field has subsided about 5 meters (Fjellså, 2005). The fixed surface piercing structures on these two fields are mainly of the steel space frame type, so-called jackets. Recently, it has become clear that also the Statfjord field (sandstone reservoir) with its concrete gravity base structures (GBS) in the Northern North Sea might experience some seabed subsidence due to extended exploitation of the hydrocarbon reserves through depletion of the gas in the field's gas cap (Stansberg et al., 2004).

Observed or anticipated seabed subsidence and / or revised environmental criteria may for fixed platforms result in a need for taking an *airgap extinction* into account, of which one consequence can be extreme waves impacting the topside structure. This is frequently referred to as *wave-in-deck loading*. Since seafloor subsidence and an apparent increase in design wave height in the Gulf of Mexico, which are the main triggers for wave-in-deck considerations for fixed structures, until recently have been related to hydrocarbon fields of which the majority of the fixed installations are jacket structures, the issue of wave-in-deck loading has mainly been investigated in connection with such platforms. *It is the jacket type of platforms that is dealt with in this thesis.*

1.4 Jacket platforms subjected to wave-in-deck loading

A wave-in-deck load itself is preceded by an increasing loading on the jacket structure below the topside caused by the approaching wave crest. When the crest strikes the platform deck, a load that is more or less impulse like, depending on the deck configuration, will act on deck level. The remains of the wave crest will pass the jacket after the initiation of the wave-in-deck loading, and thus the external loading will remain at a high level for a while or might even continue to increase also after the peak topside load.

A wave that reaches and strikes the deck may to generate forces exceeding the elastic, static capacity of the platform. According to static analysis theory the consequence may be permanent deformations. State-of-practice for (re)assessment of fixed steel platforms subjected to

extreme wave loading is to use *non-linear structural pushover analysis* (e.g. ISO/CD 19902, 2001) to determine the capacity of the load-bearing system as a whole, allowing for local damages that do not lead to global failure. However, this is a static approach that ignores dynamic effects of possible importance such as inertia- and damping response and dynamic amplification.

Dynamic effects in relation to jacket structures have been investigated by e.g. Stewart (1992), Dalane and Haver (1995), Schmucker (1996), Moan et al. (1997), Emami Azadi (1998) and HSE (1998). However, more attention needs to be paid to the dynamic structural behaviour of jackets subjected to extreme wave loading *including wave-in-deck loading with relevant phasing relative to the wave loading on the jacket*. This topic is the overall subject of this thesis. It should be noted that extreme waves may be associated with a storm surge reducing the airgap and it is assumed that this effect is taken into account prior to analysis of wave-in-deck loading.

1.5 The present doctoral work

1.5.1 Summary

The aim of the present work is:

- ⋆ To improve the understanding of the *dynamic effects of wave-in-deck loading on the response of jacket platforms* and, based on that, present results on jacket response and capacity to withstand wave-in-deck loads for the benefit of the structural engineering community.
- ⋆ To evaluate simplified methods for calculation of *wave-in-deck load magnitude and time history*, with basis in existing work.
- ⋆ To investigate the use of a simplified model to predict response to wave-in-deck loading. The model is a single degree of freedom (SDOF) type of model that utilises results, i.e. load-displacement or resistance curves, from nonlinear static pushover analysis to calculate dynamic response. The SDOF model used herein is not to be confused with e.g. commonly used generalised SDOF models.

In order to investigate the dynamic response, both the above mentioned simplified model and finite element models are used. The models are subjected to wave time histories where an impulse-like wave-in-deck load history is applied with realistic phasing relative to the wave loading on the jacket structure below. The simplified model is evaluated by comparing the computed response with the response obtained by use of finite element computations.

Although not being the main subject of this work, the SDOF model requires some explicit attention. The model was originally intended for use during reassessment of *existing jacket structures* subjected to wave-in-deck loading, a loading condition which may imply non-linear response. The basis for the model is therefore (nonlinear) structural properties *that*

are normally a part of the existing jacket documentation, that is to say the nonlinear load-displacement curves or *resistance curves* corresponding to a given (wave) load scenario, as obtained from static pushover analysis.

It is emphasised that the SDOF model presented herein is meant to represent an approximation of the dynamic response. The complexity of including *both* variation in load distribution *and* plastic behaviour in an exact calculation model would not justify the description 'simplified' model. Note that in simplified analysis of purely elastic problems, varying load distribution can be handled by use of e.g. a generalised SDOF model or modal analysis.

The following limitations apply:

- ⋆ The magnitude and time variation of wave-in-deck loading is based on interpretation of existing work.
- ⋆ The wave loading is based on the use of regular waves.
- ⋆ Vertical loads are not attended to in the structural analyses.
- ⋆ Damping is not included in the structural analyses.

The main contributions from this work are:

- ⋆ An improved understanding of the dynamic response mechanisms during wave-in-deck loading.
- ⋆ Identification of the main causes of improved dynamic performance compared to static when exposed to wave-in-deck loading, being the variation in load distribution immediately prior to wave impact on deck and the ductility reserves beyond ultimate capacity of the structure.
- ⋆ It is shown that ductile North Sea jackets may be able to resist considerable wave-in-deck loading although initially not designed for that.
- ⋆ Since we cannot change the nature of the wave loading, it is, as a consequence-reducing measure in the case of wave-in-deck loading, strongly recommended to pay explicit attention to ductile behaviour in the design and reassessment of jacket structures.
- ⋆ Based on the acceleration levels revealed during the dynamic analyses, acceleration response is identified as an important indicator of the dynamic performance of jackets under wave-in-deck loading.
- ⋆ The examination of the applicability of a simplified model and development of a modification to this model has contributed significantly to the understanding of the dynamic response versus the static response. In the course of this work, it has become clear that the model is unsuited for problems involving wave loading, due to the significant variation of the spatial load distribution with time. The model is, however, believed to have a potential for problems of non-varying load distribution. Although found unsuited for wave problems, in fact just due to the nature of the discrepancies, the model has provided valuable insight into the mechanisms that for ductile structures lead to a higher tolerance for wave-in-deck loading than indicated by static nonlinear analysis.

1.5.2 Organisation of the work

The work is divided into 8 chapters, of which the present chapter is the first. Chapter 2 represents an overview of topics related to wave-in-deck loading on jacket structures, with a main focus on the performance of the structural system as a whole — *structural system performance*. Chapter 3 briefly outlines the principles of the computer program used to carry out nonlinear finite element analyses in this work.

In Chapter 4, the focus is on the magnitude and time variation of the wave-in-deck load. Chapter 5 comprises time domain analyses of two jacket models denoted 'DS' and 'DE', respectively.

Chapter 6 treats issues related to dynamic behaviour, and particularly addresses the differences between dynamic and static behaviour. Further, a simplified model to calculate response of complex structural systems is presented. In Chapter 7, the simplified model is used to calculate response of jacket model 'DS'.

Chapter 8 comprises the conclusions of this work as well as recommendations for further work.

Chapter 2

State of the art

2.1 Introduction

This chapter represents a summary of a literature review carried out to explore the most important technical areas relevant for reassessment of jacket structures, seen from the viewpoint of a structural engineer. During the process, particularly the wave-in-deck issue as well as the dynamic response to loads caused by such captured the interest of the undersigned.

Parts of this chapter have been published previously (Hansen and Gudmestad, 2001) as a part of the present doctoral studies.

This chapter starts with an introduction to the coverage of *reassessment of offshore structures* in regulations and recommendations, Section 2.2. Section 2.3 is devoted to the environmental conditions and loading, with emphasis on wave-in-deck loading. Section 2.4 deals with system performance in general. Three approaches to the evaluation of system performance, being static analysis, dynamic analysis and structural reliability analysis, are explicitly dealt with in Sections 2.5 to 2.7. The contribution from structural components to system performance is treated separately in Section 2.8.

2.2 Reassessment in regulations

The main contributors to standardisation of the design of offshore structures have been the *American Petroleum Institute* (API) through their Recommended Practices (RP), the *Norwegian Petroleum Directorate* (NPD) — presently the Petroleum Safety Authority (PSA), the British *Health and Safety Executive* (HSE) and *Det Norske Veritas* (DNV). It is anticipated that all petroleum activities in the future will be based on the international standards developed by the International Organization for Standardization, ISO (the new ISO standard series for offshore structures, ISO 19 900, is currently being developed). However, the North Sea

conditions and the Norwegian safety policy require certain amendments to the international standards, being the reason for the existence of the NORSOK standards for activities on the Norwegian Shelf. NORSOK has substituted the NPD regulations on detail level. In US waters the recommendations by API apply, just as the HSE regulations are relevant for UK waters.

Old North Sea platforms are designed according to the API recommendations valid at the time of design, and are therefore normally, at least in first instance, re-evaluated based on API recommended practice.

The first explicit advice relating to reassessment of offshore structures came with the supplementary Section 17 to the API RP 2A in 1997. Section 17 was later fully incorporated into the 21st edition of RP 2A-WSD, whereas still being a supplement to RP 2A-LRFD. Currently, provisions for reassessment of offshore structures are included in both the draft ISO/CD 19902 (2001) and NORSOK N-004 (2004).

Reassessment of offshore structures is an inherent part of *structural integrity management* (SIM) — an '*ongoing lifecycle process for ensuring the continued fitness-for-purpose of offshores structures*' (O'Connor et al., 2005). Provisions relating to structural integrity management are included in the current version of API RP 2A and in the draft ISO 19902. API RP 2A is in the future intended split into two parts; one part relating to design of new structures, and one comprising the process of structural integrity management of existing structures including reassessment of structures.

2.3 Environmental conditions and loading

2.3.1 Waves and hydrodynamic loads

Several theories for the description of the shape and kinematics of *regular waves* exists. Regular wave theories used for calculation of wave forces on fixed offshore structures are based on the three parameters water depth (d), wave height (h) and wave period (T) as obtained from wave measurements adapted to different statistical models.

The simplest regular wave theory is the linear small amplitude wave theory (Airy theory), which gives symmetric waves having the form of a sine function about the still water level. The linear wave theory is well suited for simplified calculations, but more important: it comprises the basis for the description of *irregular waves*.

Nonlinear theories used for design purposes are Stokes higher order wave theories and Stream function theory for waves in deep water and cnoidal wave theories for shallow water. These theories give an asymmetric wave form about the still water line with high crests compared to more shallow, wide troughs.

Wave forces on individual structural elements can be calculated using Morison equation, based on hydrodynamic drag- and mass coefficients (C_{d}, C_{m}) and particle acceleration and velocity obtained by the chosen wave theory. For drag dominated structures, defined as structures consisting of structural members of small diameter compared to the wave length, the

particle velocity is the governing factor, and thus the wave crest is of importance[1]. Jackets are in the design wave condition normally categorised as drag dominated structures.

2.3.2 Wave-in-deck loading

General

Research has indicated that for North Sea structures failure due to extreme environmental conditions probably only can be associated with wave impact on topside (Dalane and Haver, 1995; Haver, 1995). A vertical distance between the extreme surface elevation (including tide and storm surge) and the underside of the lowest deck, an *airgap*, of 1.5 meters has been widely recognised as a minimum requirement for fixed offshore structures. The extreme surface elevation refers to the worst combination of tide, surge and wave height. It is evident that the 1.5 meter requirement leads to an inconsistent level of reliability, following different probability of airgap extinction, between structures located in different areas of the world having different environmental conditions.

Fixed offshore platforms are traditionally not designed to withstand the large forces generated by wave-in-deck loads. If a wave yet strikes the deck, the deck legs, which are not sized to transfer shear forces of this magnitude from the deck into the jacket, may be excessively loaded. In addition, large (up and) downwards acting vertical loads may be introduced in the structure, further reducing the deck legs' capacity to carry transverse load. The latter may also apply to the jacket legs. Thus, other failure modes than those considered during design can be governing for platforms exposed to wave-in-deck loads.

The probability that a wave hits the deck of a structure influences the structural reliability significantly. Bolt and Marley (1999) have shown that the effect of wave-in-deck loads on the system reliability depends more upon whether the load is included at all than on which load model one actually has chosen. With respect to airgap, Bolt and Marley anticipate that the future requirements will be based on reliability considerations rather than explicit requirements regarding size of the gap.

Properties of the wave such as crest height, wave steepness (Olagnon et al., 1999) and water pressure (Tørum, 1989) are determining for the size of the wave-in-deck forces. Estimation of crest height should preferably be carried out based on statistical data, since small variations in the crest height may imply large relative differences in deck inundation. Tørum (1989) found that the water pressure was largest at a distance $u_{\mathrm{cs}}^2/2g$ below the wave crest elevation and zero at a distance $u_{\mathrm{cs}}^2/2g$ above the wave crest, where u_{cs} and g are maximum crest particle velocity and acceleration due to gravity, respectively. The same trend was pointed out earlier by e.g. Bea and Lai (1978).

[1] For mass dominated structures, i.e. those being large compared to the wave length, the particle *acceleration* will be of interest. Since the particle acceleration is largest in the still water level, assumptions regarding wave crest and crest elevation will not be as important as for drag dominated structures

Methods for calculation of wave-in-deck loads

So far there is no generally agreed engineering practice on how to model impact loading from waves on topside structures. Several methods are previously used for this task, some verified against experimental data and some not. They can roughly be categorised into two groups, that is 'detailed' or 'global', the latter also denoted 'silhouette approach'.

The 'detailed' methods require a detailed deck model and allow for calculation of wave-in-deck loads on component level. They are presented by the following references:

- Kaplan et al. (1995)
- Finnigan and Petrauskas (1997)
- Pawsey et al. (1998)
- Grønbech et al. (2001)

'Global' implies that no detailed deck model is needed, and comprises the following references:

- API formulation (API LRFD, 2003; API WSD, 2002)
- ISO formulation (ISO/CD 19902, 2001) — directly adopted from API
- the DNV slamming formulation (Det Norske Veritas, 1991)
- the Shell model (HSE, 1997b)
- the MSL model (HSE, 2001, 2003)

Wave-in-deck load models are discussed in detail in Section 4.5.

2.3.3 Some historical issues regarding calculation of wave-in-deck loads

A method for estimation of wave-in-deck loads for reassessment of jacket structures was first suggested through Supplement 1 to the existing API regulations in 1997. At present, identical recommendations are also included in the draft ISO standard (ISO/CD 19902, 2001).

A modified version of the API method has been suggested by Bea et al. (1999, 2001). The modifications have so far not been implemented, but are summarised as follows:

- larger directional spreading
- omitting hurricane current
- modifying assumptions regarding surface elevation to account for wave 'runup'
- introducing drag coefficients (C_{d}) that varies with depth

The basis for these suggested modifications were, amongst others, observed in-field performance of platforms in Bay of Campeche that experienced deck wave inundation following from hurricanes. The performance of several structures was assessed using the simplified ULSLEA technique (see Section 2.4.2) and the modified API procedure. The results were validated against observed performance during hurricanes Hilda in 1964, Camille in 1969, Carmen in 1974 and Andrew in 1992.

In the early days, seen from a wave-in-deck point of view, the difference in phase angle between the wave hitting the jacket and the wave hitting the deck was not taken into account. Effectively, the wave load on the jacket and the wave-in-deck load were assumed to have their maxima simultaneously. This issue is obviously important, and was pointed out by Pawsey et al. (1998) who, to the author's knowledge, first presented a method that integrated the calculation of wave loads on the jacket and wave loads on the deck.

DHI have recently presented the results from a JIP in which one of the aims has been to develop a method for calculation of wave-in-deck loads, and include it in their inhouse nonlinear finite element program.

2.3.4 Combination of environmental loads for structural analysis

The conventional way of establishing design load for jackets in the ultimate limit state (ULS) is to add load effects from 100-years / 1 minute gust wind, 10-years current and 100-years wave height on top of 100-years still water level (Dalane and Haver, 1995). However, since the probability that these events will occur simultaneously is much smaller than 1:100 per year, structures that are designed according to such assumptions have an inherent reserve capacity.

To avoid some of the conservatism in the above mentioned method, the extreme surface elevation can be estimated by use of a joint probability distribution of tide surge and crests as proposed by e.g. Olagnon et al. (1999).

In the accidental limit state (ALS) analyses it is important to recognise the phase difference between the maxima for wave-in-deck load and wave load on the jacket structure.

2.4 System performance

2.4.1 General

Conventional design analyses of jackets presupposes linear elastic behaviour for all relevant analysis limit states as well as perfectly rigid joints. Members are validated against formulae based on linear-elastic theory, and no yield or buckling is permitted. This applies both to the ULS analysis using the design wave and to the ALS analysis using a wave with a lower probability of exceedance. Load effects, i.e. member end forces, are used for local check of joints according to formulae that are developed on the background of experiments. Interaction

ratio, IR, is defined as component load effect divided by component capacity, and failure is defined to occur when component IR exceeds 1.0.

This conventional methodology disregards the structure's inherent capability to redistribute forces in case of one or more component failures. Each member and joint has been designed to resist the actual load effects from the loads acting on the system. Structures that are configured in a manner that permits *redistribution of forces* in case of component failure may perform relatively well for load scenarios considerably more onerous than those corresponding to first component failure. Such structures are said to be *redundant*. Both the draft ISO standard, the NORSOK regulations and the API recommendations explicitly require redundant structures (ISO/CD 19902, 2001; NORSOK N-001, 2004; NORSOK N-004, 2004; API WSD, 2002; API LRFD, 2003).

During the last decade extensive research (see Section 2.4.2) on the topic *system capacity* as opposed to *component capacity* has been conducted, confirming the need to take — and benefit from taking — into account the behaviour of the complete structure as a system rather than the strength of every single component.

Moan et al. (1997), for example, distinguish between four ways to investigate *structural system performance*:

1. Scaling of the design wave load (normally the 100-years load) with constant wave height, static analysis (Section 2.5.1).

2. Scaling of wave height, static analysis (Section 2.5.1).

3. Cyclic approach based on incrementing the wave height captures possible damage accumulation or cyclic degradation, (quasi-)static analysis, i.e. dynamic effects are not incorporated (Section 2.5.2).

4. Full dynamic time history approach (Section 2.6).

The author considers the results from structural reliability analysis as a performance measure, and therefore distinguishes between the following three main approaches to system performance analysis:

1. Static analysis, incorporating pushover analysis and cyclic analysis.

2. Dynamic (time history) analysis.

3. Structural reliability analysis (requires results from static or dynamic analysis).

These different approaches are attended to in Sections 2.5 to 2.7.

2.4.2 Background

Structural capacity

During the years 1990 to 1996, SINTEF conducted a joint industry research project on re-assessment of marine structures. The results were presented in several papers that were issued during this period (Hellan et al., 1991; Stewart et al., 1993; Stewart and Tromans, 1993; Eberg et al., 1993; Hellan et al., 1993; Eide et al., 1995; Amdahl et al., 1995). The main objective was to develop an extended ULS design methodology in which *global collapse of the system, contrary to first component failure, determines the capacity of the structure*. This work forms the basis for the nonlinear finite element program USFOS, which is used later in this thesis.

Work on the topic of system capacity has also been conducted at University of California, Berkeley (Bea, 1993; Bea and Mortazavi, 1996). The work has resulted in proposed screening procedures for requalification of larger number of platforms, calibrated to Gulf of Mexico conditions, as well as a simplified assessment method of system strength called ULSLEA — Ultimate Limit State Limit Equilibrium Analysis (Bea and Mortazavi, 1996). The idea behind ULSLEA is that a depth profile of shear capacity for the structure based on simplified considerations is established and compared to a storm loading profile. The ULSLEA technique is incorporated into available software (Bea et al., 2000).

In the context of the ULSLEA technique, it is interesting to notice that e.g. HSE (1997a) has shown that shear and overturning moment capacity at the base are not necessarily good indicators of structural integrity. Better indications evinced from shear force and moment vs. the respective capacities at the *level where the failure occurs*. This supports the ULSLEA idea.

System capacity was also addressed by Vannan et al. (1994), through the Simplified Ultimate Strength approach (SUS), which is a linear procedure. The global ultimate capacity of the structure is defined as the base shear at which first component (joint, member, pile-soil bearing capacity or pile steel strength) reaches its ultimate capacity. Ultimate capacity for the different component classes is calculated based on API LRFD (1993). It was pointed out that the procedure leads to faulty indications of joint and soil failure compared to the pushover analyses.

A study in which the SUS approach was compared to the ULSLEA approach and to nonlinear static pushover analyses was reported by Stear and Bea (1997). The three analysis approaches were also compared to historical observations of platform performance. Both ULSLEA and SUS were found to give reasonable and reliable predictions of ultimate capacity. One purpose of the study was to validate the SUS approach for use in requalification for structures not passing the ULSLEA analysis. It was concluded in the reference paper that SUS is suited for this task. The author of this thesis, however, questions this conclusion since SUS seems in general to yield lower ultimate capacity than ULSLEA, meaning that in general platforms that do not pass ULSLEA will neither pass SUS. Also, results obtained by SUS have larger spreading compared to pushover analyses than those obtained by ULSLEA. These issues are not discussed by Stear and Bea.

System behaviour has already for some time been considered in connection with requalification of jackets, see e.g. Ersdal (2005), in particular when it comes to wave-in-deck loads because of the large horisontal loads. However, component based design is still the state of practice for design of new structures. A procedure for design of new jackets to meet a particular target reliability level was proposed by Manuel et al. (1998). The *structural system capacity* is explicitly addressed as a performance measure during the design process, a significant difference compared to todays design practice.

Procedures focusing on system capacity, ensuring redundant and ductile structural behaviour, are beneficial because they focus on optimal design of structures with respect to distribution of capacity throughout the structure — no bottlenecks — as well as robustness against component failure.

Structural reliability

The previously mentioned work by Manuel et al. (1998) outlines an iterative procedure to design of (new) jackets to a given target *structural* reliability[2]. The procedure distinguishes between *design level* wave height and *ultimate level* wave height. The design level wave is initially used for a conventional linear elastic design analysis, of which the purpose is to size members and perform IR unity checks. The ultimate level wave height is used as input to nonlinear pushover analysis in order to establish the ultimate capacity and subsequently the probability of failure. If the failure probability does not meet the target probability, structural members that are critical to the capacity is redesigned, followed by a new pushover analysis and calculation of failure probability. If necessary, such local redesign can be done several times until the target structural reliability is obtained.

A limited amount of work has been conducted on the effects of wave-in-deck loads on the structural reliability. Dalane and Haver (1995) carried out a reliability study of an existing jacket structure in the North Sea exposed to different levels of seabed subsidence. Not surprisingly, it was found that the annual probability of failure increases with increasing subsidence level and thus larger probability of airgap extinction. It was also stated that the description of extreme waves is the most important part of the assessment.

A HSE-study reported by Bolt and Marley (1999) illustrates that system reliability is significantly influenced by wave-in-deck load, and, as mentioned earlier, that the determining factor is whether the load on the deck is included or not, rather than which model is being used for load calculation.

Manzocchi et al. (1999) also emphasise the significance of including wave-in-deck loads, based on a study of a platform situated in the central North Sea. Smaller failure probability is yielded by wave force incrementation compared to results derived from wave height incrementation (see Section 2.5.1).

[2]Existing design codes aim at designing structures to withstand a load scenario having a given probability of occurrence. In this context it must be emphasised that the probability of occurrence of a given load scenario is not equal to the probability of structural failure induced by that load scenario.

Sørensen et al. (2004) performed reliability analyses of an example jacket for the Danish part of the North Sea using the model correction factor method (Ditlevsen and Arnbjerg-Nielsen, 1994), and emphasise that if a wave scenario leads to airgap extinction, this (probabilistic) method gives better indications of the structural performance than the RSR alone.

2.4.3 Large scale testing

To the author's knowledge only one project which includes large scale testing of space frames has been reported — the FRAMES project (Bolt and Billington, 2000). The observations from the tests confirm the significant force redistribution potential within steel structures, but also emphasise that the presence of imperfections, variable system properties and initial stress conditions in the structure are important to the system performance and should be further investigated.

2.5 Static system analysis

2.5.1 Pushover analysis

State-of-practice for system performance analysis of existing jackets is to use so-called *push-over analyses* — nonlinear (quasi-) static finite element analyses with monotonically increasing load. Permanent loads and variable functional loads are applied first, followed by the (hydrodynamic) load for which one wants to obtain ultimate capacity. This load with its associated distribution is applied by increasing its magnitude stepwise until global collapse of the structure is reached. A measure of the capacity of a structure with reference to one particular load scenario is thus obtained. This measure is referred to as *reserve strength ratio*— RSR.

$$RSR = \frac{R_{\mathrm{ult}}}{F_{\mathrm{j}}(h_n) + F_{\mathrm{d}}(h_n) + F_{\mathrm{c}} \ \ (+F_{\mathrm{w}})} \tag{2.1}$$

Here, R_{ult} is the ultimate static capacity of the structure for the given load scenario, h_n is the n-year wave height, $F_{\mathrm{j}}()$ and $F_{\mathrm{d}}()$ are wave load on jacket and deck, respectively, F_{c} is current load and F_{w} is wind load. The wind load is frequently omitted from the definition of RSR. Current design practice is to refer the RSR to the 100-years environmental load condition, for which wave-in-deck load normally will be irrelevant. However, during reassessment of offshore structures, it will also be relevant to obtain RSR relative to the 10 000-years environmental load.

The RSR is dependent upon the load predictions and calculation of system capacity. RSR is a quasi-deterministic measure, since design loads and capacities are taken as deterministic values, although based on statistical interpretation of measured data with inherent variability.

The procedure with pure scaling of the wave load intensity while keeping the load distribution constant yields a measure of reserve capacity for a given wave only, it does not indicate to

what extent the wave height can increase without leading to loss of structural integrity. A relevant question is therefore whether to increment the wave load (intensity) only or the wave height. Wave height incrementation, which requires several pushover analyses using wave load incrementation, has a clearer physical meaning. Incrementing the wave height can lead to other failure modes than those arising from pure incrementation of the wave load for *one* given wave scenario, particularly in the case where the wave reaches the cellar deck or main decks (e.g. Manzocchi et al., 1999; HSE, 1997a). It has been shown that wave height incrementation gives a slightly smaller ultimate capacity than wave load incrementation in terms of total global load / base shear (Emami Azadi, 1998). Moan et al. (1997) reports similar results, and emphasise that this is mainly due to the wave encountering the deck structure before collapse load is reached and then the loads increase rapidly as the wave is increased.

Clearly, if waves with crests lower than the underside of the deck are not alone enough to cause collapse of the platform, obtaining RSR based on wave load incrementation with wetted surface limited to the jacket (disregarding the deck) may give distorted results. This problem is attended to by Ersdal (2005), through introduction of additional parameters to describe system strength; a *reserve freeboard ratio* (RFR) and a *new failure modes* parameter (NFM). The combination of RSR and these two parameters provides a more complete evaluation of static system strength.

2.5.2 Cyclic analysis

The major difference between pushover analysis and cyclic analysis is that in the latter case the applied load vector is reversed several times. Cyclic capacity is defined as the largest load intensity at which the structure *shakes down* (Stewart et al., 1993). A structure is said to shake down when a load scenario with magnitude large enough to create permanent displacements will, when repeated with the same or smaller magnitude, after some cycles only lead to elastic deformations in the structure. The mathematical expressions or theorems that describe this behaviour are briefly outlined in e.g. Hellan et al. (1991).

If the magnitude of the load exceeds the cyclic capacity, and the structure is subjected to repeated action, the result will be either incremental collapse or low cycle fatigue (alternating plasticity). When repeated loading results in steadily increasing plastic deformation, the structure will sooner or later reach a state where the deformations are larger than what can be accepted out of practical reasons, or the structure becomes unstable. This is called *incremental collapse*. During the process of reaching shakedown or incremental collapse, the structure may fail locally due to *alternating plasticity* / *low cycle fatigue* resulting in fatigue fractures. This may prevent shakedown and accelerate the incremental collapse.

As a part of the project ‘Reassessment of Marine Structures’, and based on short- and long-term statistics, Stewart and Tromans (1993) have developed a nonlinear load history model for nonlinear cyclic analysis.

2.6 Dynamic system analysis

2.6.1 Design provisions

The draft ISO standard (ISO/CD 19902, 2001, Section 12.6.6.3) states that dynamic analyses can be performed in one of the following two ways:

1. Full transient dynamic non-linear analysis in which the environmental action is simulated in time.
2. Quasi-static, in which static non-linear analysis procedures are used in combination with the environmental load set augmented with an inertial component.

Both API LRFD (2003) Section C.3.3.2.1 and NORSOK N-004 (2004) Section K.4.2 say '.... Time history methods using random waves are preferred. Frequency domain methods may be used for the global dynamic analysis (...), provided the linearisation of the drag force can be justified'.

2.6.2 Dynamic effects

The first period of vibration of a jacket platform (in not too deep water) is typically 1-3 seconds. The load duration for the jacket (as opposed to the deck) is typically the period during which the crest part of a wave forms, i.e. half the wave cycle. The part of the wave that enters the deck will have a shorter duration, Schmucker and Cornell (1994) assume 2 - 3 seconds for a wave with $T_{\mathrm{p}} = 12$ s, when considering the time it takes from the point of contact, to travel through the deck and finally loose contact on the opposite side. An open deck configuration having smooth surfaces allows the wave to travel through the deck, whereas for a closed configuration, e.g. a solid wall, the wave contact will result in an impact of more impulsive character. The exposed area of the former is smaller, and presumably also the peak force.

The load on the deck during impact from a large wave is undoubtedly of dynamic nature, and that will influence the response from the structural system. The response is governed by parameters such as the peak load value, load duration and its variability in time and the structure's stiffness, mass distribution, ultimate capacity, ductility and post-collapse behaviour. In certain situations, a dynamic load with a limited duration can be advantageous compared to a static load with the same value as the peak value of the dynamic load history (see Section 5.3). Damping and inertial resistance, the latter mainly determined by the deck weight, may lead to a higher tolerance for lateral forces, generally and theoretically spoken. It is evident that if the load exceeds the static capacity, static equilibrium cannot be obtained. Dynamic equilibrium can and will, however, always be obtained from the analysts point of view; the question only turns into how large displacements, velocities and accelerations that can be accepted. Also from the mathematical formulation of dynamic equilibrium, in this case for a

single degree of freedom (SDOF) system, it is clear that equilibrium can be obtained also for external forces $F_{\mathrm{e}}(t)$ that exceed the static capacity $R_{\mathrm{ult}} = R_{\mathrm{r,max}}$:

$$R_{\mathrm{m}}(t) + R_{\mathrm{d}}(t) + R_{\mathrm{r}}(t) = F_{\mathrm{e}}(t) \tag{2.2}$$

Here, $R_{\mathrm{m}}(t)$, $R_{\mathrm{d}}(t)$ and $R_{\mathrm{r}}(t)$ are inertia-, damping- and stiffness induced responses, respectively. For structures that possess a certain ductility and post-collapse capacity, one can easily imagine that this equation also is valid for responses that exceed the yield limit of the structure. Transient (accidental) loads may in that case result in considerable but acceptable permanent deformations of the structure while not resulting in a complete loss of structural integrity.

The studies by Stewart (1992), Dalane and Haver (1995), Schmucker (1996), Moan et al. (1997), Emami Azadi (1998) and HSE (1998) demonstrate indeed that structures with certain qualities may be able to remain (damaged but) intact when exposed to a dynamic load history with peak load exceeding the static capacity, provided the load peak is of limited duration. Note that the opposite might as well be the situation; that the dynamic effect results in a lower resistance to a peak applied load than for a static load. Two parameters commonly used to quantify the dynamic effects on the structural response are described in the following. In this respect one distinguishes between transient and harmonic loading:

The dynamic magnification factor (DMF) is the relation between the dynamic response (displacement) caused by a peak applied load and the static response for the same load. The DMF is illustrated in Figure 2.1 for different impulse shapes.

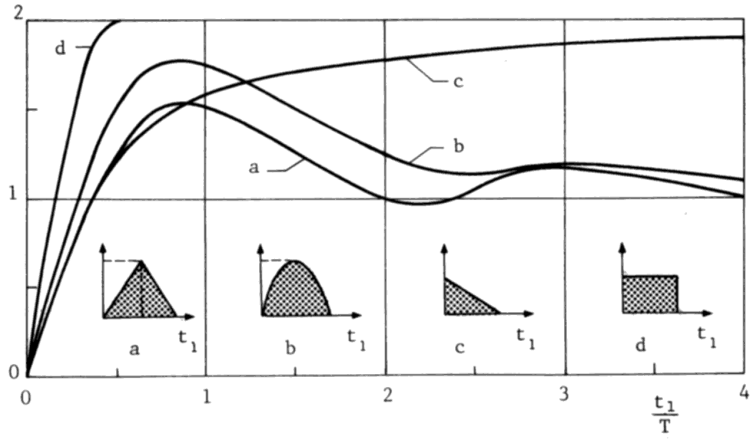

Figure 2.1: DMF as a function of impulse duration relative to structure natural period. T is the structure's natural period, t_1 is the impulse duration. (Bergan et al., 1981)

The dynamic amplification factor (DAF) is normally associated with harmonic loading, as opposed to transient loading, and is defined as the relation between the dynamic response amplitude and the static response displacement. From this definition it is clear

that for a brittle structural system that behaves linearly up to collapse, the dynamic overload ratio (see Equation 2.7) is

$$r_\nu = \frac{1}{DAF} \tag{2.3}$$

The DAF can be calculated as follows (Clough and Penzien, 1993):

$$DAF = \frac{1}{\sqrt{(1-\beta^2)^2 + (2\beta\xi)^2}} \tag{2.4}$$

where β is the ratio of applied loading frequency to the natural frequency of the structure and ξ is the ratio of the given damping to the critical damping value. For a typical jacket, the damping is 1.5 - 2% of critical damping. Figure 2.2 illustrates how the DAF varies with the frequency ratio, β, for 2% damping ratio, i.e. for $\xi = 0.02$. As the load period approaches the natural period of the structure, the dynamic amplification increases rapidly and reaches its maximum value of 25 when the load period and the natural period are equal.

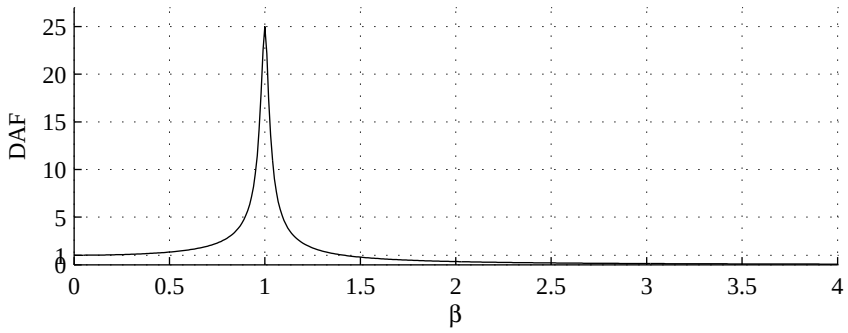

Figure 2.2: DAF as a function of frequency ratio β, $\xi = 0.02$

Sometimes it may also be relevant to analyse dynamic amplification resulting from a particular (irregular) load history, comparing the maximum dynamic response to the given load time history to the 'static' response, i.e. response excluding inertia and damping effects, to the same load history.

Further, it is assumed that the load - deformation curves obtained from static extreme wave analysis, frequently called resistance curve, may give information about dynamic performance[3]. Related to this assumption, some parameters of the resistance curve are defined (symbols are illustrated in Figure 2.3):

[3]The discussion regarding the validity of this statement is one of the main subjects of this thesis.

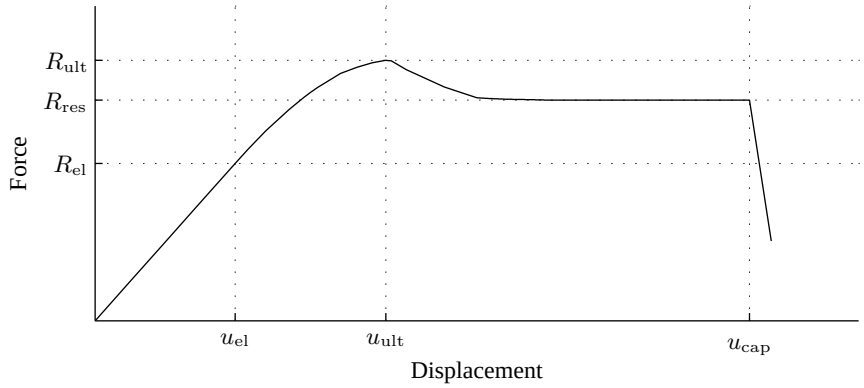

Figure 2.3: Resistance curve, system capacity properties

The ductility ratio (μ) characterises the structure's ability to deform in the post-collapse area:

$$\mu = u_{\mathrm{cap}}/u_{\mathrm{el}} \tag{2.5}$$

Note that the expression *ductility demand* frequently is used in the literature. It refers to the ductility required for a structure to remain (damaged but) intact after exposure to a given load history.

The residual resistance ratio (r_{r}) does, together with the ductility ratio, describe the performance of the structural system in the post-collapse range.

$$r_{\mathrm{r}} = R_{\mathrm{res}}/R_{\mathrm{ult}} \tag{2.6}$$

Schmucker (1996) investigated the influence of the shape of the static resistance curve on the dynamic response, focusing on the following characterising properties of the curve:

- ⋆ A secondary stiffness (as opposed to the initial elastic stiffness) that describes the slope of the resistance curve between R_{el} and R_{ult} .
- ⋆ A post ultimate stiffness which describes the transition from R_{ult} to R_{res}.
- ⋆ The previously described residual resistance ratio r_{r}.

The load history subject to investigation had a squared sinusoidal shape, and was meant to represent the complete crest part of a wave. Hansen (2002) compared the results from this load history to the results from a more impulse like load history meant to represent a wave-in-deck force impulse. For the conclusions from both studies, reference is made to the source documents.

SINTEF (1998) characterises post-collapse behaviour as follows:

Ductile	$r_{\mathrm{r}} > 0.9$	and	$\mu \gg 1$
Brittle	$r_{\mathrm{r}} < 0.7$	or	$\mu \approx 1$
Semi-ductile	$0.7 < r_{\mathrm{r}} < 0.9$	and	$\mu \gg 1$

2.6.3 Simplified dynamic analysis

Full dynamic time history analyses, which can reveal (dis)advantageous structural behaviour compared to traditional static pushover analyses, are expensive and time consuming, and several analyses are necessary in order to cover a reasonable domain of relevant wave heights. One has therefore sought to find SDOF models that can estimate the *dynamic overload ratio* (the structure's capability to resist dynamic loading relative to the resistance to static loading) as a function of the post-collapse behaviour observed by pushover analyses:

$$r_\nu = F_{\mathrm{e,max}}/R_{\mathrm{ult}} \tag{2.7}$$

Simplified expressions for the dynamic overload ratio were presented by Bea and Young (1993) on the form

$$r_\nu = f(\mu) \qquad \text{and} \qquad r_\nu = f(\mu, r_r) \tag{2.8}$$

for seismic loading, i.e. load durations typically shorter than the natural period of the structural system.

Schmucker (1996) included more parameters when presenting equations for wave loading:

$$r_\nu = f(DMF, \frac{T_{\mathrm{n}}}{t_{\mathrm{d}}}, \mu, r_{\mathrm{r}}) \tag{2.9}$$

The parameters T_{n} and t_{d} are the natural period of structure and the load duration (typically half a wave cycle), respectively. This relation is an EPP (elasto perfectly-plastic) or bi-linear EPP approach to the complex behaviour of a structural system, and does thus not account for gradual yielding or reduction in load bearing capacity for displacements beyond those related to the static ultimate capacity. In order to include the effect of gradual yielding for an elasto-plastic system with post-peak degradation Emami Azadi (1998) in addition included a parameter denoted β comprising residual strength and gradual stiffness degradation in his attempt to obtain an expression for the dynamic overload ratio:

$$r_\nu = f(DMF, r_{\mathrm{r}}, \frac{T_{\mathrm{n}}}{T}, \mu, \beta) \tag{2.10}$$

In the above equation, T denotes wave period. Note that β is a 'degradation parameter', expressed as

$$\beta = 1 - r_{\mathrm{r}}\frac{T_{\mathrm{n}}}{T_{\mathrm{eff}}} \qquad \text{where} \qquad T_{\mathrm{eff}} = 2\pi\sqrt{\frac{m}{k_{\mathrm{eff}}}} \tag{2.11}$$

T_{eff} is an effective, dynamic period near collapse, but is neither the same as the natural period of the static system near collapse nor equal to the initial natural period. k_{eff} can be expressed as a fraction of the initial stiffness k_{i}, i.e.

$$k_{\text{eff}} = \alpha k_{\text{i}} \tag{2.12}$$

where α can be taken in the range of $0.1 - 0.001$. $k_{\text{eff}} = 0.1k_{\text{i}}$ represents a very highly inertia effective system, while $k_{\text{eff}} = 0.001k_{\text{i}}$ represents a very low mass dominated system (Emami Azadi, 1998).

Moan et al. (1997) reported a comparison between a MDOF model, Schmucker's approach and an expression given on the form[4]

$$r_{\nu} = f(DMF, \mu, \beta) \tag{2.13}$$

for one single platform for end-on and broad-side loading (β is the parameter defined in Equation 2.11). The discrepancies between the results obtained using MDOF model and Equation 2.13 are found to be small, generally less than 5%. Schmucker's model yields slightly lower dynamic overload ratios, and it is argued that the reason for this is that the model does not account for the change in natural period as the structure softens in the post-collapse range.

An analytical cantilever model for calculation of dynamic response of a jacket structure is presented by HSE (1998). The mathematical formulation is presented, however, it seems unclear from the description whether information about the structural properties such as stiffness and wave loading needs to be generated by some external (finite element) software with a detailed structural model. The simplified model is reported to calculate results in good agreement with results from nonlinear dynamic finite element analyses for the structure investigated in the report.

2.6.4 Acceleration levels

NORSOK S-002 (2004) provides acceleration limits for (human) exposure to continuous vibrations from machinery during a 12 hours working day for vibration frequencies 1 Hz and above. The relevance of these recommendations is considered marginal particularly due to the frequency range considered, but also due to the fact that (transient) environmental loading resulting from wave impact on the platform topside will be perceived differently than continuous vibrations during a working day.

NS 4931 (1985) gives recommendations related to the sensitivity of human beings to low frequency horisontal vibrations with duration exceeding 10 minutes in (buildings and) fixed offshore installations for the frequency range 0.063 Hz to 1 Hz. For durations shorter than 10 minutes, no recommendations are given. The human reactions to different acceleration levels are categorised as follows:

[4]The expression is referred to be originating from Emami Azadi's Dr.Ing. thesis 'to be published', however in the published thesis the expression is extended to be on the form given in Equation 2.10.

a) Threshold levels - perception or noticing of vibrations (the two lower curves in Figure 2.4).

b) Anxiety or fear leading to significant complaints, relevant as basis for criteria for on-shore building vibrations generated by storms.

c) Disturbance to activity (the upper curve in Figure 2.4).

Important for the human reactions will be how often one experiences such vibration incidents and how long they last. Values relevant for fixed offshore installations are shown in Figure 2.4. The three curves in the figure represent from above: The acceptable acceleration level of the structure when performing non-routine or exacting work, the limit acceleration which an average human being will feel and the threshold value below which nobody will notice the vibrations.

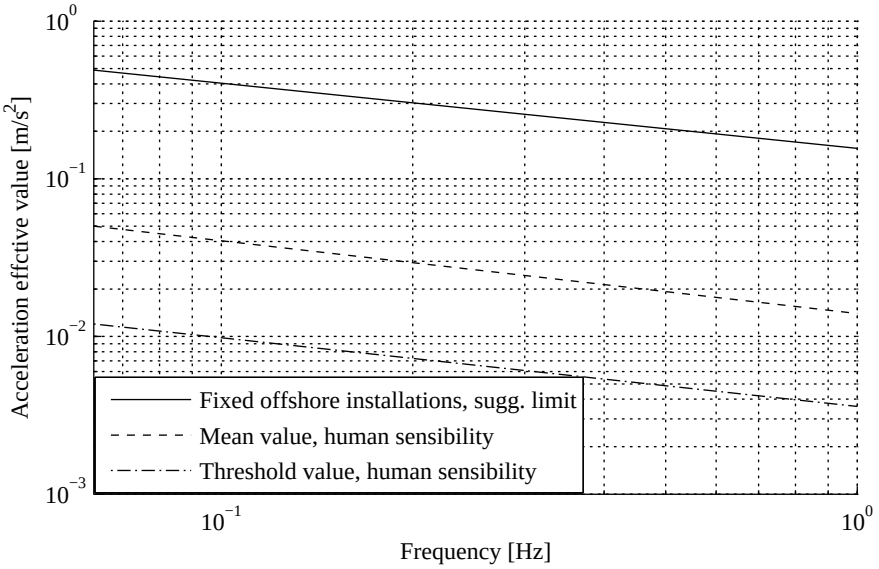

Figure 2.4: Acceleration limit values, fixed offshore installations (NS 4931, 1985)

2.6.5 Relative velocity vs. absolute water particle velocity

It has been shown that accounting for the relative velocity between water particle velocity and structural members reduces the wave load effect significantly and thereby increases the dynamic performance of a structure for a given wave scenario (Schmucker, 1996; Moan et al., 1997; Emami Azadi, 1998).

HSE (2003) reported similar results from analysis of a jack-up rig.

However, NORSOK N-003 (1999) recommends relative velocity to be included only for slender members with motion amplitude larger than the member diameter, in order not to overestimate hydrodynamic damping for structures during small motions.

2.6.6 Representative load histories

Based on analyses of time histories from three hurricanes, Bea and Young (1993) reported that the largest response amplitudes were caused by a few waves preceding and following the peak wave amplitude in these time histories.

Stewart (1992) suggested a load history comprising three wave cycles, where the force is gradually increased over the first two cycles in order to provide a 'start-up' condition for the system response. This is identical to the recommendations given later by SINTEF (1998).

A linear envelope increasing over 3 wave cycles, being constant over 2 cycles and decreasing over 3 cycles is suggested by Moan et al. (1997).

These approaches are essentially the same: a few waves before the max-wave are needed in order to start motion of the structure, and thus to get a representative inertia effect.

HSE (2003) shows that the response status, with respect to displacement and its derivatives, of a jack-up rig prior to exposure to an extreme wave which hits the deck does not influence the resulting maximum response significantly. It is noted, though, that the largest deck displacement occurs if the wave hits the hull when it has the largest displacement in the direction opposite to the wave heading direction, i.e. at the time the hull has the largest acceleration in the direction of the wave heading. The effect on the vertical reactions in the legs is, however, significant in the way that tension, i.e. deck lift off, is detected for some response conditions prior to wave impact.

2.7 Structural reliability analysis

2.7.1 General

Reliability methods are increasingly recognised as tools for supporting decisions in the petroleum industry. Related to reassessment of structures, the overall goal is to keep the safety level above the minimum requirements of the inherent safety level of the relevant design code.

Briefly, reliability methods in structural design and reassessment are structural analysis models incorporating available information about uncertainties in loads and resistances. There are mainly two types of uncertainties:

- ⋆ inherent (aleatory / type I) uncertainty — cannot be reduced by more knowledge
- ⋆ modeling (epistemic / type II) uncertainty — can be reduced by collecting more information

Currently, use of *structural reliability analysis* (SRA) is in practice mostly limited to calibration/udating of load factors in design codes. System reliability approaches are so far only applied to offshore structures where very simplified models serve the purpose (Moan, 1998a). *Quantitative reliability analysis* (QRA), however, has a wide area of application. The difference might not be obvious to the reader:

SRA Structural reliability analysis, for estimating probability of structural failure by taking into account the inherent variability of loads and the uncertainty due to lack of knowledge. Is being used for ultimate strength assessment and fatigue reliability evaluations (Moan, 1998a,b).

QRA Quantitative reliability analysis, the purpose of which is to determine likelihood of fatalities. Failure probabilities yielded by use of SRA can be included in QRA. For ALS evaluation, QRA will implicitly be used to find representative load (-combinations) or likelihood of e.g. fire or explosion, whereas SRA can be applied to determine the probability of structural collapse based on these loading events (Moan, 1998a,b).

2.7.2 Jacket structural reliability analysis in practice

The ultimate capacity for the structure must be established for different loading scenarios including, if relevant, different levels of subsidence. Current practice is to use nonlinear finite element analyses for this task. Both load and system capacity is frequently represented in terms of base shear[5] (Moan, 1998a). The load will be a function of wave heights and wave directions, while the ultimate capacity of the system is relatively independent of the variability in the (wave-)load, see e.g. Sigurdsson et al. (1994).

The dominating uncertainty parameters in the reliability calculations are those related to description of the sea state, this will be even more pronounced for waves large enough to hit the deck.

It is important that joint behaviour is represented in the finite element model, see Section 2.8.1.

The basic principle for calculation of the probability of failure is summarised in the following. The safety margin Z is a stochastic variable. This quantity is simply the difference between capacity / resistance (R) and load / load effect (S). If Z is negative, the structure fails, and positive Z indicates a safe structure. Z is in principle given on the format:

$$Z = \lambda R - (\lambda_{\mathrm{j}} S_{\mathrm{j}} + \lambda_{\mathrm{d}} S_{\mathrm{d}} + \lambda_{\mathrm{c}} S_{\mathrm{c}} + \lambda_{\mathrm{w}} S_{\mathrm{w}}) \tag{2.14}$$

where λ denotes uncertainty, R denotes structural capacity, S is load effect and indices j, d, c, and w refers to wave-on-jacket, wave-in-deck, current and wind respectively.

Lognormally distributed resistance R and load effect S are frequently assumed. Based on the failure margin, the *annual probability of failure* P_{f} is calculated. The failure probability

[5] Note the difference between *collapse base shear* and *shear capacity at the base*

depends upon expected values and inherent uncertainties as well as uncertainties in the statistical model, in load predictions, responses, member capacities and material properties. P_{f} is given by

$$P_{\mathrm{f}} = \Phi\left(-\beta\right) \tag{2.15}$$

where $\Phi\left(\right)$ is the cumulative standard normal distribution (with zero mean and unit standard deviation) and β is called *reliability index*. β is given by

$$\beta = \frac{\mu_{\mathrm{z}}}{\sigma_{\mathrm{z}}} \tag{2.16}$$

The quantities μ_{z} and σ_{z} are the mean value and standard deviation for the safety margin Z.

It should be noted that while there is an explicit connection between β and P_{f}, a given P_{f} does not reflect a certain RSR and opposite.

2.8 Components contribution to system behaviour

2.8.1 Tubular joints

The behaviour of tubular joints has been a topic subjected to considerable research over the last three decades. Increasing knowledge has improved the estimates of capacities and fatigue resistance of the joints, and the knowledge is to some extent incorporated in tools for system analysis.

Formulae for calculating the strength of tubular joints are in general derived on the basis of experiments, where failure involves significant strains. The refined formulae in the latest edition (22nd) of API RP2A, however, are calibrated against nonlinear finite element analyses as well as physical experiments.

The behaviour of the joint will be determining for the distribution of forces throughout the structural system, and therefore for the developed failure mode. Consequently, the joint behaviour will be of importance for the *overall system performance* — and thus the reliability — of the structure. This is demonstrated by e.g. Morin et al. (1998), whose objective was to investigate the influence of the joint behaviour on the overall behaviour of jacket structures. It is, amongst others, reported that the assumption of rigid joints may lead to non-conservative estimates of system capacity.

Conventional design of new structures does not include explicit modeling of joint behaviour, the joints are assumed to be perfectly rigid, meaning that moments and forces are distributed according to nominal member stiffness. In nonlinear static or cyclic analyses, which are often used for reassessment purposes, methods such as representing joint behaviour by linear (joint flexibility) or nonlinear (joint capacity) springs are used (Moan, 1998a). Other ways to represent joints can be the use of beam elements with capacities determined on the basis of tubular joint capacity formulae from recognised design codes, or to model joint behaviour by a plastic potential, taking interaction between axial loads and moments into account.

2.8.2 Tubular members

Experience has revealed that there is a considerable reserve strength in many conventionally designed jackets. As opposed to assumptions regarding other structural details in such structures, which often result in an non-conservative over-prediction of system capacity, assumptions regarding members often lead to systematic under-estimation of capacity. This is mainly caused by use of conservative buckling lengths of members. The API-regulations recommend an effective length factor of 0.8 to 0.9 for jacket braces, while NORSOK N-004 (2004) and ISO/CD 19902 (2001) recommend 0.7 to 0.8. In all cases the recommendations come to use if buckling lengths are not explicitly determined by appropriate analyses. Hellan et al. (1994) and Grenda et al. (1988) demonstrated that a more realistic estimate of the effective length factor for braces might be 0.60 - 0.65.

2.8.3 Pile / soil interaction

Failure modes that are considered in jacket pile foundations comprise pile pull-out or plunging, or plastic hinge formation (lateral pile failure). A real structure might experience a combination of these failure modes.

Methods in use to model pile/soil interaction comprise linear and nonlinear concentrated springs, springs distributed along the piles and finite element continuum models. Moan et al. (1997) demonstrated that the choice of pile/soil modeling method can affect the load distribution and failure mode in the structural model. Emami Azadi (1998) has, however, shown that the use of linear springs to represent foundation in some cases can lead to significant overestimation of the jacket-pile-soil system capacity.

HSE (1998) concludes that for one ductile jacket structure analysed, the inclusion of nonlinear foundation model results in a significant increase of the lateral displacement of the deck. The effect on the capacity to carry lateral load is, however, small.

Chapter 3

Finite element software - basis and application

3.1 Introduction

The finite element computations in this document have been carried out using USFOS, a nonlinear finite element program developed by SINTEF Civil and Environmental engineering. USFOS is originally intended for offshore (space) frame structures. The formulation is based on the displacement method using only *one* finite element per physical element in the structure and includes nonlinear material properties and nonlinear geometry / large displacements.

The objective of this chapter is to give an introduction to the methodology that is the basis for USFOS. The main references for this chapter are USFOS Theory Manual (Søreide et al., 1993), USFOS Getting Started (SINTEF GROUP, 2001) and Skallerud and Amdahl (2002).

3.2 Basic continuum mechanics applied to beam elements

3.2.1 Strain and stress

The USFOS formulation is based on use of *Green strain* E, which, to the difference from the traditional *engineering strain*, is valid for any magnitude of displacement and rotation. The stretching of an element due to transverse displacement is for instance captured by Green strain formulation, but not by engineering strain formulation. Green strain will be denoted ε herein.

The axial strain can be expressed as follows:

$$\varepsilon_x = v_{x,x} + \frac{1}{2}v_{x,x}^2 + \frac{1}{2}v_{y,x}^2 + \frac{1}{2}v_{z,x}^2 \tag{3.1}$$

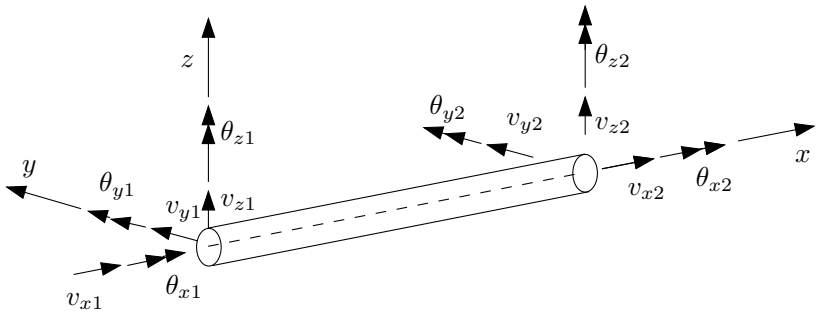

Figure 3.1: Definition of local element displacements

where v_x, v_y and v_z are displacements in x, y and z directions at any location within the beam, and subscript , x denotes differentiation once with respect to x. For moderate element deflections, Equation 3.1 simplifies to:

$$\varepsilon_x = v_{x,x} + \frac{1}{2}v_{y,x}^2 + \frac{1}{2}v_{z,x}^2 \tag{3.2}$$

The stress measure that is energy conjugate to the Green strain is the 2nd Piola-Kirchhoff stress, S. Herein, the notation σ will be used instead of S. For small strains, the 2nd Piola-Kirchhoff stress approaches the Cauchy stress, which is the energy conjugate to the engineering strain.

3.2.2 Potential energy

Potential energy considerations are used to establish the (elastic) stiffness matrix. The internal strain energy is

$$\begin{aligned} U &= \frac{1}{2}\int_V \sigma_x \varepsilon_x \mathrm{d}V \\ &= \frac{1}{2}\int_l EA\left(v_{x,x} + \frac{1}{2}v_{y,x}^2 + \frac{1}{2}v_{z,x}^2\right)^2 \mathrm{d}x + \frac{1}{2}\int_l \left(EI_z v_{y,xx}^2 + EI_y v_{z,xx}^2\right)\mathrm{d}x \end{aligned} \tag{3.3}$$

where EA and EI are axial and bending stiffness, respectively, subscript , xx denotes differentiation twice with respect to x, σ_x is the 2nd Piola-Kirchhoff stress in x-direction and l is the length of the element. The internal strain energy has one contribution from axial loading which includes axial displacement v_x, and one from bending, which includes the lateral displacements v_y and v_z .

The potential of the external loads reads

$$H = -\sum F_i v_i - \int_l q_x v_x \mathrm{d}x - \int_l q_y v_y \mathrm{d}x - \int_l q_z v_z \mathrm{d}x \tag{3.4}$$

where F_i and v_i are the concentrated loads and the resulting displacements and q is distributed load. The total potential for an (elastic) element is the sum of internal strain energy and the potential of the external loads:

$$\Pi = U + H \tag{3.5}$$

The first variation of the total potential

$$\delta\Pi = \delta U + \delta H \tag{3.6}$$

with respect to displacements expresses the state of equilibrium in the body. The requirement $\delta\Pi = 0$ is the basis for equilibrium corrections, ensuring that the internal stress state corresponds to the external force situation.

Further, the relation between two close configurations is given by the variation of increment in the total potential:

$$\delta\Delta\Pi = \delta\Delta U + \delta\Delta H \tag{3.7}$$

3.3 Finite element formulation

So far, we have considered the beam element as a continuum, its variables not restricted to certain locations or nodes. The functions $v_x(x)$, $v_y(x)$ and $v_z(x)$ denote the displacements in the three directions of the longitudinal neutral axis of the beam. In the following, the behaviour of the element will instead be represented by the behaviour at chosen locations, called nodes.

3.3.1 Shape functions

Generating a finite element model of a structure involves a division or discretisation of the structure into elements with a given number of nodes[1]. The displacement $\{\mathbf{v}\}$ of any point

[1]One major feature of USFOS is the formulation which allows for the use of only one element per physical element in the frame structure. The element formulation is capable of modeling beam-column behaviour including buckling and large deflections. The default beam column element has two nodes with three translational and three rotational degrees of freedom each.

located at the element neutral axis is described by the displacement of the nodes $\{\mathbf{v}_\mathrm{N}\}$ combined with the *shape* or *interpolation functions* $[\mathbf{\Phi}]$;

$$\{\mathbf{v}\} = [\mathbf{\Phi}]^T\{\mathbf{v}_\mathrm{N}\} \tag{3.8}$$

For a two node beam element, which is the basic element in USFOS, the displacements can be expressed in the following way:

$$\begin{aligned} v_x(x) &= \{\boldsymbol{\phi}_x\}^T\{\mathbf{v}_x\} \\ v_y(x) &= \{\boldsymbol{\phi}_y\}^T\{\mathbf{v}_y\} \\ v_z(x) &= \{\boldsymbol{\phi}_z\}^T\{\mathbf{v}_z\} \end{aligned} \tag{3.9}$$

By substituting these expressions for $v_x(x)$, $v_y(x)$ and $v_z(x)$ in the functionals $\delta\Pi$ and $\delta\Delta\Pi$, the problem of finding stationary value of the functional reduces to finding the solution of a set of algebraic equations where nodal displacements $\mathbf{v}_x$, $\mathbf{v}_y$ and $\mathbf{v}_z$ are the unknowns.

3.3.2 Stiffness matrix

The elastic tangent stiffness matrix $[\mathbf{K}_\mathrm{T}]$ is derived by substituting Equation 3.9 into the expression for $\delta\Delta U$ and arranging the terms in the order $\mathbf{v}_x$, $\mathbf{v}_y$ and $\mathbf{v}_z$, on the form

$$\{\mathbf{S}\} = [\mathbf{K}_\mathrm{T}] \begin{Bmatrix} \mathbf{v}_x \\ \mathbf{v}_y \\ \mathbf{v}_z \end{Bmatrix} \tag{3.10}$$

where $\mathbf{S}$ is the vector of force components.

3.3.3 Nonlinear material model

The inclusion of nonlinear material behaviour comprises the following elements:

- ⋆ A yield condition — defines when yield occurs
- ⋆ A flow rule — relates the plastic strain increment to the stress increment
- ⋆ A hardening rule — description of change in stress during plastic flow
- ⋆ A bounding surface — the surface that defines the outer limit of the yield surface
- ⋆ A loading condition — identifies elastic (un)loading or plastic loading

The ***yield condition*** is represented by a yield surface or yield function Γ_{y} on the form

$$\Gamma_{\mathrm{y}}(S_i, S_{\mathrm{p}i}, \beta_i, z_{\mathrm{y}}) = \Gamma_{\mathrm{y}}\left(\frac{S_i - \beta_i}{S_{\mathrm{p}i}\, z_{\mathrm{y}}}\right) = 0, \qquad i = 1, \ldots, 6 \tag{3.11}$$

where

$$\mathbf{S} = [N, V_y, V_z, M_x, M_y, M_z]^T \quad \text{and} \quad \mathbf{S}_{\mathrm{p}} = [N_{\mathrm{p}}, V_{\mathrm{p}y}, V_{\mathrm{p}z}, M_{\mathrm{p}x}, M_{\mathrm{p}y}, M_{\mathrm{p}z}]^T \tag{3.12}$$

S_i is the vector of force components, while $S_{\mathrm{p}i}$ is the vector of the plastic capacities for all force components. The factor z_{y} describes the extension of the yield surface relative to the bounding surface, and β_i describes transition of the yield surface from initial yield to full plastification of the cross section. The yield surface divides the force space into an elastic force state $\Gamma_{\mathrm{y}} < 0$ and a plastic force state $\Gamma_{\mathrm{y}} = 0$. A force state $\Gamma_{\mathrm{y}} > 0$ is in principle not allowed.

For tubular members, when neglecting torsion, shear forces and strain hardening, the yield condition simplifies to:

$$\Gamma_{\mathrm{y}} = \cos\left(\frac{\pi}{2}\frac{(N - \beta_1)}{N_{\mathrm{p}}\, z_{\mathrm{y}}}\right) - \frac{\sqrt{(M_y - \beta_5)^2 + (M_z - \beta_6)^2}}{M_{\mathrm{p}}\, z_{\mathrm{y}}} = 0 \tag{3.13}$$

The total strain, and consequently the total displacement, is assumed to consist of an elastic and a plastic part. The ***flow rule***, also called the normality criterion, states that the plastic displacement vector must be normal to a defined plastic potential Q. For ductile steel materials, the yield function can be taken as the plastic potential, and thus the flow rule reads

$$\Delta \mathbf{v}^p = \mathbf{G}\Delta\,\lambda = \begin{bmatrix} \mathbf{g}_1 & \mathbf{0} \\ \mathbf{0} & \mathbf{g}_2 \end{bmatrix} \begin{Bmatrix} \Delta\lambda_1 \\ \Delta\lambda_2 \end{Bmatrix} \tag{3.14}$$

where $\mathbf{g}_j$ is the surface normal at node j which, for an elastic-perfectly-plastic material, is given by:

$$\mathbf{g}_j^T = \frac{\partial \Gamma_{\mathrm{y}}}{\partial \mathbf{S}} = \left[\frac{\partial \Gamma_{\mathrm{y}}}{\partial N}, \frac{\partial \Gamma_{\mathrm{y}}}{\partial V_y}, \frac{\partial \Gamma_{\mathrm{y}}}{\partial V_z}, \frac{\partial \Gamma_{\mathrm{y}}}{\partial M_x}, \frac{\partial \Gamma_{\mathrm{y}}}{\partial M_y}, \frac{\partial \Gamma_{\mathrm{y}}}{\partial M_z}, \right]_j^T \tag{3.15}$$

Index j refers to nodes 1 and 2. The parameter $\Delta\lambda$ is a scalar, yet unknown, which will be zero during elastic unloading and positive during plastic loading.

The ***hardening rule*** describes the transition from one plastic state to another. Hardening can be one of the two following types, or a combination of the two:

- ⋆ *Kinematic hardening* - the yield surface moves but doesn't change shape or extend.

- ⋆ *Isotropic hardening* - the yield surface extends with increasing plastic deformations, but doesn't change shape or move.

The current version of USFOS includes only kinematic hardening. Hardening is implemented according to the ***bounding surface*** concept, meaning that in addition to the yield surface Γ_{y} a bounding surface, denoted and Γ_{b}, is used. The bounding surface is the outer limit of the expansion / translation of the yield surface, and indicates full plastification:

$$\Gamma_{\mathrm{b}}(\overline{S}_i, S_{\mathrm{p}i}, \alpha_i, z_{\mathrm{b}}) = \Gamma_{\mathrm{y}}\left(\frac{\overline{S}_i - \alpha_i}{S_{\mathrm{p}i}\, z_{\mathrm{b}}}\right) = 0, \qquad i = 1, \ldots, 6 \tag{3.16}$$

$\overline{\mathbf{S}}$ is the conjugate point having a surface normal $\overline{\mathbf{g}}$ that points in the same direction as the surface normal $\mathbf{g}$ to the force state $\mathbf{S}$ on the yielding surface. The bounding surface extension parameter z_{b} is 1. The vector α describes the translation of the bounding surface due to kinematic hardening.

When the cross section is loaded, the force vector moves from origin outwards in some direction, and when it reaches the yielding surface Γ_{y} it corresponds to yielding of the extreme fibre in the cross section. Further loading of the cross section makes the yield surface translate, while the force vector remains on the yield surface. If (kinematic) strain hardening is accounted for in the structural model, the bounding surface Γ_{b} also translates, however at a smaller rate. If the load state is increasing, the yield surface will finally contact the bounding surface, meaning that the cross section is fully plastified. From this state on, the force vector will remain on the bounding surface Γ_{b}.

Whether a load increment implies plastic straining or elastic (unloading) straining, is determined by a ***loading condition***. During a load increment that moves the force vector from one plastic state to another, the force vector must remain on the yield surface. This is obtained by the following requirement, which is called the consistency criterion:

$$\Delta\Gamma_{\mathrm{y}} = \frac{\partial\Gamma_{\mathrm{y}}}{\partial\mathbf{S}}\Delta\mathbf{S} = \mathbf{g}^T\Delta\mathbf{S} = 0 \tag{3.17}$$

Elastic (un)loading implies that the following is true:

$$\Delta\Gamma_{\mathrm{y}} < 0 \tag{3.18}$$

The consistency criterion for an elastic-perfectly-plastic material reads:

$$\begin{aligned}\Delta\Gamma_{\mathrm{y}} = \frac{\partial\Gamma_{\mathrm{y}}}{\partial N}\Delta N + \frac{\partial\Gamma_{\mathrm{y}}}{\partial V_y}\Delta V_y + \frac{\partial\Gamma_{\mathrm{y}}}{\partial V_z}\Delta V_z + \frac{\partial\Gamma_{\mathrm{y}}}{\partial M_x}\Delta M_x \\ + \frac{\partial\Gamma_{\mathrm{y}}}{\partial M_y}\Delta M_y + \frac{\partial\Gamma_{\mathrm{y}}}{\partial M_z}\Delta M_z = 0\end{aligned} \tag{3.19}$$

The consistency criterion is further used to determine the size of $\Delta\lambda$ and to establish the elasto-plastic tangent stiffness matrix, using the assumption that the displacement increment consists of an elastic and a plastic part together with the stiffness relation for the element.

3.3.4 Analysis using USFOS

The equation system is by default solved by use of a pure incremental solution procedure, however, the analyst may specify the use of equilibrium iterations.

Static pushover analysis

The load is applied in steps, implying that a full linear analysis is run at each load step. The structural geometry and state based on the introduction of plastic hinges is updated after each load step. If a plastic hinge is introduced during a load step, the load step is scaled to coincide exactly with the load level for the occurrence of the plastic hinge.

The analyst specifies the load history to be used. Normally, permanent design loads are applied first during a few load steps. Thereafter, the load for which one seeks to obtain the static capacity is applied stepwise until global collapse occurs.

The major outcome of a static pushover analysis is a load-displacement curve — a resistance curve — for a given load scenario. The resistance curve contains information about the global collapse load or capacity as well as insight into the (nonlinear) behaviour in the pre- and post-collapse domain.

Dynamic analysis

Load specification for dynamic (nonlinear) analysis comprises the load magnitude and spatial distribution as well as the time variation in the form of a scaling factor that is time dependent. Node and element loads as well as gravity loads, for example, are specified by a reference numerical value and a time history. A wave load time history, on the other hand, is specified by wave height, period, water depth and direction and a phase angle for the start of the analysis. This information comprises both the spatial distribution and the time variation.

The time step size used in the analysis must be determined considering the nature of the load history, the natural period of the structure and the amount of plastic behaviour experienced by the structure due to the load history.

The HHT-α method (Hilber et al., 1977) for numeric time integration is adopted (Søreide et al., 1993). This method can be considered as an extension of the Newmark β-method, which is used for the simplified analyses in Chapters 6 and 7. The algorithm includes the three parameters α, β and γ, which in combination control accuracy, stability and high frequency damping. The method is unconditionally stable if the following conditions are satisfied:

$$
\begin{aligned}
-\frac{1}{3} &< \alpha < 0 \\
\gamma &= \frac{1}{2} - \alpha \\
\beta &= \frac{1}{4}(1-\alpha)^2
\end{aligned}
$$

The results from a dynamic nonlinear analysis comprise response time histories of e.g. nodal displacements, velocities and accelerations as well as time histories of element forces and reaction forces. In general, the nonlinear performance obtained for a specific load history is relevant for this single load history only.

Chapter 4

Environment and forces

4.1 Introduction

4.1.1 Chapter outline

This chapter comprises considerations related to wave-in-deck force time histories.

This first section is a summary of the chapter and is followed by a brief introduction and motivation.

Typical characteristics for the North Sea environment are summarised in Section 4.2, whereas some considerations regarding wave time history and wave theories are presented in Section 4.3. Modelling of the wave forces on a jacket structure is briefly explained in Section 4.4.

Section 4.5 presents the most commonly used methods and mathematical formulations for wave-in-deck forces. The methods are divided into two main groups, namely component models and global or silhouette models. The silhouette models are again subdivided into two groups, those based on drag formulation and those based on loss-of-momentum formulation. The difference between these two types of silhouette models is particularly addressed in Section 4.5.3.

In Section 4.6 it is demonstrated how to analytically calculate wave-in-deck force histories based on linear wave theory. Further, it is described how one can use Stokes 5th order theory in a computer program to calculate simplified force time histories.

Forces calculated by the simplified methods described in Section 4.6 are compared to each other in Section 4.7.1, and to computational results in Section 4.7.2. Results from wave tank experiments on wave-in-deck forces are presented and discussed in Section 4.8.

Vertical wave-in-deck forces are briefly discussed in Section 4.9.

Section 4.10 deals with the relevance of the load time history prior to the extreme wave event.

A conclusion of the chapter including a recommended formula for calculating wave-in-deck loads is presented in Section 4.11.

4.1.2 Motivation

For a dynamic analysis of fixed offshore jacket structures exposed to wave-in-deck loading, it is not evident which wave (-history) to use. In a static analysis, a worst case scenario is used, e.g. a 100 years wave (ULS situation) or a 10 000 years wave (ALS situation) with corresponding periods. This single wave represents all smaller waves. In a dynamic analysis, a smaller wave with a period that could cause dynamic amplification could theoretically be more onerous, resulting in higher load effects. For an impact load, the form and duration of the load impulse are of main importance (Biggs, 1964). The load history prior to the extreme wave may also influences the dynamic response.

4.2 Environment

Wind

Wind loads on fixed offshore structures must be calculated and included in the structural analyses in accordance with relevant regulations for the platform location. Wind forces represent a relatively small part of the total environmental loading and are normally not a point of concern for the load bearing capacity of a conventional jacket. The topic of wind forces will not be further addressed herein. However, for major structural parts, such as for instance flare towers, wind has to be considered particularly with respect to vortex shedding and subsequent fatigue damage.

Current

NORSOK N-003 (1999) states that current for design purposes should be based on measurements at the actual and adjacent sites, in addition to hindcast predictions of wind induced currents, theoretical considerations and other information about tidal and coastal currents. In order to limit the present work, current has not been a topic of investigation. However, a surface current of 1 m/s is included in the structural analyses.

Waves

Typical wave heights and periods for return periods of 100 and 10 000 years in the southern and northern North Sea respectively can be as follows (Eik, 2005; NORSOK N-003, 1999):

Southern North Sea		Northern North Sea	
$h_{100} = 26$ m	$T_{100} = 15.5 - 16$ s	$h_{100} = 28$ m	$T_{100} = 15.5$ s
$h_{10000} = 33$ m	$T_{10000} = 16 - 16.5$ s	$h_{10000} = 35$ m	$T_{10000} = 16.3$ s

Other combinations of wave heights and periods, which give the same probability of occurrence, can be obtained in the form of contour diagrams and should also be taken into account

(NORSOK N-003, 1999). Contour diagrams provide a valuable basis for decision on relevant combinations of wave height and period, see Haver and Kleiven (2004) wherein contour diagrams for significant wave height h_s and spectral peak period T_p are given. Because the dynamic load effect depends upon the relation between the period of the loading and the natural period of the structure, it might for dynamic problems in addition be necessary to consider combinations of h and T giving a different probability of occurrence.

Waves of these heights are steep, irregular waves. For a deterministic approach such waves are normally described by Stokes wave theory or Stream function theory. Both theories account for higher crest heights than trough depths. However, linear wave theory with Wheeler stretching[1] of wave kinematics to the surface (see e.g. Gudmestad, 1993) could be used due to the possibility of analytical representation of the load time history. Generating force time histories using Stokes or Stream function wave theory requires computer tools.

4.3 Wave time history and wave kinematics

Reanalysis of offshore structures, in particular where wave-in-deck loads are expected to be a problem, should include simulation of dynamic structural response in storm situations with irregular waves. Under such conditions, there might be one or more waves that bring the response into the non-linear domain. There are these situations that need special considerations, i.e. non-linear dynamic analysis. Using the waves that cause concern in the linear simulations, including a few wave cycles prior to the extreme wave, will be an obvious approach. If the software used for non-linear analysis is not capable of analysing irregular waves, the wave history may be approximated by a sequence of regular waves.

Linear Airy wave theory with extrapolation or Wheeler stretching of wave kinematics to the surface has a relatively simple analytical formulation which in turn permits an analytical representation of the force time history. However, linear theory does not to a satisfactory degree describe real ocean waves.

State-of-practice for mathematical representation of North Sea waves is to use Stokes 5th order wave theory. As mentioned, computer software is required to calculate force time histories based on Stokes or Stream function wave theory.

4.4 Wave load on jacket structure

In accordance with state-of-practice, Morison equation (e.g. Chakrabarti, 1987) is used to calculate wave forces on the jacket structure below deck level.

[1] Other commonly used methods are Delta stretching and vertical extrapolation of wave kinematics (Gudmestad, 1993; ISO/CD 19902, 2001; NORSOK N-003, 1999).

4.5 Wave-in-deck load models

There is no general consensus on which method to use to calculate wave loads on platform decks. Several approaches exist, some verified against experimental data, some not. The methods can be divided into two main groups; firstly the global / silhouette approaches, which use an effective deck area combined with pressure induced by the water particles, and secondly the detailed component approaches where the load on each single members is calculated separately.

Unless the deck is extremely simple and lightly equipped, the use of component methods is relatively resource consuming. The use of such models is appropriate for (re)analysis of specific structures, whereas the silhouette approaches are suitable for e.g. sensitivity studies and general studies on structural behaviour.

The British Health and Safety Executive has conducted a comparative study of wave-in-deck load models (HSE, 1997b), comprising the API model, DNV slamming, Shell-, Amoco-, Kaplan- and Chevron models. They are, together with some other approaches, attended to in the following.

4.5.1 Component approaches

In the component approaches one seeks to estimate wave loading on each deck member and all equipment separately. Interaction between different structural components can be taken into account by using shielding or blocking factors, which can be determined by experiments (see e.g. Sterndorff, 2002) or computational fluid dynamics (CFD) technique. Obviously, when using this kind of approach, the deck must be modeled in detail. The amount of equipment and members in a normal platform deck necessitates, for practical purposes, computer software to carry out the calculations. Software based on the recommendations by dr. Kaplan (Kaplan et al., 1995) is commercially available. Further, Finnigan and Petrauskas (1997) have given recommendations for how to calculate maximum load from wave on deck.

Other references in general outline the principles they have applied in specific studies, rather than presenting a method to be used by others.

More detailed information about the different methods is given in the following.

Company internal models Amoco (now part of BP) has a company internal wave-in-deck load model, which was made available to HSE for comparison purposes (HSE, 1997b). It requires a detailed deck model.

Kaplan et al.'s (1995) model uses stretched (Wheeler, 1970) linear wave theory and requires a detailed deck model. The model includes drag, inertia and impact loads as well as buoyancy. The formulation handles both horisontal and vertical forces and includes time variation.

Finnigan and Petrauskas' (1997) model, which is denoted 'Chevron model' in the comparative study conducted by HSE (1997b), is based on regular Stream function wave theory and Morison equation, with direction- and equipment density dependent drag and inertia coefficients. Only horisontal loads are addressed. The method is calibrated against tests reported in the reference document. Focus is on maximum loads, and load variation with time is not addressed. The procedure cannot just like that be extended to include variation in time.

Pawsey et al. (1998) developed a procedure based on Kaplans recommendations but modified to use Stream function wave theory. Modeling of dense deck areas is somewhat simplified. The procedure was calibrated to Kaplans software. The integration of the wave-in-deck load module into the wave-load generator in the analysis software, thus including the phase difference for load on deck and load on jacket, is emphasised. This eliminates the conservatism in adding maximum load on the deck to maximum load on the jacket, which has been state-of-practice for static analyses.

DHI *WaveInDeck* (DHI*WID*) (Grønbech et al., 2001) This is commercially available software that computes time domain wave-in-deck forces on component level, based on the recommendations given by Kaplan (1992). The program handles the most commonly used wave kinematics models as well as deterministic and stochastic waves. The program is based on the concept of change in momentum, and includes also drag and buoyancy forces.

4.5.2 Silhouette models

The silhouette models are of two kinds; those based on drag formulation and those based on momentum formulation. The notation is illustrated in Figure 4.1.

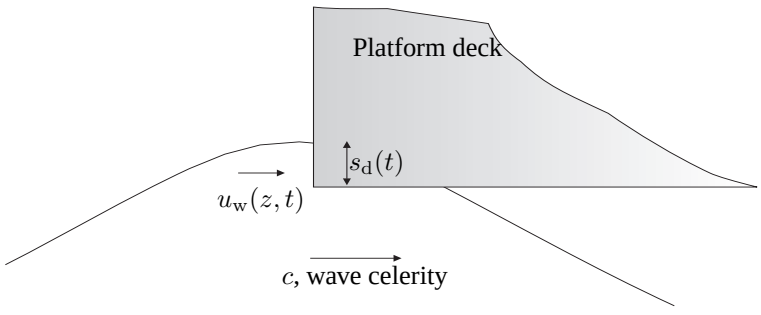

Figure 4.1: Notation for simplified wave-in-deck force formulations

Drag formulation

The drag based silhouette wave-in-deck models have in common the typical drag formulation known from Morison equation. The absolute value of the load is given by

$$F_x = \frac{1}{2}\rho A C_{\mathrm{d}} u_{\mathrm{w}}^2 \tag{4.1}$$

where ρ is sea water density u_{w} is the water particle velocity, $A = s_{\mathrm{d}} \cdot b$ is the exposed area, s_{d} is the inundation (height) and b the width of the inundated area. The drag factor C_{d} (sometimes called slamming factor and denoted C_{s}) is chosen to account for different loading scenarios. These models are typically intended for calculation of maximum load, but the simple formulation makes them also easy to apply for time domain analyses, noting that the particle velocity u_{w} and the inundated area A are time dependent variables. However, time variation has not been addressed for any of the presented models. Accordingly the models have not been subject to time domain comparison with e.g. more detailed methods or experiments.

The wave-in-deck force models in this group are briefly presented in the following.

In the API model (API WSD, 2002; API LRFD, 2003; Finnigan and Petrauskas, 1997) C_{d} is varied between 1.2 and 2.5 according to the wave direction and the equipment density on the deck. The water particle velocity u_{w} contains a sum of current velocity and wave induced particle velocity, as well as a current blockage factor and a wave kinematics factor. The method is validated against model tests that are reported by Finnigan and Petrauskas (1997). The wave induced particle velocity shall be taken as the highest velocity at the crest (or the top of the exposed area if the wave crest extends above the deck silhouette).

The ISO procedure (ISO/CD 19902, 2001) is directly adopted from API (see above).

Det Norske Veritas (1991) has the following formulation, similar to the well known Morison equation, for slamming forces:

$$F_x = \frac{1}{2}\rho A C_{\mathrm{s}} u_{\mathrm{w}}^2 \tag{4.2}$$

This formulation is used by Dalane and Haver (1995) and Haver (1995) to calculate horisontal wave-in-deck loads, and is referred to as the ‘Statoil method’ in the comparative study conducted by HSE (1997b). The formulation is similar to the API formulation presented above. The deck is assumed to be solid, i.e. the total impact area is used with no modifications related to equipment density. Water particle velocity is taken to be the velocity ‘at a representative height with respect to the exposed area’, e.g. in the center of the exposed area, and Det Norske Veritas (DNV) requires the slamming coefficient C_{s} (corresponding to API’s drag coefficient) not to be less than 3.0. A is the exposed area, ρ is sea water density and u_{w} is the water particle velocity. Only horisontal loads

are included. In the latest edition DNV (Det Norske Veritas, 2000) suggest the use of $C_{\mathrm{s}} = 2\pi$ for vertical on bottom slamming.

The formulation was basically intended for vertical loads on horisontal cylinders (braces), for wedge entry into water and flat bottom slamming. Clearly, the validity related to calculation of wave in deck forces can be questioned. This issue has been addressed by Vinje (2002). The conclusion is that the identification of a proper slamming coefficient is a problem and that this drag type formulation is unsuitable for calculation of wave-in-deck forces.

Momentum formulation

This type of formulation is based on the assumption of complete loss of momentum at impact, which in a general manner can be expressed as

$$F_x(t) = \int_{A(t)} \frac{\mathrm{d}m}{\mathrm{d}t} u_{\mathrm{w}}(z,t)\,\mathrm{d}A \tag{4.3}$$

where $\mathrm{d}m/\mathrm{d}t$ is the net mass flow imparted onto the structure per unit time and unit area and u_{w} is the water particle velocity. A is the exposed area, which is a function of the surface elevation η, which again is a function of time. The formulation makes it relatively convenient to calculate load as a function of time. This type of formulation does not include any empirical factors, such as slamming- or drag factors, and in principle any appropriate wave theory can be used. It is assumed that the water particles that hit the deck will be 'thrown away' having no further influence on the deck, and that the presence of the deck does not influence the particle movement before the particle hits the deck.

Shell To the author's knowledge there exists no open detailed firsthand reference for this method. A few sentences about the background for the Shell-method is roughly outlined by Tromans and van de Graaf (1992). The present information about the Shell method is taken from the comparative study conducted by HSE (1997b).

Although not explicitly stated in the reference, it is interpreted from the text that the horisontal water particle velocity is to be taken as the velocity at the water surface $z = \eta$. Thus η must be substituted for z in Equation 4.3. Horisontal forces as a function of time are calculated on front wall and during passage of the wave under the deck as the wave enters the deck from beneath. The net mass flow to be substituted into Equation 4.3 for wave impact on the front wall is expressed as

$$\frac{\mathrm{d}m}{\mathrm{d}t} = \rho\, u_{\mathrm{w}}(\eta,t) \tag{4.4}$$

where ρ is the sea water density. The horisontal force at the front wall is expressed as follows:

$$F(t) = \rho \int_{A(t)} \left(u_{\mathrm{w}}(\eta,t)\right)^2\,\mathrm{d}A \tag{4.5}$$

The net mass flow onto the deck as the wave passes under the deck is given as

$$\frac{\mathrm{d}m}{\mathrm{d}t} = \rho\, v_{\mathrm{w}}(\eta, t) \tag{4.6}$$

where $v_{\mathrm{w}}(\eta, t)$ is the *vertical* water particle velocity. The horisontal force as the wave passes under the deck is given as:

$$F(t) = \rho \int_{A(t)} v_{\mathrm{w}}(\eta, t) u_{\mathrm{w}}(\eta, t)\, \mathrm{d}A \tag{4.7}$$

Although not included in the description of the procedure, extension to include vertical loads is possible by using the same principle as for horisontal loads (HSE, 1997b).

MSL (HSE, 2001, 2003) The MSL method is developed from the previously described Shell model, and is intended for the closed hull-type of decks found on jack-up platforms. The procedure comprises horisontal slamming force on the front wall, vertical hydrodynamic force and buoyancy, all as a function of time.

Vinje (2001) expresses the net mass flow dependent upon the wave celerity $c = L/T$, not the water particle velocity:

$$\frac{\mathrm{d}m}{\mathrm{d}t} = \rho\, c\, \mathrm{d}A \tag{4.8}$$

In the expression for the celerity c the wave length L can be calculated from

$$L = \frac{gT^2}{2\pi} \tanh kd \tag{4.9}$$

by use of an iterative procedure, since $k = 2\pi/L$. Vinje has only addressed the impact force at the front wall, and the total expression for the force as a function of time is:

$$F(t) = \rho\, c \int_{A(t)} u_{\mathrm{w}}(z, t)\, \mathrm{d}A \tag{4.10}$$

4.5.3 Comments to the silhouette approaches

The two types of formulation of the silhouette approaches — the drag formulation and the momentum formulation — differ in nature. The drag formulation is only defined for slamming forces from waves at the deck front wall.

The drag factor C_{d} is in its original form meant to be a global representation of pressure caused by the local flow phenomena summarised around a body. In principle it is not incorrect to let the drag factor represent the sum of local flow induced pressure at wave inundation.

However, it is likely that the global effect of the pressure summarised over the inundated area might differ for different inundation levels. A given C_{d} might therefore be representative for a given inundation level, but not for another. Following this, it is likely that the C_{d}, in order to be representative, should change as the inundation increases and then decreases during the wave passage past the front wall of the deck.

The ratio of a general drag formulation (subscript 'dr') to the Shell or MSL type of formulation (subscript 'mo') is constant throughout the wave cycle:

$$\frac{F_{\mathrm{dr}}(t)}{F_{\mathrm{mo}}(t)} = \frac{C_{\mathrm{d}}}{2} \tag{4.11}$$

This means that a drag formulation with an equivalent drag factor $C_{\mathrm{d,eq}} = 2$ will give the same result as a momentum formulation with $\mathrm{d}m/\mathrm{d}t = \rho\, u_{\mathrm{w}}$.

Now comparing a general drag formulation with the Vinje (subscript 'Vi') approach:

$$\begin{aligned}
\frac{F_{\mathrm{dr}}}{F_{\mathrm{Vi}}} &= \frac{0.5\, C_{\mathrm{d}}\, \rho \int_{A(t)} (u_{\mathrm{w}}(z,t))^2 \, \mathrm{d}A}{\rho\, c \int_{A(t)} u_{\mathrm{w}}(z,t)\, \mathrm{d}A} \\
&= \frac{C_{\mathrm{d}}}{2\, c} \cdot \frac{\int_{A(t)} (u_{\mathrm{w}}(z,t))^2 \, \mathrm{d}A}{\int_{A(t)} u_{\mathrm{w}}(z,t)\, \mathrm{d}A} \\
&\leq \frac{C_{\mathrm{d}}}{2\, c} \cdot \frac{u_{\mathrm{w,max}} \int_{A(t)} u_{\mathrm{w}}(z,t)\, \mathrm{d}A}{\int_{A(t)} u_{\mathrm{w}}(z,t)\, \mathrm{d}A} \\
&\leq \frac{C_{\mathrm{d}}\, u_{\mathrm{w,max}}}{2\, c}
\end{aligned} \tag{4.12}$$

Clearly the relation between the two methods will vary through a wave cycle. Based on Equation 4.12, a lower bound for an equivalent drag / slamming factor (e.g. for use in finite element software when generating wave loads with drag formulation) can be found:

$$C_{\mathrm{d,eq}} \geq \frac{2\, c}{u_{\mathrm{max}}} \tag{4.13}$$

Examples of how $C_{\mathrm{d,eq}}$ may vary with time will be given in later sections in this chapter.

4.5.4 A practical approach to the use of drag formulation in the time domain

The method outlined in the following only takes the horisontal pressure on the upstream deck wall into account. It is assumed that the water particle movements are not disturbed prior

to the contact with the deck wall, and that the top of the wave is being 'shaved' off at the lower edge of the deck. The forces are calculated using a drag formulation combined with the exposed area and the particle velocity at the actual height. An appropriate value for the drag factor C_{d} must be used. By use of cylindrical vertical elements at the location of the deck front wall for the actual wave heading, the wave load time histories can be generated separately or together with the wave load on the jacket by any FE software that includes a wave load generator, for any wave theory that is included in the software.

This approach yields an approximation for the wave-in-deck loading and makes the calculations very convenient. The chosen C_{d} may calibrate the (maximum) force to e.g. other silhouette models.

4.6 Calculation of simplified load time histories for the load onto the deck

Analytical calculation of load time histories is relatively simple when combining the silhouette methods with Airy theory. If using Stokes or Stream Function theory, the approach described in Section 4.5.4 can be used, alternatively computer tools that serve the purpose are required.

In the following, derivation of expressions for force time histories will be given based on a general drag formulation and the Vinje formulation using linear Airy theory. The use of Stokes 5th order wave theory for the same task is attended to separately. The notation used is illustrated in Figure 4.2. Note that the drag formulation used includes the variation in time and space for the water particle velocity.

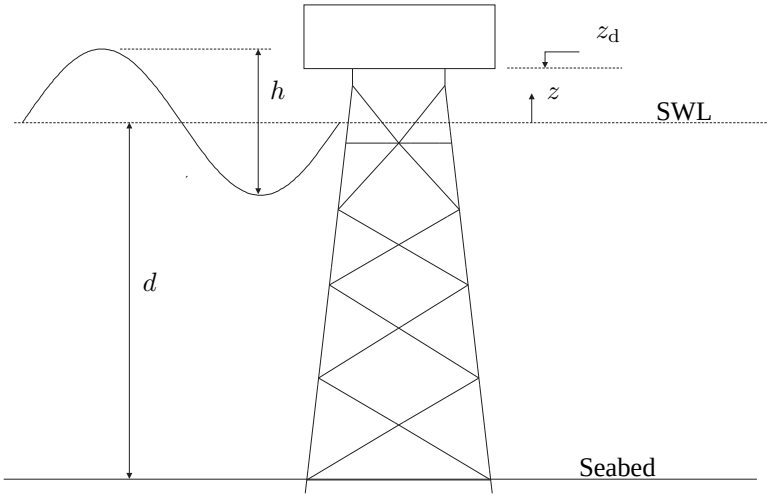

Figure 4.2: Nomenclature for calculation of force impulse

4.6.1 Derivation of deck force time history using drag formulation and Airy theory

Horisontal particle velocity according to Airy theory (Chakrabarti, 1987) including Wheeler stretching of kinematics to the surface is given as

$$u_{\mathrm{w}}(z,t) = \frac{\pi\, h}{T} \frac{\cosh\left(k(d+z)\frac{d}{d+\eta(t)}\right)}{\sinh kd} \sin\theta \tag{4.14}$$

where $\theta = kx - \omega t$ is the phase angle of the wave. Substituting Equation 4.14 for u_{w} in Equation 4.2, assuming that the wave does not break at the first impact, yields:

$$\begin{aligned}
F_x(t) &= \frac{1}{2}\rho\, C_{\mathrm{s}} \int_{A(t)} \left(u_{\mathrm{w}}(z,t)\right)^2 \,\mathrm{d}A \\
&= \frac{1}{2}\rho\, C_{\mathrm{s}}\, b \int_{z_{\mathrm{d}}}^{\eta(t)} \left(u_{\mathrm{w}}(z,t)\right)^2 \mathrm{d}z \\
&= \frac{1}{2}\rho\, C_{\mathrm{s}}\, b \int_{z_{\mathrm{d}}}^{\eta(t)} \left[\frac{\pi\, h}{T} \frac{\cosh\left(k(d+z)\frac{d}{d+\eta(t)}\right)}{\sinh kd} \sin\theta\right]^2 \mathrm{d}z \\
&= \frac{1}{2} \frac{\rho\, C_{\mathrm{s}}\, b\, \pi^2\, h^2\, \sin^2\theta}{T^2\, \sinh^2 kd} \int_{z_{\mathrm{d}}}^{\eta(t)} \cosh^2\left(k(d+z)\frac{d}{d+\eta(t)}\right)\mathrm{d}z \\
&= \frac{1}{2} \frac{\rho\, C_{\mathrm{s}}\, b\, \pi^2\, h^2}{T^2\, \sinh^2 kd} \left[\frac{z}{2} + \frac{d+\eta(t)}{4kd} \sinh\left(2k(d+z)\frac{d}{d+\eta(t)}\right)\right]_{z_{\mathrm{d}}}^{\eta(t)} \sin^2\theta \\
&= \frac{1}{4} \frac{\rho\, C_{\mathrm{s}}\, b\, \pi^2\, h^2}{T^2\, \sinh^2 kd} \Bigg[\eta(t) - z_{\mathrm{d}} + \frac{d+\eta(t)}{2kd} \sinh\left(2kd\right) \\
&\qquad\qquad - \frac{d+\eta(t)}{2kd} \sinh\left(2k(d+z_{\mathrm{d}})\frac{d}{d+\eta(t)}\right)\Bigg] \sin^2\theta
\end{aligned} \tag{4.15}$$

Substituting $\eta(t) = \frac{h}{2}\sin\theta$:

$$\begin{aligned}
F_x(t) = \frac{1}{4} \frac{\rho\, C_{\mathrm{s}}\, b\, \pi^2\, h^2}{T^2\, \sinh^2 kd} \Bigg[&\frac{h}{2}\sin\theta - z_{\mathrm{d}} + \frac{d+\frac{h}{2}\sin\theta}{2kd} \sinh\left(2kd\right) \\
&- \frac{d+\frac{h}{2}\sin\theta}{2kd} \sinh\left(2k(d+z_{\mathrm{d}})\frac{d}{d+\frac{h}{2}\sin\theta}\right)\Bigg] \sin^2\theta
\end{aligned} \tag{4.16}$$

Using this expression, time histories for wave forces acting on the topside can be established. These time histories can now, dependent on the size of the deck overhang, be phased differently compared to the wave forces acting on the load bearing structure, i.e. the jacket.

4.6.2 Derivation of deck force time history using Vinje method and Airy theory

Horisontal particle velocity $u_{\mathrm{w}}(z,t)$ according to Airy theory as given in Equation 4.14 is substituted in Equation 4.10, giving:

$$\begin{aligned}
F_x(t) &= \rho\, c \int_{A(t)} u_{\mathrm{w}}(z,t)\,\mathrm{d}A \\
&= \rho\, c\, b \int_{z_{\mathrm{d}}}^{\eta(t)} u_{\mathrm{w}}(z,t)\mathrm{d}z \\
&= \rho\, c\, b \int_{z_{\mathrm{d}}}^{\eta(t)} \left[\frac{\pi\, h}{T} \frac{\cosh\left(k(d+z)\frac{d}{d+\eta(t)}\right)}{\sinh kd} \sin\theta \right] \mathrm{d}z \\
&= \frac{\rho\, c\, b\, \pi\, h\, \sin\theta}{T\, \sinh kd} \int_{z_{\mathrm{d}}}^{\eta(t)} \cosh\left(k(d+z)\frac{d}{d+\eta(t)}\right)\mathrm{d}z \\
&= \frac{\rho\, c\, b\, \pi\, h}{T\, \sinh kd} \left[\frac{d+\eta(t)}{kd} \sinh\left(k(d+z)\frac{d}{d+\eta(t)}\right) \right]_{z_{\mathrm{d}}}^{\eta(t)} \sin\theta \\
&= \frac{\rho\, c\, b\, \pi\, h}{T\, \sinh kd} \cdot \frac{d+\eta(t)}{kd} \\
&\qquad \cdot \left[\sinh(kd) - \sinh\left(k(d+z_{\mathrm{d}})\frac{d}{d+\eta(t)}\right) \right] \sin\theta
\end{aligned} \tag{4.17}$$

Substituting $\eta(t) = h/2\sin\theta$:

$$\begin{aligned}
F_x(t) &= \frac{\rho\, c\, b\, \pi\, h}{T\, \sinh kd} \cdot \frac{d+\frac{h}{2}\sin\theta}{kd} \\
&\qquad \cdot \left[\sinh kd - \sinh\left(k(d+z_{\mathrm{d}})\frac{d}{d+\frac{h}{2}\sin\theta}\right) \right] \sin\theta
\end{aligned} \tag{4.18}$$

This is the expression for deck wave force variation with time. Again, this time history can be phased differently compared to the wave forces acting on the jacket in order to model different deck overhang.

4.6.3 Deck force time history using Stokes 5th order theory and drag or Vinje formulation

For the more complicated formulation of Stokes 5th order wave theory, numerical integration, i.e. a computer program, is required for calculation of wave-in-deck load time histories. The

program must calculate the depth profile for the particle velocity and acceleration for one given phase angle (coordinate relative to wave length). This must be repeated for every time step in order to create a velocity / acceleration time history. Summarising the velocities over the deck height and using the drag or the Vinje approach to calculated forces yields a corresponding force time history (for the deck only).

4.7 Comparison of load estimates

4.7.1 Comparison of loads established using simplified methods

The different formulations given in Sections 4.6.1 to 4.6.3 are compared using unit deck width:

- ⋆ Airy theory / drag formulation, $C_{\mathrm{d}} = 5.54$
- ⋆ Airy theory / Vinje formulation
- ⋆ Stokes 5th theory / drag formulation, $C_{\mathrm{d}} = 4.02$
- ⋆ Stokes 5th theory / Vinje formulation

The drag factors C_{d} for the drag formulations are chosen deliberately in order to calibrate the maximum force obtained by drag formulation to the maximum force obtained by Vinje formulation (for Airy- and Stokes waves, respectively). Note that these drag factors are considerably larger than the minimum requirement for cylinders suggested in the previous version of Class Note 30.5 by DNV (Det Norske Veritas, 1991). The newest version (Det Norske Veritas, 2000), however, suggest a value of 2π, which is more in line with the C_{d} values considered above. A wave with $h = 33$ m and $T = 15$ s is used, in a water depth of $d = 75$ m. A wave with these properties has a crest height of $\eta_{\max} = 16.5$ m according to linear theory. However, according to Stokes 5th order theory the crest height is 20.98 m. In order to do a relevant comparison, the deck freeboard z_{d} is chosen to give a deck inundation of 0.5 m for both wave theories. The surface profiles are illustrated in Figure 4.3.

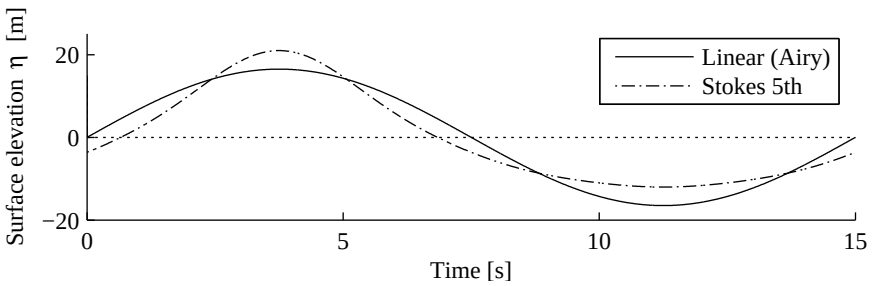

Figure 4.3: Surface elevation

The results are shown in Figure 4.4. Note that for each wave theory respectively, the Vinje approach does not differ notably from the drag formulation for the chosen C_{d}'s. For the Airy theory, the differences between the Vinje and the drag formulation vary from 0 to 2.7% through the time history, and for the Stokes theory the differences are 0 to 2%, see Figure 4.5.

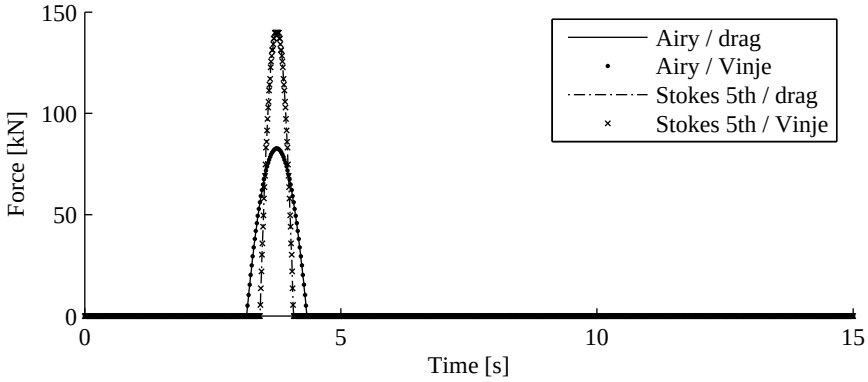

Figure 4.4: Comparison of simplified wave-in-deck calculations, wave-in-deck impact force

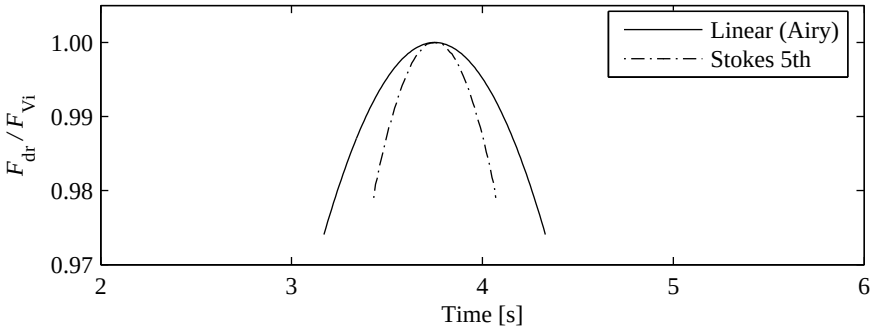

Figure 4.5: Drag force divided by Vinje force

Although the chosen C_{d} is smaller when using Stokes 5th order theory, the maximum force is considerably larger than for Airy theory. This is due to the higher crest velocity. On the other hand, because of the steeper crest, the Stokes case has a shorter lasting load impact history.

Equivalent drag factor as a function of time can be obtained by solving $F_{\mathrm{dr}} = F_{\mathrm{Vi}}$ with respect to C_{d}. The result is shown for Airy theory and Stokes 5th order theory respectively in Figure 4.6. Using Airy theory, $C_{\mathrm{d,eq}}$ varies between 5.54 and 5.69, whereas for Stokes 5th order theory $C_{\mathrm{d,eq}}$ varies from 4.02 to 4.10.

With the small differences between the drag and the Vinje approach in mind, the question of which formulation to use — drag or momentum — becomes less important. Instead, the

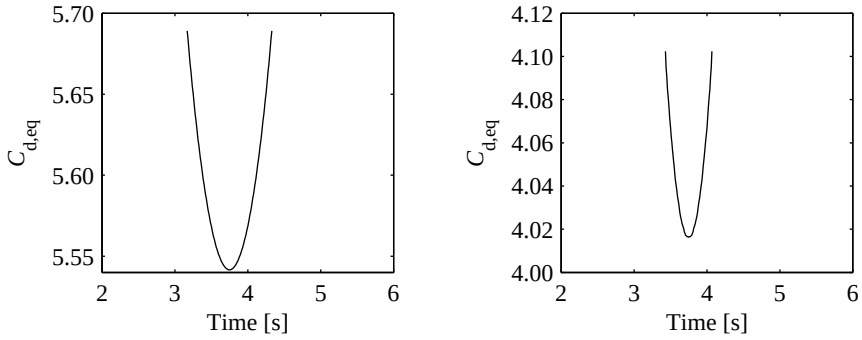

(a) $C_{\mathrm{d,eq}}$ Airy theory (b) $C_{\mathrm{d,eq}}$ Stokes 5th order theory

Figure 4.6: Equivalent drag factors for drag formulations

relevant question becomes which drag factor to use, alternatively which definition of rate of mass to use, $\mathrm{d}m/\mathrm{d}t = \rho\, u_{\mathrm{w}}$ or $\mathrm{d}m/\mathrm{d}t = \rho\, c$.

4.7.2 Simplified methods compared to computational results reported by Iwanowski et al. (2002)

This section documents comparison of force time histories obtained by the simplified methods described in Section 4.6 with reported force time histories computed with more advanced methods. Note that the methods in Section 4.6 include forces on the front wall only.

Only Stokes 5th order theory will be used, since linear (Airy) theory is not really applicable for the waves relevant for wave-in-deck forces. Based on the conclusion in the last paragraph of Section 4.7.1, it is chosen to calculate the wave-in-deck force time history in two different ways:

- ⋆ Traditional momentum approach with $\mathrm{d}m/\mathrm{d}t = \rho\, u_{\mathrm{w}}$ (identical to drag formulation with $C_{\mathrm{d}} = 2$), in the following denoted *Mom*, + Stokes 5th order theory
- ⋆ Momentum formulation with $\mathrm{d}m/\mathrm{d}t = \rho\, c$ (Vinje approach), in the following denoted *Mom-Vinje*, + Stokes 5th order theory

Iwanowski et al. (2002) presented and compared wave-in-deck load time histories calculated by use of different software. Three programs, of two different types, were used :

- ⋆ Analytical methodologies; PLATFORM program by Dr.Kaplan utilising momentum displacement and Morison equation
- ⋆ Computational fluid dynamics (CFD) technique; FSWL-2D and FLOW-3D programs using finite difference algorithms to solve the Navier-Stokes equation and volume of fluid (VOF) method to describe the free surface flow.

The results from the PLATFORM program were used as reference values when comparing the different methods.

The calculations were carried out for a 100 years design wave for the Ekofisk field in the North Sea with the characteristics $h = 24.3$ m, $T = 14.5$ s and $d = 80$ m. The crest height is, using Stokes 5th order theory, calculated to be $\eta_{\max} = 14.32$ m. Calculations were carried out for both Airy and Stokes 5th order waves with FSWL-2D and FLOW-3D, as well as by the PLATFORM program, which is based on Airy waves modified by Wheeler stretching. The Airy waves used in FSWL-2D and FLOW-3D programs are not modified by e.g. Wheeler stretching, and therefore give unrealistically large particle velocities in the crest. Only the results arising from the use of Stokes 5th order wave theory are considered herein.

The three cases reported by Iwanowski et al. are used for the purpose of comparison, comprising two different deck layouts; one simple box and one model of the deck of Ekofisk 2/4 C platform. The simple box is analysed for two inundation levels; 2 m and 4 m, whereas the 2/4 C deck is analysed for 1.5 m inundation.

Simple box, 2 m inundation

The wave forces were calculated for a simple box being 30 m wide (normal to the wave propagation direction) with wave inundation 2 m (Iwanowski et al., 2002). The Iwanowski force histories are compared to the force histories calculated in the present project in Figure 4.7.

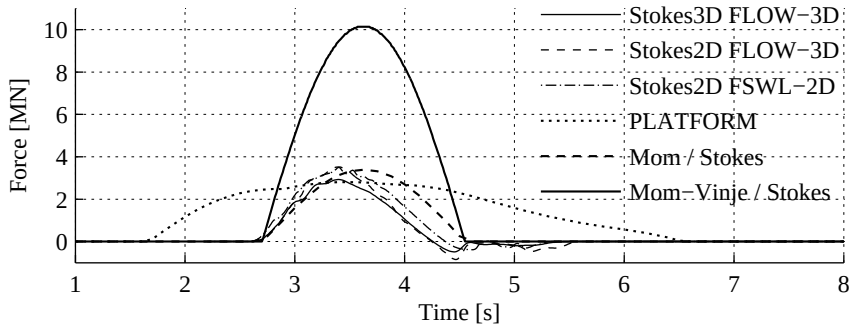

Figure 4.7: Comparison of simplified load calculations and Iwanowski results for simple box, inundation 2 m

The forces calculated by Iwanowski et al. for the Stokes wave show all quite similar trends. The start and end time for the forces are essentially the same and the maximum values range from 2.8 MN to 3.5 MN. The maximum force calculated by PLATFORM agrees well with the maximum force calculated using CFD technique, but the load history has a considerably longer duration due to the longer crest for Airy wave. The Vinje formulation yields a maximum total of 10.14 MN. This is considerably larger than the values computed by Iwanowski

et al..The explanation could be that Vinje's formula assumes that the horisontal water momentum is being stopped by the deck while some water particles in practice are being distorted upon impact with the deck. The 'Mom' formulation, however, has a maximum force of 3.4 MN which agrees well with the Iwanowski results. The shape of the impulses are similar, however the CFD-results are somewhat skewed towards the start time, while the simplified approaches by their nature produce symmetric force histories.

Simple box, 4 m inundation

For an inundation of 4 m, the Iwanowski force histories are compared to the force histories calculated in the present project in Figure 4.8.

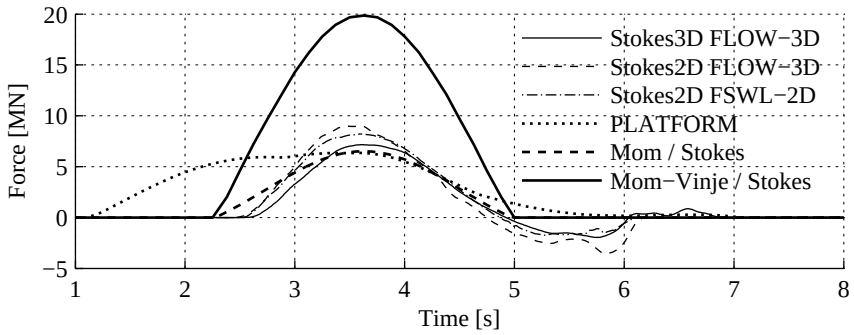

Figure 4.8: Comparison of simplified load calculations and Iwanowski results for simple box, inundation 4 m

The trends are the same as for an inundation of 2 m, except that the force magnitudes are larger. Again, the Vinje approach overestimates the maximum force (19.9 MN) considerably compared to the CFD-results (7-9 MN for FLOW-3D and FSWL-2D, 6.35 MN for PLATFORM) and the drag formulation (6.5 MN).

Simplified 2/4 C deck

Iwanowski et al. calculated the wave loads for a simple deck consisting of a lower box measuring 42.6 m x 30 m x 1.5 m centrally attached to an upper box measuring 53.1 m x 42 m x 10 m (all measures given as length x width x height, where width is measured normal to the wave heading). The wave inundation is 1.5 m, i.e. reaching but not entering the 'floor' of the upper box. A deck width of 30 m is therefore used for calculation of loads by simplified methods.

The PLATFORM program and drag formulation with $C_{\mathrm{d}} = 2$ seem to agree well for the maximum force value, but PLATFORM yields again a much longer impulse duration, see Figure 4.9. The CFD methods compute larger peak forces, which agrees better with the

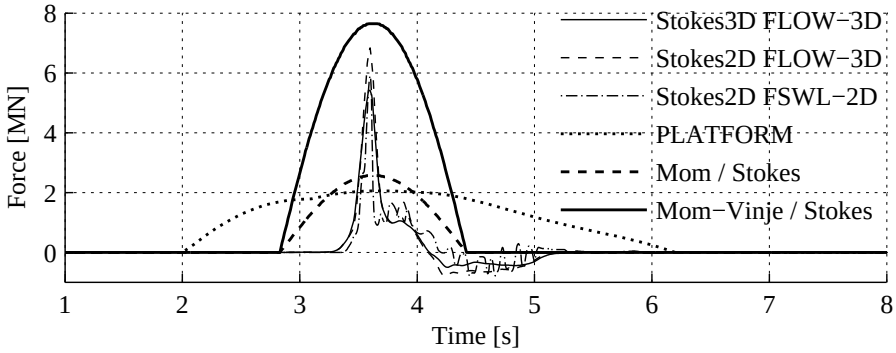

Figure 4.9: Comparison of simplified load calculations and Iwanowski results for simplified 2/4 C deck, inundation 1.5 m

Vinje formulation. The CFD techniques are able to compute the local fluid flow in the corner between the lower and the upper box more accurately. Water is trapped in this corner, with the high peak as a result. The simplified methods used in the present project are, as already mentioned, only able to predict symmetric force histories on the front wall.

A sharp peak characterises the CFD results, where the load within half a second rapidly increases from zero to maximum and decreases to about 1/5 of the maximum force. Thereafter the force further decreases more slowly within about half a second to zero, or temporarily somewhat below zero.

Summary

Clearly, if using the CFD results reported by Iwanowski et al. as a basis for validation, the simplified methods presented herein are not able to accurately predict wave-in-deck load histories. However, a representative load history for a simple hull or box type of deck can probably be produced, see Figures 4.7 and 4.8. It is, however, always important to consider the objective of the analyses. For detailed (re-)analyses meant to document the performance of actual structures, simplified methods are not adequate.

4.8 Available experimental data for wave-in-deck loading

4.8.1 Introduction

Wave-in-deck forces are sensitive to the size of the wave inundation, i.e. crest height. During experiments with regular waves, the crest height of measured waves may vary much more

than the wave height (Sterndorff, 2002). When comparing measured and numerically predicted data, it is therefore important to pay explicit attention to crest heights, not only the wave heights.

'Gulf of Mexico related' experiments reported by Finnigan and Petrauskas (1997) have been used to calibrate the API procedure and the Chevron procedure. Deck loads are reported at only one time instant per experiment, assumed to be the time of the maximum load. This coincides well with the fact that the API and the Chevron procedures aim at estimating maximum forces for static structural analysis. Due to lack of information on time variation, the results from these experiments are considered unsuitable for validation of the simplified methods described in the present work (however, maximum values calculated by use of API formulation are given in Table 4.3).

Results from experiments carried out at the Large Wave Channel (*der Grosse Wellenkanal*) at Forschungszentrum Küste in Hannover are published by Sterndorff (2002). The experiments comprise wave force time histories on typical offshore deck elements, both single elements and element groups, and focus has been on the details of the loading process. However, since no results are published for complete deck models, the results are not considered in the present work.

Early in 2002, model tests at scale 1:54 were carried out at Marintek in Trondheim in connection with a possible late life production scenario for the GBS platform Statfjord A (Stansberg et al., 2004). Global deck loads and local slamming loads were, amongst others, measured. The results from the model tests have been interpreted in a confidential report from Marine Technology Consulting AS to Statoil (Statoil, 2002), and recommendations are given regarding which time histories to use for wave-in-deck slamming load when carrying out structural analyses of Statfjord A in case of seabed subsidence possibly caused by reduced reservoir pressure. The recommendations from these experiments are attended to in the following.

4.8.2 Experiments at Marintek for Statfjord A (Statoil, 2002)

The Statfjord A experiments were carried out for two water depths: 150.1 and 151.6 m, corresponding to 0.5 and 2.0 m inundation for the 10 000 years crest of 21.7 m. The impact forces relating to this crest in these two water depths were estimated to be 75 MN and 105 MN respectively. These values were recommended for reassessment of Statfjord A.

In order to determine a representative load time history, a selection of measured time histories was investigated. For 150.1 m water depth, only measured force time histories with maximum force between 50 and 100 MN were considered, in total 31 time histories. In the same manner, only time histories having maximum forces ranging from 80 to 125 MN were investigated for a water depth of 151.6 m, this left 22 time histories.

In Table 4.1, the recommended horisontal maximum forces $F_{\mathrm{d,max}}$ and the force at the kink F_{k} (see Figure 4.12) from the Statfjord experiments are shown, together with the computed results from Iwanowski et al. (2002, note that only the results obtained by Stokes wave and FLOW-3D program in 3D mode are shown).

Table 4.1: Reported horisontal wave-in-deck loads

Reference	Iwanowski	Statoil	Statoil
Type of results	CFD 2/4 C deck	Experiments	Experiments
Wave	100 years	10 000 years	10 000 years
Inundation	1.5 m	0.5 m*	2.0 m*
Deck width	30 m	83.6 m	83.6 m
$F_{\mathrm{d,max}}$	5.4 MN	75 MN	105 MN
Pressure due to $F_{\mathrm{d,max}}$**	0.12 MN/m^2	1.79 MN/m^2	0.63 MN/m^2
F_{k}	N/A	30 MN	35 MN

*Note that the inundation is calculated from *undisturbed* wave crest height

**On the inundated area

Besides the fact that neither the inundation level nor the deck width are the same, there are several reasons that the numbers in Table 4.1 cannot be directly compared:

1. Statfjord A is a GBS platform with a huge base supporting large diameter columns. Both the presence of the base as well as the reflection of waves from the columns result in amplification of the incoming wave. Stansberg et al. (2004) indicate approximately 20% amplification of the wave height compared to a (undisturbed) regular 30 m wave with periods of some 16.5 s. Wave-in-deck loads are reported as a function of the crest height for the *undisturbed wave*, however they are actually generated by an *amplified wave*. As a consequence of this, the real inundation is greater than the value reported by Statoil (2002) or the above Table 4.1. In fact, some waves that in undisturbed condition do not enter the deck do also, due to amplification over the base, generate loads.

   This may explain the small increase in load, and the corresponding reduced water pressure on the inundated area, for the 2.0 m inundation case in the Statoil experiments compared to the 0.5 inundation case. Now considering the increase in load caused by the increased inundation; the 1.5 m increase in inundation corresponds to the load being increased by 30 MN. The pressure cause by this increase is $30/(1.5 \cdot 83.6)$ MN/m^2 = 0.24 MN/m^2. This measure might be a better indication of the water pressure caused by a wave that is not subject to amplification, which is the case for waves acting on jacket platforms.

   Ekofisk 2/4 C (which is the structure investigated by Iwanowski et al.) is a jacket platform, for which the wave amplification due to the presence of the structure itself is negligible. Obviously, the load generated by the amplified wave crest for Statfjord A cannot therefore directly be compared to the load on the deck of the jacket platform.

2. The Iwanowski results are obtained for a *100 years wave*, whereas the Statoil experiments were carried out in order to find the force time history for a *10 000 years wave*. The former has smaller particle velocity in the crest, and this is obviously reflected in the calculated forces. NORSOK N-003 (1999) recommends the 10 000 year design wave height to be 25% larger than the 100 year wave height. This leads to, for southern North Sea conditions (see Section 4.2), an increase in the crest particle velocity

of some 35%. Assuming that the particle velocity enters square into the load, a 10 000 years Ekofisk wave is estimated to give a pressure on the inundated area of 0.22 MN/m^2. This value corresponds well with the pressure calculated in item 1.

3. The definition of *crest front steepness* used during interpretation of the Statfjord experiments is $s = \eta_{\max}/(c \cdot (0.25\ T)) = 4\eta_{\max}/L$. For the 100 years wave used by Iwanowski this steepness formulation gives $s = 0.18$. From the waves generated during the Statfjord experiments, about 3/4 have crest front steepness larger than 0.3. Thus the majority of the waves forming the background for the estimate of wave-in-deck force for Statfjord A are considerably steeper than the wave used by Iwanowski.

The general trend for the global deck load is that the normalised time history for the horisontal slamming load consists of three lines as shown in Figure 4.10. It is characterised by a steep linear rise to maximum force, a steep linear decrease to about 0.4 times the maximum value, and finally a less steep but still linear decrease to zero. The durations for the three phases are 0.54 s, approximately 0.5 s and 2.1 seconds respectively. These duration values are representative for the two water depths and corresponding inundation levels reported by Statoil (2002).

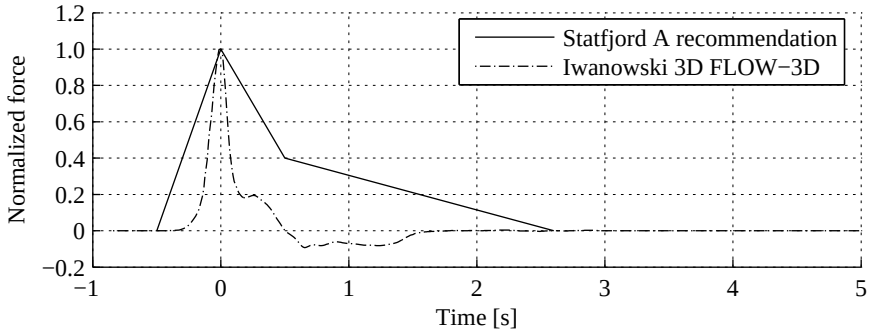

Figure 4.10: Normalised horisontal wave-in-deck load history, trend from experiments (Statoil, 2002) and computational results (Iwanowski et al., 2002)

It should be noted that this force time history represents a number of experiments in which the numerical values of both force and duration differ considerably. However, the three-line-trend is seen in most of the experiments. A single experimental wave-in-deck force time history reported by Grønbech et al. (2001) supports this finding. This time history was recorded at the deck during model tests of Ekofisk 2/4 C. The three-line-trend is also seen in Iwanowski et al. (2002) where CFD technique is used to calculate wave-in-deck forces on a simplified platform deck, see Section 4.7.2 and Figure 4.10.

4.9 Vertical loads

Till now, only horisontal forces have been considered. However, a few of the previously referred publications have treated vertical force time histories as well, that is to say Statoil (2002) and Iwanowski et al. (2002).

In the Statfjord A wave tank experiment, vertical forces were measured and interpreted (Statoil, 2002). Recommendations for wave-in-deck forces in the form of reference forces (max. and min.) and time history shape for reassessment of Statfjord A GBS were given.

The recommended design values for maximum positive vertical forces for water depths $d = 150.1$ m and $d = 151.6$ m are 67 and 80 MN, respectively, i.e. somewhat smaller than the horisontal forces (referred in Section 4.8.2). The minimum force, which is negative (suction), is about 50 - 60% of the value of the maximum force. Note that these values relate to a deck width of 83.6 m. There is however, considerable uncertainty related to these numbers, and they should only be regarded a rough but indeed representative outline of the observed wave-in-deck force. These recommended forces for design are shown in Table 4.2 together with the forces from the CFD results reported by Iwanowski et al. for 30 m deck width. Note that only the CFD results obtained by Stokes 3D FLOW-3D are used.

Table 4.2: Reported vertical wave-in-deck forces

Reference	Iwanowski	Statoil	Statoil
Type of results	CFD 2/4 C deck	Experiments	Experiments
Inundation	1.5 m	0.5 m	2.0 m
Deck width	30 m	83.6 m	83.6 m
$F_{\mathrm{v,max}}$	41 MN	67 MN	80 MN
$F_{\mathrm{v,min}}$	-22 MN	-35 MN	-50 MN

The time history for vertical forces recommended for the reanalysis of Statfjord A, which originates from the Statoil experiments, is characterised by a linear rise from zero to maximum, with a duration of about 0.5 seconds, thereafter a linear drop to minimum force, which is negative, in about 1 second. Finally, the force increases linearly from its minimum to zero in about 3.5 seconds. This recommendation is given on background of 31 measured load histories, to which a representative load time history was fitted by means of least square method. The Statoil recommendation is compared to the Iwanowski CFD results for the simplified 2/4 C deck in Figure 4.11. Both time histories are normalised against their respective maximum force. The time variation of the vertical force is essentially the same for these two independent studies, of which one is theoretical and the other one experimental.

It can be seen that vertical wave-in-deck forces are of considerable magnitude, and act both upwards and downwards. They result in deck uplift loads, and they give additional compressive forces in platform legs which can lead to different failure modes than the platform originally was designed to sustain.

Vertical forces should therefore be considered during reassessment of offshore platforms. *In order to limit the present work, vertical loads are not included in this study.* It is stated,

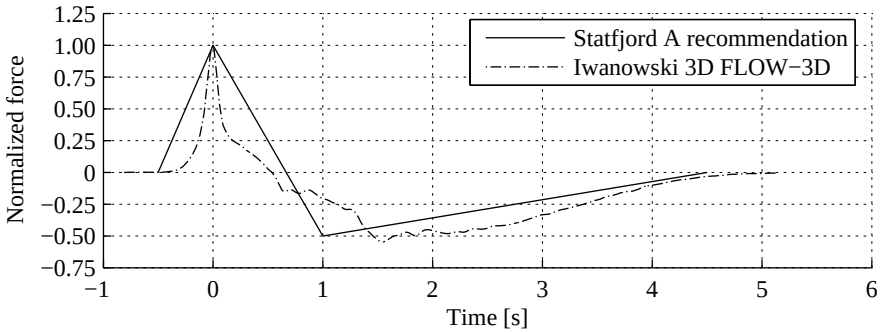

Figure 4.11: Normalised vertical wave-in-deck force history, trend from experiments (Statoil, 2002) and computational results (Iwanowski et al., 2002)

though, that vertical forces are important in the further study of structural response to wave-in-deck forces.

4.10 Representative load histories

A number of authors have given recommendations for the pre-history duration to be included in the wave time history prior to the extreme wave, see the paragraph on this matter on page 24.

4.11 Discussion

Time history for horisontal wave-in-deck loading

It is concluded that most support is found for the trilinear type of (load) time history referred to in Section 4.8 and Figure 4.10. *It is chosen to use this load history in the present project*, however, for practical reasons the start time is rounded to the nearest 1/10 (Figure 4.12).

The load time history is described in full by this time history and a reference load, taken as the maximum load $F_{\mathrm{d,max}}$ corresponding to the inundation level in question.

The validity range of the time history in terms of inundation is uncertain. In the reference report Statoil (2002) this type of time history is reported to be representative for inundation levels 0.5 m and 2.0 m. However, these levels are calculated based on an undisturbed wave, whereas the real inundation will be larger due to amplification of the incoming wave over the gravity base. It is therefore anticipated that the time history is more representative for larger inundations, and less for smaller inundations. However, for the reason of simplification and due to the limited amount of data, the time history is used regardless of inundation level in this work.

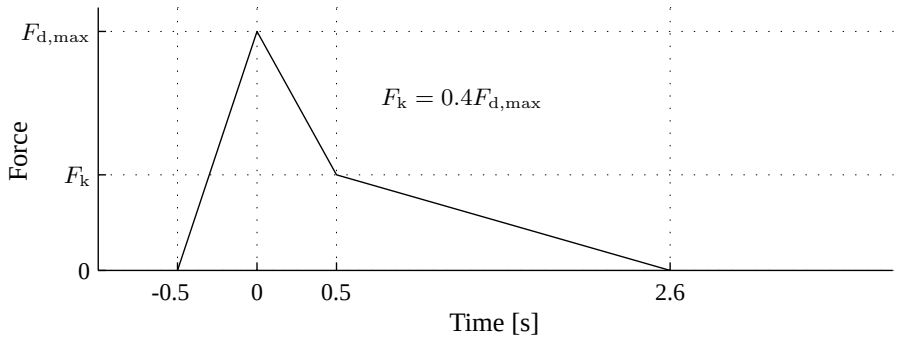

Figure 4.12: Time history to be used in analyses in the present work

Reference load $F_{\mathrm{d,max}}$ for horisontal wave-in-deck loading

It should be noted that the load level for an actual wave-in-deck situation depends on the local geometry of the deck, which is unknown in the present project. It is, however, decided to use the regression curves obtained from the experimental data during the Statfjord A experiments as a basis. The reported experimental data for $d = 151.6$ m are split into 3 different *crest front steepness* ranges. The linear regression curve for steepness $s < 0.3$ is used (Stansberg et al., 2004, Figure 9) herein, since the Stokes 5th order waves relevant for the present study will belong to this range (note that crest front steepness expressed as $s = \eta_{\max}/(c \cdot (0.25\,T)) = 4\eta_{\max}/L$ is defined different than traditional wave steepness). From the uppermost subfigure of Figure 9 in the given reference, the variation of wave-in-deck force with inundation is found to be 10.9 MN/m. Dividing by the deck width of 83.6 m leaves 0.1304 MN/m^2. In order to ommit the influence of the wave amplification over the gravity base, the load is set to zero for a wave crest that just reaches the underside of the deck. Larger wave crests generate forces that are proportional to the inundation with a factor of 0.13 MN per m inundation for unit deck width:

$$F_{\mathrm{d,max}} = 0.13\, s_{\mathrm{d}}\, b \quad \text{[MN]} \tag{4.19}$$

This equation is related to a 10 000 years wave at the Statfjord field in the northern North Sea, with a corresponding crest particle velocity. It is assumed that the particle velocity enters square into the equation for the force. This is true for both a drag formulation and a general momentum formulation (but not for the Vinje formulation). In order to allow for adjustment of the force to represent the actual wave and to include current, Equation 4.19 is modified as follows:

$$F_{\mathrm{d,max}} = 0.13\, s_{\mathrm{d}}\, b\, \frac{(u_{\mathrm{cs}} + u_{\mathrm{ce}})^2}{u_{\mathrm{ref}}^2} \quad \text{[MN]} \tag{4.20}$$

where u_{cs} is the water particle velocity at the wave crest, u_{ce} is the current velocity and u_{ref} is the particle velocity representing the 10 000 years wave at the Statfjord field, which by use

of Stokes 5th order theory is found to be 9.8 m/s. In Table 4.3 the reference (i.e. maximum) values for the deck-force calculated by this method for several different scenarios are listed. Also included is the maximum force calculated by Iwanowski et al. (2002) for the simplified Ekofisk 2/4 C deck, as well as force values calculated according to the Vinje formulation and the drag formulation recommended in the API regulations with $C_{\mathrm{d}} = 2.0$ (API recommends a drag factor between 1.2 and 2.5, where 2.0 corresponds to end-on or broadside loading of moderately equipped deck). The forces are calculated for a deck width $b = 30$ m and an inundation $s_{\mathrm{d}} = 1.5$ m.

Table 4.3: Wave-in-deck forces for a case with $s_{\mathrm{d}} = 1.5$ m and $b = 30$ m

Reference	Wave type	h [m]	T [s]	d [m]	c [m/s]	u_{cs} [m/s]	u_{ce} [m/s]	$F_{\mathrm{d,max}}$ [MN]
Statfjord A	*10.000 yr., measured (basis)*	*36.5*	*15.8*	*150*		*9.80*	*0*	*5.87*
Statfjord A	100 yr., Eq. 4.20	29.0	14.4	150		8.25	0	4.16
Statfjord A	10.000 yr., API **	36.5	15.8	150		9.80	0	4.43
Statfjord A	10.000 yr., Vinje formulation	36.5	15.8	150	26.17	9.80	0	11.83
Statfjord A	10.000 yr. + curr., Eq. 4.20	36.5	15.8	150		9.80	1	7.13
Statfjord A	10.000 yr. + curr., API *	36.5	15.8	150		9.80	1	5.38
Iwanowski	100 yr., calc. Iwanowski **	24.3	14.5	80		N/A	N/A	5.40
Iwanowski	100 yr., Eq. 4.20	24.3	14.5	80		7.57	0	3.50
Iwanowski	100 yr., API *	24.3	14.5	80		7.57	0	2.64
Iwanowski	100 yr., Vinje formulation	24.3	14.5	80	22.22	7.57	0	7.76
SNS***	100 yr., Eq. 4.20	26.0	15.5	75		8.17	0	4.08
SNS	100 yr., API *	26.0	15.5	75		8.17	0	3.08
SNS	10.000 yr., Eq. 4.20	33.0	16.0	75		11.28	0	7.77
SNS	10.000 yr., API *	33.0	16.0	75		11.28	0	5.87
SNS	10.000 yr., Vinje formulation	33.0	16.0	75	23.75	11.28	0	12.36
SNS	10.000 yr. + curr., Eq. 4.20	33.0	16.0	75		11.28	1	9.21
SNS	10.000 yr. + curr., API *	33.0	16.0	75		11.28	1	6.96

* using Cd = 2.0, corresponding to moderately equipped deck, end on / broad side loading

** Calculated by use of CFD methods (Iwanowski et al., 2002)

*** SNS denotes a location in the southern North Sea

Table 4.3 illustrates that the API recommendations with $C_{\mathrm{d}} = 2.0$ in general yields lower forces than Equation 4.20. The fraction is about 75%. If increasing the C_{d} to 2.5 (end-on or broadside loading of heavily equipped / solid deck), the fraction would be 75% $\cdot 2.5/2.0 = 94\%$, i.e. Equation 4.20 would still yield conservative forces compared to the API regulations.

It can be shown that the API formulation with $C_{\mathrm{d}} = 2.65$ yields the same result for $F_{\mathrm{d,max}}$ as Equation 4.20 (API formulation is given by Equation 4.1 with $u_{\mathrm{w}} = u(\eta_{\mathrm{max}}) = u_{\mathrm{cs}} + u_{\mathrm{ce}}$).

The Vinje formulations yields larger forces compared to the other methods. The explanation could be that the formulation is based on the conservative assumption of *total* loss of momentum at impact.

The maximum force calculated according to Equation 4.20 for the Iwanowski wave is 3.50 MN. This is considerably smaller than the value calculated in the reference paper for this deck (5.4 MN). However, the API formulation yields even smaller forces — only about 50% of the value calculated by Iwanowski et al.

Conclusion

The above discussion is considered to support Equation 4.20 being a rough but reasonable estimate for horisontal wave force on deck for an example jacket structure. This equation together with the force history given in Figure 4.12 is sufficient to establish wave-in-deck load histories for analyses of (jacket) structures subjected to wave-in-deck loads.

Chapter 5

Time domain analyses

5.1 Introduction

This chapter comprises the static and dynamic analyses of two different jacket platforms, denoted ‘DS’ and ‘DE’, subjected to extreme wave loading including wave-in-deck loading. The analyses are carried out using the nonlinear finite element program USFOS.

The objective is to investigate the dynamic effect of wave-in-deck loading, and to compare the resulting dynamic performance with that obtained using static pushover analysis, the latter being state-of-art for (re)assessment of jacket structures. Static behaviour is in general a simplification of a dynamic behaviour — a simplification that cannot always be justified, and of which knowing the implications is essential.

General information relevant for both analysed structural models is given in Section 5.2, whereas the finite element analyses of jacket models ‘DS’ and ‘DE’ are treated in Sections 5.3 and 5.4, respectively. Section 5.5 deals with response acceleration levels and acceptable acceleration values, and Section 5.6 comprises a discussion related to the results obtained in this chapter.

5.2 General

5.2.1 Limitations

In order to simplify, damping is not included in the calculations in the present doctoral thesis, and all initial values of displacement, velocity and acceleration are set to zero. These matters are discussed at the end of this chapter.

Relative velocity of the structure compared to the water particle velocity is not accounted for in the calculations of drag forces. NORSOK N-003 (1999) recommends that for structures

experiencing small motions — i.e. motion amplitudes not exceeding the member diameters — hydrodynamic damping should be included in the form of an equivalent viscous damping rather than by using relative velocity. The draft ISO/CD 19902 (2001) states that relative velocity shall not be included for fixed structures, but that hydrodynamic damping may be included through a viscous damping term in the dynamic equilibrium equation. Since (viscous) damping is not included in the analyses herein, no hydrodynamic damping is included. The consequence is an overestimation of the response. It is further referred to the discussion regarding the omission of damping in Section 5.6.

5.2.2 Integration of the equation of motion

In USFOS the HHT-α method (Hilber et al., 1977) for numeric time integration is adopted (Søreide et al., 1993). Predictor-Corrector time domain integration is used with integration parameters controlling high frequency damping $\alpha = -0.3$, $\beta = 0.423$ and $\gamma = 0.800$. Convergence criterion for iterations is set to 10^{-5}.

5.2.3 Analyses

For each model and its respective load scenarios three analyses are carried out:

1) Traditional static pushover analysis — the state-of-art method used to assess the integrity of existing structures. Pushover analysis provides the static load deformation curve, also called resistance curve (R_{f}), including initial elastic stiffness and ultimate capacity for the load pattern corresponding to the given wave data and water depth. Note that this is the type of analysis referred to as static analysis in the following, as opposed to dynamic analysis.

2) Time domain analysis without effects of inertia and damping, elastic — an elastic static time simulation, in the following denoted quasi-static analysis or static time domain simulation. The purpose of this analysis is to know the elastic static displacement of the reference point at the deck at any time, i.e. for varying load distribution and intensity. This has obviously no meaning anymore if / when the (static) wave load reaches and exceeds the static capacity.

3) Full dynamic time domain analysis — providing response time histories of e.g. displacement, velocity and acceleration as well as base shear and overturning moment.

5.2.4 Loading - general

In order to set the structure in deformed equilibrium position corresponding to permanent static loads (self weight, weight of equipment and live loads etc.), these load must be applied in a static manner — i.e. without dynamic effects — before the dynamic analysis is initiated. It is chosen to apply the permanent loads without dynamic effects during one second before

the dynamic analysis is initiated. Thereafter, the dynamic, i.e. environmental, loads are applied and the dynamic effects (inertia, and damping if included) are 'switched on'. In this way, structural motion arising from loads that by nature are static is avoided. This first 'static' second is not included in any of the presented results in this chapter.

Details of loading that are unique to the different models are described in connection with the description of the actual structural model. All details of the structural models are given in the input files attached in Appendix C.

Self weight

The self weight of all members is generated automatically. In addition, a number of node masses representing e.g. deck weight and weight of equipment are applied.

Wind

No wind loads are included in the analyses.

Hydrodynamic loads

Wave load on jacket structure The wave load is specified by wave theory, wave height (h), period (T), direction, phase and water depth (d). The wave load histories are generated by USFOS. Stoke 5th order theory (Skjelbreia and Hendrickson, 1960) is used, and the structure is subjected to one wave cycle. The load histories are based on a wave with and annual probability of exceedance of 10^{-4} (a 10 000 years wave), and the water depth is varied in order to represent different levels of subsidence. Tide and storm surge is assumed to be included in the different water depths.

Wave load on deck structure The topic of wave-in-deck forces is thoroughly discussed in Chapter 4. The wave-in-deck loads are applied in accordance with the conclusions from that chapter. The time history is repeated in Figure 5.1. The reference force values $F_{\mathrm{d,max}}$ are given under the section of each structural model, respectively.

The peak horisontal wave in deck load is assumed to occur when the wave crest is at the deck front wall. The deck force is applied to the top of the deck legs and distributed equally, meaning 1/4 to each leg.

Current The current speed at the *still water level* is set to 1.0 m/s, and there is further provided a depth profile of current velocity for each analysed model, see Sections 5.3.3 and 5.4.3. Since the depth profiles do not extend above the still water level, current velocity values in the wave crest are extrapolated by USFOS. This results in e.g. varying surface current through the wave period for both analysis models 'DS' and 'DE'.

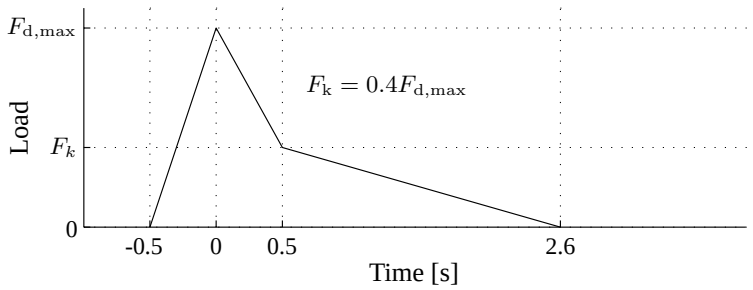

Figure 5.1: Time history for wave load on topside structure for use in analyses in the present work

Buoyancy The jacket legs, pile sleeves, risers and caissons are flooded (see Appendix C for details). Buoyancy will be calculated for non-flooded elements if submerged. The buoyancy loads are included in the self weight load case, which means it is applied as a permanent, static load.

5.3 Jacket 'DS' - description and analyses

5.3.1 General

The model jacket 'DS' is based on a static linear analysis model of an existing North Sea jacket, provided by Statoil. The jacket from which the analysis model originates is a four legged jacket, supported by sixteen ø 1.828 m (72 inch) piles driven to approximately 76 m below the seabed. It has a K-brace configuration, five risers and four caissons. The area between the deck legs is 22 m x 22 m. The water depth at the field is 70 meters. See e.g. Figures 5.3 and 5.8.

The model supplied by Statoil consisted of input files to be used in FE analysis program SESAM. This model was converted to UFO-format, which can be read by USFOS. During the conversion, the model was somewhat simplified:

- ⋆ The deck structure was replaced by a simple but stiff dummy deck structure.
- ⋆ For simplicity, the platform legs were fixed to the seabed for all six degrees of freedom.

In the analysis model, the lowest deck is located at $z = z_{\mathrm{d}} = 95.5$ m. The model coordinate system is right-handed and has its origin at the seabed. In order to simulate subsidence of seabed and the structure, the z-value of the sea surface is set differently from one analysis (load) scenario to another.

SI-units are used in the analyses (s, m and kg).

The deck is assumed to be 47 m x 47 m. The model structure has a first natural period T_{n} of 1.60 s.

All input files for the structural analyses can be found in Appendix C. These include all information in detail.

5.3.2 Materials and cross sections

Two different materials have been used, one typical steel material and one dummy material with higher stiffness but very small density. The latter is used for the deck dummy structure, and the former for the rest of the structure. The yield stress is 355 N/mm^2.

A number of different circular cross sections are used, having diameters ranging from 0.457 m to 3 m and wall thickness from 0.020 m to 0.095 m. For details, see Appendix C.

5.3.3 Loads

Self weight

The generated weight of all members sums up to $3.78 \cdot 10^6$ kg. In addition, a node mass of $11 \cdot 10^6$ kg representing the deck weight and weight of equipment and personnel is applied at node 40041 (which is located in the center of gravity of the deck structure).

Hydrodynamic loads

The reference force values for the wave-in-deck force are given in Table 5.1.

Table 5.1: Model 'DS'; wave-in-deck forces to be used in analysis

Water depth d [m]	Crest $\eta_{\max}$ [m]	Deck inund. s_{d} [m]	$F_{\mathrm{d,max}}$ [MN] (Fig. 5.1)	F_{k} [MN] (Fig. 5.1)
75.0	20.75	0.25	2.406	0.9623
76.0	20.68	1.18	11.15	4.461
77.0	20.62	2.12	19.71	7.884
78.0	20.56	3.06	28.03	11.21
79.0	20.50	4.00	36.09	14.43
80.0	20.44	4.94	43.89	17.56
81.0	20.38	5.88	51.45	20.58

Note that for $d = 75 - 77$ m the maximum total force will occur at approximately $t = 5$ s — i.e. not simultaneously with the peak wave-in-deck load at $t = 4.1$s — due to the small magnitude of the wave-in-deck load (see also Figure 5.2). In the following, the maximum total load and the maximum static displacement for these water depths are referred to the maximum values occurring around $t = 5$ s.

The hydrodynamic load histories including wave-in-deck load and current load are shown in Figure 5.2 for the different analysed water depths. The wave crest is at the deck front wall at $t = 4.1$ s. The force peaks at this time instant represent the wave-in-deck forces, which increase in size as the water depth and the corresponding deck inundation increase.

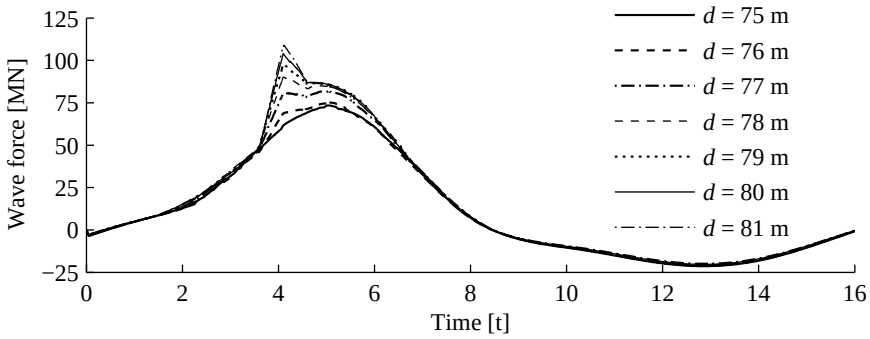

Figure 5.2: Hydrodynamic load history generated for model 'DS' for wave height $h = 33$ m and wave period $T = 16$ s for different water depths

If ignoring the wave-in-deck force, there are only minor variations in the magnitude of the horisontal wave load as the water depth increases.

The load histories are based on a 33 m high (10 000 years-) wave with a period of 16 s. The water depth is varied in order to represent different levels of subsidence; $d = 75, 76, \cdots, 81$ m.

The following current profile is used in the analyses:

z [m]	Velocity scaling factor
0.0	1.00
-25.0	0.52
-85.0	0.28

Between these specified values of the velocity scaling factor linear interpolation is used. Above still water level $z = 0$ m the scaling factor is extrapolated.

5.3.4 Results from analyses

In the dynamic analyses the time steps used range from 0.005 s to 0.05 s. This corresponds to $0.003T_{\mathrm{n}}$ and $0.03T_{\mathrm{n}}$, respectively.

The displacement is recorded at a reference point at deck level, node 40041 with coordinates $x = -1.084$ m, $y = -1.107$ m and $z = 99.000$ m. This is the node at which the mass representing the weight of deck and equipment is applied.

Performance based on pushover analysis Figure 5.3 illustrates the different static collapse modes for model ‘DS’ for two different inundation levels. As the water depth increases and the deck load increases accordingly, a larger part of the total force has to be transferred from the deck through the braces in the upper bay and down into the lower part of the jacket structure. These braces are originally not intended to transfer large wave loads, and will therefore represent the ‘bottlenecks’ when the platform is exposed to large wave-in-deck loads.

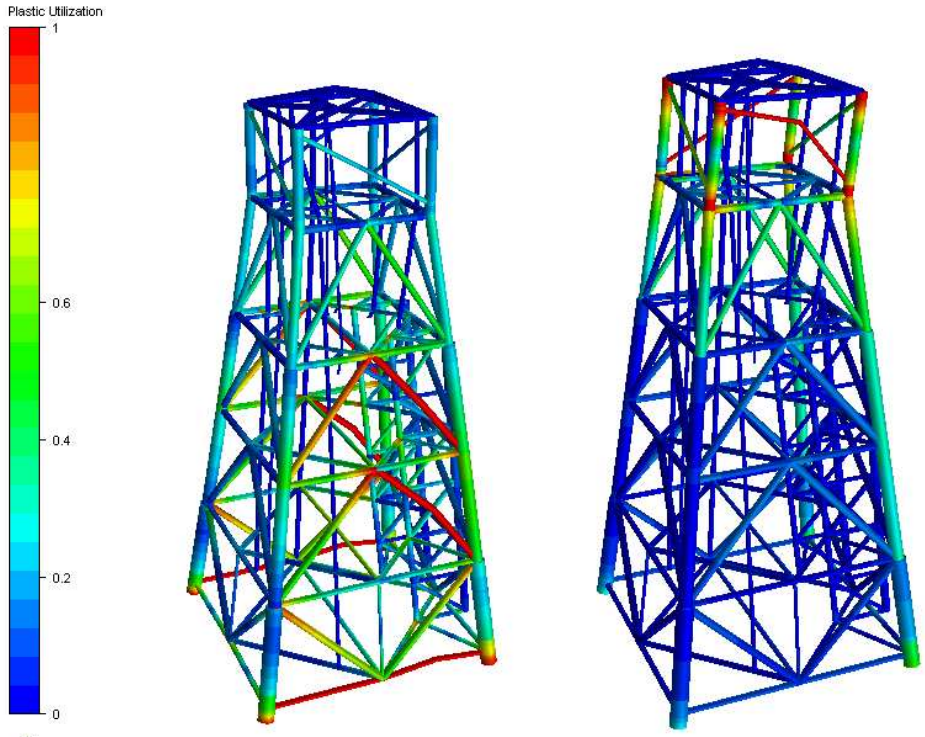

(a) Depth 75 m / inundation 0.25 m (b) Depth 81 m / inundation 5.88 m

Figure 5.3: Static collapse modes for different water depths and corresponding inundation levels

The static ultimate capacity for base shear is 160.2 MN for 0.25 m deck inundation, while it is dramatically reduced to 79.8 MN for 5.88 m inundation. This change in capacity and stiffness curve can be seen in Figure 5.4, in which the static stiffness curve is compared for the load pattern following from different water depths. Further, the clear decrease in initial elastic stiffness with increasing deck inundation should be noted from the figure. This is due to the fact that a larger part of the forces acts on the deck level, having a larger effect on the displacement of the reference point in the deck.

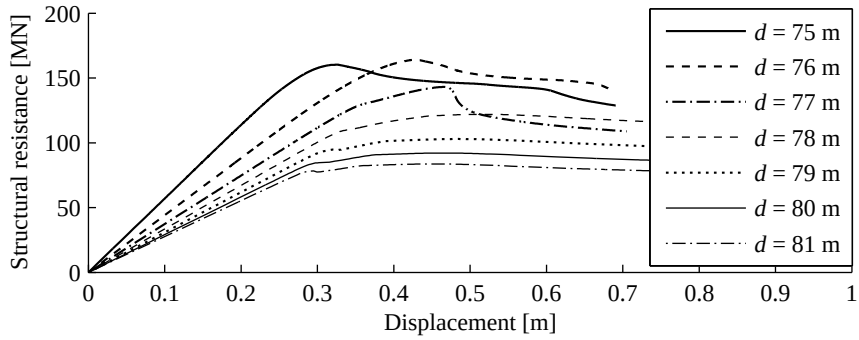

Figure 5.4: Model ‘DS’: Stiffness curves for in terms of base shear (BS) for different water depths

Performance based on time domain analysis The resulting displacement histories for different water depths (and corresponding inundation levels) are given in Figure 5.5.

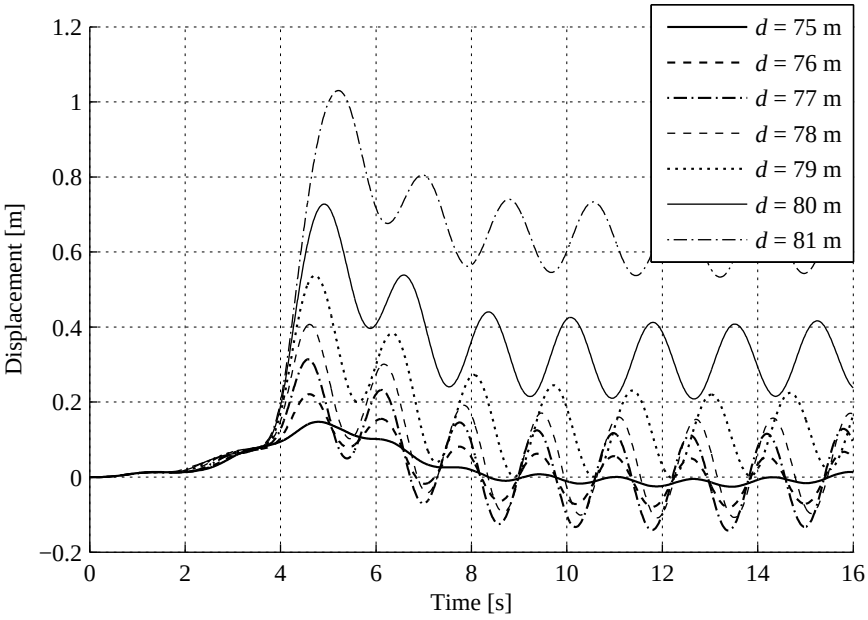

Figure 5.5: Model ‘DS’: Dynamic displacment response for different water depths / inundation levels

The displacement response does, as expected, increase with increasing subsidence / inundation. This increase gets more pronounced as the wave load approaches and exceeds the static ultimate capacity. However, where pushover analyses indicate a total collapse for the peak in

the load time history (i.e. the ultimate capacity is exceeded at least once during the load history), dynamic time domain simulations compute a large but limited maximum displacement.

All analysed cases have a certain dynamic amplification of the response (15% - 54%), even where the wave load is less than half the static capacity, see Table 5.2. The dynamic amplification is calculated by comparing the dynamic maximum response to the *nonlinear* static maximum displacement, as obtained by interpolation of maximum wave load on the resistance curve. An example of dynamic response vs. *elastic* static response is given in Figure 5.6. For this water depth the elastic static response is approximately equal to the real nonlinear static response.

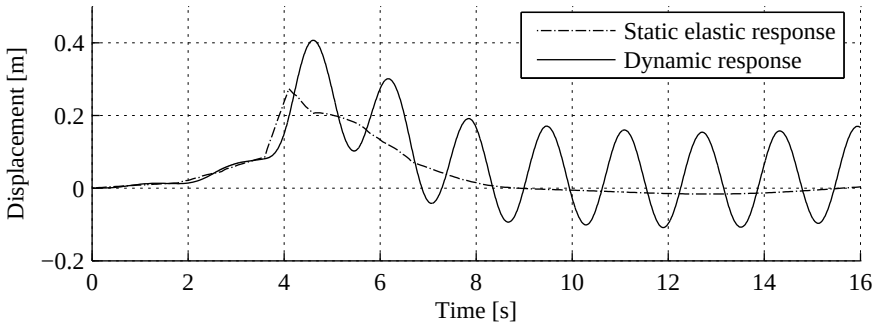

Figure 5.6: Model 'DS': Dynamic and static response response history, water depth 78 m / inundation 3.06 m

In Figure 5.7 time histories of accelerations are given for three chosen analysis cases, the ones having smallest and largest water depth and inundation, and the one with largest resulting accelerations.

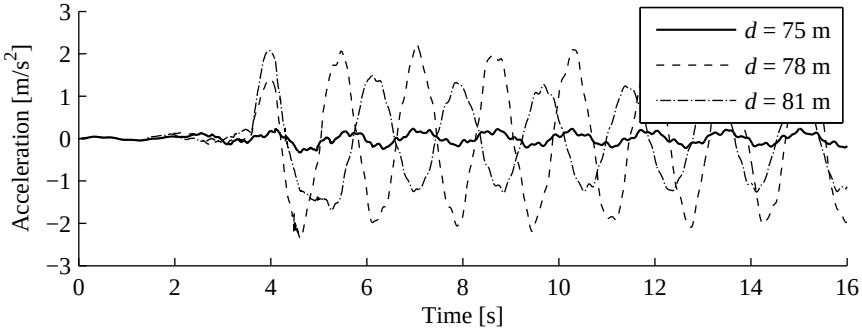

Figure 5.7: Acceleration response for different water depths / inundation levels

For $d = 75$ m the response is purely elastic, and the accelerations are relatively small, maximum acceleration is 0.23 m/s^2. The case with $d = 78$ m has moderate acceleration during the first cycle (1.4 m/s^2), but the largest accelerations in the following cycles is obtained for

this case, $\ddot{u} = 2.2$ m/s^2. During the first cycle, the $d = 81$ m case has the largest acceleration, $\ddot{u} = 2.1$ m/s^2. Thereafter the accelerations for this case are reduced to approximately 1.3 - 1.5 m/s^2. The implications of these levels of acceleration are further discussed in Section 5.5.

The reason that accelerations in cycles following the first cycle are reduced for deeper water than 78 m, is that the larger loads lead to a significant degree of plastic material behaviour resulting in damping of the motion response.

The term 'dynamic capacity' (to sustain transient loads) cannot be uniquely defined or interpreted because dynamic response depends on both the structural natural period and the frequencies of the external load (see Figure 2.1). Intuitively, one might interpret 'dynamic capacity' as the most onerous load history that the structure is able to sustain. However, the fact that the structure can sustain a given load history does not give any information about the response to other load histories.

For practical purposes, a *displacement limit* related to one or more given reference points in the structure may quantify the capacity to withstand dynamic load. If the load history leads to exceedance of this displacement, the capacity is by definition exceeded. An absolute maximum allowable limit for the displacement can be decided from structural considerations, e.g. a given fraction of the displacement corresponding to total collapse. However, there might be other limitations on the displacement, e.g. safety limitations. There is little help in having the platform deformed but standing, if rupture of pipes could lead to explosions and subsequent fires. The platform must also, in a deformed state, be able to withstand subsequent (large) waves, this is the ALS (accidental limit state) requirement in structural standards.

Static pushover performance versus dynamic performance The main results from the analyses are shown in Table 5.2 in numerical form. Elastic load limit and corresponding displacement are extracted at *first yield*, regardless of the location of the yielding element.

Table 5.2: Model 'DS'; results from non-linear static and dynamic analyses, $h = 33$ m, $T = 16$ s

Water depth [m]	Deck inund. [m]	Total wave load BS[a] [MN]	First yield BS[a] [MN]	First yield u [m]	Stat. cap. BS[a] [MN]	Stat. cap. u [m]	Maximum displ. Stat.[b] [m]	Maximum displ. Stat.[c] [m]	Maximum displ. Dyn. [m]
75.0[d]	0.25	73.4	95.3	0.16	161.1	0.33	0.13	0.13	0.15
76.0[d]	1.18	75.1	90.0	0.20	165.0	0.43	0.17	0.16	0.22
77.0[d]	2.12	81.7	85.3	0.22	143.7	0.47	0.22	0.22	0.31
78.0	3.06	90.2	82.0	0.24	122.4	0.52	0.27	0.27	0.41
79.0	4.00	97.9	76.0	0.24	103.3	0.49	0.35	0.32	0.54
80.0	4.94	103.9	66.7	0.22	92.4	0.48	N/A	0.36	0.73
81.0	5.88	108.9	59.7	0.21	83.9	0.46	N/A	0.40	1.03

[a] BS = base shear

[b] Displacement for given load without dynamic effects (interpolated on the resistance curve)

[c] Elastic displacement

[d] Max. total load, subsequent to max. wave-in-deck load, see page 67

At 0.25 m inundation, the total wave load is smaller than the elastic load limit of the structure. The dynamic maximum displacement does not exceed the displacement corresponding to the elastic load limit, and no yielding is detected during dynamic analysis for this case. At the next two inundation levels, s_{d}= 1.18 m and s_{d}= 2.12 m, the wave load peak is still smaller than the elastic load limit, however the elastic limit displacement is exceeded during dynamic analysis due to dynamic amplification, meaning that the structure experiences some yielding.

At 3.06 m inundation the total wave load exceeds the elastic load limit. At 4.00 m inundation the dynamic maximum displacement is larger than the displacement corresponding to static ultimate capacity. At s_{d}= 4.94 m and s_{d}= 5.88 m (corresponding to water depths of 80 m and 81 meters, respectively) the load peak in the dynamic analyses exceeds the static ultimate capacity of the structure. Static displacement, in the meaning time domain displacement excluding dynamic effects, is theoretically infinite for these last two cases. However, the displacements estimated from dynamic analyses are 0.728 m and 1.030 m, respectively. If these displacements are admissible, the platform can by definition withstand these load histories, and thus it can withstand these particular waves that generate loads exceeding the static ultimate capacity.

Plots of the structure with yielding zones highlighted show that the collapse modes are similar during dynamic and pushover analyses for all analysed water depths respectively. An example is given in Figure 5.8.

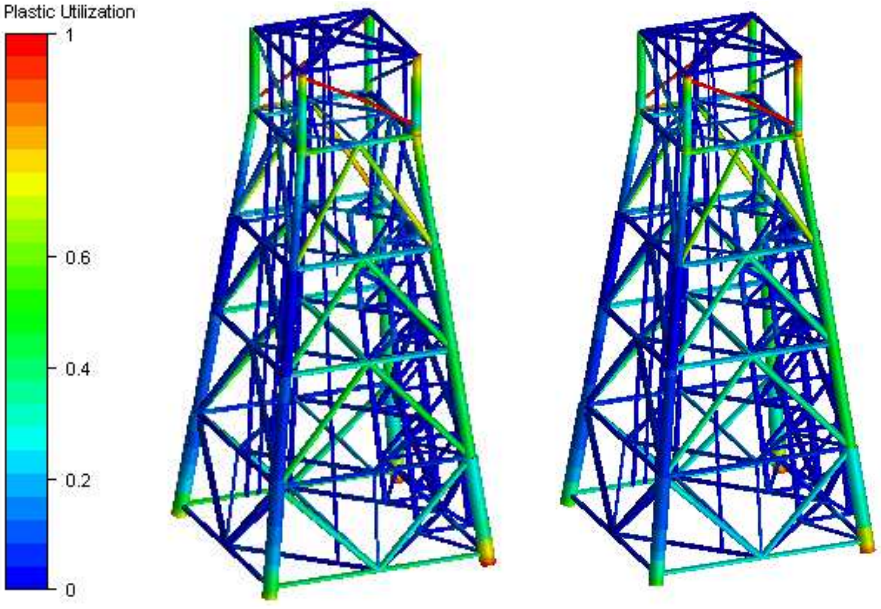

(a) Pushover case (b) Dynamic case

Figure 5.8: Structural plastic state at dynamic max. displacement, water depth 78 m

Contribution from stiffness and inertia In Figure 5.9 the variation of the structural restoring forces and the inertia forces is illustrated. The response is clearly dominated by restoring forces, but for $d = 78$ m and $d = 81$ m it can be seen that around the time of maximum response the inertia force amplifies the response.

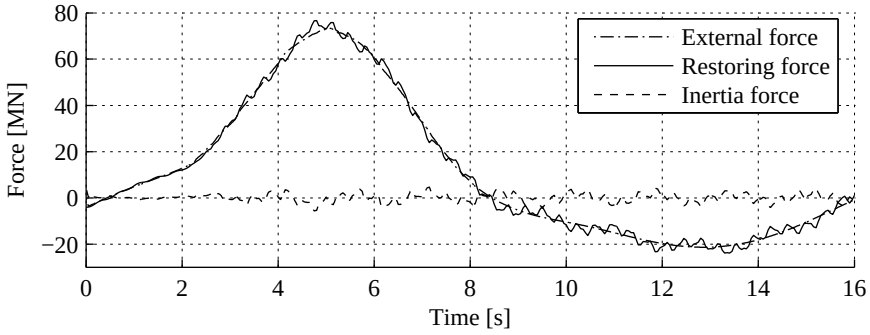

(a) $d = 75$ m

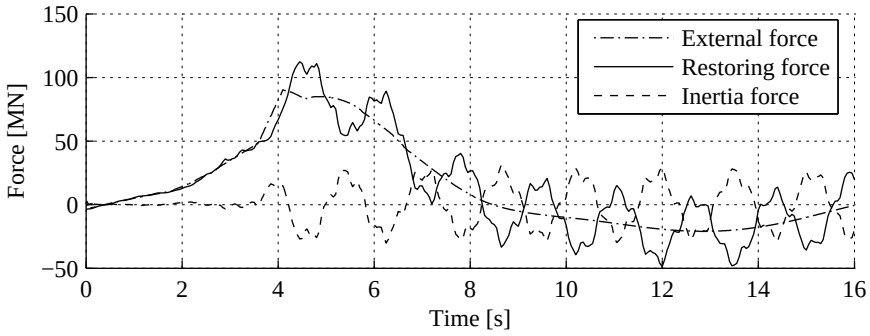

(b) $d = 78$ m

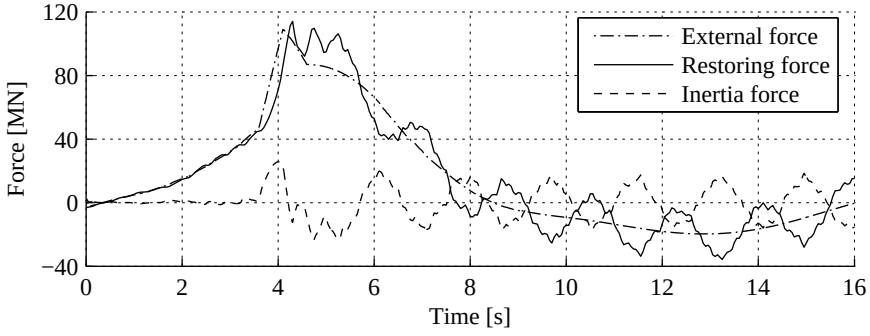

(c) $d = 81$ m

Figure 5.9: Model 'DS': Contributions from structural restoring forces and inertia forces

For $d = 75$ m / $s_{\mathrm{d}} = 0.25$ m, the inertia response is insignificant, a fact that supports the use of quasi-static considerations for jackets under regular wave loading not including topside impact.

5.4 Jacket 'DE' - description and analyses

5.4.1 General

This model is based on the dynamic analysis model of an existing North Sea jacket, provided by SINTEF. 'DE' is X-braced and has bucket foundations. It has 4 legs and the area between the deck legs is 20 x 20 meters. The jacket is originally designed for a water depth of 70 meters.

The lower deck beams are located at $z = z_{\mathrm{d}} = 25.75$ m, and the mudline at $z = -70$ m.

The model coordinate system, which is right-handed, has its origin 70 m above the seabed. This elevation corresponds to the sea surface for the design water depth. Note that the sea surface will be lifted to positive z-values for the analyses in the present thesis in order to simulate subsidence of seabed and structure.

SI-units are used (s, m and kg).

The bucket foundations are modeled by use of linear spring-to-ground elements, identical to the original computer model provided by SINTEF.

The received model consisted of an input file for the NIRWANA computer program. The model has been manually converted to UFO-format, i.e. not by any conversion program. The following modifications have been done to the structural model:

- ⋆ The section names are changed, however every element has the same section type
- ⋆ A minor structural part was removed, this included 3 nodes, the masses applied to these nodes and 7 elements.
- ⋆ A dummy deck structure is added to attract wave loading on deck.

The deck is not modeled in detail in the computer model, but a size of 40 x 40 meters is used for this work. It is assumed that the deck is centered on the deck legs with an overhang of 10 m on all sides. The structural model has a first natural period of 1.18 s.

The input files to the structural analyses with detailed information can be found in Appendix C.

5.4.2 Materials and cross sections

A number of different materials have been used. The materials are identical to the ones used in the original NIRWANA model. They include one typical steel material and one dummy

material with zero density, as well as several steel materials with different densities used to include contents of piping and risers. The yield stress is 355 N/mm^2.

The cross sections that are used are circular with diameters ranging from 0.215 m to 3.8 m and wall thickness from 0.005 m to 0.090 m.

For details, see Appendix C.

5.4.3 Loads

Self weight

The generated self weight of all members sums up to $2.7 \cdot 10^6$ kg. In addition, 11 node masses representing deck weight and a bridge are applied, in total approximately $10 \cdot 10^6$ kg.

Hydrodynamic loads

The reference values for the wave-in-deck forces are given in Table 5.3. Note that for $d = 76$ m the maximum total force will occur at $t = 5.1$ s — i.e. not simultaneously with the peak wave-in-deck load at $t = 4.9$ s — due to the small magnitude of the wave-in-deck load. The maximum total load and the maximum static displacement for this water depth are referred to the values at $t = 5.1$ s.

Table 5.3: Model 'DE'; wave-in-deck forces to be used in analysis

Water depth d [m]	Crest $\eta_{\max}$ [m]	Deck inund. s_{d} [m]	$F_{\mathrm{d,max}}$ [MN] (Fig. 5.1)	F_{k} [MN] (Fig. 5.1)
76.0	20.68	0.93	7.480	2.992
77.0	20.62	1.87	14.80	5.918
78.0	20.56	2.81	25.74	10.29
79.0	20.50	3.75	33.83	13.53
80.0	20.44	4.69	41.67	16.67
81.0	20.38	5.63	49.27	19.71

The hydrodynamic load histories including wave-in-deck load and current load are shown in Figure 5.10 for the different analysed water depths. The peak wave in deck load is taken to occur at $t = 4.9$ s, when the wave crest is at the deck front wall. The force peaks at this time instant represent the wave-in-deck forces, which increase in size as the water depth and the corresponding deck inundation increase.

If ignoring the wave-in-deck force, there are only minor variations in the magnitude of the horisontal wave load as the water depth increases.

The load histories are based on a 33 m high (10 000 years-) wave with a period of 16 s. Load scenarios based on water depths $d = 76, 77, \cdots, 81$ m are analysed.

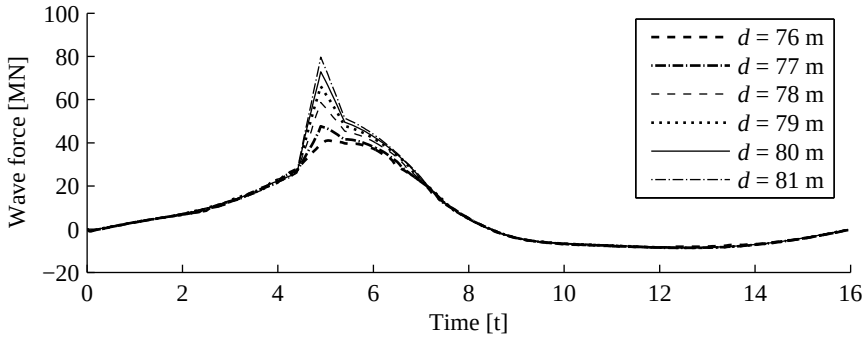

Figure 5.10: Hydrodynamic load history generated for model 'DE' for $H = 33$ m and $T = 16$ s for different water depths

The current profile used in the analyses is as follows:

z [m]	Velocity scaling factor
0.0	1.0
-50.0	0.3
-67.0	0.0
-70.0	0.0

Values of the scaling factor are extrapolated / interpolated above / below still water level $z = 0$ m.

5.4.4 Results from analyses

In the dynamic analyses the time steps used range from 0.001 s to 0.05 s. This corresponds to $0.0008T_{\mathrm{n}}$ and $0.04T_{\mathrm{n}}$, respectively. The tiny time steps have been necessary to capture all nonlinear incidents.

The displacement is recorded at a reference point centrally located at deck level — node 212 — which has coordinates $x = 30.000$ m, $y = -6.000$ m and $z = 25.75$ m.

Performance based on pushover analysis The static ultimate capacity for base shear show only minor variations, ranging from 83.8 MN to 86.3 MN (Figure 5.11 and Table 5.4). The largest capacity is found for a water depth of 78 m, corresponding to an inundation of 2.81 m. Whereas the ultimate capacity does not show any significant sensitivity to the load distribution (limited to those distributions analysed herein), the initial elastic stiffness clearly does. Similar to model 'DS', the latter is attributed to the fact that a larger part of the forces act on the deck level, having a larger effect on the displacement of the reference point in the deck.

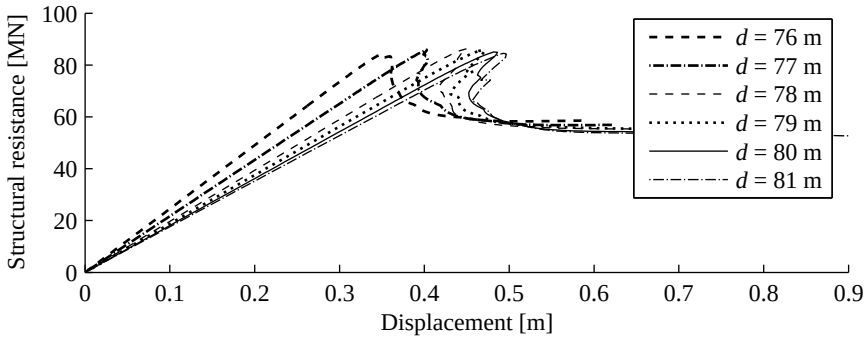

Figure 5.11: Model 'DE': Stiffness curves in terms of base shear (BS) for different water depths

All analysis cases show the same pre-collapse behaviour; linear elastic displacement followed by yielding that can be separated into three different stages. Firstly, a thin piping element (el. 1313, ca. elevation -42 m) at the bottom of the second bay from below yields. This is followed by yielding of a part of a tension brace (el. 1172, ca. elevation -45 m) in the lowest bay. This brace supports a vertical riser, and the yielding part is located between the jacket leg and the riser support. These two first yielding incidents are isolated incidents. The major part of the nonlinear global behaviour starts at 65 to 80% of the capacity, the largest fraction for the smallest inundation (Table 5.4). The degradation of the stiffness starts at and beyond this 'main yield', the former for the smaller inundations and the latter for the larger inundations. It is thus concluded that the behaviour is close to linear until close to the static ultimate capacity.

Table 5.4: Model 'DE'; results from non-linear static analyses $h = 33$ m, $T = 16$ s

Water depth [m]	Deck inund. [m]	Total wave load BS[a] [MN]	First yield BS[a] [MN]	First yield u [m]	Sec. yield BS[a] [MN]	Sec. yield u [m]	Main yield BS[a] [MN]	Main yield u [m]	Ult. cap. BS[a] [MN]	Ult. cap. u [m]
76.0[b]	0.93	41.11	33.77	0.136	48.48	0.196	68.62	0.278	83.83	0.347
77.0	1.87	47.69	25.01	0.114	44.71	0.205	67.57	0.310	85.91	0.403
78.0	2.81	58.71	20.03	0.100	41.60	0.210	63.49	0.321	86.31	0.450
79.0	3.75	66.18	18.10	0.095	40.06	0.212	61.18	0.325	85.65	0.467
80.0	4.69	72.86	16.88	0.092	39.07	0.214	58.90	0.324	85.05	0.482
81.0	5.63	79.66	16.06	0.090	38.34	0.216	55.80	0.316	84.52	0.494

[a] BS = base shear

[b] Max. total load, subsequent to max. wave-in-deck load, see page 76

It seems clear that model 'DE' has a relatively brittle behaviour when exposed to such load histories. The resistance curves are close to linear until the ultimate capacity is reached, followed by a significant drop in capacity combined with an elastic snap-back behaviour.

Figure 5.12 shows the static collapse modes for the smallest and largest inundation levels.

The collapse modes are not significantly different from each other. The compression braces in the 2nd and 3rd bay are the weak spots of this structure. X-brace configuration is normally considered to be redundant, but this presupposes horisontal braces at the intersection between the different X-levels, i.e. at the bottom and top of the X's, making the complete structure consisting of (stiff) triangles. With the present layout the X configuration is not redundant, as reflected in the resistance curves.

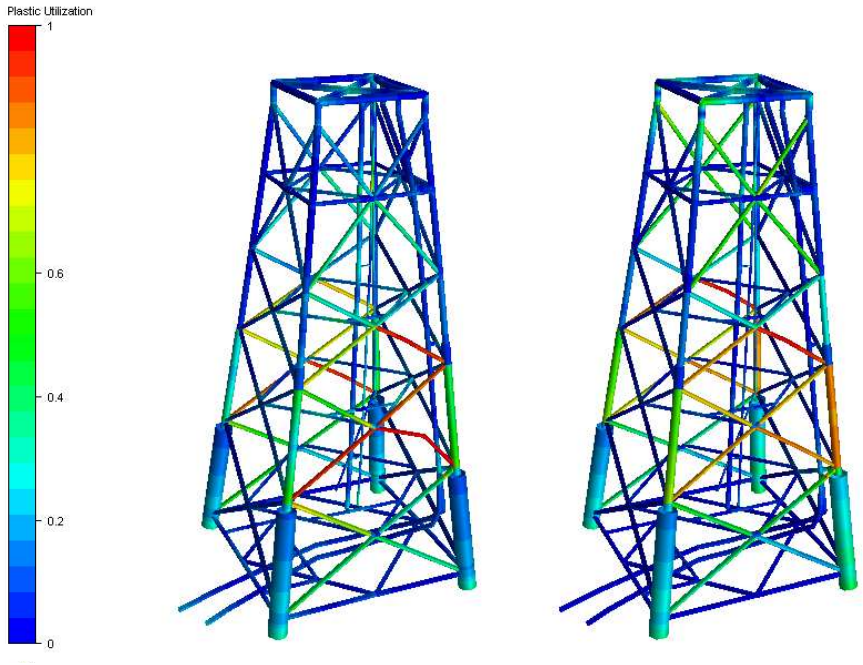

(a) Depth 76 m / inundation 0.93 m (b) Depth 81 m / inundation 5.63 m

Figure 5.12: Static collapse modes for different water depths and corresponding inundation levels

A brittle global behaviour might be acceptable if the structure is designed to a large level of reserve capacity, as is the case for the present structure. However, one should be aware that if one of the vital compression braces has reduced or lost capacity or has an initial deflection caused by some accidental loading, the structure's ultimate capacity might be considerably reduced compared to the intact condition.

Performance based on time domain analysis The resulting displacement histories for different water depths (and corresponding inundation levels) are given in Figure 5.13. It has not been possible to produce time domain analyses of acceptable numerical quality for water depths from 79.5 m and beyond, due to numerical instability. The largest depth analysed is therefore 79 m, corresponding to an inundation of 3.75 m. The brace configuration of the

model causes instability for responses resulting from loading above this level.

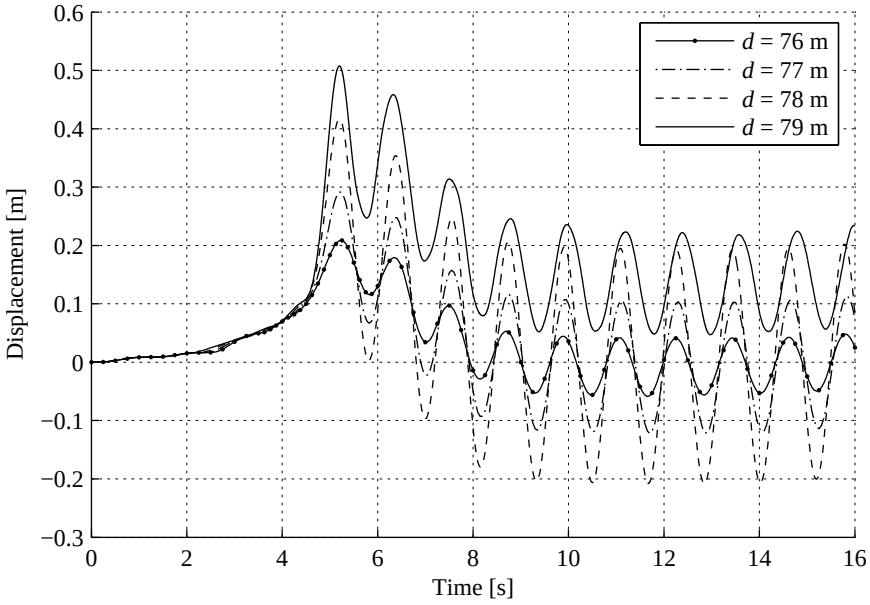

Figure 5.13: Model 'DE': Dynamic displacment response for different water depths / inundation levels

All dynamic analyses show positive dynamic amplification compared to the static nonlinear displacement, which is interpolated on the resistance curve for the maximum external load (Table 5.5). The amplification is in the range 24% to 46%. An example of dynamic amplification of the displacement response compared to the static *elastic* analysis results, which do not differ significantly from the static nonlinear results due to the linear brittle behaviour of the structure, is given in Figure 5.14 for $d = 78$ m.

The brittle nature of the 'DE' model results in unstable behaviour for load conditions having a peak exceeding some 80% of the static capacity. To the contrary, the ductile 'DS' model is able to remain (damaged but) intact even for wave load histories that for a limited time exceed the static capacity.

In Figure 5.15 time histories of accelerations are given for the four relevant analysis cases. For $d = 76$ m the response is close to purely elastic and the largest accelerations are approximately 1.5 m/s^2. At $d = 77$ m the acceleration peaks are 3.2 - 3.3 m/s^2, and for $d = 78$ m the peaks are rather close to 5.9 m/s^2. The last case, $d = 79$ m, has very irregular accelerations due to many plastic incidents. The largest acceleration value is negative, and is close to 6.1 m/s^2. This negative peak is followed by a positive peak of 4.8 m/s^2. Thereafter the acceleration peaks remain at $\pm$ 2 - 4 m/s^2, but are decreasing due to material damping. The implications of this level of acceleration are further discussed in Section 5.5.

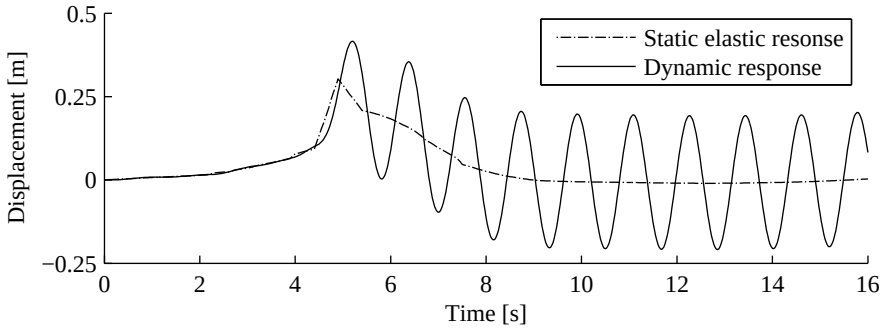

Figure 5.14: Dynamic and static response response history, water depth 78 m / inundation 3.06 m

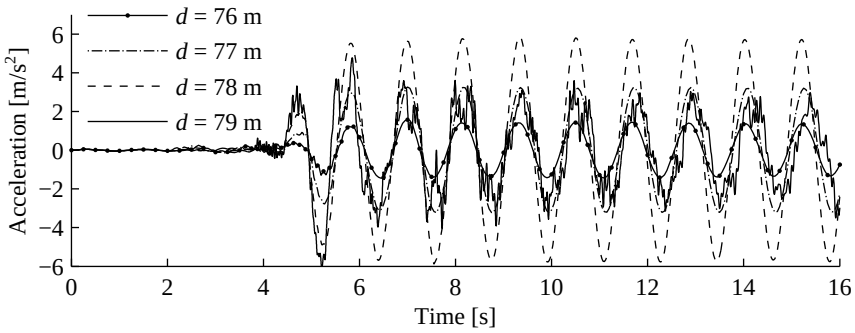

Figure 5.15: Acceleration response for different water depths / inundation levels

Static pushover performance versus dynamic performance Plots of the structure with yielding zones highlighted show that the collapse modes are similar during dynamic analysis and pushover analysis for all analysed water depths with one exception, namely the $d = 79$ m / $s_{\mathrm{d}} = 3.75$ m case. In this case, the maximum dynamic displacement corresponds to a post collapse displacement in the pushover analysis. This is reflected by the larger deflections of individual compression members for the pushover case as illustrated in Figure 5.16. It is interesting to notice that a displacement that according to pushover analysis corresponds to a post collapse condition and snap back behaviour can be obtained without structural instability during a dynamic analysis.

The main results from the analyses are shown in Table 5.5 in numerical form. Elastic load limit and corresponding displacement are extracted at *first yield*, regardless of location of the yielding element. Note that all analysed wave conditions result in load peaks exceeding the elastic load limit (first yield) of the structure.

At $d = 76$ m / $s_{\mathrm{d}} = 0.93$ m the only elements yielding are those corresponding to first and second yield as given in Table 5.4. The main nonlinear domain is not entered. The total wave

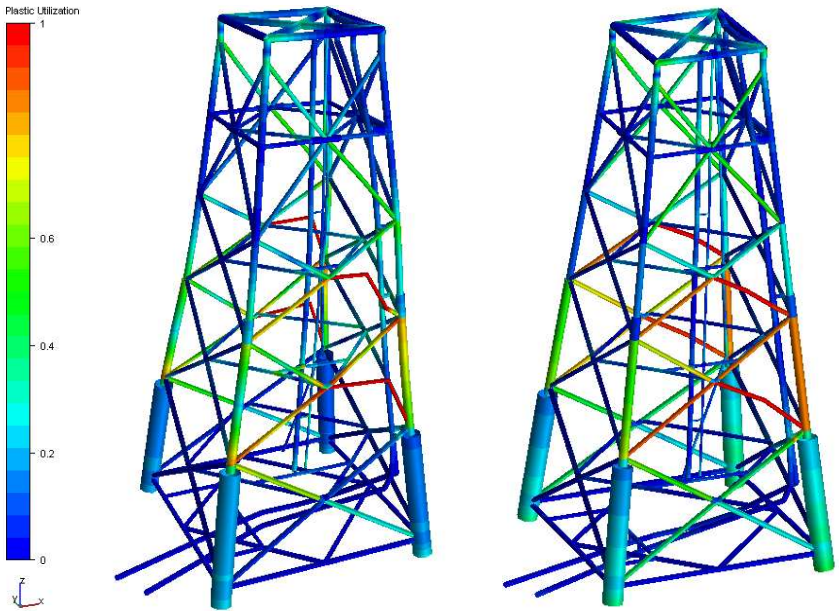

(a) Pushover case (b) Dynamic case

Figure 5.16: Structural plastic state at dynamic max. displacement, water depth 79 m

Table 5.5: Model ‘DE’; results from non-linear static and dynamic analyses , $h =$ 33 m, $T = 16$ s

Water depth [m]	Deck inund. [m]	Total wave load BS[a] [MN]	First yield BS[a] [MN]	First yield u [m]	Stat. cap. BS[a] [MN]	Stat. cap. u [m]	Maximum displ. Stat.[b] [m]	Maximum displ. Stat.[c] [m]	Maximum displ. Dyn. [m]
76.0[d]	0.93	41.11	33.77	0.14	83.83	0.35	0.17	0.17	0.21
77.0	1.87	47.69	25.01	0.11	85.91	0.40	0.22	0.22	0.29
78.0	2.81	58.71	20.03	0.10	86.31	0.45	0.30	0.30	0.42
79.0	3.75	66.18	18.10	0.10	85.65	0.47	0.35	0.36	0.51
80.0	4.69	72.86	16.88	0.09	85.05	0.48	0.40	0.41	N/A
81.0	5.63	79.66	16.06	0.09	84.52	0.49	0.46	0.46	N/A

[a] BS = base shear

[b] Displacement for given load without dynamic effects (interpolated on the resistance curve)

[c] Elastic displacement

[d] Max. total load, subsequent to max. wave-in-deck load, see page 76

load is smaller than the load corresponding to ‘second yield’ during pushover analysis. No plastic hinges are introduced during the dynamic analysis.

At the next inundation level, $d = 77$ m / $s_{\mathrm{d}} = 1.87$ m, the wave load peak exceeds the second yield pushover load, but not the ‘main yield’ load. The same is valid for the displacement

response — it does not exceed the main yield displacement limit. No plastic hinges are introduced.

For $d = 78$ m / $s_{\mathrm{d}} = 2.81$ m the wave load condition is similar to the previous described case; the wave load peak exceeds the second yield pushover load, but not the 'main yield' load. However, in this case the dynamic displacement response exceeds the 'main yield' displacement limit, and the structure experiences considerable yielding — but no plastic hinges.

The load generated for $d = 79$ m / $s_{\mathrm{d}} = 3.75$ m exceeds the main yield load limit, but not the ultimate capacity. The structural response enters into the nonlinear domain, and includes considerable yielding and several plastic hinges in the second and third bay.

Contribution from stiffness and inertia In Figure 5.17 the variation of the structural restoring forces and the inertia forces is illustrated. As for model 'DS', the response is dominated by the restoring forces. The inertia forces clearly amplify the response at its maximum around $t = 5.1$ s.

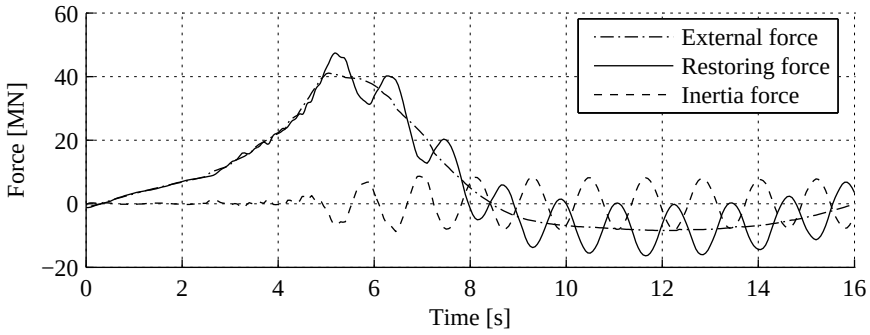

(a) $d = 76$ m

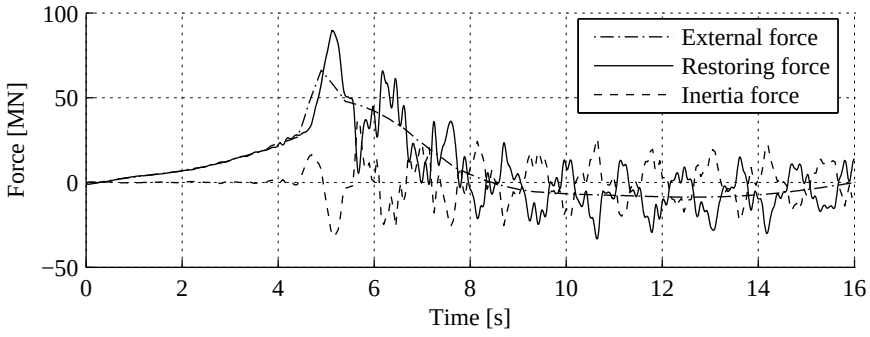

(b) $d = 79$ m

Figure 5.17: Model 'DE': Contributions from structural restoring forces and inertia forces

5.5 Acceleration levels

NS 4931 (1985) gives recommendations related to the sensitivity of human beings to low frequency horisontal vibrations in buildings and fixed offshore installations. For the first natural vibration frequency for jacket model 'DS', which is 0.63 Hz, the limit acceleration which an average human being will feel is given as approximately 0.017 m/s^2. For the same frequency, 0.0043 m/s^2 is given as a threshold value below which nobody will notice the vibrations. The acceptable acceleration level of the structure when performing non-routine or exacting work is approximately 0.19 m/s^2.

NORSOK S-002 (2004) provides acceptable acceleration limits for (human) exposure to continuous vibrations from machinery during a 12 hours working day. The recommendations are only given for vibration frequencies 1 Hz and above, thus recommendations for 1 Hz are considered herein. For areas that are normally unmanned, 2 m/s^2 is an upper limit of acceptable acceleration, whereas 0.05 m/s^2 is acceptable for process, utilities and drilling areas.

The accelerations calculated for model 'DS' are considerably larger than the 'comfort levels' indicated in NS 4931, see Figure 2.4. The magnitude is more in agreement with the upper acceptable limit for continuous vibrations in normally unmanned areas given in NORSOK S-002. All limit values are, however, related to operating situations, whereas wave-in-deck slamming is an extreme event. 2 m/s^2 acceleration corresponds to accelerating from 0 to 216 km/h in 30 seconds. In a car this is to be considered a considerable but not excessive acceleration, being less than half the acceleration relevant for the most powerful sports cars. As 'structural ground' acceleration it will, however, surely be experienced as a frightening event. A certain fright should be considered acceptable, in lieu of the fact that wave-in-deck loading is an accidental event. It is, though, a relevant question if the different equipment located on the platform is designed to sustain such accelerations, and — if required — can maintain operation. It is known that generators can 'trip' (stop temporarily) in case of large accelerations. Such an incident was e.g. observed on Sleipner A for a large wave impact on the platform legs (Gudmestad, 2005).

The acceleration response of model 'DE' is of considerably worse nature. A maximum of some 6 m/s^2, equal to 0 - 648 km/h in 30 s, is three times as much as the acceleration that 'DS' experiences. This is an extremely large acceleration, unacceptable even for accidental conditions.

5.6 Discussion

Dynamic performance vs. static

It is important to be aware that the static ultimate capacity of a platform does not uniquely characterise the structural performance, neither does the load - displacement curve. The capacity depends on the load pattern, i.e. the distribution of external forces on the structure. Static ultimate capacity is, however, a unique and informative measure of nonlinear structural performance *when related to a given load distribution*. Dynamic performance should, on the

other hand, rather be evaluated against allowable displacements and accelerations at relevant locations in the structure *for each single load scenario*.

All the dynamic analyses carried out in this chapter show dynamic amplification compared to the static analyses. This corresponds to findings in HSE (1998). The amplification ranges from some 15% to some 54% (for water depth $d = 80$ m and $d = 81$ m for model 'DS' the term dynamic amplification does not give any meaning, since the wave load exceeds the static capacity).

The example model 'DS' has shown to be able to respond to dynamic (wave-in-deck) loads with short duration peaks exceeding the static ultimate capacity of the structure with only limited deformations, as opposed to global collapse. In other words, for the situations analysed herein dynamic considerations are beneficial and important, as they increase the confidence in the structural performance compared to static considerations.

'DS' is a ductile structure, see Figure 5.4. To the contrary, model 'DE' can be regarded a brittle structure (Figure 5.11). Brittle structures are structures with negligible ductile reserves beyond the static ultimate capacity. Such structures may, when subjected to dynamic loads, collapse for load histories with maxima considerably smaller than static capacity, due to dynamic amplification. In that case, dynamic considerations are even more important than for ductile structures. The ductility reserves of a structure is obviously of great importance when it comes to vulnerability to (accidental) wave-in-deck loads.

For the structures and loading conditions analysed herein, it is clear that it is the ductility of the structure, as opposed to the inertia of the mass, that increases the structural ability to resist external loading when accounting for dynamic effects.

A wave-in-deck load history of the nature analysed herein will always lead to dynamic amplification for a traditional jacket structure with a natural period of a few seconds. This is determined by the relation between the duration of the impulse-like part of the load history, in our case the wave-in-deck load, and the natural period of the structure (e.g. Biggs, 1964).

Omission of damping

Damping is not included in the presented analyses. For structures, linear viscous undercritical damping is normally assumed, i.e. the damping is proportional to the velocity $\dot{u}$ and $c < 2m\omega$ in the dynamic equilibrium equation for a SDOF system (e.g. Equation 6.23). Undercritical damping implies that the structure will oscillate but there is a damping 'force' present in the system which continuously reduces the vibration amplitudes. In case of a small damping ratio, this effect is small or negligible during the first vibration cycles. In this project the load histories are of a nature implying that the maximum displacement and the permanent displacement are reached during these first oscillations. Damping is therefore assumed to have small or negligible effect on the maximum amplitudes of motion resulting from the force histories used. The inclusion of damping would in the present work firstly be of importance if including a pre-load history generating a start-up condition for the wave-in-deck loading, or if analysing load histories with more than one peak.

In addition to having an explicit effect on the response to external loading, damping also influences the natural frequency of a structural system. In the case of undercritical damping the frequency is reduced. However, within the range of damping that apply to typical structures this effect is negligible (Biggs, 1964). In this respect it is justifiable to omit damping.

Initial values

In the analyses all initial values of displacement, velocity and acceleration are set to zero. In reality, these values will be different from zero at the time when the analysis is initiated. The choice of initial values will influence the maximum response in the way that they will be determining for where in a vibration cycle the structure will be at deck wave impact, and it will be determining for the magnitude of the response immediately prior to wave impact. HSE (2003) analysed a jack-up rig and showed that the largest deck displacement occurred if the wave hit the hull when it had the largest displacement in the direction opposite to the wave heading direction, i.e. at the time the hull has the largest acceleration in the direction of the wave heading, but that the variation in response caused by different phasing is relatively small.

Reasonable initial values different from zero can only be included based on a precondition of either loading or response. However, one set of initial values would lead to reduced maximum response whereas another set would lead to an increase. It would therefore be necessary to analyse the actual extreme wave scenario several times to cover a representative range of wave or response conditions prior to wave impact and determine the condition that results in the largest maximum response. One should in that case have the results from the above mentioned HSE study in mind.

Based on the near static nature of jacket response to wave loading, implying small accelerations, and the results from the HSE study, it is considered likely that setting the initial values equal to zero does not imply significant misestimation of the maximum response following from the response immediately prior to the wave impact. However, the magnitude of the misestimation can only be revealed by running analyses with different preconditions, being a recommended task for the future.

Further use of analysis results

The analyses of model ‘DS’ that are carried out in this chapter will be used further in Chapter 7, where the results from a simplified method to estimate dynamic response (described in Chapter 6) will be compared to the response histories given in the present chapter.

Chapter 6

Simplified response analysis

6.1 Introduction

6.1.1 Chapter outline

This chapter comprises the theory and application of a simplified calculation model for assessment of dynamic response. The calculation model is in essence a single degree of freedom (SDOF) model that utilises information from a static analysis of the structure in question to calculate an approximate dynamic response to a given load history. Parts of this chapter has been published previously (van Raaij and Jakobsen, 2004) as a part of the present doctoral studies.

The present section comprises a summary of the chapter and is followed by a brief introduction / motivation.

In Section 6.2 general issues regarding dynamic versus static response to loading are treated.

Section 6.3 presents the theory of the SDOF model, as well as two slightly different calculation examples.

How to use the SDOF calculation model to calculate dynamic response of a multi degree of freedom (MDOF) structure is illustrated in Section 6.4. A cantilever beam is used as example structure.

In Section 6.5 a modification to the SDOF model is suggested and outlined, and response time histories with and without this modification are compared.

A summary of this chapter is given in Section 6.6.

6.1.2 Motivation

The data used for structural reassessment of offshore steel frame structures are commonly those that were used during the design phase, but modified according to the present situa-

tion. Such data often include an FE analysis model which is well suited for static nonlinear pushover analysis, as well as results (i.e. natural frequencies and mode shapes) from modal analysis. Rarely there exists analysis models that can be used for (nonlinear) dynamic time domain analyses without putting considerable effort into improvement of the model. This motivates the development of a very simple calculation model that uses information from pushover analysis and eigenvalue analysis to approximate dynamic response to given load histories.

A SDOF system needs 2 out of the 3 variables stiffness k, mass m and natural period T_{n} to be adequately described. The idea is to use the stiffness relation obtained by nonlinear static pushover analysis of the complete MDOF structure, i.e. the resistance function, to describe the stiffness of the SDOF model. The natural period is taken from eigenvalue analysis of the structure. Thus static pushover analysis and eigenvalue analysis yields enough information to establish a SDOF model of the structure. Of course also relevant load histories are needed before the analyses can be carried out, this matter is discussed in Chapter 4.

SDOF analysis methodology is also recommended by NORSOK N-004 (2004) for the purpose of estimating response to explosion loads, for which the load history normally comprise one single load peak of impulsive character. The suggested approach is based on a presupposed deflection mode, and is identical to a method explained by Biggs (1964).

Extreme wave analysis by use of a SDOF model is recommended by Skallerud and Amdahl (2002) as a screening procedure, of which the purpose is to identify the wave scenarios that need more accurate analysis. It is further recommended to establish a deformation spectrum (displacement response vs. natural period) for each of these wave scenarios in order to obtain an understanding of the response sensitivity to the natural period of the structural system. This is useful and necessary because of the uncertainty connected to the calculated natural period of a structure. The application of the suggested SDOF model is in accordance with that of the model outlined in Section 6.3 of this thesis.

6.2 Dynamic versus static response - resistance to external loading and inertia forces

When representing a MDOF structural system with an equivalent SDOF model, the structural response to the actual external loads is typically assumed to be governed by only one (e.g. the first) vibration mode. However, this is true only if the external force has a distribution that is identical to the distribution of inertia forces for the first vibration mode. In the following, this will be illustrated. Finite element (matrix) formulation is used to emphasise the *spatial distribution* of external and internal forces.

If imagining e.g. a cantilever with only transverse degrees of freedom in one plane (i.e. a discretisation of the cantilever in Figure 6.1), the importance of the possible difference in spatial distribution of external forces and inertia forces becomes evident. The dynamic equilibrium equation for the MDOF structural system reads:

$$\{\mathbf{R}_{\mathrm{m}}\} + \{\mathbf{R}_{\mathrm{d}}\} + \{\mathbf{R}_{\mathrm{r}}\} = \{\mathbf{F}_{\mathrm{e}}\} \tag{6.1}$$

where $\{\mathbf{R}_\mathrm{m}\} = [\mathbf{m}]\{\ddot{\mathbf{u}}\}$ is the vector (in the sense single column matrix) of inertia forces, $\{\mathbf{R}_\mathrm{d}\}$ is the vector of damping forces and $\{\mathbf{R}_\mathrm{r}\} = [\mathbf{k}]\{\mathbf{u}\}$ is the vector of structural restoring forces, frequently called static resistance forces. Damping will be omitted in the following, in order to focus on the interplay between the external loading and the inertia loading. Statically the force vs. the response is described by $\{\mathbf{R}_\mathrm{r}\} = \{\mathbf{F}_\mathrm{e}\}$, and similarly for the dynamic case $\{\mathbf{R}_\mathrm{r}\} + \{\mathbf{R}_\mathrm{m}\} = \{\mathbf{F}_\mathrm{e}\}$:

$$\text{Static:} \{\mathbf{R}_\mathrm{r}\} = \{\mathbf{F}_\mathrm{e}\} \qquad \text{Dynamic: } \{\mathbf{R}_\mathrm{r}\} = \{\mathbf{F}_\mathrm{e}\} - \{\mathbf{R}_\mathrm{m}\} \tag{6.2}$$

The implications of this is that a static and a dynamic load with identical distribution will not generate restoring forces with identical distributions (unless the external force and the inertia force have identical distributions).

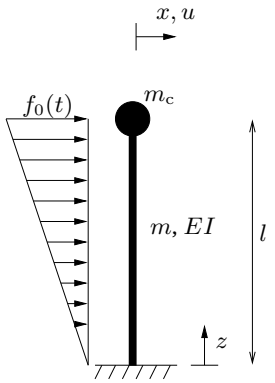

Figure 6.1: Cantilever with concentrated and distributed mass

To illustrate the above (within the elastic domain), the cantilever model shown in Figure 6.1 is used as example. A triangularly distributed load $f(z,t)$, quantified by $f_0(t)$ at $z = l$, is chosen because it can easily be analysed analytically and has a similar distribution as wave loading. The expression for the load variation along the cantilever is thus

$$f(z) = f_0 \frac{z}{l} \tag{6.3}$$

The total force is $F_\mathrm{e} = f_0 l/2$.

Static displacement response to the given external load can be calculated using e.g. the moment-area method, which states that for a cantilever beam the displacement of the free end is

$$u(l) = \int_0^l \frac{M(z)\,(l-z)}{EI} \mathrm{d}z \tag{6.4}$$

where $M(z)$ is the value of the moment diagram at location z. By use of the above equation together with the expression for the load $f(z)$ (Equation 6.3), the lateral displacement of the concentrated mass can be shown to be

$$u(l) = f_0 \frac{11l^4}{120EI} \tag{6.5}$$

The relation between the total external force F_e and the displacement of the concentrated mass is thus

$$F_\mathrm{e} = \frac{60EI}{11l^3}\, u(l) = \frac{5.45EI}{l^3}\, u(l) \tag{6.6}$$

The above is the direct physical relationship between the given external load and the structural displacement at the reference point (the tip). Except for the fact that it is defined only in the elastic domain, it can be seen as analogous to the resistance curve obtained by static pushover analysis. The stiffness is

$$k_\mathrm{f} = \frac{5.45EI}{l^3} \tag{6.7}$$

where k_f means stiffness related to external load (subscript f). The reaction shear V equals the resistance force, since this is a static consideration.

Considering *dynamic* behaviour due to an impulse load (undamped system), the structure will respond in a combination of forced and free vibrations depending on the external load. The structure will vibrate freely as long as the external loads are (nearly) constant in magnitude and spatial distribution, or after these loads have become zero. The inertia forces (during free or forced vibrations) may in general have a different spatial distribution than an external loading, and so the structural stiffness both in the elastic and plastic range will differ.

A cantilever with evenly distributed mass and stiffness and a concentrated mass at the free end has a 'free vibration stiffness' k_i in the first mode which can be calculated based on static consideration, applying external forces equal to (dynamic) inertia forces. In the following, subscripts cm and dm refer to concentrated and distributed mass, respectively. The 'load' corresponding to the inertia force is governed by the acceleration along the beam. The acceleration is proportional to the displacement and therefore assumptions must be made regarding the deflected shape, i.e. the first mode shape, of a beam with evenly distributed mass and a concentrated mass at the free end. A good estimate for the first mode shape is (Blevins, 1979):

$$\phi(z) = \frac{3}{2}\left(\frac{z}{l}\right)^2 - \frac{1}{2}\left(\frac{z}{l}\right)^3 \tag{6.8}$$

The applied ('inertia') force from concentrated mass is

$$F_\mathrm{cm} = m_\mathrm{c}\ddot{u}(l) \tag{6.9}$$

and the load from the distributed mass is:

$$F_{\mathrm{dm}} = m\int_0^l \ddot{u}(z)\mathrm{d}z = m\ddot{u}(l)\int_0^l \phi(z)\mathrm{d}z = \frac{3l}{8}m\ddot{u}(l) \tag{6.10}$$

The static relation between the 'inertia' force and the displacement at the free end is

$$F_{\mathrm{cm}} + F_{\mathrm{dm}} = k_{\mathrm{i}}u(l) = k_{\mathrm{i}}(u_{\mathrm{cm}} + u_{\mathrm{dm}}) \tag{6.11}$$

where u_{cm} and u_{dm} are the displacements of the free end resulting from the inertia load of the concentrated mass and the distributed mass, respectively. The displacement of the free end of a cantilever due to a concentrated load can for instance be found from tables, and is in our case:

$$u_{\mathrm{cm}} = \frac{F_{\mathrm{cm}}l^3}{3EI} \tag{6.12}$$

The displacement u_{dm} must be calculated using static methods, such as the moment-area method expressed in Equation 6.4. In the present case u_{dm} can be shown to be:

$$u_{\mathrm{dm}} = \frac{22F_{\mathrm{dm}}l^3}{105EI} \tag{6.13}$$

Choosing $m_{\mathrm{c}} = 3.5 \cdot 10^6$ kg and $m = 0.925 \cdot 10^6$ kg/m (these are the values used later in this chapter), the 'free vibration stiffness' can be calculated from Equation 6.11:

$$k_{\mathrm{i}} = \frac{F_{\mathrm{cm}} + F_{\mathrm{dm}}}{u_{\mathrm{cm}} + u_{\mathrm{dm}}} = \frac{3.42EI}{l^3} \tag{6.14}$$

The implication of the above is that subjected to a triangular load distribution, the cantilever behaves considerably stiffer (ref. k_{f}, Equation 6.7) than under the action of inertia force / free vibrations only (ref. k_{i}, Equation 6.14).

The reaction shear $V(t)$ has one contribution from external load and one from inertia forces, $V(t) = V_{\mathrm{f}}(t) + V_{\mathrm{i}}(t)$. The contribution from load is straight forward found by an equilibrium consideration of a purely static system exposed to the external load (at an instant in time):

$$V_{\mathrm{f}}(t) = k_{\mathrm{f}} \cdot u(l,t) = \int_0^l f(z,t)\,\mathrm{d}z = F_{\mathrm{e}}(t) \tag{6.15}$$

The contribution from inertia forces is found by considering the free vibration part of the response, by integrating the inertia forces over the length of the cantilever:

$$V_{\mathrm{i}}(t) = -\int_0^l m(z)\ddot{u}(z,t)\,\mathrm{d}z - m_{\mathrm{c}}\ddot{u}(l,t) \tag{6.16}$$

$$= -\left(m\int_0^l \phi(z)\,\mathrm{d}z + m_{\mathrm{c}}\right)\ddot{u}(l,t) \tag{6.17}$$

$$= -m_{\mathrm{i}}\ddot{u}(l,t) \tag{6.18}$$

where m_{i} is an equivalent mass that will be commented upon shortly. Note in particular that if the external forces are zero and the cantilever is in a pure state of free vibrations, the following relation is valid:

$$m_{\mathrm{i}}\ddot{u}(l,t) + k_{\mathrm{i}} \cdot u(l,t) = 0 \quad \Rightarrow \quad V(t) = V_{\mathrm{i}}(t) = k_{\mathrm{i}} \cdot u(l,t) = -m_{\mathrm{i}}\ddot{u}(l,t) \tag{6.19}$$

From the above equation it is clear that m_{i} is an equivalent mass of the cantilever associated with the free vibration stiffness (Equation 6.14). Accordingly, a mass m_{f} can be explicitly associated with the 'external load stiffness' k_{f} (Equation 6.7). In case of harmonic vibrations where $\ddot{u} = -\omega^2 u$, the relation between m_{i} and the free vibration stiffness k_{i} is equal to the relation between m_{f} and k_{f}:

$$\frac{k_{\mathrm{i}}}{m_{\mathrm{i}}} = \frac{k_{\mathrm{f}}}{m_{\mathrm{f}}} = \omega^2 \tag{6.20}$$

The contribution from inertia forces to reaction forces can thus also be expressed by m_{f}, and the total reaction force can be calculated as follows:

$$V(t) = V_{\mathrm{f}}(t) + V_{\mathrm{i}}(t) = F_{\mathrm{e}}(t) - \frac{k_{\mathrm{i}}}{k_{\mathrm{f}}} m_{\mathrm{f}}\ddot{u}(l,t) \tag{6.21}$$

Compared to a real SDOF system, where the reaction force equals the stiffness term in the dynamic equilibrium equation, the SDOF simplification of a MDOF structure obviously have some implications. The effect of the fraction multiplier $k_{\mathrm{i}}/k_{\mathrm{f}}$ (< 1) is a reduction of the magnitude of the inertia term. In the case where both the external force and the acceleration have the same direction, which is the case when a structure or mass is accelerated from zero by the force, the consequence is an increase in the reaction force magnitude. This can be interpreted as a increased stiffness (compared to elastic static stiffness) attributed to the inertia of the mass. Further it leads to a reduced stiffness during free vibrations that follows after being exposed to a load impulse. Both effects are clearly seen in the example in Section 6.4 (Figures 6.12 and 6.15).

6.3 SDOF model

The essence of static structural analysis is that the structure cannot resist larger external loads F_{e} than its static maximum resistance or capacity. However, when considering the dynamic equilibrium equation for a SDOF system given in Equation 6.22, one can see that it is possible for a structure to withstand loads exceeding the static capacity, provided such loads are counteracted by inertia and damping forces. In practice, this may be the case when the external force is of limited duration.

$$R_{\mathrm{m}}(t) + R_{\mathrm{d}}(t) + R_{\mathrm{r}}(t) = F_{\mathrm{e}}(t) \tag{6.22}$$

Here, $R_{\mathrm{m}}(t) = m\,\ddot{u}(t)$, $R_{\mathrm{d}}(t) = c\,\dot{u}(t)$ and $R_{\mathrm{r}}(t) = k\,u(t)$ are inertia, damping and internal restoring forces respectively. Biggs (1964) suggested that the dynamic equilibrium equation might be extended into the nonlinear (plastic) region by letting R_{r} be a predefined, unique function of the displacement u, *hereafter denoted* R_{f} *when explicitly referred to.*

In the following, the SDOF model based on this assumption will be outlined. The intention is to use this SDOF model to estimate dynamic response for complex structural systems, in the present case jacket platforms.

6.3.1 Model outline

The equation of motion of a SDOF system in the elastic domain is given by Equation 6.23, alternatively by Equation 6.22.

$$m\,\ddot{u}(t) + c\,\dot{u}(t) + k\,u(t) = F_{\mathrm{e}}(t) \tag{6.23}$$

The behaviour of the jacket structure, which is sought modeled by the SDOF model, is represented by the behaviour of a centrally located reference point at the deck[1]. The variables $u(t)$, $\dot{u}(t)$ and $\ddot{u}(t)$ in the SDOF equation of motion represent the horisontal displacement, velocity and acceleration of this reference point. These variables are functions of time t. Further, m, c, k and $F_{\mathrm{e}}(t)$ denote mass, damping, stiffness and external load, respectively.

In the following, damping will be omitted.

In order to allow for nonlinear material behaviour prior to and following attainment of ultimate capacity, the stiffness term $k\,u(t)$ is replaced by the nonlinear stiffness term $R_{\mathrm{f}}(u)$ as stated introductorily in this section. This *resistance function* $R_{\mathrm{f}}(u)$ for a jacket structure can be obtained from pushover analysis. Resistance functions will be dealt with in Section 6.3.2. The subscript 'f' refers to the fact that the resistance function is the result of a given external load.

[1] This is in accordance with current practice for establishment of resistance curve by use of pushover analysis

The nonlinear equation of motion for the model thus reads

$$m_{\mathrm{f}}\ddot{u} + R_{\mathrm{f}}(u) = F_{\mathrm{e}}(t) \tag{6.24}$$

where m_{f} is *the mass associated with the stiffness k_{f} relevant for the spatial distribution of the given external load*. The model is illustrated in Figure 6.2. The spring stiffness indicated in the model is the secant stiffness, and is related to the resistance function by $k(u) = R_{\mathrm{f}}(u)/u$.

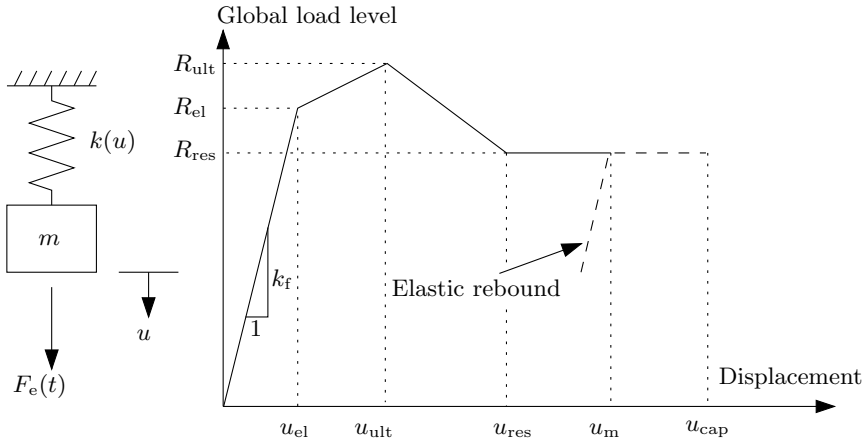

Figure 6.2: SDOF model

The nonlinear resistance curve $R_{\mathrm{f}}(u)$ obviously must be known prior to solving the equation of motion. This is hardly a problem because of the important role resistance curves play in documentation of the static performance of a jacket structure. It is evident that resistance curves differ for different distribution of the external load, and thus the resistance function must be obtained for the load distribution in question. Once a representative resistance function is available, it can be used either 'as is' or approximated by a few straight lines. The latter is convenient if the curve is not distinct (see for instance Figure 6.3), and the reason for this is mathematical circumstances during establishment of the resistance curve.

As already mentioned, the response of the reference point at deck level is taken to represent the structural behaviour.

6.3.2 Resistance functions

Relevant static characteristics of a jacket structure exposed to wave loading include nonlinear resistance curves (static load - displacement curves), denoted $R(u)$. The resistance curve illustrates the structural restoring force or resistance R as a function of the displacement u of a reference point of the structure, and thus gives information about the structures stiffness

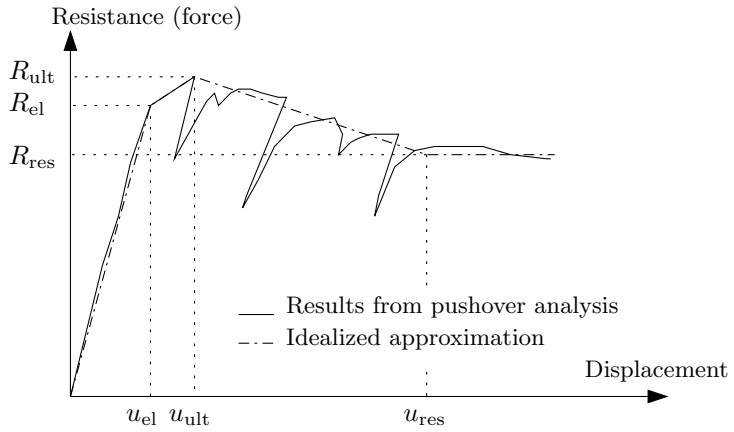

Figure 6.3: Load - deformation relationship

characteristics. Resistance curves are established by use of FE analyses subjecting the structure to all relevant wave scenarios. They are basically used to document the inherent reserves of the structure when exposed to a given load scenario.

A typical resistance curve for a North Sea jacket subjected to horisontal wave load is shown in Figure 6.3. The displacement is measured horisontally, commonly at deck level. The global load level represents (static) resistance against the wave load, and is often normalised against the design load in order to give the reserve strength ratio, RSR. An approximation of the resistance curve with 4 straight lines is also indicated in the figure, in order to illustrate the possibility for analytical representation of the curve.

6.3.3 Numerical solution

Solving Equation 6.24 for $\ddot{u}$ yields:

$$\ddot{u} = \frac{1}{m_{\mathrm{f}}}(F_{\mathrm{e}}(t) - R_{\mathrm{f}}(u)) \tag{6.25}$$

In this equation, u is not known, and the differential equation must be solved numerically. The load value $F_{\mathrm{e}}(t)$ for every time step must be known, and R_{f} must be an unique function of u. Having a prescribed value for the displacement start value $u^{(0)}$, $\ddot{u}^{(0)}$ can be calculated from Equation 6.24 for $R_{\mathrm{f}} = R_{\mathrm{f}}(u = u^{(0)})$. Next step is to estimate $u^{(1)}$, and having this value, $\ddot{u}^{(1)}$ can be calculated. The procedure must then be repeated for the desired number of time steps. There are several methods for estimating $u^{(s+1)}$ from previous values of u and $\ddot{u}$. In this work the 2. central difference, which is a special case of the Newmark β integration equations (see Section A.1 in Appendix A), is used.

The 2. central difference method has several advantages. No spurious (numerical) damping is involved, and the solution becomes exact as $\Delta t \to 0$. It is explicit (only information from

present and previous time intervals is needed to estimate the displacement at the next interval) and thus requires a minimum of computation time at each time interval.

The method has two disadvantages of which the consequences can easily be avoided by selecting the time interval properly. One is that the resulting displacement time history includes a negative period error and thus a shortening of the period. The period error increases rapidly as the relation $\Delta t/T_{\mathrm{n}}$ increases and approaches the stability limit which will be explained shortly. Using e.g. $\Delta t \leq 0.05T_{\mathrm{n}}$ ensures that the period shortening is not larger than approximately 0.5% (Newmark, 1959). The second disadvantage is that the 2. central difference is only conditionally stable, $\Delta t < (1/\pi) \cdot T_{\mathrm{n}} = 0.318\,T_{\mathrm{n}}$ being the criterion for stability. Selecting the time interval as indicated above to minimise the period error, the stability criterion is automatically fulfilled. The 2. central difference reads:

$$u^{(s+1)} = 2u^{(s)} - u^{(s-1)} + \ddot{u}^{(s)}(\Delta t)^2 \tag{6.26}$$

This expression leaves $u^{(1)}$ a problem since no value of $u^{(s-1)}$ is known. For this special case Biggs (1964) suggests to use

$$u^{(1)} = \frac{1}{2}\ddot{u}^{(0)}(\Delta t)^2 \tag{6.27}$$

or

$$u^{(1)} = \frac{1}{6}\left(2\ddot{u}^{(0)} + \ddot{u}^{(1)}\right)(\Delta t)^2 \tag{6.28}$$

of which the former corresponds to assuming the acceleration to be constant during the first time step. The latter corresponds to assuming that the acceleration varies linearly through the first time step, and must be solved by trial and error since $\ddot{u}^{(1)}$ depends upon $u^{(1)}$. If the acceleration is zero at first time step, Equation 6.28 must be used, in order not to have zero acceleration also at the second time step, since if a load is applied, the acceleration will be different from zero at the second time step.

For a given structure, if and when *rebound* occurs depends on the of the load history. Provided the load history is such that the displacement is reversed before the ductility limit of the structure (u_{cap}) is reached, the structure will rebound, in first instance elastically. The maximum value of the displacement, u_{m}, is not known in advance, but has to be found during the calculations: at first occurrence of $u^{(s+1)} < u^{(s)}$, u_{m} is set equal to $u^{(s)}$. The resistance $R_{\mathrm{f}}(u)$ is further expressed by

$$R_{\mathrm{f}}(u) = k_{\mathrm{f}}(u - u_{\mathrm{p}}) \tag{6.29}$$

which means that elastic rebound is a general elastic vibration problem but with a different neutral axis u_{p} equal to the permanent displacement. The governing equation of motion during elastic rebound is

$$m_{\mathrm{f}}\ddot{u} + k_{\mathrm{f}}(u - u_{\mathrm{p}}) = F_{\mathrm{e}}(t) \tag{6.30}$$

The permanent displacement u_{p} can be derived by compatibility considerations at maximum displacement $u = u_{\mathrm{m}}$:

$$m_{\mathrm{f}}\ddot{u} + R_{\mathrm{f}}(u_{\mathrm{m}}) = m_{\mathrm{f}}\ddot{u} + k_{\mathrm{f}}(u - u_{\mathrm{p}}) = F_{\mathrm{e}}(t) \tag{6.31}$$

When solved with respect to u_{p} Equation 6.31 reads

$$u_{\mathrm{p}} = u_{\mathrm{m}} - \frac{R_{\mathrm{f}}(u_{\mathrm{m}})}{k_{\mathrm{f}}} \qquad \text{or} \qquad u_{\mathrm{p}} = u_{\mathrm{m}} + \frac{m_{\mathrm{f}}\ddot{u} - F_{\mathrm{e}}}{k_{\mathrm{f}}} \quad \text{at} \quad u = u_{\mathrm{m}} \tag{6.32}$$

If the external force is constant from the time where $u = u_{\mathrm{m}}$, the amplitude in the following free vibration is $-m_{\mathrm{f}}\ddot{u}/k_{\mathrm{f}} = u_{\mathrm{m}} - u_{\mathrm{p}} - F_{\mathrm{e}}(t)/k_{\mathrm{f}}$. The last term vanishes if the force is zero.

6.3.4 Example

As an example, the outlined mathematical model is applied to a genuine SDOF structural system. It will be illustrated how two different resistance functions result in different response.

The first part of the example is identical to the example on page 21 - 26 in Biggs (1964, note that Biggs uses British units lb and feet, these units are also used in the present example in order to simiplify comparison). The example model and load history are illustrated in Figure 6.4, and the displacement response is sought. The mass used in the example is $m = 2$ lb $\cdot$ s^2 / ft. The resistance function (Figure 6.5(a)) to be used is elastic perfectly plastic, with the break point at $u_{\mathrm{el}} = u_{\mathrm{ult}} = 0.055$ ft and $R_{\mathrm{el}} = R_{\mathrm{ult}} = 110$ lb. This yields an elastic stiffness of $k = 2000$ lb/ft.

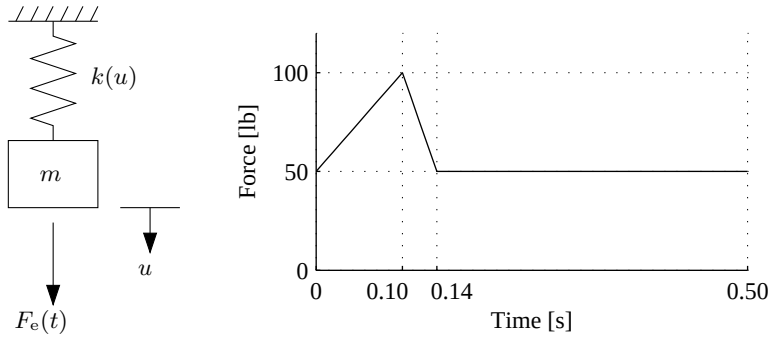

(a) SDOF model (b) External force history

Figure 6.4: Example model layout

The natural period is $T_{\mathrm{n}} = 0.199$ s. In Biggs book, a time step of $\Delta t = 0.02$ is used. However, in order to reduce the period error a time step of $\Delta t = 0.01$ s is used herein. The

resulting displacement response history is given in Figure 6.5(b). The maximum displacement is $u_{\mathrm{m}} = 0.099$ ft and the permanent set is $u_{\mathrm{p}} = 0.044$ ft. The amplitude of the residual vibrations is 0.030 ft.

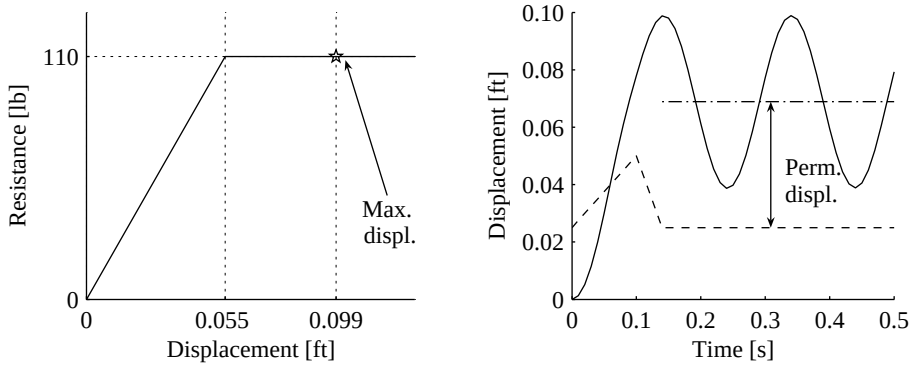

(a) Resistance function (b) Displacement response history

Figure 6.5: Resistance function and displacement response, elastic perfectly plastic case

Now look at an example where the resistance function is somewhat changed, see Figure 6.6(a). The initial elastic stiffness is kept unchanged, but at $u = u_{\mathrm{el}} = 0.045$ ft / the elastic limit is reached corresponding to a resistance of $R = R_{\mathrm{el}} = 90$ lb, and the plastic domain is entered. The ultimate capacity is reached when $u = u_{\mathrm{ult}} = 0.075$ ft and $R = R_{\mathrm{ult}} = 110$ lb. Thereafter the capacity drops linearly to $R_{\mathrm{res}} = 85$ lb at $u = 0.090$ ft. The residual capacity is thus $= 85$ lb.

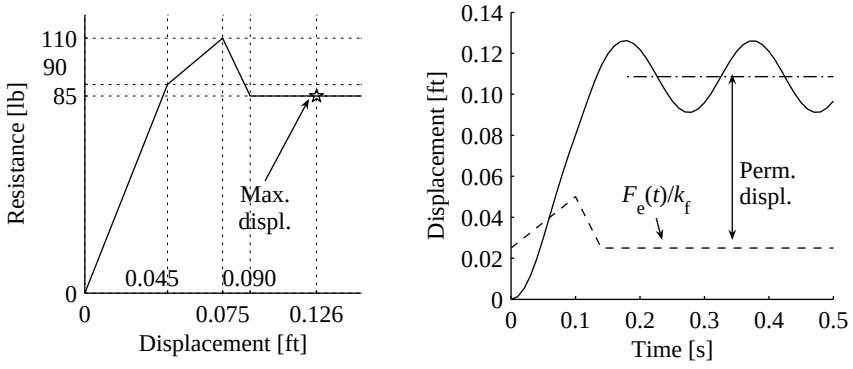

(a) Resistance function (b) Displacement response history

Figure 6.6: Resistance function and displacement response, elasto-plastic case

The maximum displacement is 0.126 ft, some 27% increased compared to the first example, and the permanent set is 0.084 ft has thus increased by a factor of almost 2. This is attributed

to the change in the resistance curve. In general, reduced area under the resistance curve will give increased maximum- and permanent displacement if the other parameters are kept.

6.4 Application of the SDOF model to a real structural system

Skallerud and Amdahl (2002) and Hansen (2002) have attempted to assess dynamic response of a jacket platform by use of a nonlinear SDOF model as described previously. In both references it is assumed that $F_{\mathrm{e}}(t)$ is the total external load, and that a representative resistance function $R_{\mathrm{f}}(u)$ for fixed offshore platforms can be established by use of static nonlinear pushover analysis, subjecting the structure to the same external load (-distribution) that is to be used during the dynamic analysis. The resistance function is related to the displacement u at some reference point, normally at the deck level of the platform.

Under these assumptions, the SDOF model of the structure is based on the relationship between the reaction force (base shear or overturning moment) and the displacement of the top of the structure due to external loading. The inertia forces in such a SDOF model then have to be 'tuned' to the spatial distribution of the studied external loading. That means that an equivalent mass for the SDOF model has to be adopted according to $m_{\mathrm{f}} = k_{\mathrm{f}}/\omega^2$, where k_{f} is the stiffness, i.e. the first derivative of $R_{\mathrm{f}}(u)$ with respect to displacement in the elastic domain. The circular frequency ω is obtained from eigenvalue analysis of the structure. Note that the equivalent mass is neither the physical mass integrated over the span nor a generalised mass in the traditional sense.

In this section, the cantilever model from Section 6.2 will be used as an example:

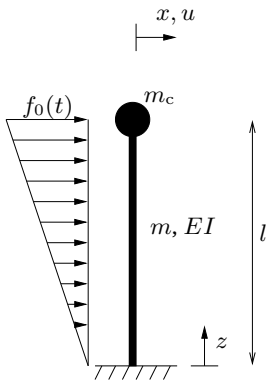

Figure 6.7: Cantilever with concentrated and distributed mass

The cantilever[2] has a height $l = 5$ m, and a circular cross section with outer diameter $D = 400$ mm and wall thickness $t_{\mathrm{w}} = 150$ mm. Youngs modulus is $2.1 \cdot 10^{11}$ N/m^2.

[2]Note that the structure properties should not be taken literally to represent a cantilever structure.

The concentrated and distributed masses are $m_c = 3.500 \cdot 10^6$ kg and $m = 0.925 \cdot 10^6$ kg/m, respectively. The first natural period is 5.4 s. The external load has a triangular distribution, and is quantified by $f_0(t)$. The load *distribution* in itself is time-invariant.

$$f(z,t) = f_0(t)\frac{z}{l} \tag{6.33}$$

The total force is $F_e(t) = f_0(t)l/2$.

The finite element analysis in this section are carried out using USFOS (Hellan et al., 1998).

6.4.1 Static analysis

The objective of the static FE analysis is to establish the resistance curve R_f to be used in dynamic SDOF analysis of the structure. The given triangular load distribution is used. The resistance curve is illustrated in Figure 6.8.

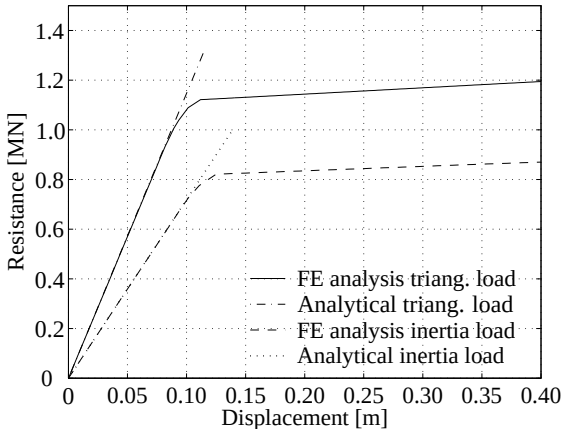

Figure 6.8: Finite element analysis, static resistance

The resistance function extends into the nonlinear region. It has a stiffness in the elastic domain of $k_f = 11.4$ MN/m. First yield occurs at $u = 78$ mm, at a load level of 0.883 MN. The cross section is fully plastified at $u = 112$ mm, at load level 1.121 MN.

The resistance curve R_i obtained when inertia of the mass is applied as static load is also included in Figure 6.8. The inertia load is calculated based on the deflected shape used in Section 6.2, which is

$$\phi(z) = \frac{3}{2}\left(\frac{z}{l}\right)^2 - \frac{1}{2}\left(\frac{z}{l}\right)^3 \tag{6.34}$$

Exposed to this load, first yield occurs at $u = 90$ mm, at a load level of 0.648 MN. This corresponds to an elastic stiffness of $k_i = 7.2$ MN/m. Note that this represents the stiffness during

free vibrations. Full plastification is reached at a load level of 0.821 MN, corresponding to a displacement of $u = 125$ mm.

The resistances arising from Equations 6.6 and 6.14, which represent the analytical approach, are also illustrated. The calculated elastic stiffnesses are $k_{\mathrm{f}} = 11.47$ MN/m and $k_{\mathrm{i}} = 7.19$ MN/m, respectively.

6.4.2 Dynamic analysis

A load time history is created by defining the time variation of $f_0(t)$. The normalised time variation used in this example is illustrated in Figure 6.9. The load starts at zero, maximum load occurs at $t = 0.5$ s and the returns to zero again at $t = 1.0$ s.

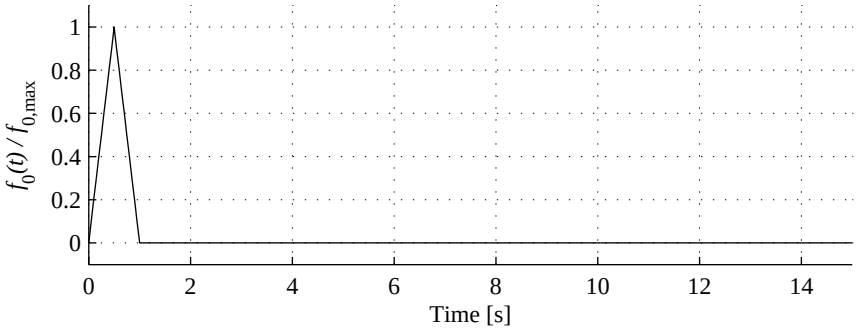

Figure 6.9: Scaling factor for external load

The dynamic displacement response history is calculated by use of SDOF model described in Section 6.3, with the resistance function obtained by FE analysis (see previous section), and with mass $m_{\mathrm{f}} = k_{\mathrm{f}}/\omega^2$. The circular frequency ω is obtained from eigenvalue analysis of the structure using FE analysis. The results are compared to displacements calculated at the free end of the cantilever model by use of finite element analysis.

The reaction base shear is calculated according to Equation 6.21 and compared to reaction base shear obtained by FE analysis.

Results, elastic case

A total maximum load $F_{\mathrm{e}}(t = 0.5s) = 1$ MN is obtained by choosing $f_0(t = 0.5s) = 0.4$ MN/m. The resulting displacement calculated by the SDOF model and finite element analysis, respectively, is given in Figure 6.10. The maximum displacement for the SDOF model is 0.0499 m. The corresponding value for the finite element model is exactly the same, 0.0499 m. From the figure, one can see the excellent agreement between the displacement response for this case.

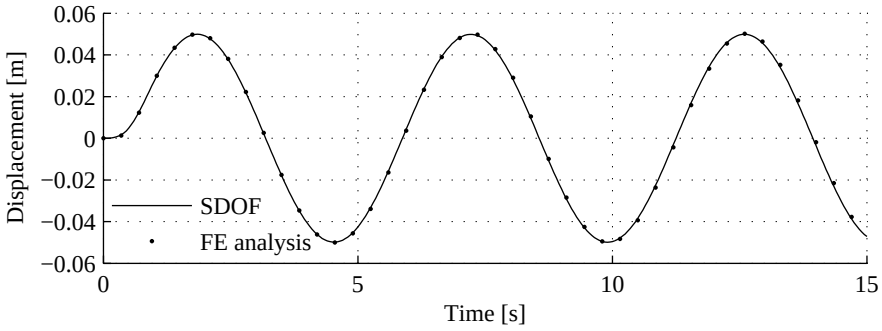

Figure 6.10: Displacement of free end of cantilever

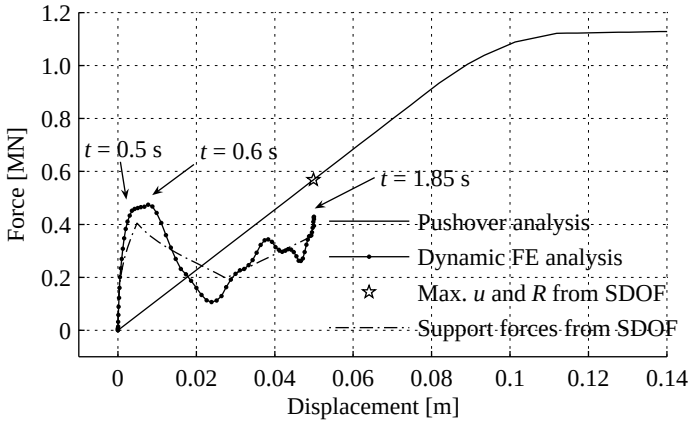

Figure 6.11: Restoring forces in dynamic analysis over 2 s vs. pushover analysis

In Figure 6.11 the structural resistance R_{f} obtained from static finite element analysis is plotted together with the (dynamic) reaction forces from both finite element analysis and SDOF computation. The solid - dotted line is the support reaction force vs. the displacement of the free end in the dynamic finite element analysis plotted for each 0.025 s of the first 2 seconds of simulation. From $t = 0$ (at $u = R_{\mathrm{f}}(u) = 0$) to $t = 0.5$ s the reaction force increases rapidly, analogous to a very stiff response. This is the time needed to accelerate the mass. Shortly thereafter (approximately at $t = 0.6$ s) the maximum reaction force is reached. Further, the reaction force decreases and increases a few times until maximum displacement is reached at $t = 1.85$ s. These variations indicate that higher order vibration modes are excited. The reaction forces (dash-dotted line) calculated from the SDOF model by Equation 6.21 agrees fairly well with the reaction forces from the finite element analysis. Of course the higher order vibrations are not captured.

In Figure 6.12 the reaction forces for all time steps up to $t = 15$ s are illustrated, together

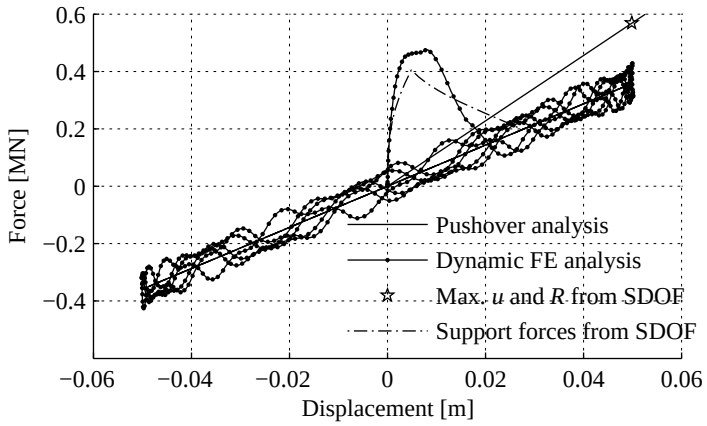

Figure 6.12: Restoring forces in dynamic analysis vs. pushover analysis

with the static structural resistance. One can see how the reaction forces after the initial peak settles in a new and softer 'global' state, and varies along a straight line representing the free vibration stiffness. The local variations around this softer'global' state are due to higher order vibrations. The reaction force from the SDOF model agrees very well during these free vibrations.

Clearly, it can be seen that the structure behaves softer during free vibrations than under (increasing) external forces. The dynamic stiffness during free vibrations is from the figure taken to be approximately 7.2 MN/m, which agrees well with the free vibration stiffness calculated previously by finite element analysis (7.2 MN/m) and the analytically obtained value (7.19 MN/m) — see Section 6.4.1.

Results, plastic case

So far, we have restricted the behaviour to the elastic region. Using a total load of 3 MN in the dynamic analysis, the displacements enter the plastic region. The response history is illustrated in Figure 6.13.

The SDOF model predicts slightly larger maximum displacement — 0.163 m — than the finite element model — 0.155 m. The results from both methods indicate some plastic deformation and therefore permanent displacement of the free end of the cantilever. The SDOF model computes a permanent displacement caused by plastic deformation of 0.064 m, which is significantly larger than the permanent displacement from the finite element analysis — 0.03 m (this value cannot be directly extracted from USFOS, and is therefore approximated from Figures 6.13 and 6.15).

This is likely due to the difference between the nonlinear behaviour under inertia forces and the nonlinear behaviour under external loading alone, as obtained in pushover analysis. The difference can be noticed in Figure 6.8.

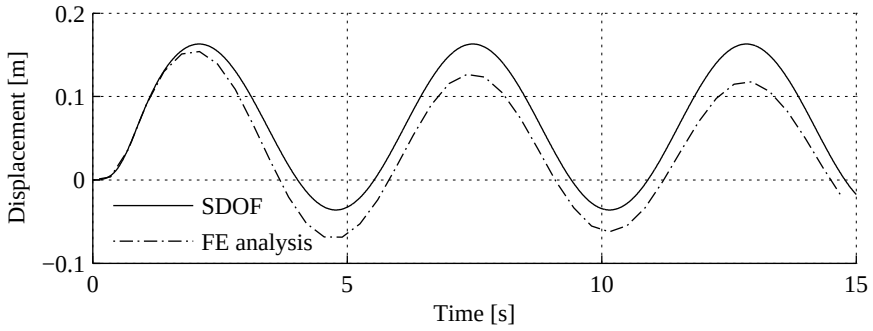

Figure 6.13: Displacement of free end of cantilever

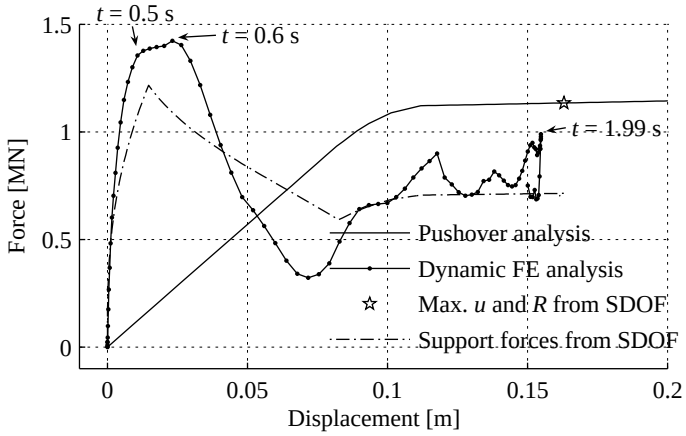

Figure 6.14: Restoring forces in dynamic analysis over 2.25 s vs. pushover analysis

In Figure 6.14, one can see that the course of the reaction force in time is similar to the elastic case (studied in Figures 6.11 and 6.12), except the magnitude which is larger. Maximum displacement is reached at $t = 1.99$ s. The local variations indicate that higher order vibration modes are excited, like in the elastic case. The reaction forces calculated from the SDOF model by Equation 6.21 (dash-dotted line) has an acceptable agreement with the reaction forces from the finite element analysis in the initial phase. However, when settling in free vibrations, one can clearly see that the SDOF model has resulted in larger permanent displacements.

A 'global' free vibration stiffness of 7.2 MN/m seems to be a representative estimation also in this case, according to Figure 6.15 which shows structural reaction force for all time steps.

It is expected that the difference between the displacement obtained by the SDOF model and finite element analysis will be reduced if the difference between the nonlinear behaviour of the two 'load cases', i.e. inertia forces and external loads, is accounted for by an adjusted

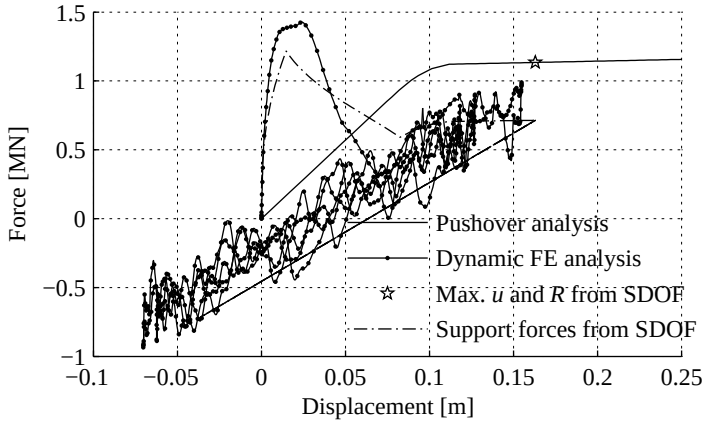

Figure 6.15: Restoring forces in dynamic analysis vs. pushover analysis

mass term. This matter is treated in the following.

6.5 A modified mass term

6.5.1 The modification factor α_{m}

Again the dynamic equilibrium equation for the employed SDOF system is presented:

$$m_{\mathrm{f}}\,\ddot{u} + R_{\mathrm{f}}(u) = F_{\mathrm{e}}(t) \tag{6.35}$$

This equation predicts well the displacements that remain within the elastic domain where $R_{\mathrm{f}}(u) = k_{\mathrm{f}}u$, but fails to predict displacements that enter the plastic domain. It is likely that this is because the effect of the nonlinear behaviour under inertia loading is not captured, and in the following an attempt is made to include this effect by modifying the inertia force term $m_{\mathrm{f}}\ddot{u}$. If we look at static equilibrium at an instant in time for the cantilever under free vibrations and include nonlinear behaviour through the term $R_{\mathrm{i}}(u)$ we have

$$\begin{aligned} R_{\mathrm{i}}(u) &= -\int_0^l m(z)\,\ddot{u}(z,t)\,\mathrm{d}z - m_{\mathrm{c}}\,\ddot{u}(l,t) \\ &= -m_{\mathrm{i}}\,\ddot{u}(l,t) \end{aligned} \tag{6.36}$$

where R_{i} is the *static resistance curve obtained under a load with the same distribution as inertia loading* as shown in Figure 6.8. While Equation 6.36 defines the nonlinear behaviour under inertia loading, in Equation 6.35 the nonlinear behaviour under inertia loading is governed by R_{f} which however is representative for the external loading only. In order to combine them and account for the nonlinear behaviour under both $m_{\mathrm{i}}\ddot{u}$ and F_{e} in one equation

i.e. make them refer to the same stiffness, Equation 6.36 is scaled with a factor $R_{\mathrm{f}}(u)/R_{\mathrm{i}}(u)$, giving

$$R_{\mathrm{f}}(u) = -\frac{R_{\mathrm{f}}(u)}{R_{\mathrm{i}}(u)} m_{\mathrm{i}}\, \ddot{u}(l,t) \tag{6.37}$$

The mass m_{i} is associated with the stiffness during free vibrations k_{i} in the same way as m_{f} is associated with k_{f}:

$$\frac{k_{\mathrm{f}}}{m_{\mathrm{f}}} = \frac{k_{\mathrm{i}}}{m_{\mathrm{i}}} = \omega^2 \;\; \Rightarrow \;\; m_{\mathrm{i}} = \frac{k_{\mathrm{i}}\, m_{\mathrm{f}}}{k_{\mathrm{f}}} \tag{6.38}$$

Substituting for m_{i} from Equation 6.38 into Equation 6.37:

$$R_{\mathrm{f}}(u) = -\frac{k_{\mathrm{i}}}{k_{\mathrm{f}}} \frac{R_{\mathrm{f}}(u)}{R_{\mathrm{i}}(u)}\, m_{\mathrm{f}}\, \ddot{u}(l,t) \tag{6.39}$$

The adjusted mass term in the right hand side of Equation 6.39 is used in the SDOF model. The fraction multiplier is from now on denoted α_{m}:

$$\alpha_{\mathrm{m}} = \frac{k_{\mathrm{i}}}{k_{\mathrm{f}}} \frac{R_{\mathrm{f}}(u)}{R_{\mathrm{i}}(u)} \tag{6.40}$$

The modified dynamic equilibrium finally reads:

$$\alpha_{\mathrm{m}}\, m_{\mathrm{f}}\, \ddot{u} + R_{\mathrm{f}}(u) = F_{\mathrm{e}}(t) \tag{6.41}$$

$\alpha_{\mathrm{m}}$is effectively the normalised (against elastic behaviour) nonlinear behaviour under external load divided by normalised nonlinear behaviour under inertia loading, and captures the possible difference in the nonlinear behaviour for the two 'load cases' external load and inertia forces.

Applying this modification factor to the mass term, only the 'dynamic part' of the equilibrium equation is influenced. Thus, if the load has a static nature, the acceleration will be nearly zero, and the contribution from the mass term and thus $\alpha_{\mathrm{m}}$is negligible.

At each time step during the calculation, there exists a given relation between u and $\ddot{u}$, determined by the dynamic equilibrium equation. This equilibrium equation differs for the (possibly non-linear) phase where the displacement u increases, and the elastic rebound phase. In the first phase where the displacement increases, Equation 6.41 is determining. In the rebound phase, where $\alpha_{\mathrm{m}}$by definition is 1.0, Equation 6.42 below is determining (this expression for equilibrium in the rebound phase is identical to the expression given for the non-modified SDOF model).

$$m_{\mathrm{f}}\, \ddot{u} + k_{\mathrm{f}}(u - u_{\mathrm{p}}) = F_{\mathrm{e}}(t) \tag{6.42}$$

At the point where the displacement is at its maximum and the structure starts to rebound, these two equations must both be valid.

The mass modifier α_{m} will in case of plastic behaviour be discontinuous at $u = u_{\mathrm{m}}$ (unless if the external loading has identical distribution to the generated inertia force). This discontinuity leads to a discontinuity in R_{f} at the same point; the value of $R_{\mathrm{f}}(u_{\mathrm{m}})$ picked from the resistance curve used in Equation 6.41 is different from the value of $R_{\mathrm{f}}(u_{\mathrm{m}}) = k_{\mathrm{f}}(u_{\mathrm{m}} - u_{\mathrm{p}})$ in Equation 6.42. This sudden change in the R_{f}-value does not really have a physical meaning, but is is a consequence of modifying the mass term in the SDOF model, and ensures a representative prediction of the physical values displacement, velocity and acceleration.

The simplest way to calculate u_{p} is to use Equation 6.42 as a basis. The permanent displacement is thus:

$$u_{\mathrm{p}} = u + \frac{m_{\mathrm{f}}\ddot{u} - F_{\mathrm{e}}}{k_{\mathrm{f}}} \quad \text{at} \quad u = u_{\mathrm{m}} \tag{6.43}$$

With this modified SDOF model, the displacement for the previously described case with plastic response (Section 6.4.2) is recalculated. The resulting displacement history is shown in Figure 6.16, together with the results from the case without adjusted mass term.

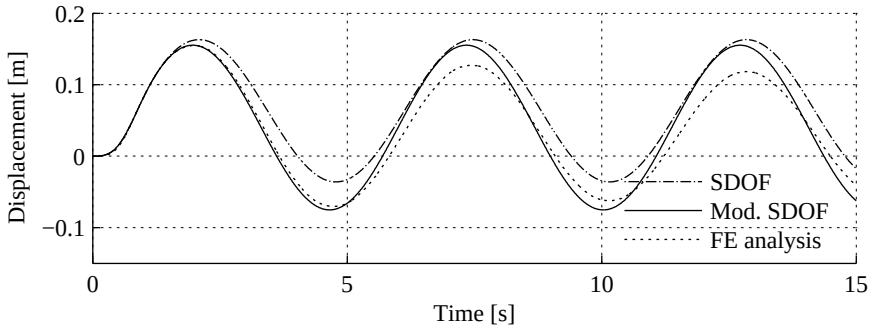

Figure 6.16: Displacement of free end of cantilever

The agreement with the finite element analysis is improved, particularly during the first positive displacement amplitude. The maximum displacement calculated by the modified SDOF model is 0.155 m, and the permanent displacement is 0.040 m. The maximum displacement computed by finite element analysis is 0.155 m, i.e. the agreement is very good. As mentioned earlier, the permanent displacement cannot be extracted from USFOS, but was previously (Section 6.4.2) taken to be approximately 0.03 m. The modified SDOF model estimates the permanent displacement well.

The reaction force calculated by use of the SDOF model with and without adjusted mass term is shown in Figure 6.17, as well as the reaction force from finite element analysis. The agreement has clearly improved.

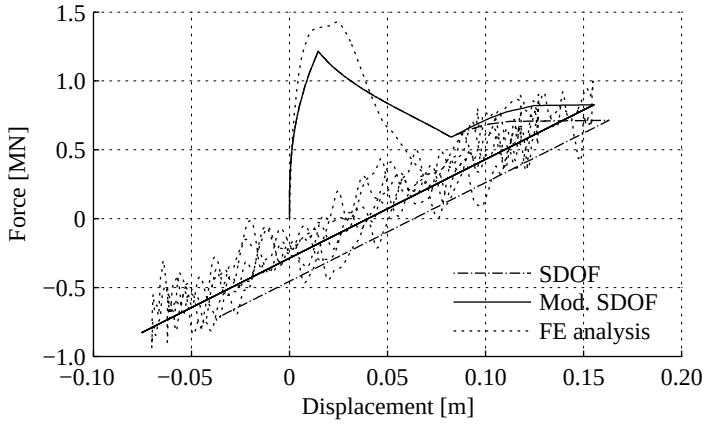

Figure 6.17: SDOF, restoring forces with / without modified mass term

6.5.2 The implications of α_{m}

If $R_{\mathrm{f}}(u)/R_{\mathrm{i}}(u) \geq k_{\mathrm{f}}/k_{\mathrm{i}}$ for a given u, then $\alpha_{\mathrm{m}}(u) \geq 1.0$ for this value of u. Opposite, if $R_{\mathrm{f}}(u)/R_{\mathrm{i}}(u) \leq k_{\mathrm{f}}/k_{\mathrm{i}}$, then $\alpha_{\mathrm{m}}(u) \leq 1.0$. This can be illustrated as shown in Figure 6.18, where R_{f}, R_{i} and finally $R_{\mathrm{i}} \cdot k_{\mathrm{f}}/k_{\mathrm{i}}$ for two different types of stiffness characteristics are plotted. In cases where the curve for $R_{\mathrm{i}} \cdot k_{\mathrm{f}}/k_{\mathrm{i}}$ lies underneath the R_{f} curve, $\alpha_{\mathrm{m}}(u) \geq 1.0$. This, in turn, indicates that R_{i} has a less favourable load (i.e. mass) distribution in the sense of plastic behaviour than R_{f}. Correspondingly, if $R_{\mathrm{i}} \cdot k_{\mathrm{f}}/k_{\mathrm{i}}$ lies above the R_{f} curve, $\alpha_{\mathrm{m}}(u) \leq 1.0$.

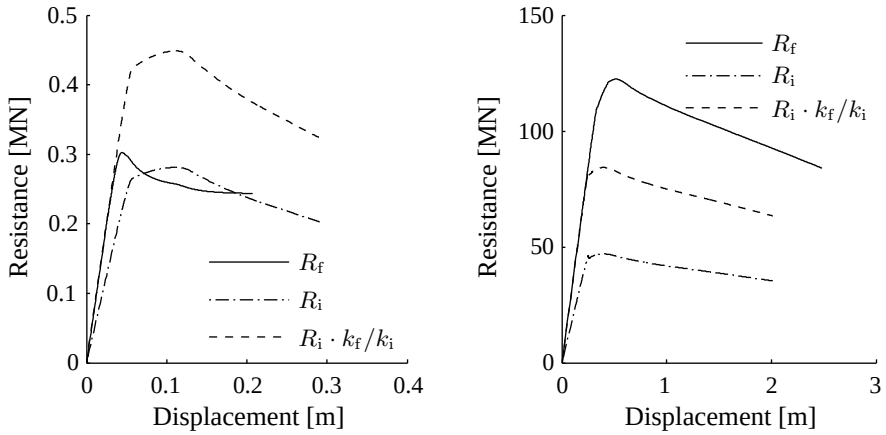

(a) $\alpha_{\mathrm{m}} \leq 1$ (b) $\alpha_{\mathrm{m}} \geq 1$

Figure 6.18: Typical scenarios for stiffness characteristics for $\alpha_{\mathrm{m}} \leq 1$ and $\alpha_{\mathrm{m}} \geq 1$

If $\alpha_{\mathrm{m}}(u) = 1.0$, meaning that $R_{\mathrm{f}}(u)/R_{\mathrm{i}}(u) = k_{\mathrm{f}}/k_{\mathrm{i}}$ or $R_{\mathrm{f}}(u)/k_{\mathrm{f}} = R_{\mathrm{i}}(u)/k_{\mathrm{i}}$ for the range of displacements in question, the response is not influenced and the original SDOF and the modified SDOF model will give identical results.

$\alpha_{\mathrm{m}}(u) < 1.0$ results in increase in the acceleration absolute value, and $\alpha_{\mathrm{m}}(u) > 1.0$ correspondingly leads to reduced absolute value of the acceleration. The influence of this increase / reduction on the displacement depends on the direction of the acceleration compared to the direction of the displacement. In general, a reduction of the intensity of the acceleration leads to a reduction of the displacement magnitude (compared to the pure SDOF model).

In practice this means:

$\alpha_{\mathrm{m}}(u) < 1.0 \;\rightarrow$ increased $\lvert\ddot{u}\rvert$	$\ddot{u} < 0 \;\rightarrow\; u$ decreases
	$\ddot{u} > 0 \;\rightarrow\; u$ increases
$\alpha_{\mathrm{m}}(u) > 1.0 \;\rightarrow$ reduced $\lvert\ddot{u}\rvert$	$\ddot{u} < 0 \;\rightarrow\; u$ decreases
	$\ddot{u} > 0 \;\rightarrow\; u$ increases

The sign of the acceleration depends on the relative size of the static resistance and the external load, as follows:

$$\ddot{u} = \frac{1}{\alpha_{\mathrm{m}}(u)\, m_{\mathrm{f}}} \left(F_{\mathrm{e}}(t) - R_{\mathrm{f}}(u)\right) \tag{6.44}$$

If we assume that plastic deformation happens for positive displacement — which is the condition in the analysed cases in the present project — the acceleration is negative if $F_{\mathrm{e}}(t) < R_{\mathrm{f}}(u)$.

For wave loading conditions that lead to significant plastic deformation, the static resistance R_{f} when approaching u_{m} will normally be constant or decreasing for increasing displacement u. Simultaneously, the external load is still considerable, and is most likely larger than the resistance R_{f}. Under such conditions, the real value of the acceleration is likely to be positive.

Loading conditions of highly impulsive nature, e.g. explosion loading, will lead to a different behaviour as long as the natural period of the structure is considerably longer than the load duration, which is only a fraction of a second. As the displacement approaches its (positive) maximum, the impulsive load history is already past, thus $F_{\mathrm{e}}(t) \ll R_{\mathrm{f}}(u)$ and the acceleration is negative. A structural configuration and load distribution giving $\alpha_{\mathrm{m}}(u) < 1.0$, such as the cantilever described previously, will experience a 'more negative' acceleration when subject to the modified SDOF model, and the (positive) maximum displacement will be reduced. This is documented in Section 6.5.1.

6.6 Summary

In this chapter the structural response to external load as opposed to that of inertia forces has been discussed. It is demonstrated how dynamic considerations, including the presence of

mass in a structural system, alter the deflected shape, and consequently the global stiffness, obtained by static considerations.

Further, a simplified method to assess structural dynamic response has been outlined. The method is a single-degree-of-freedom (SDOF) model based on the following structural properties:

- ⋆ An equivalent stiffness (nonlinear if relevant) as obtained from static methods, e.g. push-over analysis, subjecting the structure to the relevant load distribution.
- ⋆ An equivalent mass which is associated with the initial elastic stiffness from the pushover analysis mentioned above and with the natural period of the structure (as obtained from eigenvalue analysis).

The application of the SDOF model has been demonstrated on a cantilever with distributed and concentrated mass, which can be regarded a strong idealisation of jacket type structures. The resulting response time histories have been compared to response obtained by finite element analysis of the cantilever structure.

In the case where the response remains elastic, very good agreement has been obtained between SDOF computation and finite element analysis for displacement response. There is also good agreement for the support forces.

For the plastic case there is a deviation both in the calculated displacement time history, permanent displacement and support force between SDOF and finite element analysis. Better agreement is achieved between the SDOF analyses and the finite element analyses by taking into account the nonlinear behaviour under pure inertia loading. An adjustment of the mass term in the SDOF equilibrium equation is particularly suggested for this task.

The SDOF model is in the following sought validated against finite element analyses of a jacket structure (Chapter 7).

Chapter 7

Simplified response analysis of jacket structure — model ‘DS’

7.1 Introduction

This chapter comprises simplified dynamic analyses of jacket model ‘DS’ using the single degree of freedom (SDOF) model presented in Chapter 6.3. The results from the simplified analyses are validated against results from finite element analyses.

The objective of the chapter is to investigate to what extent the SDOF model can predict dynamic response of jacket structures exposed to wave(-in-deck) loading, and further to identify factors that contribute to discrepancies between the results obtained using the SDOF model and those obtained using finite element analysis.

In Section 7.2 information about the model ‘DS’ and its loading conditions is briefly repeated. The analysis results are presented in Section 7.3, and a thorough discussion of the results is given in Section 7.4.

7.2 Structural model and external loading

The structural model, load scenarios and finite element analyses are described in detail in Chapter 5 and in the analysis input files in Appendix C. The model is shown in Figure 7.1.

The external load time histories are repeated in Figure 7.2. An important aspect of these load histories is the fact that the distribution of the load along the jacket varies with time as the wave travels through the structure. This implies that a static resistance curve R_{f} calculated for a particular load scenario (wave height, -period, water depth) is chosen to correspond to the load at one single instant in time of the wave cycle. It is therefore necessary to carefully

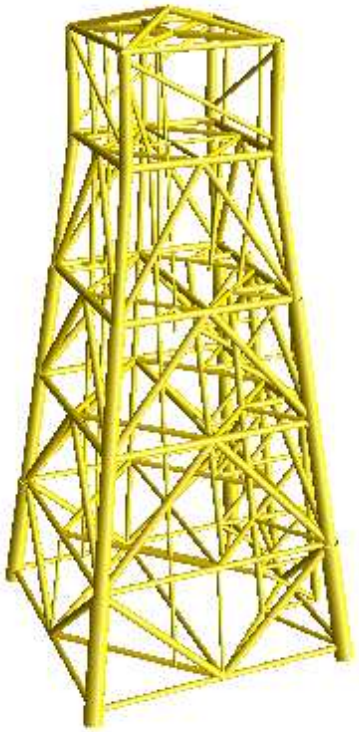

Figure 7.1: Model ‘DS’

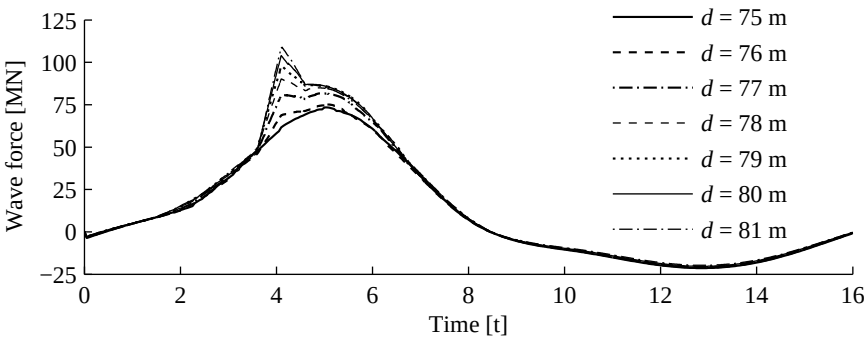

Figure 7.2: Model DS, load history generated, $H = 33$ m and $T = 16$ s for different water depths

consider at which phase angle the load distribution is most representative for the dynamic response results, and use this distribution to obtain R_{f}.

In this study, the most relevant distribution is taken to occur when the load at deck level is

at its maximum, since this load distribution is likely to be the major initiator of the dynamic behaviour. The details of the static analyses carried out in order to obtain the resistance curves R_{f} of the model, which are necessary for the simplified assessment, are also described in Chapter 5. For simplicity, the structural resistance curves are illustrated again in Figure 7.3, together with the resistance curve R_{i} obtained for a load distribution identical to the distribution of inertia forces in the first vibration mode.

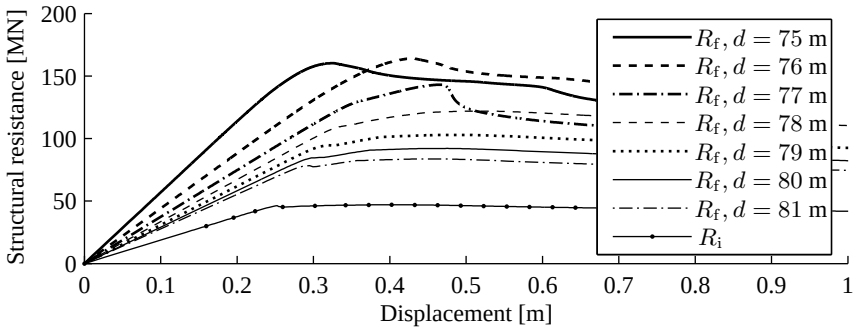

Figure 7.3: Stiffness curves in terms of base shear (BS) for different water depths

7.3 SDOF analyses

7.3.1 Summary

SDOF analysis is run for each case that is analysed in Section 5.3, in total for 7 cases. The results, comprising maximum and permanent displacements are summarised in Table 7.1. For all cases except for water depths $d = 80$ m and $d = 81$ m the modified SDOF analyses give maximum displacement u_{m} and permanent displacement u_{p} identical to[1] or larger than found using the original SDOF. At water depth $d = 81$ m the SDOF analyses break down due to excessive displacements. FE analysis in general yields larger u_{m} than the SDOF methods where no or only little plasticity is involved, and smaller u_{m} in cases with many plasticity incidents and significant permanent displacement. The permanent displacements calculated by the FE method are in general smaller than those calculated by the SDOF methods. The difference is significant when much plastic deformation is present.

The response time histories generated with the SDOF model for four selected cases are, together with the results from FE analysis, illustrated in Figures 7.5 to 7.9. Note that an additional curve is included in all subfigures of these figures. This curve represents the response calculated by use of FE analysis for a case where the *distribution* of the load is kept constant during the complete load time history, denoted 'FE c.d.' (c.d. is an abbreviation of 'constant distribution'). The value of the total load at each time instant is not changed.

[1] SDOF and modified SDOF giving identical results means that the behaviour is linear.

Table 7.1: Results from SDOF analyses of model DS, $h = 33$ m, $T = 16$ s

Water depth [m]	Deck inund. [m]	Wave load BS * [MN]	Orig. SDOF u_{m} [m]	Orig. SDOF u_{p} [m]	Mod. SDOF u_{m} [m]	Mod. SDOF u_{p} [m]	FE analysis u_{m} [m]	FE analysis u_{p} [m]
75.0	0.25	73.4	0.139	0.000	0.139	0.000	0.147	0.000
76.0	1.18	75.1	0.203	0.000	0.203	0.000	0.221	0.000
77.0	2.12	81.7	0.287	0.001	0.290	0.013	0.314	0.000
78.0	3.06	90.2	0.369	0.031	0.387	0.068	0.407	0.038
79.0	4.00	97.9	0.554	0.224	0.609	0.298	0.537	0.126
80.0	4.94	103.9	2.018	1.782	1.890	1.670	0.728	0.324
81.0	5.88	108.9	NA **	NA **	NA **	NA **	1.030	0.645

* BS = base shear

** Displacement grows unlimited, meaning total collapse

7.3.2 Results, details

The variable α_{m} (the mass modifier described in Section 6.5) is, when different from 1.0, positive for all the analysed cases with exception of negligible variations around 1.0 due to minor differences in $k_{\mathrm{i}}/k_{\mathrm{f}}$ and $R_{\mathrm{f}}/R_{\mathrm{i}}$. This is illustrated in Figure 7.4. For $d = 75$ m and $d = 76$ m $\alpha_{\mathrm{m}} \equiv 1$ because no plastic behaviour is detected by the SDOF models.

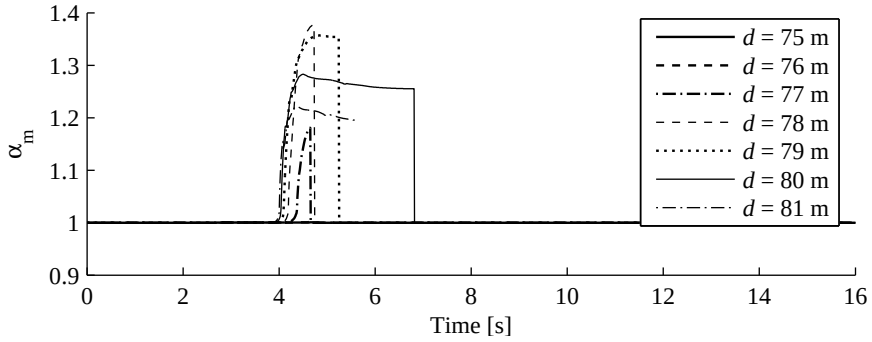

Figure 7.4: Time histories of α_{m}

If α_{m} exceeds 1.0, the absolute value of the acceleration will decrease. When the maximum displacement is approached in a case with some (but not excessive) plastic behaviour, the acceleration is frequently negative, retarding the movement (see Figures 7.6(c) and 7.7(c)). A reduced retardation (attributed to α_{m}) leads to increased displacement compared to a SDOF computation disregarding the effect of α_{m}. Thus for the medium water depths analysed and their corresponding 'medium' forces, the modified SDOF model gives larger displacements than the original SDOF model.

Water depths $d = 75$ m and $d = 77$ m, see Figures 7.5 and 7.6 The dynamic response calculated for the case with $d = 75$ m by both FE analysis and SDOF analyses is purely elastic, and the original and the modified SDOF therefore give identical results. For $d = 77$ m the structure experiences some plastic deformations, resulting in the modified SDOF model giving slightly larger displacements than the original SDOF model. The stiffness properties used for the SDOF analyses are calculated for the load distribution when the deck load is at its maximum at $t = 4.1$ s (see Section 7.2). For these water depths this neither coincides with the largest total load on the platform nor is the most unfavourable with respect to displacement of the deck.

For $d = 75$ m the SDOF models compute displacement-, velocity- and acceleration responses in relatively good agreement with the FE analyses. They underestimate the maximum displacement by some 6%. Essentially the SDOF results are between the 'FE wave' and 'FE c. d.' results.

The SDOF models underestimates the maximum displacement by some 8 - 9% for $d = 77$ m, the modified SDOF giving 1% larger displacement than the original SDOF. At this water depth, the SDOF responses clearly follow the responses for the FE constant load distribution case, whereas the FE variable distribution case has both larger velocity and accelerations, resulting in larger vibration amplitudes following the maximum displacement. This illustrates the significance of the variation in load distribution through the wave cycle, an effect which is not captured in the SDOF models.

Water depth $d = 79$ m, see Figure 7.7 The modified SDOF model computes 13% larger maximum displacement than the 'FE wave' analysis, and the original SDOF model results in 3% overestimation. The modified SDOF gives a value which is almost 10% larger than the original SDOF. The displacement response resulting from the 'FE c. d.' analysis is of the same nature as the SDOF analyses, whereas the 'FE wave' analysis have larger 'residual' amplitudes following the maximum displacement. This is true for both displacement-, velocity- and acceleration response.

Water depths $d = 80$ m and $d = 81$ m, see Figures 7.8 and 7.9 Both the 'FE c. d.' analysis and the SDOF analyses highly overestimates the displacement compared to the 'FE wave' analysis. The effect of the variable distribution of the load becomes even more pronounced than in the cases with smaller water depths and correspondingly smaller total load.

The modified SDOF computes 6% smaller displacement than the original SDOF at $d = 80$ m.

The SDOF analyses and the 'FE c. d.' analysis breaks down for the $d = 81$ m case. The acceleration grows unlimited, and therefore also the displacement. However, the 'FE wave' analysis with variable load distribution results in limited maximum displacement (1.03 m) and acceleration (2.07 m/s^2).

Again, the effect of the variation of the load distribution following the variation in sea surface level is seen to be to a considerable extent determining for the response.

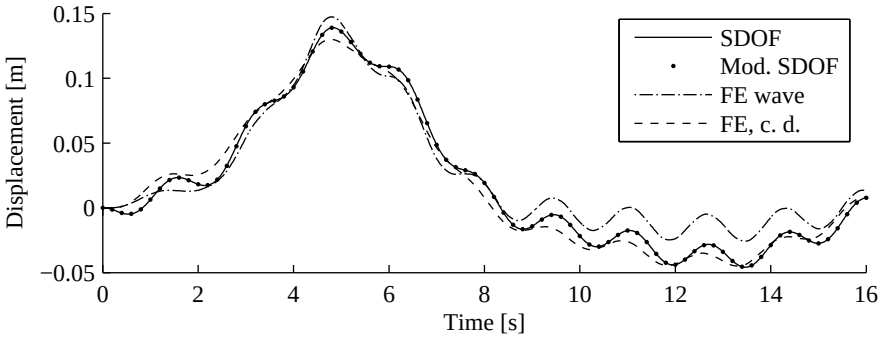

(a) Displacement

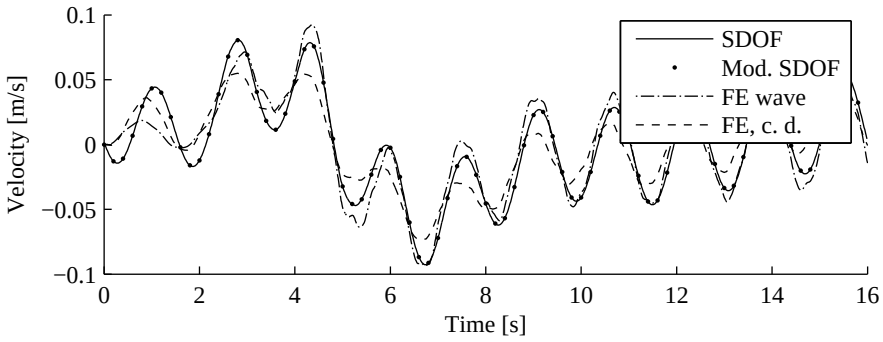

(b) Velocity

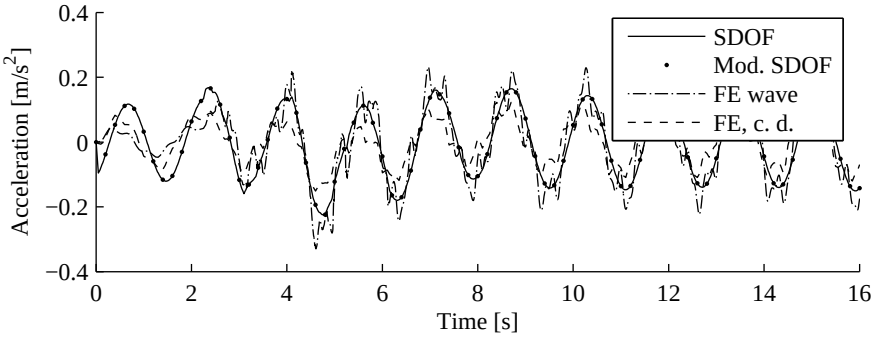

(c) Acceleration

Figure 7.5: Response at $d = 75$ m

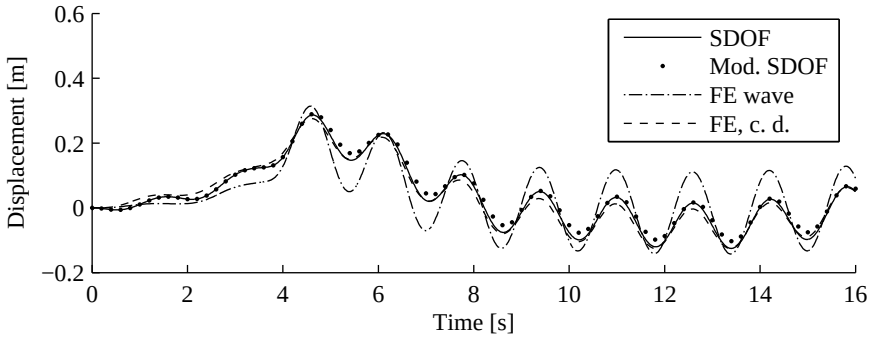

(a) Displacement

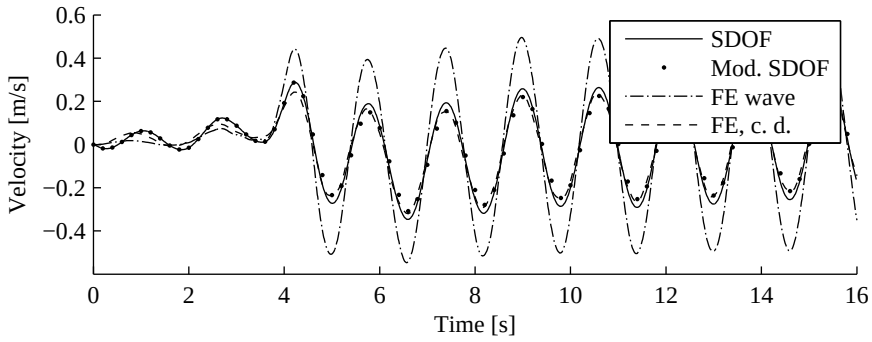

(b) Velocity

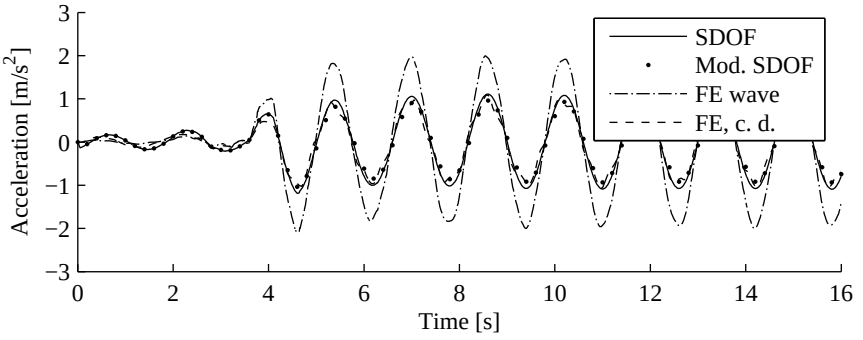

(c) Acceleration

Figure 7.6: Response at $d = 77$ m

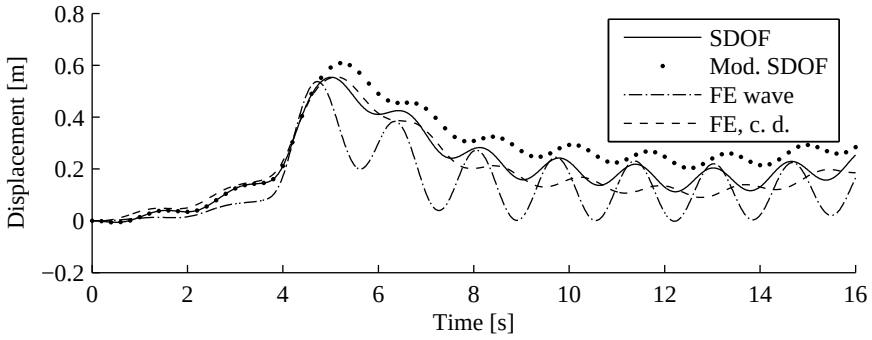

(a) Displacement

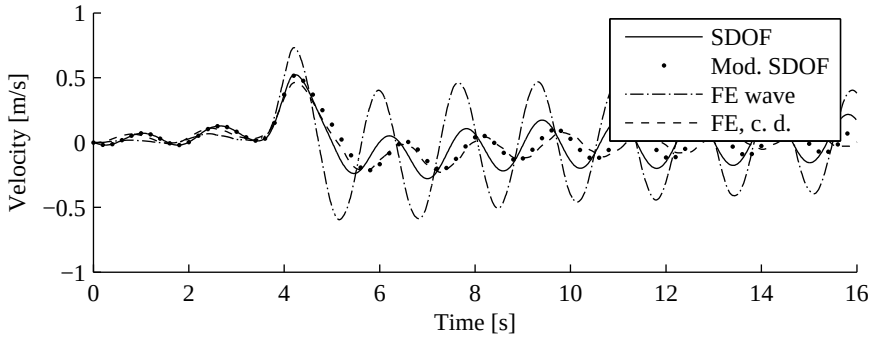

(b) Velocity

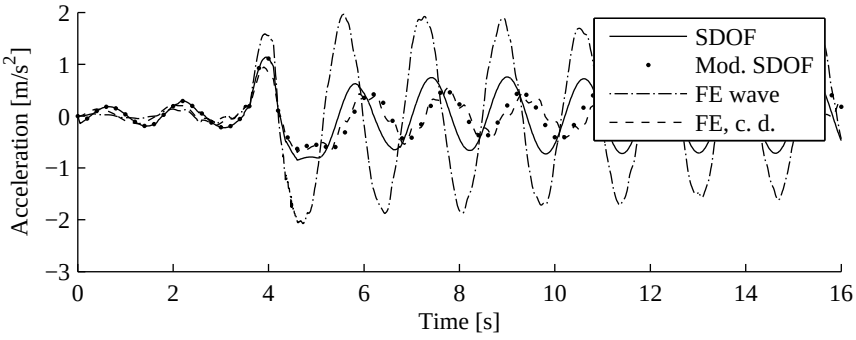

(c) Acceleration

Figure 7.7: Response at $d = 79$ m

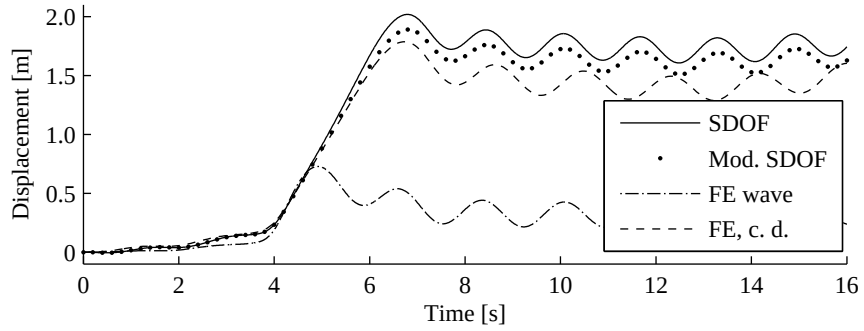

(a) Displacement

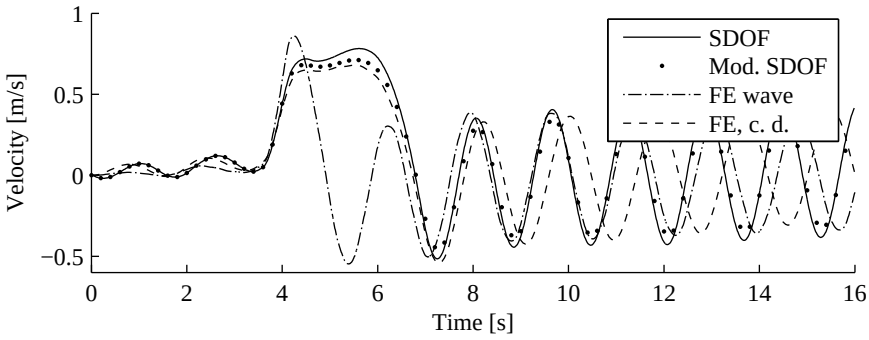

(b) Velocity

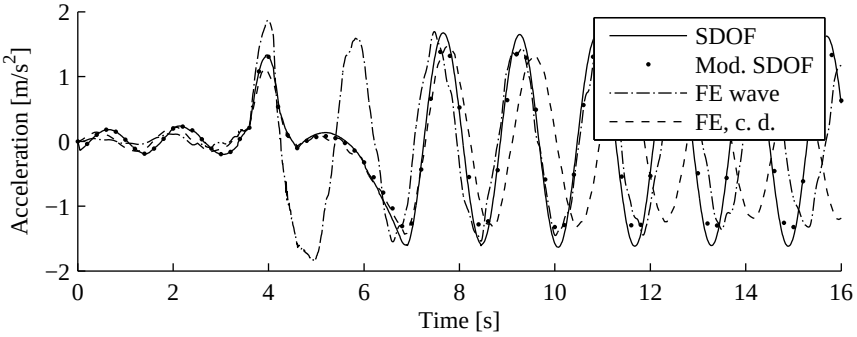

(c) Acceleration

Figure 7.8: Response at $d = 80$ m

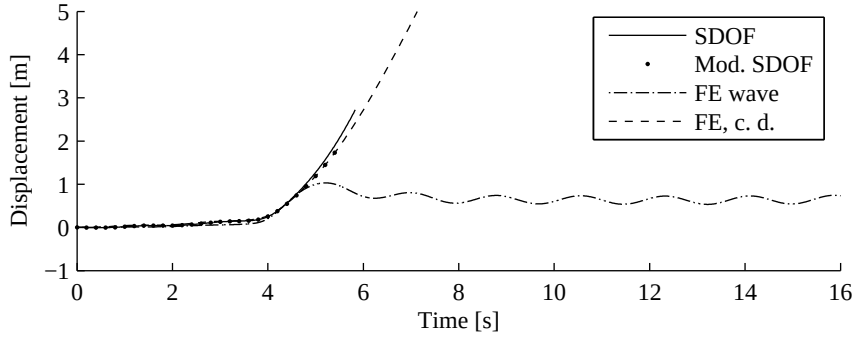

(a) Displacement

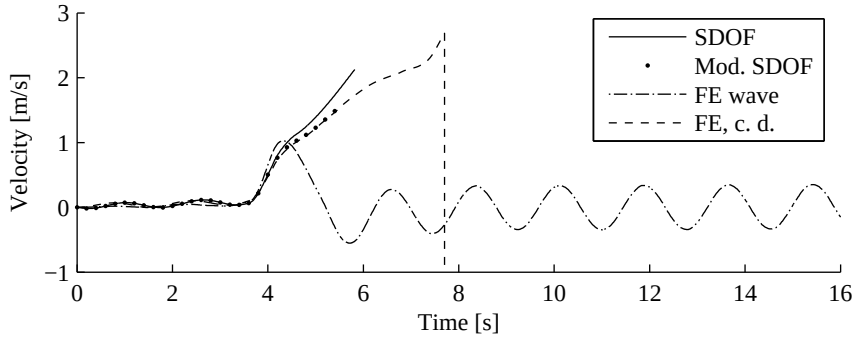

(b) Velocity

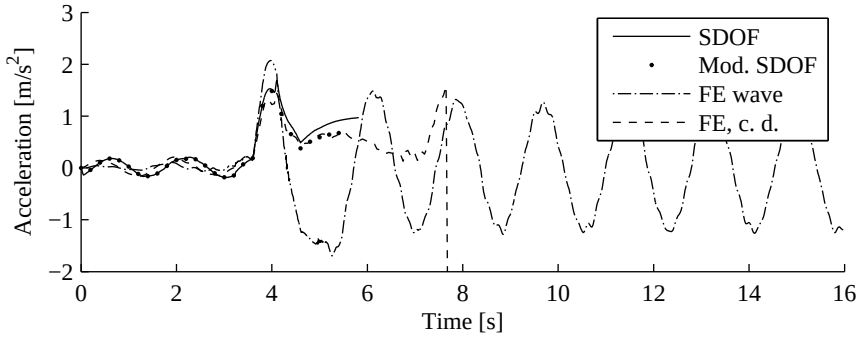

(c) Acceleration

Figure 7.9: Response at $d = 81$ m

7.4 Discussion

Surface elevation

Figures 7.5 to 7.9, in particular the two last ones, illustrate clearly that the effect of the variation in surface elevation through the wave cycle is significant.

The static resistance curve R_{f} is based on the load distribution at *one* chosen instant in time. The SDOF model is based solely on this resistance curve, it is thus implicitly assumed that the load distribution at any time instant is identical to the distribution used to establish the R_{f} curve. This is obviously an assumption with important implications.

If neglecting the dynamic effects (damping, if included, and inertia forces), what remains is a time depended static displacement. For the SDOF models this displacement curve is based on the stiffness as given by the static resistance curve, whereas a FE program will compute the displacements from the instant and true load distribution. The displacement response arising from such a time domain simulation of the $d = 79$ m case (plasticity is neglected) illustrates this, see Figure 7.10.

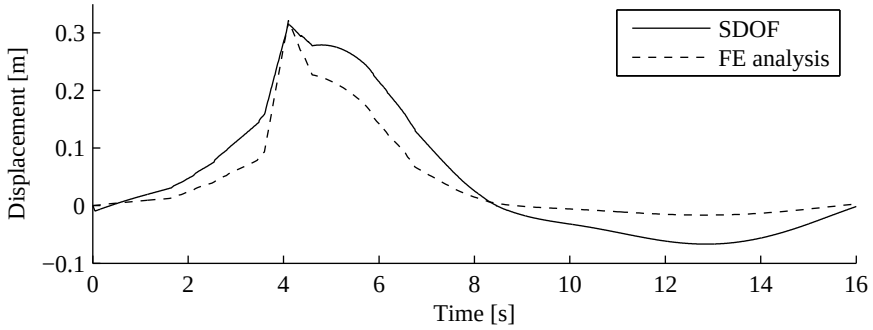

Figure 7.10: Example of elastic displacement response without inertia effects

Clearly, the effect of the load on the displacement of the reference point (at the deck level) in the FE analysis is smaller than in the SDOF analysis, except for at that time instant where the FE model is subjected to a load distribution which equals the distribution that characterises the SDOF model. At all other times, the FE model is subjected to a load distribution which has less effect on the displacement of the reference point, i.e. a load distribution which makes the structure respond stiffer. We can define a *load effect*, limited to elastic behaviour, as follows:

$$\alpha_{\mathrm{F}}(t) = \frac{u_{\mathrm{s,FE}}(t)}{u_{\mathrm{s,SDOF}}(t)} = \frac{F_{\mathrm{e}}(t)}{k_{\mathrm{FE}}(t)} \cdot \frac{k_{\mathrm{f}}}{F_{\mathrm{e}}(t)} = \frac{k_{\mathrm{f}}}{k_{\mathrm{FE}}(t)} \tag{7.1}$$

where $k_{\mathrm{FE}}(t) = F_{\mathrm{e}}(t)/u_{\mathrm{s,FE}}$, i.e. the total force divided by the 'static' displacement of the reference point calculated by FE analysis. Note that this measure is not defined for zero

displacement. Note also that load effect must be defined relative to a chosen load distribution, in our case the distribution relevant at the time for maximum wave-in-deck load. For the above case $\alpha_{\mathrm{F}} \leq 1$ for all nonzero values of u, indicating that the real effect of the load is smaller than it would have been if the load distribution remained constant and equal to the max-load distribution (which is the basis for the SDOF models). The SDOF models are thus 'pessimistic' during most of the simulation time. If the chosen load distribution is the one giving the largest displacement response for the reference point (i.e. giving the lowest stiffness), the calculated stiffness (k_{f}) is smaller than the true stiffness $k_{\mathrm{FE}}(t)$ arising from the instant load distribution at all time instants except for the time of the maximum loading.

SDOF analyses vs. 'FE wave' analyses

The SDOF models compute maximum displacements that are in good agreement with the FE analysis results for load conditions that give elastic or near elastic response, despite the fact that the resistance curve is based on a load distribution that is only true at one single instant in time. The general reason for this is that such load conditions imply limited wave-in-deck loads. With limited wave-in-deck loads the vibration amplitudes are accordingly limited, and the main contribution to the total displacement is the static, elastic displacement. I.e. there will only be limited displacement oscillations around the curves given in Figure 7.10, which have the same values at maximum displacement.

It is, however, clear from the response curves given that the FE analysis with variable load distribution ('FE wave') differ in nature from both the SDOF results and the results from the FE analysis with constant load distribution ('FE c. d.').

Acceleration for a SDOF model is determined from

$$\ddot{u} = \frac{1}{m\ \alpha_{\mathrm{m}}(u)} \left(F(t) - R_{\mathrm{f}}(u)\right) \tag{7.2}$$

If transferring this to the FE model, one must imagine that the term $F(t) - R_{\mathrm{f}}(u)$, is smaller because of the smaller load effect / larger stiffness which affects R_{f}. In other words, the structural stiffness is greater in 'real life' than given by R_{f}. Smaller load effect leads to smaller acceleration. But as the time of maximum wave-in-deck loading is approached, the stiffness of the FE model decreases, and the term in parentheses grows quicker in the FE model than in the SDOF model. This results in a more rapid increase in acceleration and therefore displacement response for the FE model than for the SDOF model. Which one of the models - FE or SDOF - that finally will give the largest (maximum) displacement depends on how pronounced the load effect is prior to this, as well as other factors such as degree of plastic behaviour. The load effect will typically be less pronounced for load conditions that give small wave-in-deck loads and more pronounced for conditions that give large wave-in-deck loads.

For all the analysed cases the 'FE wave' analyses give larger positive acceleration peak value around the time for the maximum load than the SDOF models. The consequences of this

is that the 'FE wave' model yields slightly larger displacement than the SDOF model, however *only for analysis cases with elastic response or with limited plastic deformation*. The SDOF model will enter the plastic domain earlier in the load history than the 'FE wave' model, and the displacements, which obviously grow faster in this domain, will reach a larger value before the unloading starts. This influences the maximum displacement increasingly for increasing inundation. The SDOF model therefore overestimate maximum displacements increasingly compared to the 'FE wave' analyses as the inundation and the external load increase.

Skallerud and Amdahl (2002, Section 9.4) present an example of application of their SDOF model[2] to an undamped jacket platform with ductile and semi-ductile (static) resistance. The results are presented in form of ductility spectra and the maximum response for the actual natural period of the system. The resulting maximum displacement responses are compared to results from finite element analysis of the jacket (reported by Stewart (1992)). The SDOF analyses underpredicted the FE results by some 20 - 30%. The agreement is in the book characterised as 'not bad in view of the inaccurate representation of the resistance curve and the load history'. The exact meaning of 'inaccurate representation of the load history' is, however, not clear. It might imply that the load history is read from the illustration of the load in Stewart's paper, it might comprise the fact that the variation of load distribution for the jacket cannot be included in the SDOF model, or it might be a combination of the two. It is, however, in the opinion of the author of this thesis, impossible to know how much of the deviation that really can be attributed to inaccurate input values, and how much is a result of the simplification of the jacket structure to a SDOF model. It is, on the other hand, clear from this thesis that the simplification of a MDOF system to a SDOF system of the type used in this thesis in itself leads to a considerable miscalculation of the response compared to finite element analysis. The deviation mainly arises from disregarding the time variation of the load distribution in the SDOF analysis, and this miscalculation is increased with increasing permanent plastic deformations.

Modified SDOF vs. original SDOF

The combination of structural configuration and external load distribution result in $\alpha_{\mathrm{m}}(u) \geq 1.0$ for relevant displacements for all analysed cases. This leads to smaller acceleration absolute value for the modified SDOF model (for details on $\alpha_{\mathrm{m}}(u)$ see Section 6.5.2). Compared to the original SDOF model, the result is a reduction of displacement if the acceleration has the same sign as the displacement, and an increase of displacement if acceleration and displacement have opposite sign.

The modified SDOF model computes reduced displacements compared to the original SDOF model under loading conditions that lead to a large degree of plastic deformation. For loading conditions that result in elastic or near elastic response, the modified SDOF model will yield increased displacements. This is in accordance with the description of α_{m}'s manner of

[2] This SDOF model is formulated identically to the 'original SDOF model' presented in this thesis — see Section 6.3.

operation in Section 6.5.2. However, the differences between the two SDOF approaches are relatively small.

Chapter 8

Conclusions and recommendations

8.1 Summary and conclusions

The aim of this doctoral work has been to improve the understanding of the dynamic effects of wave-in-deck loading on the response of jacket platforms. Finite element analyses have been used to simulate response time series. In addition, and as an inherent part of the work, simplified methods for calculation of wave-in-deck load magnitude and time history have been evaluated and the use of a simplified model to predict response to wave-in-deck loading has been investigated.

In the following, the work carried out is summarised. The item lists comprise the conclusions drawn from each part of the work.

Wave-in-deck loading

An overview over existing methods or approaches for the estimation of wave-in-deck loading is given.

Further, formulae for calculation of simplified load time histories based on linear (Airy) wave theory combined with drag and two different momentum wave-in-deck load approaches, denoted *Mom* and *Mom-Vinje*, are presented. In addition, these drag and momentum approaches are used to obtain wave-in-deck load histories with wave kinematics based on Stokes 5th order wave theory.

The formulae mentioned above was compared with reported wave-in-deck load time histories from a study in which computational fluid dynamics (CFD) technique was used to calculate wave-in-deck loading on idealised platform decks.

The findings were:

- The momentum approach denoted *Mom* is identical to a drag approach with $C_{\mathrm{d}} = 2$.

- ⋆ The *Mom-Vinje* momentum approach is *approximately* equal to a drag approach, however in our case for an equivalent C_{d} of ~ 5.6 for Airy theory and ~ 4.1 for Stokes 5th order theory. The C_{d} needed to match the *Mom-Vinje* approach and a drag approach is dependent on the wave scenario.
- ⋆ With the two above items in mind, it is concluded that the question of whether to use drag or momentum formulation reduces to a question of which drag factor to use, alternatively which one of of the two momentum approaches to use.
- ⋆ A simplified formulae are probably adequate for establishment of wave-in-deck force histories for a simple hull- or box-like deck geometry.

The main results from wave-in-deck load experiments related to a possible subsidence scenario at the Statfjord field in the northern North Sea are referred. These results are further evaluated for the purpose of being used as a basis for the calculation of wave-in-deck load time histories for the jacket models used in this thesis.

An expression for the estimation of a reference load value (Equation 4.20), which together with the given time history (Figure 4.12) is sufficient to establish a 'rough but reasonable' load time history for wave-in-deck loading on jacket structures, has been presented. The method in general, and its validity range in particular, should be subject to wave tank testing in order to obtain more data supporting, or possibly updating, the method.

The results from the Statfjord experiments also show that the vertical wave-in-deck loads are of the same magnitude as the horisontal loads. The vertical loading should be included in any platform (re)assessment study that includes wave-in-deck forces. Vertical loads have been outside the scope of the present work.

Time domain finite element analyses of jacket structures

Two jacket models with different brace configurations, and therefore different post collapse behaviour, are analysed under static and dynamic assumptions using finite element methodology. The external loading comprises extreme wave loading, wave-in-deck loading as defined in Chapter 4, current and buoyancy loading. Increasing wave-in-deck loading is simulated by increasing the water depth, corresponding to increasing seabed subsidence.

The following conclusions are drawn from the results of the analyses:

- ⋆ Wave-in-deck forces influence a structure not only by their magnitude, which is significant compared to the wave load on the jacket itself, but also because they alter the load distribution in a manner that introduces high forces into (relatively) weaker parts of the structure such as the deck legs (immediately below the deck).
- ⋆ Whereas static ultimate capacity is a unique and informative measure of nonlinear structural performance *when related to a given load distribution*, the dynamic performance should be evaluated against allowable response values, such as displacements and accelerations, at relevant locations in the structure *for each single load scenario*.

- ⋆ Typical jacket structures with a first natural period of a few seconds will experience dynamic amplification, i.e. increase of response, when subjected to wave-in-deck load histories as the ones used herein. This applies to both the displacement response and the base shear forces.
- ⋆ Typical jacket structures that can be characterised as ductile may resist dynamic loading with higher peak load than its static capacity relevant for the same load distribution. For load durations typical for wave-in-deck loading, this favourable effect is attributed to the beyond-ultimate-capacity ductility of the structure as opposed to any attenuating effects of the inertia of the mass (in fact, all analyses show dynamic amplification).

  On the other hand, brittle jackets may collapse under dynamic loading that is considerably smaller than the static capacity associated with the load distribution in question.
- ⋆ In case of wave-in-deck loading, acceptable displacements may correspond to excessive accelerations. It is therefore important to pay explicit attention to acceleration response during (re)assessment of structures. In the present study, accelerations are considerably more pronounced for the brittle structural model than for the ductile one, although the latter has larger displacement response.

The simplified model for response analyses

The nature of structural response to external load as opposed to that of inertia forces is discussed. The *static* deflected shape of a structural system due to a given load distribution is used as a basis. It is demonstrated how *dynamic* considerations, including the presence of mass, alter the deflected shape — and consequently the global stiffness — of the structure.

- ⋆ The mass distribution, which leads to a different distribution for the inertia forces than for the externally applied load, results during vibrations in a deflected shape differing from the static deflected shape. During vibration, the deflected shape of the jacket may be more or less curved (‘softer’ or ‘stiffer’) than the static deflected shape. As a consequence, yielding may be initiated at a different displacement level and the ultimate capacity expressed as e.g. base shear may be changed (relative to static behaviour).

A simplified method to assess structural dynamic response is presented. The method is a single-degree-of-freedom (SDOF) model built around a static pushover analysis with a given external load distribution. The application of the SDOF model is demonstrated on a cantilever with distributed and concentrated mass subjected to a triangularly distributed load. The resulting response is compared to response obtained by finite element analysis of the cantilever structure. The following conclusions are drawn:

- ⋆ In the case where the response remains elastic, good agreement is obtained between SDOF computation and finite element analysis for displacement response. There is also good agreement for the support forces.

- ⋆ In the case where the response is brought into the plastic domain there is a clear deviation both in the calculated displacement time history, permanent displacement and support force between the SDOF analysis and the finite element analysis.

In lieu of the deviations between the SDOF model and FE analyses found when using the above mentioned ('original') SDOF model, a modification to the mass term is suggested. The modification is based on the stated differences in behaviour under externally applied loading and inertia 'loading'. The modification is included in a 'modified SDOF model' in the form of a *mass term multiplier* which is dependent on the instant displacement, denoted $\alpha_{\mathrm{m}}(u)$ where u is the displacement. This mass term modifier is determined based on the resistance curve under the applied loading in question and the resistance curve under loading with the same distribution as the inertia forces in the relevant vibration mode.

Examining the mass multiplier and applying the modified SDOF model to the cantilever structure it becomes clear that:

- ⋆ The mass modifier α_{m} provides a quantification of the differences between the distribution of externally applied load and inertia forces, the latter corresponding to the vibration mode in question and the mass distribution, in terms of stiffness and capacity.
- ⋆ The mass modifier α_{m} directly influences the magnitude of the acceleration.
- ⋆ By taking into account the nonlinear behaviour under pure inertia loading using α_{m} , better agreement is achieved between the SDOF analyses and the FE analyses.

The original and the modified SDOF models are further used to compute the response of a real jacket, namely the jacket model 'DS' which was previously analysed by use of finite element technique. The response determined by use of FE analysis is used to evaluate the quality of the results computed by the SDOF models. In addition, another set of FE analyses is run for all loading scenarios with a load time history of which the magnitude is identical to the wave load time history, but with a *non-varying spatial load distribution*.

The conclusions drawn from this part of the work are:

- ⋆ Loading conditions that imply limited wave-in-deck loading do lead to elastic or near elastic response, i.e. to no or only limited plastic deformations. These loading conditions do only generate limited dynamic response compared to the quasi-static response. For the larger levels of inundation and correspondingly larger wave-in-deck loading, the dynamic part of the response is increasing. The wave-in-deck loading then contributes significantly to the structural dynamics.
- ⋆ For loading conditions leading to limited dynamic response, i.e. conditions with limited wave-in-deck loading, the SDOF models yields maximum displacement response in good agreement with the FE analyses.
- ⋆ As the loading conditions worsens and the inundation and the plastic permanent displacement increase the SDOF models overestimate the response increasingly.

- ⋆ The differences between the original and the modified SDOF model are minor compared to the deviations from the finite element results for cases involving a certain degree of plastic deformation.
- ⋆ The effect of the variation of the load distribution through a wave cycle is considerable, and is not included in the SDOF models. This effect is the main error source when applying the SDOF models to a case that includes varying load distribution. This should motivate future investigation of the SDOF models and in particular the mass modifier α_{m} for loading situations with non-varying load distributions.
- ⋆ The miscalculation of the response attributed to the time variation of the load distribution when using any of the SDOF models becomes more pronounced for increasing plastic deformation.
- ⋆ Within a short time prior to maximum wave-in-deck load, that is as the wave crest approaches the deck front wall and the sea surface elevation increases, the total wave load distribution changes rapidly in the way that the resultant horisontal load vector translates upwards (in positive z-direction). If relating the external load to the resulting horisontal displacement of the topside, the effect corresponds to a stiffer jacket behaviour changing towards a softer jacket behaviour.

  This rapid change in load *distribution* prior to maximum load leads to a different development of accelerations for real wave-in-deck loading compared to loading with non-varying distribution. The development of the acceleration for the real wave-in-deck loading is favourable in the sense that it retards the structural motion and thereby contributes to the structural ability to resist large dynamic load of limited duration.

8.2 Recommendations for further work

It is further desirable to perform investigations of dynamic response under wave-in-deck loading including damping and relevant pre-load histories implying initial values different from zero.

The effect of using overturning moment instead of base shear as a measure of loading and capacity in the SDOF models could be a further step from the present work. It would also be interesting to use a load time history based on the dashed curve of Figure 7.10 as opposed to the solid curve (the curves represent displacements, however, loads are given by multiplying with the elastic stiffness).

Acceleration levels are identified as a point of concern in this work, however the effect of brittle vs. ductile structural behaviour on acceleration levels could be investigated more thoroughly.

Waves that are large enough to reach the deck of an offshore platform generate not only horisontal but also vertical forces. The vertical forces are of considerable magnitude, and their influence on the dynamic performance of offshore structures should be subject to further investigations.

Validation of the recommendations relating to wave-in-deck load time history in Chapter 4 through tank tests of wave-in-deck loading on jacket decks would be strongly recommended. Particularly the validity range in terms of inundation should be examined.

Bibliography

Amdahl, J., Skallerud, B. H., Eide, O. I., and Johansen, A. (1995). Recent developments in reassessment of jacket structures under extreme storm cyclic loading, part II: Cyclic capacity of tubular members. In *Proceedings of the 14th International Conference on Offshore Mechanics and Arctic Engineering (OMAE) 1995*, Copenhagen, Denmark.

API LRFD (1993). *Recommended practice for planning, designing and constructing fixed offshore platforms - Load and resistance factor design (API RP2A-LRFD)*. American Petroleum Institute, Washington, DC, USA, first edition.

API LRFD (2003). *Recommended practice for planning, designing and constructing fixed offshore platforms - Load and resistance factor design (API RP2A-LRFD)*. American Petroleum Institute, Washington, DC, USA, first edition. Reaffirmed May 2003.

API WSD (2002). *Recommended practice for planning, designing and constructing fixed offshore platforms - Working stress design (API RP2A-WSD)*. American Petroleum Institute, Washington, DC, USA, twenty-first (2000) edition. Including errata and supplement 1.

Bea, R., Mortazavi, M., Stear, J., and Jin, Z. (2000). Development and verification of Template Offshore Capacity Analysis Tools (TOPCAT). In *Proceedings of the 32nd Annual Offshore Technology Conference 2000*, Houston, Texas, USA.

Bea, R. G. (1993). Reliability based requalification criteria for offshore platforms. In *Proceedings of the 12th International Conference on Offshore Mechanics and Arctic Engineering (OMAE) 1993*, Glasgow, Scotland.

Bea, R. G., Iversen, R., and Xu, T. (2001). Wave-in-deck forces on offshore platforms. *Journal of Offshore Mechanics and Arctic Engineering*, volume 123:pp. 10 – 21.

Bea, R. G. and Lai, N. W. (1978). Hydrodynamic loadings on offshore platforms. In *Proceedings of the 10th Annual Offshore Technology Conference 1978*, volume 1, pages 155 – 168, Houston, Texas, USA. OTC 3064.

Bea, R. G. and Mortazavi, M. M. (1996). ULSLEA: A limit equilibrium procedure to determine the ultimate limit state loading capacities of template-type platforms. *Journal of Offshore Mechanics and Arctic Engineering*, volume 118(no. 4):pp. 267 – 275.

Bea, R. G., Xu, T., Stear, J., and Ramos, R. (1999). Wave forces on decks of offshore platforms. *Journal of Waterway, Port, Coastal, and Ocean Engineering*, volume 125(no. 3):pp. 136 – 144.

Bea, R. G. and Young, C. (1993). Loading and capacity effects on platform performance in extreme condition storm waves and earthquakes. In *Proceedings of the 25th Annual Offshore Technology Conference 1993*, Houston, Texas, USA.

Bergan, P. G., Larsen, P. K., and Mollestad, E. (1981). *Svingning av konstruksjoner*. Tapir. (In Norwegian).

Biggs, J. M. (1964). *Introduction to structural dynamics*. McGraw-Hill.

Blevins, R. D. (1979). *Formulas for natural frequency and mode shape*. Van Nostrand Reinhold Company Inc.

Bolt, H. M. and Billington, C. J. (2000). Results from ultimate load tests on 3d jacket-type structures. In *Proceedings of the 32nd Annual Offshore Technology Conference 2000*, Houston, Texas, USA.

Bolt, H. M. and Marley, M. (1999). Regional sensitivity and uncertainties in airgap calculations. In *Proceedings from HSE / E & P Forum Airgap Workshop*, London, England.

Chakrabarti, S. K. (1987). *Hydrodynamics of offshore structures*. Computational Mechanics Publications.

Clough, R. W. and Penzien, J. (1993). *Dynamics of structures*. McGraw-Hill, Inc., second edition.

Dalane, J. I. and Haver, S. (1995). Requalification of an unmanned jacket structure using reliability methods. In *Proceedings of the 27th Annual Offshore Technology Conference 1995*, Houston, Texas, USA. OTC 7756.

Det Norske Veritas (1991). *Environmental conditions and environmental loads*. Oslo, Norway. Classification note No. 30.5.

Det Norske Veritas (2000). *Environmental conditions and environmental loads*. Oslo, Norway. Classification note No. 30.5.

Ditlevsen, O. and Arnbjerg-Nielsen, T. (1994). Model correction factor method in structural reliability. *Journal of Engineering Mechanics, ASCE*, vol. 120(no. 1):1 – 10.

Eberg, E., Hellan, Ø., and Amdahl, J. (1993). Nonlinear re-assessment of jacket structures under extreme storm cyclic loading: Part III - the devlopment of structural models for cyclic response. In *Proceedings of the 12th International Conference on Offshore Mechanics and Arctic Engineering (OMAE) 1993*, Glasgow, Scotland.

Eide, O. I., Amdahl, J., Skallerud, B. H., and Johansen, A. (1995). Recent developments in reassessment of jacket structures under extreme storm cyclic loading, part I: Overview. In *Proceedings of the 14th International Conference on Offshore Mechanics and Arctic Engineering (OMAE) 1995*, Copenhagen, Denmark.

Eik, K. J. (2005). Personal communication, Statoil ASA.

Emami Azadi, M. R. (1998). *Analysis of static and dynamic pile-soil-jacket behaviour*. PhD thesis, Norges teknisk-naturvitenskapelige universitet (NTNU), Trondheim, Norway. No. 1998:52.

Ersdal, G. (2005). *Assessment of existing offshore structures for life extension*. PhD thesis, University of Stavanger (UiS), Norway. To be published.

Finnigan, T. D. and Petrauskas, C. (1997). Wave-in-deck forces. In *Proceedings of the 7th International Offshore and Polar Engineering Conference 1997*, volume III, pages 19–24, Honolulu, Hawaii, USA.

Fjellså, O. (2005). Personal communication, BP Norway.

Grenda, K. G., Clawson, W. C., and Shinners, C. D. (1988). Large-scale ultimate strength testing of tubular K-braced frames. In *Proceedings of the 20th Annual Offshore Technology Conference 1988*, Houston, Texas, USA.

Grønbech, J., Sterndorff, M. J., Grigorian, H., and Jacobsen, V. (2001). Hydrodynamic modelling of wave-in-deck forces on offshore platform decks. In *Proceedings of the 33nd Annual Offshore Technology Conference 2001*, Houston, Texas, USA. OTC 13189.

Gudmestad, O. T. (1993). Measured and predicted deep water wave kinematics in regular and irregular seas. *Journal of Marine Structures*, volume 6(no. 1):pp. 1 – 73.

Gudmestad, O. T. (2000). Challenges in requalification and rehabilitation of offshore platforms. On the experience and developments of a Norwegian operator. *Journal of Offshore Mechanics and Arctic Engineering*, volume 122(no. 1):pp. 3 – 6.

Gudmestad, O. T. (2005). Personal communication, Statoil ASA / Universtiy of Stavanger.

Hansen, K. (2002). Use of simplified structural models to predict dynamic response to wave-in-deck loads. In *Structural Dynamics EURODYN 2002*, volume volume 2, pages pp. 1209 – 1215, München, Germany.

Hansen, K. and Gudmestad, O. T. (2001). Reassessment of jacket type of platforms subject to wave-in-deck forces – current practice and future development. In *Proceedings of the 11th International Offshore and Polar Engineering Conference 2001*, Stavanger, Norway.

Haver, S. (1995). Uncertainties in force and response estimates. In *Uncertainties in the design process, Offshore structures/metocean workshop*, Surrey, England. E & P Forum Report No. 3.15/229.

Haver, S. and Kleiven, G. (2004). Environmental contour lines for design purposes - why and when? In *Proceedings of the 23st International Conference on Offshore Mechanics and Arctic Engineering (OMAE) 2004*, Vancouver, British Columbia, Canada.

Hellan, Ø., Amdahl, J., Brodtkorb, B., Holmås, T., and Eberg, E. (1998). *USFOS Users Manual*. SINTEF report STF71 F88039, rev. 98-04-01, Trondheim, Norway.

Hellan, Ø., Moan, T., and Drange, S. O. (1994). Use of nonlinear pushover analyses in ultimate limit state design and integrity assessment of jacket structures. In *Proceedings of the 7th International Conference on the Behaviour of Offshore Structures (BOSS) 1994*, Cambridge, Massachusetts, USA.

Hellan, Ø., Skallerud, B., Amdahl, J., and Moan, T. (1991). Reassessment of offshore steel structures: Shakedown and cyclic nonlinear FEM analyses. In *Proceedings of the 1st International Offshore and Polar Engineering Conference 1991*, volume IV, pages 34–42, Edinburgh, Scotland.

Hellan, Ø., Tandberg, T., and Hellevig, N. C. (1993). Nonlinear re-assessment of jacket structures under extreme storm cyclic loading: Part IV - case studies on existing north-sea platforms. In *Proceedings of the 12th International Conference on Offshore Mechanics and Arctic Engineering (OMAE) 1993*, Glasgow, Scotland.

Hilber, H. M., Hughes, T. J. R., and Taylor, R. L. (1977). Improved numerical dissipation for time integration algorithms in structural dynamics. *Earthquake Engineering and Structural Dynamics*, volume 5:pp. 283 – 292.

Hooper, J. R. and Suhayda, J. N. (2005). Hurricane Ivan as a geologic force: Mississippi delta front seafloor failures. In *Proceedings of the Offshore Technology Conference 2005*, Houston, Texas, USA. OTC 17737.

HSE (1997a). Comparison of reserve strength ratios of old and new platforms. Technical Report OTO 97 046, Health & Safety Executive, United Kingdom. Prepared by Brown & Root Ltd.

HSE (1997b). Review of wave-in-deck load assessment procedures. Technical Report OTO 97 073 (MaTSU/8781/3420), Health & Safety Executive, United Kingdom. Prepared by BOMEL and Offshore Design.

HSE (1998). Dynamic push-over analysis of jacket structures. Technical Report OTO 98 092 (AME/ 37037B01/R/02.2), Health & Safety Executive, United Kingdom. Prepared by Mott MacDonald Oil Gas & Maritime Division.

HSE (2001). Assessment of the effect of wave-in-deck loads on a typical jack-up. Technical Report Offshore Technology Report 2001 / 034, Health & Safety Executive, United Kingdom. Prepared by MSL Engineering Ltd.

HSE (2003). Sensitivity of jack-up reliability to wave-in-deck calculation. Technical Report Research Report 019, Health & Safety Executive, United Kingdom. Prepared by MSL Engineering Ltd.

ISO/CD 19902 (2001). *Petroleum and Natural Gas Industries - Fixed Steel Offshore Structures*.

Iwanowski, B., Grigorian, H., and Scherf, I. (2002). Subsidence of the ekofisk platforms: wave in deck impact study. various wave models and computational methods. In *Proceedings of the 21st International Conference on Offshore Mechanics and Arctic Engineering (OMAE) 2002*, Oslo, Norway.

Kaplan, P. (1992). Wave impact forces on offshore structures: Reexamination and new interpretations. In *Proceedings of the 24th Annual Offshore Technology Conference 1992*, Houston, Texas, USA.

Kaplan, P., Murray, J. J., and Yu, W. C. (1995). Theoretical analysis of wave impact forces on platform deck structures. In *Proceedings of the 14th International Conference on Offshore Mechanics and Arctic Engineering (OMAE) 1995*, Copenhagen, Denmark.

Kvitrud, A. and Leonhardsen, R. L. (2001). Driftserfaringer av offshore stålkonstruksjoner, med fokus på de innrapporterte skadene på bærekonstruksjonene, og knyttet mot årsaker og tiltak. Norsk Stålforening, Oslo 31 May 2001. In Norwegian.

Langen, I. and Sigbjörnsson, R. (1979). *Dynamisk analyse av konstruksjoner*. Tapir. (In Norwegian).

Madland, M. V. (2005). Personal communication, University of Stavanger.

Manuel, L., Schmucker, D. G., Cornell, C. A., and Carballo, J. E. (1998). A reliability-based design format for jacket platforms under wave loads. *Journal of Marine Structures*, volume 11(no. 10):pp. 413 – 428. Elsevier.

Manzocchi, G. M., Shetty, N. K., and Gierlinski, J. T. (1999). Implications of wave-in-deck forces on the reliability of offshore platforms. In *Proceedings from HSE / E & P Forum Airgap Workshop*, London, England.

Moan, T. (1998a). Research & applications developments. In *Proceedings of an International Workshop on Platform Requalification*, Lisbon, Portugal. Arranged at OMAE 1998.

Moan, T. (1998b). Target levels for structural reliability and risk analysis of offshore structures. In *Risk and Reliability in Marine Technology*. A.A. Balkema.

Moan, T., Hellan, Ø., and Emami Azadi, M. R. (1997). Nonlinear dynamic versus static analysis of jacket systems for ultimate limit state check. In *Proceedings from International Conference on Advances in Marine Structures III*, Dunfermline, Scotland.

Morin, G., Bureau, J. M., Contat, N., and Goyet, J. (1998). Influence of tubular joints failure modes on jacket structures global failure modes. In *Proceedings of the 17th International Conference on Offshore Mechanics and Arctic Engineering (OMAE) 1998*, Lisbon, Portugal.

Mouawad, J. (2005). Katrina may reshape oil platform criteria. Newspaper article, International Herald Tribune, 16 September 2005. http://www.iht.com/articles/2005/09/15/business/rigs.php.

Newmark, N. M. (1959). A method of computation for structural dynamics. *Journal of the Engineering Mechanics Division, ASCE*, vol. 85(EM 3):67 – 94.

NORSOK N-001 (2004). *Structural design*, 4th edition. http://www.standard.no/.

NORSOK N-003 (1999). *Actions and action effects*, 1st edition. http://www.standard.no/.

NORSOK N-004 (2004). *Design of steel structures*, 2nd edition. http://www.standard.no/.

NORSOK S-002 (2004). *Working environment*, 4th edition. http://www.standard.no/.

NS 4931 (1985). *Veiledning for bedømmelse av menneskers reaksjoner på lavfrekvente horisontale bevegelser (0.063 til 1 Hz) i faste konstruksjoner, særlig bygninger og installasjoner til havs*. Norges Standardiseringsforund (NSF).

O'Connor, P. E., Bucknell, J. R., DeFranco, S. J., Westlake, H. S., and Puskar, F. J. (2005). Structural integrity management (SIM) of offshore facilities. In *Proceedings of the Offshore Technology Conference 2005*, Houston, Texas, USA. OTC 17545.

Olagnon, M., Nerzic, R., and Prevosto, M. (1999). Extreme water level from joint distribution of tide, surge and crests: a case study. In *Proceedings of the 9th International Offshore and Polar Engineering Conference 1999*, Brest, France.

Pawsey, S., Driver, D., Gebara, J., Bole, J., and Westlake, H. (1998). Characterization of environmental loads on subsiding offshore platforms. In *Proceedings of the 17th International Conference on Offshore Mechanics and Arctic Engineering (OMAE) 1998*, Lisbon, Portugal.

Pemex / IMP (1998). *Criterio transitorio para la evaluación y el diseño de plataformas marinas fijas en la Sonda de Campeche* , segunda edición. Pemex Exploración y Producción, Instituto Mexicano del Petróleo (IMP), Mexico. In spanish.

Schmucker, D. G. (1996). *Near-failure behavior of jacket-type offshore platforms in the extreme wave environment*. PhD thesis, Stanford University, Stanford, California, USA.

Schmucker, D. G. and Cornell, C. A. (1994). Dynamic behaviour of semi-ductile jackets under extreme wave and wave-in-deck forces. In *Proceedings of the 7th International Conference on the Behaviour of Offshore Structures (BOSS) 1994*, Cambridge, Massachusetts, USA.

Sgouros, G. E., Pritchett, W. M., Schafer, D. R., and Jones, D. L. (2005). Shell's experience with Hurricane Ivan. In *Proceedings of the Offshore Technology Conference 2005*, Houston, Texas, USA. OTC 17733.

Sigurdsson, G., Skjong, R., Skallerud, B., and Amdahl, J. (1994). Probabilistic collapse analysis of jackets. In *Proceedings of the 13th International Conference on Offshore Mechanics and Arctic Engineering (OMAE) 1994*, Houston, Texas, USA.

SINTEF (1998). Ultiguide phase 2. Evaluation report on dynamic effects. Technical Report SINTEF: STF22 F98685, DNV: DNV 98-3097, SINTEF and DNV.

SINTEF GROUP (2001). *USFOS Getting Started*. Structural Engineering, Marintek, SINTEF GROUP. 'Light version' of the USFOS Theory Manual.

Skallerud, B. and Amdahl, J. (2002). *Nonlinear analysis of offshore structures*. Research Studies Press Ltd.

Skjelbreia, L. and Hendrickson, J. (1960). Fifth order gravity wave theory. In *Proceedings of Seventh Conference on Coastal Engineering*, pages 184 – 196, the Hague, the Netherlands.

Stansberg, C. T., Baarholm, R., Fokk, T., Gudmestad, O. T., and Haver, S. (2004). Wave amplification and possible deck impact on gravity based structure in 10^{-4} probability extreme crest heights. In *Proceedings of the 23st International Conference on Offshore Mechanics and Arctic Engineering (OMAE) 2004*, Vancouver, BC, Canada.

Statoil (2002). Statfjord A, slamming forces for design. Technical Report MTC-27-2, Statoil. Confidential report prepared by Marine Technology Consulting AS.

Stear, J. D. and Bea, R. G. (1997). Evaluating simplified analysis approaches for estimating the load capacities of Gulf of Mexico jacket-type platforms. In *Proceedings of the 16th International Conference on Offshore Mechanics and Arctic Engineering (OMAE) 1997*, Yokohama, Japan.

Sterndorff, M. J. (2002). Large-scale model tests with wave loading on offshore platform deck elements. In *Proceedings of the 21st International Conference on Offshore Mechanics and Arctic Engineering (OMAE) 2002*, Oslo, Norway.

Stewart, G. (1992). Non-linear structural dynamics by the pseudo-force influence part II: Application to offshore platform collapse. In *Proceedings of the 2nd International Offshore and Polar Engineering Conference 1992*, San Francisco, California, USA.

Stewart, G., Moan, T., Amdahl, J., and Eide, O. I. (1993). Nonlinear re-assessment of jacket structures under extreme storm cyclic loading: Part I - philosophy and acceptance criteria. In *Proceedings of the 12th International Conference on Offshore Mechanics and Arctic Engineering (OMAE) 1993*, Glasgow, Scotland.

Stewart, G. and Tromans, P. S. (1993). Nonlinear re-assessment of jacket structures under extreme storm cyclic loading: Part II - representative environmetal load histories. In *Proceedings of the 12th International Conference on Offshore Mechanics and Arctic Engineering (OMAE) 1993*, Glasgow, Scotland.

Søreide, T. H., Amdahl, J., Eberg, E., Holmås, T., and Hellan, Ø. (1993). *USFOS - A computer program for progressive collapse analysis of steel offshore structures. Theory Manual*. SINTEF report STF71 F88038, rev. 93-04-02, Trondheim, Norway.

Sørensen, J. D., Friis-Hansen, P., Bloch, A., and Nielsen, J. S. (2004). *Reliability analysis of offshore jacket structures with wave load on deck using the Model Correction Factor Method*. Draft, appendix in report 'Pålidelighedsvurdering af platforme udsat for bølgelast på dæk' prepared for Energistyrelsen (Denmark) by DHI Water and Environment, EFP-2001, j.nr. 1313/01-0019.

Tromans, P. S. and van de Graaf, J. W. (1992). A substantiated risk assessment of a jacket structure. In *Proceedings of the 24th Annual Offshore Technology Conference 1992*, Houston, Texas, USA. OTC 7075.

Tørum, A. (1989). Wave forces on pile in surface zone. *Journal of Waterway, Port, Coastal, and Ocean Engineering*, volume 115(no. 4).

van Raaij, K. and Jakobsen, J. B. (2004). Simplified dynamic analysis relevant for jackets exposed to wave-in-deck loading. In *Proceedings of the 14th International Offshore and Polar Engineering Conference 2004*, Toulon, France.

Vannan, M. T., Thompson, H. M., Griffin, J. J., and Gelpi, S. L. (1994). An automated procedure for platform strength assessment. In *Proceedings of the 26th Annual Offshore Technology Conference 1994*, Houston, Texas, USA. OTC 7474.

Vinje, T. (2001). Presentation given at Wave-in-deck Seminar at Statoil 17 January 2001. Printed in compendium from the seminar.

Vinje, T. (2002). Comments to the dnv rules regarding slamming pressures. Open note prepared for Statoil.

Wheeler, J. D. (1970). Method for calculating forces produced by irregular waves. *Journal of Petroleum Technology*, page 359.

Wisch, D., Stear, J., Versowsky, P., Welsch, J., and Abadin, J. (2005). Experiences from select shelf and deepwater fixed platforms during Hurricane Ivan. In *Proceedings of the Offshore Technology Conference 2005*, Houston, Texas, USA. OTC 17735.

Appendix A

Mathematical issues

A.1 2. central difference — a special case of the Newmark β method

In this appendix, it will be shown that the Newmark β method of numerical integration with parameters $\beta = 0$ and $\gamma = 1/2$ reduces to the 2. central difference method.

The general governing equations for the Newmark β method are given as follows (Langen and Sigbjörnsson, 1979):

$$u^{(s+1)} = u^{(s)} + \dot{u}^{(s)}\Delta t + (1/2 - \beta)\ddot{u}^{(s)}(\Delta t)^2 + \beta\ddot{u}^{(s+1)}(\Delta t)^2 \tag{A.1}$$

$$\dot{u}^{(s+1)} = \dot{u}^{(s)} + (1 - \gamma)\ddot{u}^{(s)}\Delta t + \gamma\ddot{u}^{(s+1)}\Delta t \tag{A.2}$$

Substitute $\beta = 0$ and $\gamma = 1/2$ into equations A.1 and A.2, respectively:

$$u^{(s+1)} = u^{(s)} + \dot{u}^{(s)}\Delta t + \frac{1}{2}\ddot{u}^{(s)}(\Delta t)^2 \tag{A.3}$$

$$\dot{u}^{(s+1)} = \dot{u}^{(s)} + \frac{1}{2}\ddot{u}^{(s)}\Delta t + \frac{1}{2}\ddot{u}^{(s+1)}\Delta t \tag{A.4}$$

If $u^{(s+1)}$ is expressed by equation A.3, then $u^{(s)}$ is expressed by

$$u^{(s)} = u^{(s-1)} + \dot{u}^{(s-1)}\Delta t + \frac{1}{2}\ddot{u}^{(s-1)}(\Delta t)^2 \tag{A.5}$$

and accordingly if $\dot{u}^{(s+1)}$ is expressed by equation A.4, then $\dot{u}^{(s)}$ is expressed by

$$\dot{u}^{(s)} = \dot{u}^{(s-1)} + \frac{1}{2}\ddot{u}^{(s-1)}\Delta t + \frac{1}{2}\ddot{u}^{(s)}\Delta t \tag{A.6}$$

Now we subtract each side of equationA.5 from A.3:

$$u^{(s+1)} - u^{(s)} = u^{(s)} - u^{(s-1)} + \dot{u}^{(s)}\Delta t - \dot{u}^{(s-1)}\Delta t + \frac{1}{2}(\Delta t)^2\left(\ddot{u}^{(s)} - \ddot{u}^{(s-1)}\right) \tag{A.7}$$

Now we substitute equation A.6 for $\dot{u}^{(s)}$ into equation A.7:

$$\begin{aligned} u^{(s+1)} - u^{(s)} \;=\; u^{(s)} - u^{(s-1)} + \dot{u}^{(s-1)}\Delta t + \frac{1}{2}(\Delta t)^2\left(\ddot{u}^{(s-1)} + \ddot{u}^{(s)}\right) \\ -\dot{u}^{(s-1)}\Delta t + \frac{1}{2}(\Delta t)^2\left(\ddot{u}^{(s)} - \ddot{u}^{(s-1)}\right) \end{aligned} \tag{A.8}$$

Collecting terms:

$$u^{(s+1)} = 2u^{(s)} - u^{(s-1)} + (\Delta t)^2\ddot{u}^{(s)} \tag{A.9}$$

Equation A.9 is the equation known as the 2. central difference, and facilitates estimation of the displacement at the following time step based on the acceleration at the previous time step and the displacement at the two previous time steps.

Appendix B

Comments related to the finite elements analyses

B.1 Using static analysis models for dynamic analysis

An analysis model prepared for static analyses is frequently not suited for dynamic analysis without putting considerable effort into improvement of the model. The reason is that most equipment, additional attachments, life boat platform etc. are modeled as forces while in reality being masses. In a dynamic analysis model the masses are required.

Also, masses that by nature are distributed, such as water filling in cellar deck, deck members or legs, grouting in legs etc. are commonly modeled as distributed element forces in static analyses. In order to establish a representative mass model for dynamic analysis, these must be converted to masses, evenly distributed over the exposed area or lumped to the nearest node. Today most finite element programs require such masses to be represented by an increased density of the elements in question, alternatively as lumped masses at the nodes, both being time consuming processes where the potential to do something wrong is considerable.

In the opinion of the author, any finite element program that is intended for both static and dynamic analyses of frame structures should support input options such as distributed and concentrated mass at *any place of an (beam) element span* in addition to the common option mass on node. Obviously, a source of error will be avoided when not having to calculate total mass from masses that are distributed by nature. In particular, the upgrading of old (static) models to dynamic models will be simplified due to such options.

It is also strongly recommended that preparation of input files to traditional static FE analyses should be carried out with focus on mass as opposed to force in all cases where external loading arise from masses. This will facilitate the use of *one* analysis model for both static and dynamic analysis.

Appendix C

Input files to finite element analysis

C.1 Model ‘DS’

C.1.1 Structure file stru.fem

```
 HEAD

,
,            Node ID            X             Y             Z    Boundary code
 NODE          10101        21.000       -21.000         0.000   1 1 1 1 1 1
 NODE          10107        21.000        21.000         0.000   1 1 1 1 1 1
 NODE          10113       -21.000        21.000         0.000   1 1 1 1 1 1
 NODE          10119       -21.000       -21.000         0.000   1 1 1 1 1 1
 NODE          10201        20.750       -20.750         2.000
 NODE          10202        20.750        -7.620         2.000
 NODE          10203        23.130        -7.620         2.000
 NODE          10204        20.750         0.000         2.000
 NODE          10205        23.130         7.620         2.000
 NODE          10206        20.750         7.620         2.000
 NODE          10207        20.750        20.750         2.000
 NODE          10209         0.000        20.750         2.000
 NODE          10213       -20.750        20.750         2.000
 NODE          10216       -20.750         0.000         2.000
 NODE          10219       -20.750       -20.750         2.000
 NODE          10222         0.000       -20.750         2.000
 NODE          10223        20.390       -20.390         4.884
 NODE          10224        20.390        20.390         4.884
 NODE          10225       -20.390        20.390         4.884
 NODE          10226       -20.390       -20.390         4.884
 NODE          10229        13.130        -7.620         2.000
 NODE          10232        22.067        -7.620        10.500
 NODE          10233        12.067        -7.621        10.500
 NODE          10239        13.130         7.620         2.000
 NODE          10241        19.873       -19.873         9.020
 NODE          10242        22.067         7.620        10.500
 NODE          10243        12.067         7.621        10.500
```

```
NODE         10247        19.873        19.873         9.020
NODE         10253       -19.873        19.873         9.020
NODE         10259       -19.873       -19.873         9.020
NODE         10301        18.500       -18.500        20.000
NODE         10302        18.500        -7.622        20.000
NODE         10303        20.880        -7.620        20.001
NODE         10304        18.500         0.000        20.000
NODE         10305        20.880         7.620        20.001
NODE         10306        18.500         7.622        20.000
NODE         10307        18.500        18.500        20.000
NODE         10309         0.000        18.500        20.000
NODE         10310        -3.800        18.500        20.000
NODE         10311        -6.100        18.500        20.000
NODE         10312        -8.400        18.500        20.000
NODE         10313       -18.500        18.500        20.000
NODE         10316       -18.500         0.000        20.000
NODE         10317        -5.500       -13.000        20.000
NODE         10319       -18.500       -18.500        20.000
NODE         10322         0.000       -18.500        20.000
NODE         10329        10.878        -7.622        20.000
NODE         10332        19.630        -7.620        30.000
NODE         10333         9.631        -7.619        30.000
NODE         10339        10.878         7.622        20.000
NODE         10342        19.630         7.620        30.000
NODE         10343         9.631         7.619        30.000
NODE         10401        16.000       -16.000        40.000
NODE         10402        16.000        -7.616        40.000
NODE         10403        18.380        -7.620        39.999
NODE         10404        16.000         0.000        40.000
NODE         10405        18.380         7.620        39.999
NODE         10406        16.000         7.616        40.000
NODE         10407        16.000        16.000        40.000
NODE         10409         0.000        16.000        40.000
NODE         10412        -8.400        16.000        40.000
NODE         10413       -16.000        16.000        40.000
NODE         10416       -16.000         0.000        40.000
NODE         10417        -5.500       -10.500        40.000
NODE         10419       -16.000       -16.000        40.000
NODE         10422         0.000       -16.000        40.000
NODE         10429         8.384        -7.616        40.000
NODE         10432        17.442        -7.620        47.505
NODE         10433         7.446        -7.616        47.505
NODE         10439         8.384         7.616        40.000
NODE         10442        17.442         7.620        47.505
NODE         10443         7.446         7.616        47.505
NODE         10501        13.625       -13.625        59.000
NODE         10502        13.625        -7.616        59.000
NODE         10503        16.005        -7.620        59.000
NODE         10504        13.625         0.000        59.000
NODE         10505        16.005         7.620        59.000
NODE         10506        13.625         7.616        59.000
NODE         10507        13.625        13.625        59.000
NODE         10509         0.000        13.625        59.000
NODE         10510        -5.480        13.625        59.000
NODE         10511        -7.780        13.625        59.000
NODE         10512       -10.080        13.625        59.000
NODE         10513       -13.625        13.625        59.000
NODE         10514       -13.625        10.325        59.000
NODE         10516       -13.625         0.000        59.000
NODE         10517        -5.500        -8.125        59.000
NODE         10519       -13.625       -13.625        59.000
NODE         10520        -7.153       -13.625        59.000
NODE         10521        -3.536       -10.089        59.000
NODE         10522         0.000       -13.625        59.000
NODE         10525        -3.300        10.325        59.000
NODE         10527         0.000         5.000        59.000
NODE         10528         8.629        -4.996        59.000
```

```
NODE         10529          6.009         -7.616         59.000
NODE         10530         -3.800         11.940         59.000
NODE         10531         -6.100         11.940         59.000
NODE         10532         -8.400         11.940         59.000
NODE         10533         -5.500         10.325         59.000
NODE         10534         -7.794         10.325         59.000
NODE         10535        -10.089         10.325         59.000
NODE         10538          8.629          4.996         59.000
NODE         10539          6.009          7.616         59.000
NODE         10540          4.064          9.561         59.000
NODE         10600          8.454        -11.000         80.000
NODE         10601         11.000        -11.000         80.000
NODE         10602         11.000         -8.456         80.000
NODE         10603         11.000         -6.204         80.000
NODE         10604         11.000          0.000         80.000
NODE         10605         11.000          6.204         80.000
NODE         10606         11.000          8.456         80.000
NODE         10607         11.000         11.000         80.000
NODE         10608          8.454         11.000         80.000
NODE         10609          0.000         11.000         80.000
NODE         10610         -5.480         11.000         80.000
NODE         10611         -7.780         11.000         80.000
NODE         10612        -10.080         11.000         80.000
NODE         10613        -11.000         11.000         80.000
NODE         10614        -11.000          7.700         80.000
NODE         10616        -11.000          0.000         80.000
NODE         10617         -5.500         -5.500         80.000
NODE         10618        -11.000         -8.454         80.000
NODE         10619        -11.000        -11.000         80.000
NODE         10620         -8.454        -11.000         80.000
NODE         10621         -5.220        -11.000         80.000
NODE         10622          0.000        -11.000         80.000
NODE         10623          0.000          0.000         80.000
NODE         10624         -3.300          7.700         80.000
NODE         10625         -5.498          7.700         80.000
NODE         10626         -7.790          7.700         80.000
NODE         10627        -10.083          7.700         80.000
NODE         10628         -3.800          9.313         80.000
NODE         10629         -6.100          9.313         80.000
NODE         10630         -8.400          9.313         80.000
NODE         10631          2.750          8.250         80.000
NODE         10638          0.000          5.000         80.000
NODE         20621         11.000        -11.000         81.855
NODE         20624         11.000        -11.000         94.450
NODE         20631         11.000         11.000         81.855
NODE         20634         11.000         11.000         94.450
NODE         20641        -11.000         11.000         81.855
NODE         20644        -11.000         11.000         94.450
NODE         20651        -11.000        -11.000         81.855
NODE         20654        -11.000        -11.000         94.450
NODE         20712         11.000         11.000         95.500
NODE         20715          0.000         11.000         95.500
NODE         20716         -3.800         11.000         95.500
NODE         20717         -6.000         11.000         95.500
NODE         20718         -8.400         11.000         95.500
NODE         20719        -11.000         11.000         95.500
NODE         20732        -11.000        -11.000         95.500
NODE         20734         -6.000        -11.000         95.500
NODE         20739         11.000        -11.000         95.500
NODE         20750         11.000         -5.500         95.500
NODE         20752         11.000          5.500         95.500
NODE         20760          0.000          5.500         95.500
NODE         20765        -11.000         -8.250         95.500
NODE         30210         -3.800         20.000          2.000   1 1 0 0 0 0
NODE         30211         -6.100         20.000          2.000   1 1 0 0 0 0
NODE         30212         -8.400         20.000          2.000   1 1 0 0 0 0
NODE         30217         -5.500        -15.250          2.000   1 1 0 0 0 0
```

```
 NODE          30421         -3.536        -10.089         55.000
 NODE          30427          0.000          5.000         58.000
 NODE          30428          8.626         -5.000         58.000
 NODE          30438          8.626          5.000         58.000
 NODE          30440          4.063          9.563         58.000
'
'            Elem ID     np1      np2   material   geom    lcoor    ecc1    ecc2
 BEAM         11201    10101    10201    10001    10001   10193
 BEAM         11202    10107    10207    10001    10001   10194
 BEAM         11302    10113    10213    10001    10001   10195
 BEAM         11402    10119    10219    10001    10001   10196
 BEAM         12103    10219    10222    10001    10010   10197
 BEAM         12104    10222    10201    10001    10010   10197
 BEAM         12105    10319    10222    10001    10006   10199   10013       0
 BEAM         12106    10222    10322    10001    10009   10200
 BEAM         12107    10301    10222    10001    10006   10199   10015       0
 BEAM         12200    10204    10206    10001    10010   10202
 BEAM         12201    10201    10223    10001    10001   10193
 BEAM         12202    10207    10224    10001    10001   10194
 BEAM         12203    10201    10202    10001    10010   10202
 BEAM         12204    10202    10204    10001    10010   10202
 BEAM         12205    10301    10204    10001    10006   10207   10015       0
 BEAM         12206    10206    10207    10001    10010   10202
 BEAM         12207    10307    10204    10001    10006   10209   10029       0
 BEAM         12208    10223    10241    10001    10002   10193
 BEAM         12209    10224    10247    10001    10002   10194
 BEAM         12210    10241    10301    10001    10002   10193
 BEAM         12211    10247    10307    10001    10002   10194
 BEAM         12302    10213    10225    10001    10001   10195
 BEAM         12303    10207    10209    10001    10010   10217
 BEAM         12304    10209    10213    10001    10010   10217
 BEAM         12305    10307    10209    10001    10006   10219   10029       0
 BEAM         12306    10209    10309    10001    10009   10220
 BEAM         12307    10313    10209    10001    10006   10219   10031       0
 BEAM         12309    10225    10253    10001    10002   10195
 BEAM         12311    10253    10313    10001    10002   10195
 BEAM         12402    10219    10226    10001    10001   10196
 BEAM         12403    10213    10216    10001    10010   10226
 BEAM         12404    10216    10219    10001    10010   10226
 BEAM         12405    10313    10216    10001    10006   10209   10031       0
 BEAM         12406    10216    10316    10001    10009   10229
 BEAM         12407    10319    10216    10001    10006   10207   10013       0
 BEAM         12409    10226    10259    10001    10002   10196
 BEAM         12411    10259    10319    10001    10002   10196
 BEAM         12501    10222    10229    10001    10010   10234   10082       0
 BEAM         12502    10229    10204    10001    10010   10234       0   10087
 BEAM         12503    10204    10239    10001    10010   10234   10079       0
 BEAM         12504    10239    10209    10001    10010   10234       0   10082
 BEAM         12505    10209    10216    10001    10010   10001   10083   10079
 BEAM         12506    10216    10222    10001    10010   10001   10087   10083
 BEAM         12507    10202    10229    10001    10011   10234
 BEAM         12508    10201    10229    10001    10012   10241
 BEAM         12509    10206    10239    10001    10011   10234
 BEAM         12510    10207    10239    10001    10012   10243
 BEAM         12511    10209    10222    10001    10011   10220
 BEAM         12600    10203    10202    10001    10011   10234
 BEAM         12601    10203    10233    10001    10020   10246
 BEAM         12602    10229    10233    10001    10016   10247
 BEAM         12603    10203    10232    10001    10018   10247
 BEAM         12604    10232    10233    10001    10020   10234
 BEAM         12605    10233    10329    10001    10015   10247
 BEAM         12606    10303    10233    10001    10021   10251
 BEAM         12607    10232    10303    10001    10019   10247
 BEAM         12610    10205    10206    10001    10011   10234
 BEAM         12611    10205    10243    10001    10020   10246
 BEAM         12612    10239    10243    10001    10016   10247
 BEAM         12613    10205    10242    10001    10018   10247
```

```
BEAM        12614   10242   10243   10001   10020   10234
BEAM        12615   10243   10339   10001   10015   10247
BEAM        12616   10305   10243   10001   10021   10251
BEAM        12617   10242   10305   10001   10019   10247
BEAM        13103   10319   10322   10001   10013   10197
BEAM        13104   10322   10301   10001   10034   10197
BEAM        13105   10319   10422   10001   10007   10263       0   10010
BEAM        13107   10301   10422   10001   10007   10263       0   10012
BEAM        13200   10304   10306   10001   10013   10202
BEAM        13201   10301   10401   10001   10003   10113
BEAM        13202   10307   10407   10001   10003   10133
BEAM        13203   10301   10302   10001   10013   10202
BEAM        13204   10302   10304   10001   10013   10202
BEAM        13205   10301   10404   10001   10007   10268       0   10042
BEAM        13206   10306   10307   10001   10013   10202
BEAM        13207   10307   10404   10001   10007   10270       0   10044
BEAM        13302   10313   10413   10001   10003   10153
BEAM        13303   10307   10309   10001   10034   10217
BEAM        13305   10307   10409   10001   10007   10272       0   10012
BEAM        13307   10313   10409   10001   10007   10272       0   10010
BEAM        13321   10309   10310   10001   10038   10217
BEAM        13322   10310   10311   10001   10038   10217
BEAM        13323   10311   10312   10001   10038   10217
BEAM        13324   10312   10313   10001   10013   10217
BEAM        13402   10319   10419   10001   10003   10173
BEAM        13403   10313   10316   10001   10013   10226
BEAM        13404   10316   10319   10001   10013   10226
BEAM        13405   10313   10416   10001   10007   10270       0   10044
BEAM        13407   10319   10416   10001   10007   10268       0   10042
BEAM        13500   10317   10322   10001   10010   10001       0   10083
BEAM        13501   10322   10329   10001   10013   10234   10082       0
BEAM        13502   10329   10304   10001   10010   10234       0   10087
BEAM        13503   10304   10339   10001   10010   10234   10079       0
BEAM        13504   10339   10309   10001   10013   10234       0   10082
BEAM        13505   10309   10316   10001   10010   10001   10083   10079
BEAM        13506   10316   10317   10001   10010   10001   10087       0
BEAM        13507   10302   10329   10001   10010   10234
BEAM        13508   10301   10329   10001   10012   10290
BEAM        13509   10306   10339   10001   10010   10234
BEAM        13510   10307   10339   10001   10012   10292
BEAM        13511   10309   10322   10001   10012   10220
BEAM        13600   10303   10302   10001   10010   10234
BEAM        13601   10329   10332   10001   10013   10295
BEAM        13602   10329   10333   10001   10014   10247
BEAM        13603   10303   10332   10001   10018   10247
BEAM        13604   10332   10333   10001   10012   10234
BEAM        13605   10333   10429   10001   10014   10247
BEAM        13606   10333   10403   10001   10020   10300
BEAM        13607   10332   10403   10001   10017   10247
BEAM        13610   10305   10306   10001   10010   10234
BEAM        13611   10339   10342   10001   10013   10295
BEAM        13612   10339   10343   10001   10014   10247
BEAM        13613   10305   10342   10001   10018   10247
BEAM        13614   10342   10343   10001   10012   10234
BEAM        13615   10343   10439   10001   10014   10247
BEAM        13616   10343   10405   10001   10020   10300
BEAM        13617   10342   10405   10001   10017   10247
BEAM        14103   10419   10422   10001   10014   10197
BEAM        14104   10422   10401   10001   10031   10197
BEAM        14105   10419   10522   10001   10007   10263   10005   10006
BEAM        14107   10401   10522   10001   10007   10263   10007   10008
BEAM        14200   10404   10406   10001   10014   10202
BEAM        14201   10401   10501   10001   10004   10193
BEAM        14202   10407   10507   10001   10004   10194
BEAM        14203   10401   10402   10001   10014   10202
BEAM        14204   10402   10404   10001   10014   10202
BEAM        14205   10401   10504   10001   10007   10319   10007   10038
```

```
BEAM        14206   10406   10407   10001   10014   10202
BEAM        14207   10407   10504   10001   10007   10321   10021   10040
BEAM        14302   10413   10513   10001   10004   10195
BEAM        14303   10407   10409   10001   10031   10217
BEAM        14305   10407   10509   10001   10007   10272   10021   10008
BEAM        14307   10413   10509   10001   10007   10272   10023   10006
BEAM        14322   10409   10412   10001   10036   10217
BEAM        14324   10412   10413   10001   10014   10217
BEAM        14402   10419   10519   10001   10004   10196
BEAM        14403   10413   10416   10001   10014   10226
BEAM        14404   10416   10419   10001   10014   10226
BEAM        14405   10413   10516   10001   10007   10321   10023   10040
BEAM        14407   10419   10516   10001   10007   10319   10005   10038
BEAM        14500   10417   10422   10001   10010   10001       0   10083
BEAM        14501   10422   10429   10001   10034   10234   10082       0
BEAM        14502   10429   10404   10001   10010   10234       0   10087
BEAM        14503   10404   10439   10001   10010   10234   10079       0
BEAM        14504   10439   10409   10001   10034   10234       0   10082
BEAM        14505   10409   10416   10001   10010   10001   10083   10079
BEAM        14506   10416   10417   10001   10010   10001   10087       0
BEAM        14507   10402   10429   10001   10022   10234
BEAM        14508   10401   10429   10001   10012   10343
BEAM        14509   10406   10439   10001   10022   10234
BEAM        14510   10407   10439   10001   10012   10345
BEAM        14511   10409   10422   10001   10012   10220
BEAM        14600   10403   10402   10001   10022   10234
BEAM        14601   10403   10433   10001   10023   10348
BEAM        14602   10429   10433   10001   10015   10247
BEAM        14603   10403   10432   10001   10018   10350
BEAM        14604   10432   10433   10001   10012   10234
BEAM        14605   10433   10529   10001   10015   10350
BEAM        14606   10433   10503   10001   10012   10353
BEAM        14607   10432   10503   10001   10018   10247
BEAM        14610   10405   10406   10001   10022   10234
BEAM        14611   10405   10443   10001   10023   10348
BEAM        14612   10439   10443   10001   10015   10247
BEAM        14613   10405   10442   10001   10018   10350
BEAM        14614   10442   10443   10001   10012   10234
BEAM        14615   10443   10539   10001   10015   10350
BEAM        14616   10443   10505   10001   10012   10353
BEAM        14617   10442   10505   10001   10018   10247
BEAM        15102   10519   10520   10001   10031   10197
BEAM        15103   10520   10522   10001   10031   10197
BEAM        15104   10522   10501   10001   10031   10197
BEAM        15105   10519   10622   10001   10008   10263       0   10002
BEAM        15107   10501   10622   10001   10008   10263       0   10004
BEAM        15200   10504   10506   10001   10014   10202
BEAM        15201   10501   10601   10001   10005   10193
BEAM        15202   10507   10607   10001   10005   10194
BEAM        15203   10501   10502   10001   10031   10202
BEAM        15204   10502   10504   10001   10014   10202
BEAM        15205   10501   10604   10001   10008   10373       0   10034
BEAM        15206   10506   10507   10001   10031   10202
BEAM        15207   10507   10604   10001   10008   10375       0   10036
BEAM        15302   10513   10613   10001   10005   10195
BEAM        15303   10507   10509   10001   10031   10217
BEAM        15305   10507   10609   10001   10008   10272       0   10004
BEAM        15307   10513   10609   10001   10008   10272       0   10002
BEAM        15321   10509   10510   10001   10036   10217
BEAM        15322   10510   10511   10001   10036   10217
BEAM        15323   10511   10512   10001   10036   10217
BEAM        15324   10512   10513   10001   10036   10217
BEAM        15401   10513   10514   10001   10039   10226
BEAM        15402   10519   10619   10001   10005   10196
BEAM        15403   10514   10516   10001   10039   10226
BEAM        15404   10516   10519   10001   10031   10226
BEAM        15405   10513   10616   10001   10008   10375       0   10036
```

```
BEAM        15407    10519    10616    10001    10008    10373        0   10034
BEAM        15500    10521    10522    10001    10032    10001        0   10083
BEAM        15501    10522    10529    10001    10040    10234    10082       0
BEAM        15502    10504    10528    10001    10012    10001    10087       0
BEAM        15503    10504    10538    10001    10012    10234    10079       0
BEAM        15504    10539    10540    10001    10040    10001
BEAM        15507    10502    10529    10001    10037    10234
BEAM        15508    10501    10529    10001    10012    10397
BEAM        15509    10506    10539    10001    10037    10234
BEAM        15510    10507    10539    10001    10012    10399
BEAM        15511    10527    10522    10001    10045    10220
BEAM        15512    10540    10509    10001    10040    10234        0   10082
BEAM        15514    10517    10521    10001    10032    10402
BEAM        15515    10516    10517    10001    10032    10001    10087       0
BEAM        15517    10520    10521    10001    10009    10404
BEAM        15520    10525    10516    10001    10032    10001        0   10079
BEAM        15521    10509    10527    10001    10045    10220
BEAM        15522    10538    10539    10001    10012    10407
BEAM        15523    10528    10529    10001    10012    10395
BEAM        15524    10509    10525    10001    10032    10001    10083       0
BEAM        15525    10525    10533    10001    10025    10410
BEAM        15526    10533    10534    10001    10025    10410
BEAM        15527    10534    10535    10001    10025    10410
BEAM        15528    10535    10514    10001    10025    10410
BEAM        15529    10530    10533    10001    10043    10001
BEAM        15530    10510    10530    10001    10043    10415
BEAM        15531    10531    10534    10001    10044    10416
BEAM        15532    10511    10531    10001    10044    10415
BEAM        15533    10532    10535    10001    10043    10418
BEAM        15534    10512    10532    10001    10043    10415
BEAM        15600    10503    10502    10001    10037    10234
BEAM        15610    10505    10506    10001    10037    10234
BEAM        16100    10600    10602    10001    10012    10422
BEAM        16101    10619    10620    10001    10031    10197
BEAM        16102    10620    10621    10001    10031    10197
BEAM        16103    10621    10622    10001    10031    10197
BEAM        16104    10622    10600    10001    10031    10197
BEAM        16105    10600    10601    10001    10031    10197
BEAM        16200    10606    10608    10001    10012    10407
BEAM        16201    10601    10602    10001    10031    10202
BEAM        16202    10602    10603    10001    10031    10202
BEAM        16203    10603    10604    10001    10031    10202
BEAM        16204    10604    10605    10001    10031    10202
BEAM        16205    10605    10606    10001    10031    10202
BEAM        16206    10606    10607    10001    10031    10202
BEAM        16302    10607    10608    10001    10031    10217
BEAM        16303    10608    10609    10001    10031    10217
BEAM        16321    10609    10610    10001    10031    10217
BEAM        16322    10610    10611    10001    10031    10217
BEAM        16323    10611    10612    10001    10031    10217
BEAM        16324    10612    10613    10001    10031    10217
BEAM        16400    10618    10620    10001    10012    10402
BEAM        16403    10614    10616    10001    10031    10226
BEAM        16404    10616    10618    10001    10031    10226
BEAM        16405    10618    10619    10001    10031    10226
BEAM        16420    10613    10614    10001    10031    10226
BEAM        16500    10617    10622    10001    10032    10001        0   10069
BEAM        16501    10622    10604    10001    10032    10234    10068   10073
BEAM        16502    10604    10631    10001    10032    10234    10065       0
BEAM        16503    10624    10616    10001    10032    10001        0   10065
BEAM        16504    10616    10617    10001    10032    10001    10073       0
BEAM        16511    10609    10638    10001    10009    10220
BEAM        16512    10623    10622    10001    10009    10220
BEAM        16513    10604    10623    10001    10009    10410
BEAM        16514    10623    10616    10001    10009    10410
BEAM        16515    10638    10623    10001    10009    10220
BEAM        16520    10631    10609    10001    10032    10234        0   10068
```

```
BEAM         16521    10609    10624    10001    10032   10001   10069       0
BEAM         16522    10624    10625    10001    10025   10234
BEAM         16523    10625    10626    10001    10025   10234
BEAM         16524    10626    10627    10001    10025   10234
BEAM         16525    10627    10614    10001    10025   10234
BEAM         16526    10628    10625    10001    10043   10463
BEAM         16527    10610    10628    10001    10043   10464
BEAM         16528    10629    10626    10001    10044   10465
BEAM         16529    10611    10629    10001    10044   10001
BEAM         16530    10630    10627    10001    10043   10467
BEAM         16531    10612    10630    10001    10043   10464
BEAM         26106    20654    20621    10001    20003   20001
BEAM         26107    10601    20621    10001    10005   10200
BEAM         26109    20621    20624    10001    10005   10200
BEAM         26110    20624    20739    10001    10005   10200
BEAM         26206    20624    20631    10001    20003   20005
BEAM         26301    10607    20631    10001    10005   10220
BEAM         26306    20634    20641    10001    20003   20007
BEAM         26307    10613    20641    10001    10005   10220
BEAM         26309    20641    20644    10001    10005   10220
BEAM         26310    20644    20719    10001    10005   10220
BEAM         26406    20644    20651    10001    20003   20011
BEAM         26601    10619    20651    10001    10005   10200
BEAM         26602    20651    20654    10001    10005   10200
BEAM         26603    20654    20732    10001    10005   10200
BEAM         26604    20631    20634    10001    10005   10220
BEAM         26605    20634    20712    10001    10005   10220
BEAM         30020    30217    10317    10001    30003   10199
BEAM         30021    30210    10310    10001    30001   30002
BEAM         30022    30211    10311    10001    30002   30002
BEAM         30023    30212    10312    10001    30001   30002
BEAM         30030    10317    10417    10001    30003   10199
BEAM         30040    10417    10517    10001    30003   10199
BEAM         30041    10310    10530    10001    30001   30010
BEAM         30042    10311    10531    10001    30002   30010
BEAM         30043    10312    10532    10001    30001   30010
BEAM         30044    30428    10528    10001    30812   30013
BEAM         30045    30438    10538    10001    30812   30014
BEAM         30046    30440    10540    10001    30005   10410
BEAM         30047    30427    10527    10001    30005   10410
BEAM         30049    30421    10521    10001    30006   10410
BEAM         30050    10517    10617    10001    30003   10199
BEAM         30051    10530    10628    10001    30001   10272
BEAM         30052    10531    10629    10001    30002   10272
BEAM         30053    10532    10630    10001    30001   10272
BEAM         30054    10528    10603    10001    30812   30022
BEAM         30055    10538    10605    10001    30812   30023
BEAM         30056    10540    10631    10001    30005   30024
BEAM         30057    10527    10638    10001    30005   10410
BEAM         30059    10521    10621    10001    30006   30026
BEAM         30060    10617    20765    10001    30003   30027
BEAM         30061    10628    20716    10001    30001   30028
BEAM         30062    10629    20717    10001    30002   30029
BEAM         30063    10630    20718    10001    30001   30028
BEAM         30064    10603    20750    10001    30812   30031
BEAM         30065    10605    20752    10001    30812   30032
BEAM         30066    10631    20760    10001    30005   30033
BEAM         30067    10638    20760    10001    30005   30034
BEAM         30069    10621    20734    10001    30006   30035
BEAM         30209    10209    10309    10001    31066   10272
BEAM         30309    10309    10409    10001    31066   10272
BEAM         30409    10409    10509    10001    31066   10272
BEAM         30509    10509    10609    10001    31066   10272
BEAM         30609    10609    20715    10001    31066   10410
'
'            Geom ID       Do         Thick    Shear_y   Shear_z
PIPE          10001       3.000       0.050
```

```
 PIPE         10002       3.000       0.075
 PIPE         10003       2.400       0.050
 PIPE         10004       2.400       0.040
 PIPE         10005       1.800       0.040
 PIPE         10006       1.300       0.030
 PIPE         10007       1.300       0.035
 PIPE         10008       1.100       0.035
 PIPE         10009       0.650       0.020
 PIPE         10010       1.000       0.025
 PIPE         10011       0.900       0.025
 PIPE         10012       0.800       0.025
 PIPE         10013       1.000       0.030
 PIPE         10014       1.200       0.030
 PIPE         10015       1.200       0.025
 PIPE         10016       1.200       0.020
 PIPE         10017       1.600       0.045
 PIPE         10018       1.600       0.035
 PIPE         10019       1.600       0.030
 PIPE         10020       0.800       0.020
 PIPE         10021       0.900       0.020
 PIPE         10022       1.100       0.030
 PIPE         10023       1.000       0.020
 PIPE         10024       1.940       0.095
 PIPE         10025       0.800       0.035
 PIPE         10031       1.200       0.035
 PIPE         10032       0.800       0.030
 PIPE         10034       1.000       0.035
 PIPE         10036       1.200       0.040
 PIPE         10037       1.100       0.025
 PIPE         10038       1.000       0.040
 PIPE         10039       1.200       0.055
 PIPE         10040       0.800       0.040
 PIPE         10043       0.560       0.025
 PIPE         10044       0.510       0.025
 PIPE         10045       1.000       0.045
 PIPE         20003       0.750       0.035
 PIPE         30001       0.935       0.038
 PIPE         30002       0.722       0.033
 PIPE         30003       0.780       0.033
 PIPE         30005       0.559       0.025
 PIPE         30006       0.457       0.025
 PIPE         30812       0.813       0.025
 PIPE         31066       1.067       0.025
’
’            Geom ID
’ GENBEAM      10026    8.00000E-02    1.00000E-06    1.00000E-06    4.00000E-02
’                       1.00000E-05    1.00000E-05    4.00000E-02    6.00000E-02
’                       1.00000E-05
’ GENBEAM      10027    6.00000E-02    1.00000E-06    1.00000E-06    4.00000E-02
’                       1.00000E-05    1.00000E-05    4.00000E-02    6.00000E-02
’                       1.00000E-05
’ GENBEAM      10028    1.92000E+00    1.00000E-06    1.00000E-06    1.00000E-06
’                       1.00000E-05    1.00000E-05    1.00000E-05    1.00000E-05
’                       1.00000E-05
’
’            Loc-Coo          dx             dy             dz
 UNITVEC       10001         0.000          0.000          1.000
’ UNITVEC       10029        -0.014         -0.011          1.000
’ UNITVEC       10030        -0.032          0.144          0.989
’ UNITVEC       10031        -0.144          0.032          0.989
’ UNITVEC       10032         0.011          0.014          1.000
’ UNITVEC       10033        -0.148          0.050          0.988
’ UNITVEC       10035        -0.050          0.148          0.988
’ UNITVEC       10036         0.011         -0.014          1.000
’ UNITVEC       10037        -0.144         -0.032          0.989
’ UNITVEC       10038        -0.032         -0.144          0.989
’ UNITVEC       10039        -0.014          0.011          1.000
```

```
' UNITVEC       10040         -0.050         -0.148          0.988
' UNITVEC       10042         -0.148         -0.050          0.988
' UNITVEC       10043          0.014          0.011          1.000
' UNITVEC       10044          0.032         -0.144          0.989
' UNITVEC       10045          0.144         -0.032          0.989
' UNITVEC       10046         -0.011         -0.014          1.000
' UNITVEC       10047          0.148         -0.050          0.988
' UNITVEC       10049          0.050         -0.148          0.988
' UNITVEC       10050         -0.011          0.014          1.000
' UNITVEC       10051          0.144          0.032          0.989
' UNITVEC       10052          0.032          0.144          0.989
' UNITVEC       10053          0.014         -0.011          1.000
' UNITVEC       10054          0.050          0.148          0.988
' UNITVEC       10056          0.148          0.050          0.988
 UNITVEC       10113          0.696         -0.696          0.174
 UNITVEC       10125          0.948          0.092          0.304
' UNITVEC       10126          0.530          0.838          0.128
' UNITVEC       10127         -0.838         -0.530          0.128
' UNITVEC       10128         -0.092         -0.948          0.304
' UNITVEC       10129         -0.224         -0.934          0.277
' UNITVEC       10130          0.412         -0.828          0.380
' UNITVEC       10131          0.828         -0.412          0.380
' UNITVEC       10132          0.934          0.224          0.277
 UNITVEC       10133          0.696          0.696          0.174
' UNITVEC       10145         -0.092          0.948          0.304
' UNITVEC       10146         -0.838          0.530          0.128
' UNITVEC       10147          0.530         -0.838          0.128
' UNITVEC       10148          0.948         -0.092          0.304
' UNITVEC       10149          0.934         -0.224          0.277
' UNITVEC       10150          0.828          0.412          0.380
' UNITVEC       10151          0.412          0.828          0.380
' UNITVEC       10152         -0.224          0.934          0.277
 UNITVEC       10153         -0.696          0.696          0.174
' UNITVEC       10165         -0.948         -0.092          0.304
' UNITVEC       10166         -0.530         -0.838          0.128
' UNITVEC       10167          0.838          0.530          0.128
' UNITVEC       10168          0.092          0.948          0.304
' UNITVEC       10169          0.224          0.934          0.277
' UNITVEC       10170         -0.412          0.828          0.380
' UNITVEC       10171         -0.828          0.412          0.380
' UNITVEC       10172         -0.934         -0.224          0.277
 UNITVEC       10173         -0.696         -0.696          0.174
' UNITVEC       10185          0.092         -0.948          0.304
' UNITVEC       10186          0.838         -0.530          0.128
' UNITVEC       10187         -0.530          0.838          0.128
' UNITVEC       10188         -0.948          0.092          0.304
' UNITVEC       10189         -0.934          0.224          0.277
' UNITVEC       10190         -0.828         -0.412          0.380
' UNITVEC       10191         -0.412         -0.828          0.380
' UNITVEC       10192          0.224         -0.934          0.277
 UNITVEC       10193          0.992          0.015          0.122
 UNITVEC       10194         -0.992          0.015         -0.122
 UNITVEC       10195         -0.992         -0.015          0.122
 UNITVEC       10196          0.992         -0.015         -0.122
 UNITVEC       10197          0.000         -0.124         -0.992
 UNITVEC       10199          0.000         -0.992          0.124
 UNITVEC       10200          1.000          0.000          0.000
 UNITVEC       10202          0.124          0.000         -0.992
 UNITVEC       10207          0.000         -0.696         -0.718
 UNITVEC       10209          0.000         -0.696          0.718
 UNITVEC       10217          0.000          0.124         -0.992
 UNITVEC       10219          0.000         -0.992         -0.124
 UNITVEC       10220         -1.000          0.000          0.000
 UNITVEC       10226         -0.124          0.000         -0.992
 UNITVEC       10229          0.000         -1.000          0.000
 UNITVEC       10234          0.000          0.000         -1.000
 UNITVEC       10241          0.865          0.502          0.000
```

```
 UNITVEC       10243         -0.865          0.502          0.000
 UNITVEC       10246         -0.609          0.000         -0.793
 UNITVEC       10247         -0.992          0.000         -0.124
 UNITVEC       10251          0.733          0.000         -0.680
 UNITVEC       10263          0.000          0.992         -0.124
 UNITVEC       10268          0.000          0.737         -0.676
 UNITVEC       10270          0.000          0.737          0.676
 UNITVEC       10272          0.000          0.992          0.124
 UNITVEC       10290          0.819          0.574          0.000
 UNITVEC       10292         -0.819          0.574          0.000
 UNITVEC       10295         -0.753          0.000          0.659
 UNITVEC       10300         -0.753          0.000          0.658
 UNITVEC       10319          0.000          0.767         -0.642
 UNITVEC       10321          0.000          0.767          0.642
 UNITVEC       10343          0.740          0.672          0.000
 UNITVEC       10345         -0.740          0.672          0.000
 UNITVEC       10348         -0.566          0.000         -0.824
 UNITVEC       10350          0.992          0.000          0.124
 UNITVEC       10353         -0.802          0.000          0.597
 UNITVEC       10373          0.000          0.839         -0.545
 UNITVEC       10375          0.000          0.839          0.545
 UNITVEC       10395         -0.707          0.707          0.000
 UNITVEC       10397          0.619          0.785          0.000
 UNITVEC       10399         -0.619          0.785          0.000
 UNITVEC       10402         -0.707         -0.707          0.000
 UNITVEC       10404          0.699         -0.715          0.000
 UNITVEC       10407          0.707          0.707          0.000
 UNITVEC       10410          0.000          1.000          0.000
 UNITVEC       10415         -0.708         -0.706          0.000
 UNITVEC       10416         -0.690          0.724          0.000
 UNITVEC       10418         -0.691          0.723          0.000
 UNITVEC       10422          0.707         -0.707          0.000
 UNITVEC       10463         -0.689          0.725          0.000
 UNITVEC       10464         -0.709         -0.706          0.000
 UNITVEC       10465         -0.690          0.723          0.000
 UNITVEC       10467         -0.692          0.722          0.000
 UNITVEC       20001         -0.496          0.000         -0.868
 UNITVEC       20005          0.000         -0.496         -0.868
 UNITVEC       20007          0.496          0.000         -0.868
 UNITVEC       20011          0.000          0.496         -0.868
 UNITVEC       30002          0.000          0.997          0.083
 UNITVEC       30010          0.000          0.978          0.209
 UNITVEC       30013         -0.588         -0.809          0.005
 UNITVEC       30014         -0.588          0.809          0.005
 UNITVEC       30022         -0.885          0.449          0.126
 UNITVEC       30023         -0.885         -0.449          0.126
 UNITVEC       30024          0.704          0.704          0.088
 UNITVEC       30026          0.876          0.474          0.091
 UNITVEC       30027          0.831          0.416          0.369
 UNITVEC       30028          0.000         -0.994          0.108
 UNITVEC       30029         -0.059         -0.992          0.108
 UNITVEC       30031          0.000         -0.999          0.045
 UNITVEC       30032          0.000          0.999          0.045
 UNITVEC       30033          0.686          0.686          0.243
 UNITVEC       30034          0.000         -0.999          0.032
 UNITVEC       30035          0.999          0.000          0.050
'
'            Ecc-ID            Ex             Ey             Ez
 ECCENT        10002          0.015          0.000          0.000
 ECCENT        10004         -0.015          0.000          0.000
 ECCENT        10005          0.026          0.026          0.207
 ECCENT        10006         -0.235          0.000          0.000
 ECCENT        10007         -0.026          0.026          0.207
 ECCENT        10008          0.235          0.000          0.000
 ECCENT        10010         -0.145          0.000          0.000
 ECCENT        10012          0.145          0.000          0.000
 ECCENT        10013         -0.009         -0.009         -0.069
```

```
 ECCENT        10015          0.009         -0.009         -0.069
 ECCENT        10021         -0.026         -0.026          0.207
 ECCENT        10023          0.026         -0.026          0.207
 ECCENT        10029          0.009          0.009         -0.069
 ECCENT        10031         -0.009          0.009         -0.069
 ECCENT        10034          0.000          0.015          0.000
 ECCENT        10036          0.000         -0.015          0.000
 ECCENT        10038          0.000         -0.235          0.000
 ECCENT        10040          0.000          0.235          0.000
 ECCENT        10042          0.000         -0.145          0.000
 ECCENT        10044          0.000          0.145          0.000
 ECCENT        10065          0.000         -0.080          0.000
 ECCENT        10068         -0.080          0.000          0.000
 ECCENT        10069          0.080          0.000          0.000
 ECCENT        10073          0.000          0.080          0.000
 ECCENT        10079          0.000         -0.105          0.000
 ECCENT        10082         -0.105          0.000          0.000
 ECCENT        10083          0.105          0.000          0.000
 ECCENT        10087          0.000          0.105          0.000
'
'            Mat  ID     E-mod       Poiss     Density   Thermal
 ELASTIC      10001   2.100E+11   3.000E-01   7.850E+03    .000E+00
 ELASTIC      10002   2.100E+11   3.000E-01   5.760E+02    .000E+00
'
'
'
'
' Material specifications
' -----------------------
'
'            Mat  ID     E-mod    Poiss   Yield      Density    Thermal
 MISOIEP      10001   2.100E+11   0.3   355.0E+6   7.850E+03    .000E+00
' MISOIEP      10002   2.100E+11   0.3   355.0E+6   5.760E+02    .000E+00
 MISOIEP      40001   2.100E+15   0.3   355.0E+6   1.000E-05    .000E+00
'
'
' Dummy cross section for deck dummy structure
' --------------------------------------------
'
 PIPE         40001       1.000       0.100
'
' Extra nodes for dummy structure attracting wave-in-deck loads
' -------------------------------------------------------------
'
 NODE          40001         11.000         23.500         95.500
 NODE          40002         23.500         11.000         95.500
 NODE          40003         23.500        -11.000         95.500
 NODE          40004         11.000        -23.500         95.500
 NODE          40005        -11.000        -23.500         95.500
 NODE          40006        -23.500        -11.000         95.500
 NODE          40007        -23.500         11.000         95.500
 NODE          40008        -11.000         23.500         95.500
 NODE          40011         11.000         23.500        103.500
 NODE          40012         23.500         11.000        103.500
 NODE          40013         23.500        -11.000        103.500
 NODE          40014         11.000        -23.500        103.500
 NODE          40015        -11.000        -23.500        103.500
 NODE          40016        -23.500        -11.000        103.500
 NODE          40017        -23.500         11.000        103.500
 NODE          40018        -11.000         23.500        103.500
 NODE          40021          0.000          0.000         95.500
 NODE          40041         -1.084         -1.107         99.000
'
'
' Extra elements for dummy structure attracting wave-in-deck loads
' ----------------------------------------------------------------
'
```

```
’            Elem ID     np1      np2   material   geom    lcoor    ecc1    ecc2
 BEAM         40001    20712    40001    40001    40001   10001
 BEAM         40002    20712    40002    40001    40001   10001
 BEAM         40003    20739    40003    40001    40001   10001
 BEAM         40004    20739    40004    40001    40001   10001
 BEAM         40005    20732    40005    40001    40001   10001
 BEAM         40006    20732    40006    40001    40001   10001
 BEAM         40007    20719    40007    40001    40001   10001
 BEAM         40008    20719    40008    40001    40001   10001
 BEAM         40011    40001    40011    40001    40001   10200
 BEAM         40012    40002    40012    40001    40001   10200
 BEAM         40013    40003    40013    40001    40001   10200
 BEAM         40014    40004    40014    40001    40001   10200
 BEAM         40015    40005    40015    40001    40001   10200
 BEAM         40016    40006    40016    40001    40001   10200
 BEAM         40017    40007    40017    40001    40001   10200
 BEAM         40018    40008    40018    40001    40001   10200
 BEAM         40021    20719    20718    40001    40001   10001
 BEAM         40022    20718    20717    40001    40001   10001
 BEAM         40023    20717    20716    40001    40001   10001
 BEAM         40024    20716    20715    40001    40001   10001
 BEAM         40025    20715    20712    40001    40001   10001
 BEAM         40026    20732    20765    40001    40001   10001
 BEAM         40027    20765    20719    40001    40001   10001
 BEAM         40028    20732    20734    40001    40001   10001
 BEAM         40029    20734    20739    40001    40001   10001
 BEAM         40030    20739    20750    40001    40001   10001
 BEAM         40031    20750    20752    40001    40001   10001
 BEAM         40032    20752    20712    40001    40001   10001
 BEAM         40033    20719    40021    40001    40001   10001
 BEAM         40034    40021    20712    40001    40001   10001
 BEAM         40035    20732    40021    40001    40001   10001
 BEAM         40036    40021    20739    40001    40001   10001
 BEAM         40037    40021    20760    40001    40001   10001
 BEAM         40038    20760    20715    40001    40001   10001
 BEAM         40041    20719    40041    40001    40001   10001
 BEAM         40042    40041    20712    40001    40001   10001
 BEAM         40043    20732    40041    40001    40001   10001
 BEAM         40044    40041    20739    40001    40001   10001
’
’
’ Linear elements, deck dummy frame (infinitely stiff)
’ ----------------------------------------------------
’
 Lin_Elem   0    Elem    40021   40022   40023   40024
                         40025   40026   40027   40028
                         40029   40030   40031   40032
                         40033   40034   40035   40036
                         40037   40038
                         40041   40042   40043   40044
’
’
’ Number of points for wave calculation
’ -------------------------------------
’
 WAVE_INT    81   40011 40012 40013 40014 40015 40016 40017 40018
’
’
’ Node mass representing loads on topside
’ and weight of topside, totally 11000 t
’ ---------------------------------------
’
 NODEMASS  40041 11000E+03
’
’
’ Group definitions
’ ------------------
```

```
'
' Risers and appurtenances
'
GroupDef  52  Elem  30020     30021     30022     30023  ! Risers:
                    30030
                    30040     30041     30042     30043
                    30050     30051     30052     30053
                    30060     30061     30062     30063
                    30209     30309     30409     30509     30609
'
'
                    30044     30045     30046     30047     30049 ! Caissons:
                    30054     30055     30056     30057     30059
                    30064     30065     30066     30067     30069
'
'
' Elements to generate wave load on deck
'
Groupdef  55  Elem  40001   40002   40003   40004  ! Horizontal
                    40005   40006   40007   40008  ! Horizontal
                    40011   40012   40013   40014  ! Vertical
                    40015   40016   40017   40018  ! Vertical
'
' Deck frame
'
Groupdef  56  Elem  40021   40022   40023   40024
                    40025   40026   40027   40028
                    40029   40030   40031   40032
                    40033   40034   40035   40036
                    40037   40038
'
' Pyramid carrying node mass representing deck weigth
'
Groupdef  57  Elem  40041   40042   40043   40044
'
' Launch frames
'
Groupdef  58  Elem  12507   12600   12601   12602   12603
                    12604   12605   12606   12607

                    13507   13600   13601   13602   13603
                    13604   13605   13606   13607

                    14507   14600   14601   14602   14603
                    14604   14605   14606   14607

                    15507   15600
'
                    12509   12610   12611   12612   12613
                    12614   12615   12616   12617
                    13509   13610   13611   13612   13613
                    13614   13615   13616   13617
                    14509   14610   14611   14612   14613
                    14614   14615   14616   14617
                    15509   15610
'
'
' Definitions of nonstructural elements
'
' Group 52  Risers and appurtenances
' Group 55  Elements to generate wave load on deck
' ------------------------------------------------
'
NonStru Group 52 55
NonStru Visible
'
'
```

```
’
```

C.1.2 Load file load.fem

```
HEAD

’
’ Dead weight of structural steel and masses on nodes
’ ---------------------------------------------------
’
’            Load Case       Acc_X         Acc_Y          Acc_Z
 GRAVITY            1           0.             0.          -9.81
’
’
’ Wind load positive x-direction (i.e. from PN), in total 4 MN
’ ------------------------------------------------------------
’
’           Load Case  Node ID     fx        fy        fz
’ NODELOAD       5     40041     4.0E+6      0.0       0.0
’
’
’ Wind load positive y-direction (i.e. from PW), in total 3 MN
’ ------------------------------------------------------------
’
’           Load Case  Node ID     fx        fy        fz
’ NODELOAD       6     40041      0.0     3.0E+6       0.0
’
’
’ Specify calculation of buoyancy
’ (NB! If buoyancy is calculated, flooded members
’ must be correctly given in the load file.)
’ ---------------------------------------------
’
’           Ildcs  Option
 BUOYANCY     1    NoWrite
’
’
’ Wave loads
’ ----------
’
’ Wave-in-deck load (for magnitude see file deckforce_values.xls) for deck width 47 m.
’
’           Load Case  Node ID     fx        fy        fz
 NODELOAD      9       20712     FDECKX.     0.0       0.0
 NODELOAD      9       20719     FDECKX.     0.0       0.0
 NODELOAD      9       20732     FDECKX.     0.0       0.0
 NODELOAD      9       20739     FDECKX.     0.0       0.0
’
’ Wave load on jacket
’
’           Ildcs  <type>   H    Period   Direction Phase  Surf_Lev Depth
 WAVEDATA     10   Stoke    WAVEH    PERIOD     0.0     145   SURFACE   DEPTH
’
’
’ Current profile
’ ---------------
’
’           Ildcs  Speed Direction Surf_Lev  Depth    [Profile]
 CURRENT      10     1.0     0.0   SURFACE   DEPTH           0.0  1.00
                                                        -25.0  0.52
                                                        -85.0  0.28
’
’
```

```
' Hydrodynamic factors
' --------------------
'
' General depth dependent factors:
'            Z    Cd
 Hydro_Cd   4.00  0.65
            3.01  0.65
            3.00  1.05
           -4.00  1.05
           -4.01  1.208
           -85.0  1.208
'
'            Z    Cm
 Hydro_Cm   3.00  1.6
           -4.00  1.6
           -4.01  1.2
           -85.0  1.2
'
' Deck dummy structure:
 Hyd_CdCm   0.0   0.0    40001     40002     40003     40004
                         40005     40006     40007     40008
                         40021     40022     40023     40024
                         40025     40026     40027     40028
                         40029     40030     40031     40032
                         40033     40034     40035     40036
                         40037     40038
                         40041     40042     40043     40044
                         40011     40012     40013     40014
                         40015     40016     40017     40018
'
' The dragfactor for (two at the time of) elements 40011 - 40018
' is calculated based on Cs = 3 and that they each cover 23.5 m
' of the deck wall width.
' Hyd_CdCm  70.5   0.0   40011 40018    ! Forces -y direction
' Hyd_CdCm  70.5   0.0   40012 40013    ! Forces -x direction
' Hyd_CdCm  70.5   0.0   40014 40015    ! Forces +y direction
' Hyd_CdCm  70.5   0.0   40016 40017    ! Forces +x direction
'
' Launch runners (only runners, not complete frame):
 Hyd_CdCm   3.71  2.16   12603     13603     14603
                         12607     13607     14607
                         12613     13613     14613
                         12617     13617     14617
'
'
' Marine growth
' -------------
'
'               Z          Add_Thick
 M_GROWTH       2.02       0.00
                2.01       0.00
                2.00       0.10
              -40.00       0.10
              -40.01       0.05
              -85.00       0.05
'
'
' Flooded members (for this to take effect, BUOYANCY
' must be specified in the control file)
' -------------------------------------------------
'
' Jacket legs:
 Flooded       11201     12201     13201     14201     15201
               11202     12202     13202     14202     15202
               11302     12302     13302     14302     15302
               11402     12402     13402     14402     15402
               12208     12209     12210     12211
```

```
              12309     12311
              12409     12411
'
' Risers:
 Flooded      30020     30021     30022     30023
              30030
              30040     30041     30042     30043
              30050     30051     30052     30053
              30060     30061     30062     30063
              30209     30309     30409     30509     30609
'
' Caissons:
 Flooded      30044     30045     30046     30047     30049
              30054     30055     30056     30057     30059
              30064     30065     30066     30067     30069
'
' Inertia load 2. mode (rotation about y-axis) corr. to 100 MN
' ------------------------------------------------------------
'
'           Load Case  Node ID        L O A D   I N T E N S I T Y
 NODELOAD         11     10201    1.72058E+03    6.35468E+02   -9.26136E+02
                                  -8.07533E+00    3.29358E+01   -7.94597E+00
 NODELOAD         11     10202    1.84548E+03    7.36961E+02   -5.62172E+03
                                   2.18215E+00    1.02594E+01   -7.63549E+00
 NODELOAD         11     10203    3.35593E+03    1.11577E+03   -1.29511E+04
                                  -1.68105E+01    7.16382E+01   -5.15676E+00
 NODELOAD         11     10204    8.25939E+03    4.30639E+03   -1.31702E+04
                                  -5.12777E+01    8.97072E+01    3.15385E+01
 NODELOAD         11     10205    1.55276E+03    1.88858E+03   -1.54810E+04
                                  -1.85993E+01    8.04582E+01   -2.57808E+00
 NODELOAD         11     10206    8.63752E+02    7.57086E+02   -6.82029E+03
                                  -1.00291E+01    1.12179E+01    1.24910E+01
 NODELOAD         11     10207    1.74754E+03    8.51582E+02   -2.15698E+03
                                  -1.20596E+01    3.31406E+01    3.06246E+00
 NODELOAD         11     10209    1.80729E+04    8.29171E+03   -8.31930E+03
                                  -7.54355E+01    1.60345E+02    2.11299E+00
 NODELOAD         11     10213    1.58816E+03    4.59551E+02    8.99791E+02
                                  -1.22714E+01    3.07695E+01    8.34052E+00
 NODELOAD         11     10216    1.74958E+04    5.80026E+03    1.87310E+04
                                  -3.83053E+01    1.75713E+02    8.18503E+00
 NODELOAD         11     10219    1.80330E+03    7.56512E+02    2.08379E+03
                                  -1.00702E+01    3.16082E+01   -3.68588E+00
 NODELOAD         11     10222    1.95084E+04    5.84324E+03    8.82288E+03
                                  -1.31709E+02    4.05811E+01    5.66770E+01
 NODELOAD         11     10223    4.70829E+03    1.71846E+03   -2.09591E+03
                                  -1.87969E+01    4.37514E+01   -7.41981E+00
 NODELOAD         11     10224    4.71628E+03    2.21800E+03   -4.90901E+03
                                  -1.58512E+01    4.03715E+01    2.98933E+00
 NODELOAD         11     10225    4.48409E+03    1.39095E+03    2.12250E+03
                                  -1.64524E+01    4.14430E+01    6.98494E+00
 NODELOAD         11     10226    4.97287E+03    2.02738E+03    4.92014E+03
                                  -1.37946E+01    4.25544E+01   -3.34740E+00
 NODELOAD         11     10229    3.75534E+03    2.32023E+03   -5.41748E+03
                                  -1.90380E+01    3.48682E+01   -1.03688E+01
 NODELOAD         11     10232    1.60142E+04    5.73351E+03   -2.18191E+04
                                  -4.20574E+01    1.06574E+02   -5.47700E+00
 NODELOAD         11     10233    7.64212E+03    3.01125E+03   -3.87128E+03
                                  -1.25006E+01    6.74712E+01   -1.99235E+00
 NODELOAD         11     10239    1.79205E+03   -2.43914E+02   -7.48608E+03
                                  -6.78993E+00    2.86194E+01    1.65921E+01
 NODELOAD         11     10241    2.49303E+04    9.55258E+03   -6.81582E+03
                                  -1.41281E+02    3.34423E+02   -5.78929E+01
 NODELOAD         11     10242    1.40270E+04    7.37184E+03   -2.61252E+04
                                  -3.86942E+01    1.17889E+02   -3.11069E+00
 NODELOAD         11     10243    6.68462E+03    2.54620E+03   -5.48887E+03
                                  -2.30449E+01    7.53160E+01    1.49598E+00
 NODELOAD         11     10247    2.42510E+04    1.08171E+04   -1.60560E+04
```

```
                                -1.23179E+02    3.08976E+02    2.30313E+01
NODELOAD        11      10253    2.36934E+04    8.14520E+03    6.94018E+03
                                -1.25955E+02    3.16729E+02    5.42957E+01
NODELOAD        11      10259    2.55105E+04    9.65258E+03    1.61226E+04
                                -1.05751E+02    3.25446E+02   -2.64770E+01
NODELOAD        11      10301    1.77812E+05    7.08137E+04   -2.76987E+04
                                -5.24381E+01    1.63649E+02   -6.83919E+00
NODELOAD        11      10302    9.05324E+03    3.56683E+03   -5.50652E+03
                                -1.85105E+01    1.07932E+01    1.62054E+00
NODELOAD        11      10303    3.19476E+04    1.27446E+04   -2.34687E+04
                                -6.84496E+01    1.57231E+02   -2.91562E+00
NODELOAD        11      10304    1.11143E+04    4.49698E+03   -8.58753E+03
                                -7.14228E+00    2.13839E+01    1.95610E+00
NODELOAD        11      10305    3.10169E+04    1.27350E+04   -2.81893E+04
                                -3.37166E+01    1.71492E+02   -1.18212E+00
NODELOAD        11      10306    8.79541E+03    3.58599E+03   -6.70000E+03
                                 1.02661E+01    1.16155E+01    1.23844E+00
NODELOAD        11      10307    1.69313E+05    7.18369E+04   -6.59542E+04
                                -2.94312E+01    1.54185E+02    2.09711E+01
NODELOAD        11      10309    3.00895E+04    1.17509E+04   -3.33467E+03
                                -4.50365E+01    5.07801E+01    1.03411E+02
NODELOAD        11      10310    2.37468E+03    9.25581E+02   -2.38936E+02
                                -5.27489E-02    9.36830E-02   -1.60371E-02
NODELOAD        11      10311    1.78983E+03    6.99578E+02   -1.76233E+02
                                -4.51400E-02    6.81394E-02   -1.65249E-02
NODELOAD        11      10312    4.03318E+03    1.58066E+03   -3.73095E+02
                                -1.11123E-01    1.52789E+00   -6.39527E-02
NODELOAD        11      10313    1.64966E+05    6.08154E+04    2.78517E+04
                                -6.53305E+01    9.77040E+01    1.44076E+01
NODELOAD        11      10316    2.66989E+04    9.70631E+03    7.23429E+03
                                -8.30361E+01    6.41646E+01    2.36646E+02
NODELOAD        11      10317    7.49096E+03    2.85872E+03    6.08944E+02
                                -3.41369E-01   -9.80778E-02    1.50456E+00
NODELOAD        11      10319    1.77116E+05    6.30937E+04    6.58568E+04
                                -4.57276E+01    1.53059E+02    4.05152E+00
NODELOAD        11      10322    3.09269E+04    1.19132E+04    3.34649E+03
                                -4.15652E+01    3.87717E+01   -1.06607E+02
NODELOAD        11      10329    2.52222E+04    9.85907E+03   -5.55060E+03
                                -5.68943E+01    1.10614E+02    5.73504E+00
NODELOAD        11      10332    5.77996E+04    2.41597E+04   -2.65120E+04
                                -8.01639E+01    2.02171E+02    1.82484E+00
NODELOAD        11      10333    1.98130E+04    7.75362E+03   -1.73093E+03
                                -1.95125E+01    7.64966E+01    2.47884E+00
NODELOAD        11      10339    2.45600E+04    9.77166E+03   -8.62545E+03
                                 5.75644E-01    1.06755E+02    5.43095E+00
NODELOAD        11      10342    5.78692E+04    2.13757E+04   -3.20256E+04
                                -7.16642E+01    2.12153E+02   -2.30060E+00
NODELOAD        11      10343    1.98348E+04    7.52673E+03   -3.36243E+03
                                -2.68302E+01    7.93189E+01    1.48370E+00
NODELOAD        11      10401    3.29482E+05    1.33247E+05   -5.33494E+04
                                -5.75436E+03    1.32291E+04   -2.46092E+03
NODELOAD        11      10402    2.20144E+04    8.78771E+03   -4.97178E+03
                                 7.19734E+00    1.77530E+01    1.15231E+01
NODELOAD        11      10403    7.35529E+04    3.05601E+04   -2.29546E+04
                                -6.62249E+01    2.25247E+02   -1.56762E+00
NODELOAD        11      10404    8.17653E+04    3.23386E+04   -7.43288E+03
                                 4.05523E+00    1.91161E+02   -1.31378E+01
NODELOAD        11      10405    7.43283E+04    2.90737E+04   -2.79984E+04
                                -8.99705E+01    2.27892E+02   -1.29760E+01
NODELOAD        11      10406    2.22584E+04    8.85909E+03   -6.44434E+03
                                -2.74435E+01    1.78705E+01   -5.39653E+00
NODELOAD        11      10407    3.13592E+05    1.35442E+05   -1.29452E+05
                                -4.87722E+03    1.22722E+04    9.95937E+02
NODELOAD        11      10409    1.09950E+05    4.18560E+04   -4.06637E+03
                                -1.06526E+02    5.05102E+01    2.40307E+02
NODELOAD        11      10412    1.48634E+04    5.52175E+03    2.76361E+02
                                -3.86680E-01    1.54586E+01   -3.75031E+00
```

```
NODELOAD        11     10413    3.04658E+05    1.14859E+05    5.55395E+04
                               -5.06740E+03    1.24620E+04    2.28742E+03
NODELOAD        11     10416    9.97830E+04    3.70039E+04    8.67793E+03
                               -5.45478E+01    2.15585E+02    4.92285E+02
NODELOAD        11     10417    1.32773E+04    5.24539E+03   -1.45725E+01
                               -2.10216E+00   -1.88609E+00    4.57676E+00
NODELOAD        11     10419    3.31199E+05    1.19484E+05    1.31983E+05
                               -4.37703E+03    1.29326E+04   -1.08922E+03
NODELOAD        11     10422    1.11129E+05    4.46516E+04    3.66327E+03
                               -8.55974E+01   -5.00908E+01   -1.77850E+02
NODELOAD        11     10429    4.17776E+04    1.49265E+04   -7.71931E+02
                               -2.55820E+01    7.74192E+01    7.22084E+00
NODELOAD        11     10432    8.53540E+04    3.61985E+04   -1.93647E+04
                               -1.17827E+02    2.51011E+02   -1.10815E+01
NODELOAD        11     10433    4.24930E+04    1.58766E+04    9.43944E+02
                               -5.29546E+01    1.50029E+02    3.81934E+00
NODELOAD        11     10439    4.23545E+04    1.80138E+04   -3.38344E+03
                               -2.45961E+01    7.19636E+01   -6.20918E-01
NODELOAD        11     10442    8.58869E+04    3.42587E+04   -2.40412E+04
                               -9.56761E+01    2.50242E+02   -1.27626E+01
NODELOAD        11     10443    4.27122E+04    1.76602E+04   -1.28275E+03
                               -3.22844E+01    1.42767E+02   -2.36325E+00
NODELOAD        11     10501    4.81691E+05    2.02569E+05   -6.64739E+04
                               -6.48372E+02    1.86307E+03   -3.45958E+02
NODELOAD        11     10502    3.31784E+04    1.43074E+04   -3.86129E+03
                                4.55150E+00    1.35172E+01    1.26654E+01
NODELOAD        11     10503    7.82129E+04    3.46029E+04   -1.14771E+04
                               -6.96544E+01    1.62513E+02    2.53708E+00
NODELOAD        11     10504    1.22476E+05    5.19982E+04   -1.49429E+04
                                3.48395E+01    2.68468E+02    2.89489E+00
NODELOAD        11     10505    7.81588E+04    3.33669E+04   -1.47873E+04
                               -1.13604E+02    1.43140E+02   -2.65399E+00
NODELOAD        11     10506    3.31479E+04    1.42573E+04   -5.60804E+03
                               -3.38149E+01    1.19942E+01   -5.95365E+00
NODELOAD        11     10507    4.64678E+05    2.01072E+05   -1.57923E+05
                               -1.12136E+03    2.13751E+03    1.74202E+02
NODELOAD        11     10509    1.43502E+05    5.92406E+04   -7.16273E+03
                               -1.52069E+02    1.52453E+02   -1.44504E+01
NODELOAD        11     10510    1.53204E+04    5.93559E+03    7.62690E+01
                               -2.99075E-01    9.00502E+00    1.37162E+00
NODELOAD        11     10511    9.49971E+03    3.63121E+03    3.84821E+02
                               -1.13369E-01    3.33968E+00    7.88837E-02
NODELOAD        11     10512    1.19641E+04    4.55881E+03    9.77631E+02
                               -1.24143E-01    6.40279E+00   -4.54171E-01
NODELOAD        11     10513    4.34174E+05    1.67582E+05    6.66427E+04
                               -7.16049E+02    1.76605E+03    3.97439E+02
NODELOAD        11     10514    3.54468E+04    1.37663E+04    6.01520E+03
                               -1.26615E+00    4.52191E+00   -8.51692E+00
NODELOAD        11     10516    1.60227E+05    6.08314E+04    2.15337E+04
                               -9.25438E+01    3.04078E+02    3.58835E+02
NODELOAD        11     10517    1.34950E+04    5.37697E+03    9.45487E+02
                                1.27769E+00    1.59754E+00    2.02951E+00
NODELOAD        11     10519    4.78596E+05    1.77492E+05    1.60087E+05
                               -7.98977E+02    2.10437E+03   -2.04497E+02
NODELOAD        11     10520    2.63181E+04    1.00332E+04    4.51627E+03
                               -2.63533E+00    4.16334E+01    1.48651E-01
NODELOAD        11     10521    1.01739E+04    4.05868E+03    6.60386E+02
                               -1.03009E+00    2.23186E+00   -5.46472E-01
NODELOAD        11     10522    1.71251E+05    6.70841E+04    9.83471E+03
                               -8.68935E+01    1.51849E+02   -2.04135E+02
NODELOAD        11     10525    1.99506E+04    7.66459E+03   -1.64706E+00
                               -1.56854E+01    1.62653E+01    6.49028E+00
NODELOAD        11     10527    4.42850E+04    1.76795E+04    4.42100E+02
                               -2.74180E+01    3.87832E-01    1.62919E+01
NODELOAD        11     10528    8.70261E+03    3.53487E+03   -1.11734E+02
                               -5.86158E+00    5.95952E+00    1.99210E+00
NODELOAD        11     10529    4.50712E+04    1.76802E+04    2.06660E+03
```

```
                                -4.59918E+00    6.93629E+01    7.94512E+00
NODELOAD        11      10530    2.48051E+03    9.63558E+02   -1.11082E+01
                                -1.88742E-01    4.09326E-01    1.37761E-01
NODELOAD        11      10531    2.23749E+03    8.55340E+02    5.81248E+01
                                -1.58642E-01    4.38563E-01    2.65298E-02
NODELOAD        11      10532    2.49479E+03    9.46603E+02    1.56934E+02
                                -1.57124E-01    5.56084E-01   -7.97184E-02
NODELOAD        11      10533    5.84273E+03    2.22786E+03    1.57476E+02
                                -2.70107E-01    1.67522E+00    1.23002E-01
NODELOAD        11      10534    5.81564E+03    2.21372E+03    3.55122E+02
                                -2.70784E-01    2.00201E+00   -1.75873E-02
NODELOAD        11      10535    7.21482E+03    2.75535E+03    7.24328E+02
                                -3.15143E-01    3.62976E+00   -2.23153E-01
NODELOAD        11      10538    8.73773E+03    3.79689E+03   -1.98758E+02
                                 3.77786E+00    4.04064E+00   -1.87439E+00
NODELOAD        11      10539    3.83056E+04    1.67610E+04    2.28962E+02
                                -4.38310E+01    7.47535E+01   -2.28153E+00
NODELOAD        11      10540    9.81347E+03    4.24026E+03   -3.56192E+00
                                -2.30977E+00   -1.96922E+00    3.18655E+00
NODELOAD        11      10600    3.14438E+04    1.22759E+04    9.13580E+02
                                -4.15300E+00    5.40939E+01    7.11683E+00
NODELOAD        11      10601    3.00945E+05    1.19453E+05   -2.09723E+04
                                -7.24605E+02    3.29408E+03   -4.86428E+02
NODELOAD        11      10602    1.59609E+04    6.44194E+03   -1.46739E+03
                                -5.11045E+00    6.05895E+00    3.17693E+00
NODELOAD        11      10603    2.04068E+04    8.34753E+03   -1.94193E+03
                                 1.29740E+00    2.99181E+00    7.37588E+00
NODELOAD        11      10604    2.34488E+05    9.84415E+04   -1.86298E+04
                                -8.55546E+01    9.08796E+02   -3.57982E+02
NODELOAD        11      10605    1.94470E+04    8.47258E+03   -2.09879E+03
                                -1.06109E+01    2.16964E+00    1.81766E+00
NODELOAD        11      10606    1.49036E+04    6.57302E+03   -2.06971E+03
                                -3.52336E+00    2.65808E+00    7.23875E-01
NODELOAD        11      10607    2.73933E+05    1.22530E+05   -5.30987E+04
                                -1.42955E+03    2.11729E+03    8.73938E+01
NODELOAD        11      10608    2.89842E+04    1.27279E+04   -3.33945E+03
                                -1.81264E+00    4.42345E+01    5.41303E+00
NODELOAD        11      10609    2.05424E+05    8.37122E+04   -7.57936E+03
                                -3.00357E+02    1.11226E+02    1.27478E+02
NODELOAD        11      10610    2.00712E+04    7.49916E+03   -1.03316E+03
                                -9.24446E-01    2.77470E+00    1.17427E+00
NODELOAD        11      10611    1.25782E+04    4.65213E+03   -3.79423E+02
                                -3.49681E-01    4.89773E+00   -4.47580E-01
NODELOAD        11      10612    9.58142E+03    3.56978E+03    3.46425E+02
                                 2.94588E-01    7.04940E+00   -7.74647E-01
NODELOAD        11      10613    2.86971E+05    1.07666E+05    2.28755E+04
                                -6.61626E+02    3.10259E+03    4.58336E+02
NODELOAD        11      10614    2.73280E+04    1.04225E+04    2.82865E+03
                                -3.61142E+00    4.17357E+00   -8.01044E+00
NODELOAD        11      10616    2.31726E+05    8.83655E+04    2.00690E+04
                                -1.08457E+02    8.50257E+02    3.49282E+02
NODELOAD        11      10617    2.09070E+04    8.11452E+03    3.21561E+02
                                 1.43630E+00    2.07974E+00    3.53803E+00
NODELOAD        11      10618    2.99717E+04    1.15989E+04    4.37564E+03
                                -2.81262E+01    4.59371E+00    3.22778E+00
NODELOAD        11      10619    2.84509E+05    1.10518E+05    5.51529E+04
                                -1.31516E+03    2.19126E+03   -1.06502E+02
NODELOAD        11      10620    1.77405E+04    6.91890E+03    2.04187E+03
                                -6.63361E-01    1.03761E+01    4.23801E-01
NODELOAD        11      10621    2.00344E+04    7.84879E+03    1.24149E+03
                                -1.10635E+00    9.33106E+00    4.24627E-01
NODELOAD        11      10622    2.36298E+05    9.28694E+04    9.68639E+03
                                -3.61887E+02    1.20610E+02   -3.32465E+02
NODELOAD        11      10623    2.73770E+04    1.09378E+04    7.13572E+01
                                -2.11029E-01   -2.94829E+00    3.75703E+00
NODELOAD        11      10624    2.42614E+04    8.96399E+03   -6.44686E+02
                                -3.40146E+00    3.59078E+00    5.88320E+00
```

```
NODELOAD        11      10625    8.74185E+03    3.21669E+03   -1.59321E+02
                                -2.69063E-01    1.37074E+00   -2.43427E-02
NODELOAD        11      10626    8.72086E+03    3.23308E+03    8.08899E+01
                                -4.93483E-01    3.50638E+00   -4.24231E-01
NODELOAD        11      10627    6.76448E+03    2.55358E+03    4.65475E+02
                                -8.16074E-01    4.13272E+00   -5.50797E-01
NODELOAD        11      10628    3.63125E+03    1.35510E+03   -1.45354E+02
                                -3.96003E-01    2.15344E-01    9.93765E-02
NODELOAD        11      10629    3.30990E+03    1.21512E+03   -1.26740E+02
                                -4.69769E-01    7.39224E-01   -1.67918E-01
NODELOAD        11      10630    3.66754E+03    1.34520E+03   -3.08635E+01
                                -4.84330E-01    1.72632E+00   -4.71778E-01
NODELOAD        11      10631    2.04964E+04    8.47986E+03   -3.38955E+02
                                -5.80237E+00   -5.26256E+00    4.80057E+00
NODELOAD        11      10638    7.89787E+03    3.16512E+03   -1.39985E+01
                                -1.01592E+00   -1.68461E-04    4.00900E-01
NODELOAD        11      20621    1.15713E+05    4.32370E+04   -7.32843E+03
                                -1.31843E+02    1.03084E+03   -2.25938E+01
NODELOAD        11      20624    1.57515E+05    6.35380E+04   -6.71574E+03
                                -1.79731E+02    1.67776E+02    9.56981E+01
NODELOAD        11      20631    9.98205E+04    4.72947E+04   -1.85219E+04
                                -4.29650E+02    4.05458E+02    1.98130E+02
NODELOAD        11      20634    1.49042E+05    6.44723E+04   -2.11128E+04
                                -8.42502E+01    3.91859E+02    5.64445E+01
NODELOAD        11      20641    1.10899E+05    3.92117E+04    8.04125E+03
                                -1.24887E+02    9.74325E+02    3.42288E+01
NODELOAD        11      20644    1.51089E+05    5.72571E+04    7.62133E+03
                                -1.68632E+02    1.42566E+02   -5.02537E+01
NODELOAD        11      20651    1.03756E+05    4.25671E+04    1.92286E+04
                                -3.83080E+02    4.08638E+02   -1.75880E+02
NODELOAD        11      20654    1.55313E+05    5.80484E+04    2.20182E+04
                                -5.74920E+01    4.02297E+02   -9.38915E+00
NODELOAD        11      20712    7.07210E+03    3.02105E+03   -9.83375E+02
                                -3.19311E-01    6.39688E-01    1.04883E-01
NODELOAD        11      20715    2.22658E-04    9.04276E-05   -9.87926E-06
                                -1.56722E-08    1.28901E-07    3.47945E-08
NODELOAD        11      20716    6.58092E-05    2.62484E-05   -7.68154E-07
                                -5.74321E-10    1.81962E-08    4.04998E-09
NODELOAD        11      20717    5.04533E-05    1.99112E-05    3.66192E-07
                                -4.41831E-10    1.00046E-08    2.22654E-09
NODELOAD        11      20718    5.48401E-05    2.13905E-05    1.53066E-06
                                -4.79990E-10    1.18180E-08    2.62976E-09
NODELOAD        11      20719    7.07152E+03    2.72308E+03    3.55621E+02
                                -3.19700E-01    6.39278E-01    1.04875E-01
NODELOAD        11      20732    7.36884E+03    2.72277E+03    1.02570E+03
                                -3.19338E-01    6.39713E-01    1.04874E-01
NODELOAD        11      20734    2.51444E-04    9.52167E-05    2.46102E-05
                                -2.02096E-09    2.96472E-07    6.59554E-08
NODELOAD        11      20739    7.36944E+03    3.02071E+03   -3.13346E+02
                                -3.19726E-01    6.39308E-01    1.04873E-01
NODELOAD        11      20750    1.86692E-04    7.73065E-05   -1.23080E-05
                                -7.14671E-08    3.21627E-09    3.17069E-08
NODELOAD        11      20752    1.82888E-04    7.73109E-05   -2.08812E-05
                                -7.14203E-08    3.21719E-09    3.17060E-08
NODELOAD        11      20760    1.21920E-04    4.89988E-05   -2.49612E-06
                                -2.85693E-08    2.13754E-09    1.26831E-08
NODELOAD        11      20765    2.50171E-04    9.29073E-05    3.21422E-05
                                -1.78551E-07    4.31579E-09    7.92659E-08
NODELOAD        11      40021    7.58453E-04    3.01669E-04    2.22144E-06
                                -2.45675E-07    4.64083E-07    2.09467E-07
NODELOAD        11      40041    8.98900E+07    3.57664E+07    1.45959E+06
                                -2.58088E-07    5.19076E-07    2.12706E-07
'
```

C.1.3 Control file to static analysis

```
' ========================================================================
' ||           Ultimate load analysis for typical North Sea jacket      ||
' ||                                                                    ||
' ||           Control file to USFOS, file name: statctr.fem            ||
' ========================================================================
'
HEAD      Static pushover analysis of jacket based
                       on Draupner S

'
'    Units:     Force         : Newton
'               Length        : Meters
'               Rotation      : Rad
'
'    Files:     Control file  : statctr.fem
'               Geometry file : stru.fem
'               Load file     : load.fem
'               Result file   : statres.fem
'
' ----------------------------------------------------------------
'
' Overview, basic load cases
' --------------------------
'
'     1.  Permanent loads (gravity- and live loads)
'     5.  Wind +X, in total 3 MN
'     6.  Wind +Y, in total 3 MN
'    10.  Wave (and current) +X direction
' ---------------------------------------
'
' Analysis control data
' ---------------------
'
XFOSFULL                      ! All available data stored for RAF-file
CSAVE    0   -1    1          ! Saving of data restart, xfos and out-file
CPRINT   1    2    1          ! What to write on outfile
CMAXSTEP  4000
'
'          epsol     gamstp  ifunc  pereul  ktrmax  dentsw  cmax  ifysw  deters
CPROPAR    1.0E-20   0.05    2.0    0.05    10      1       999    0     1
'
'
'
' Displacement control nodes
' --------------------------
'
CNODES     1
'          nodex     idof    dfact
           40041      1       1.0
'
' Load combinations
' -------------------------
'
 CCOMB    1   1
 CCOMB    2   9    12
'
' Static pushover analysis specification
' --------------------------------------
'
'          nloads    npostp  mxpstp mxpdis
CUSFOS     4         450     0.1   0.1
'          lcomb     lfact   mxld   nstep   minstp
            1        0.2     1.0     0      0.010
            2        0.10    0.5     0      0.005
```

```
            2        0.05    0.7     0      0.001
            2        0.01    1.2     0      0.001
            2        0.001   3.0     0      0.0001
'            11       0.05    0.25    0      0.010  ! For treghetslasten
'            11       0.005   0.50    0      0.001  ! For treghetslasten
'
'
' Rayleigh damping 1.5 %
' ----------------------
'
'           alpha1       alpha2
'RAYLDAMP   0.00997      0.00366
'
'
' Specify calculation of relative velocity
' ----------------------------------------
'
'REL_VELO
'
```

C.1.4 Control file to quasi-static analysis

```
' ========================================================================
' ||           Ultimate load analysis for typical North Sea jacket      ||
' ||                                                                    ||
' ||           Control file to USFOS, file name: kvasictr.fem           ||
' ========================================================================
'
HEAD      Static analysis in time domain of jacket based
                      on Draupner S

'
'    Units:     Force         : Newton
'               Length        : Meters
'               Rotation      : Rad
'
'    Files:     Control file  : kvasictr.fem
'               Geometry file : stru.fem
'               Load file     : load.fem
'               Result file   : kvasires.fem
'
' ---------------------------------------------------------------
'
' Overview, basic load cases
' --------------------------
'
'     1.  Permanent loads and live loads
'     5.  Wind +X
'     6.  Wind +Y
'    10.  Wave and current +X direction
' ----------------------------------------
'
' Global results to be saved
' --------------------------
'
 DynRes_G  WaveLoad
 DynRes_G  WaveElev
 DynRes_G  WaveOVTM
 DynRes_G  ReacBSH
 DynRes_G  ReacOVTM
 DynRes_N  Disp   40041   1
 DynRes_N  Vel    40041   1
 DynRes_N  Acc    40041   1
'
```

```
'
' Defining all elements elastic
' -----------------------------
'
 Lin_Elem   0    All
'
'
' Analysis control data
' ---------------------
'
XFOSFULL                      ! All available data stored for RAF-file
CSAVE    0  -10    1          ! Saving of data restart, xfos and out-file
CPRINT   1    2    1          ! What to write on outfile
CMAXSTEP   2000
'
'          epsol     gamstp  ifunc  pereul  ktrmax  dentsw  cmax  ifysw  deters
CPROPAR    1.0E-20   0.05    2.0    0.05    10      1       999    0     1
'
'
' Displacement control nodes
' --------------------------
'
CNODES     1
'          nodex     idof    dfact
           40041      1       1.0
'
'
' Dynamic analysis specification
' ------------------------------
'
'            npostp   mxpstp    mxpdis
 POSTCOLL      10      1.00     0.10
'
'           End_Time   Delta_T   Dt_Res   Dt_term
 Static       17.0      0.05      0.05      1.0
'
 Ini_time      1.0
'
 WavCase1   31   1
'
'
'             ID   <type>    Time         Factor
 TIMEHIST     51   Points     0.0          .0
                              1.0         1.0
                             20.0         1.0
'
'             ID   <type>    Time         Factor
 TIMEHIST     52   Points     0.0          .0
                              4.6         0.0
                              5.1         1.0
                              5.6         0.4
                              7.7         0.0
                             20.0         0.0
'
'             ID   <type>  Dtime Factor   Start_time
 TIMEHIST     53   Switch    0     1.0       1.0

'
'
'           Ildcs   Tim Hist
 LOADHIST     1        51
 LOADHIST     9        52
 LOADHIST    10        53
'
'
' Rayleigh damping 1.5 %
' ----------------------
```

```
'
'           alpha1       alpha2
'RAYLDAMP   0.00997      0.00366
'
'
' Specify calculation of relative velocity
' ---------------------------------------
'
'REL_VELO
'
```

C.1.5 Control file to dynamic analysis

```
' ========================================================================
' ||           Ultimate load analysis for typical North Sea jacket      ||
' ||                                                                    ||
' ||           Control file to USFOS, file name: dynctr.fem             ||
' ========================================================================
'
HEAD    Dynamic pushover analysis of jacket
        based on Draupner S

'
'    Units:     Force         : Newton
'               Length        : Meters
'               Rotation      : Rad
'
'    Files:     Control file  : dynctr.fem
'               Geometry file : stru.fem
'               Load file     : load.fem
'               Result file   : dynres.fem
'
' ---------------------------------------------------------------
'
' Overview, basic load cases
' --------------------------
'
'     1.  Permanent loads and live loads
'     5.  Wind +X
'     6.  Wind +Y
'    10.  Wave and current +X direction
' ----------------------------------------
'
' Global results to be saved
' --------------------------
'
 DynRes_G  WaveLoad
 DynRes_G  WaveElev
 DynRes_G  WaveOVTM
 DynRes_G  ReacBSH
 DynRes_G  ReacOVTM
 DynRes_N  Disp   40041   1
 DynRes_N  Vel    40041   1
 DynRes_N  Acc    40041   1
'
' Analysis control data
' ---------------------
'
XFOSFULL                      ! All available data stored for RAF-file
CSAVE    0  -10    1          ! Saving of data restart, xfos and out-file
CPRINT   1    2    1          ! What to write on outfile
CMAXSTEP   2000
'
CDYNPAR    -0.3
```

```
PCOR_ON
'          cmin      cneg      itmax      isol      epsit      cminneg
CITER       0.0       -2         30        1        0.00001       -0.0
'
'          epsol     gamstp  ifunc  pereul  ktrmax  dentsw  cmax  ifysw  deters
CPROPAR    1.0E-20   0.05    2.0    0.05    10      1       999    0     1
'
'
' Displacement control nodes
' --------------------------
'
CNODES     1
'          nodex     idof    dfact
           40041      1       1.0
'
'
' Dynamic analysis specification
' ------------------------------
'
'            npostp   mxpstp    mxpdis
 POSTCOLL      10      1.00     0.10
'
'           End_Time   Delta_T   Dt_Res   Dt_Term
 Static        1.0      0.05     0.05     1.0
 Dynamic       3.5      0.05     0.05     1.0
 Dynamic       7.0      0.005    0.05     1.0
 Dynamic      17.0      0.01     0.05     1.0
 Eigenval      0.0
'
 Ini_time      1.0
'
'              ScaleFac
'EigForce          29798  ! Totalt 100 MN
'
'             ID   <type>    Time         Factor
 TIMEHIST     51   Points     0.0          .0
                              1.0         1.0
                             20.0         1.0
'
'             ID   <type>    Time         Factor
 TIMEHIST     52   Points     0.0          .0
                              4.6         0.0
                              5.1         1.0
                              5.6         0.4
                              7.7         0.0
                             20.0         0.0
'
'             ID   <type>  Dtime Factor   Start_time
 TIMEHIST     53   Switch    0     1.0       1.0

'
'
'           Ildcs   Tim Hist
 LOADHIST     1        51
 LOADHIST     9        52
 LOADHIST    10        53
'
'
' Rayleigh damping 1.5 %
' ----------------------
'
'           alpha1       alpha2
'RAYLDAMP   0.00997      0.00366
'
'
' Specify calculation of relative velocity
' ----------------------------------------
```

```
’
’REL_VELO
’
```

C.1.6 Batch file for analysis run

```
#! /bin/sh
#  ================================================
#  ||   Made by: Katrine Hansen 4 March 2001     ||
#  ||   File name: go                            ||
#  ||   Run file for jacket analysis Draupner S  ||
#  ||   Usage: go  Wave_height  Period  Depth    ||
#  ================================================

SURFACE=$3
FdX75=601451
FdX76=2788216
FdX77=4927353
FdX78=7006456
FdX79=9021671
FdX80=10973730
FdX81=12863360


case $3
in
  75)
    FDECKX=$FdX75
  ;;
  76)
    FDECKX=$FdX76
  ;;
  77)
    FDECKX=$FdX77
  ;;
  78)
    FDECKX=$FdX78
  ;;
  79)
    FDECKX=$FdX79
  ;;
  80)
    FDECKX=$FdX80
  ;;
  81)
    FDECKX=$FdX81
  ;;
  *)
    echo ’No deck load given for chosen water depth’

    exit
  ;;
esac

echo $FDECKX

# Lager resultatkatalog hvis denne ikke eksisterer
# ------------------------------------------------

if ! test -d /cygdrive/d/UsfosWork/dsres/h$1t$2d$3
   then mkdir /cygdrive/d/UsfosWork/dsres/h$1t$2d$3
fi

cd /cygdrive/d/UsfosWork/dsres/h$1t$2d$3
```

```
cp /cygdrive/d/UsfosWork/draupnerS/load.fem load.fem

sed s/WAVEH/$1/g load.fem > l1.tmp
sed s/PERIOD/$2/g l1.tmp > l2.tmp
sed s/DEPTH/$3/g l2.tmp > l3.tmp
sed s/SURFACE/$SURFACE/g l3.tmp > l4.tmp
sed s/FDECKX/$FDECKX/g l4.tmp > l5.tmp

mv l5.tmp load.fem
rm l?.tmp

# Kjrer kvasistatisk usfos
# --------------------

usfos 25 << EOF5
d:/UsfosWork/draupnerS/kvasi/kvasictr
d:/UsfosWork/draupnerS/stru
load
kvasires
EOF5

echo 'Kvasistatic analysis finished'

# Kjrer dynamisk usfos
# ---------------------

usfos 25 << EOF7
d:/UsfosWork/draupnerS/dynamic/dynctr
d:/UsfosWork/draupnerS/stru
load
dynres
EOF7

echo 'Dynamic analysis finished'


# Lager tillegg til load.fem med pushover-lasten
# ----------------------------------------------

cp kvasires_wave_load.fem pushoverload.fem
cp /cygdrive/d/UsfosWork/draupnerS/vi_kommando1.liste .

vim -s vi_kommando1.liste pushoverload.fem

sed 's/  113  /   12  /g' pushoverload.fem > pushover1.fem

cat pushover1.fem >> load.fem
rm pushove*.fem
rm vi_kommando1.liste

# Kjrer statisk usfos
# --------------------

usfos 25 << EOF1
d:/UsfosWork/draupnerS/static/statctr
d:/UsfosWork/draupnerS/stru
load
statres
EOF1

echo 'Static analysis finished'
```

C.2 Model ‘DE’

```
 HEAD      Reducing subdivided elements into one element.

,
,            Node ID            X             Y             Z    Boundary code
 NODE             1       -1.581       -18.881       -69.381   1 1 1 1 1 1
 NODE             4       21.600        -9.919       -68.800
 NODE             5       25.500        -8.500       -68.800
 NODE             8       21.600        -9.919       -67.000
 NODE             9       21.600        -5.713       -67.000
 NODE            11       -5.133       -12.809       -69.381   1 1 1 1 1 1
 NODE            13       21.600        -5.713       -68.800
 NODE            14       27.156        -4.298       -68.800
 NODE            15       33.560        -6.300       -67.400
 NODE            16       39.160        -9.900       -64.400
 NODE            20       46.756       -20.756       -55.000
 NODE            21       44.900       -19.900       -58.400
 NODE            22       21.600       -17.489       -67.000
 NODE            25       10.111        -6.000       -67.000
 NODE            26       21.600         5.489       -67.000
 NODE            27       10.111       -17.489       -67.000
 NODE            28       10.111         5.489       -67.000
 NODE            29        9.778       -26.222       -70.000
 NODE            30        9.778        14.222       -70.000
 NODE            31       30.000       -25.889       -67.000
 NODE            32       49.889        -6.000       -67.000
 NODE            33       50.222        14.222       -70.000
 NODE            34       30.000        13.889       -67.000
 NODE            35       38.910        13.889       -67.000
 NODE            36       50.222       -26.222       -70.000
 NODE            37       38.909        12.383       -66.999
 NODE            38       49.630        13.630       -64.666
 NODE            39       47.499        11.499       -45.492
 NODE            40       49.889        13.889       -67.000
 NODE            41       40.570        13.243       -61.188
 NODE            42       40.570        11.728       -61.188
 NODE            43       45.836       -20.732       -55.000
 NODE            44       10.370        13.630       -64.666
 NODE            45       10.111        13.889       -67.000
 NODE            46       12.501        11.499       -45.492
 NODE            47       10.111       -25.889       -67.000
 NODE            48       49.889       -25.889       -67.000
 NODE            49       10.370       -25.630       -64.666
 NODE            50       49.630       -25.630       -64.666
 NODE            51       30.000        12.510       -54.596
 NODE            52       30.977        12.444       -54.000
 NODE            53       48.444        -5.023       -54.000
 NODE            54       48.510        -6.000       -54.596
 NODE            55       29.023        12.444       -54.000
 NODE            56       11.556        -5.023       -54.000
 NODE            58       11.490        -6.000       -54.596
 NODE            59       47.499       -23.499       -45.492
 NODE            60       47.583       -19.690       -46.251
 NODE            61       48.444        -6.977       -54.000
 NODE            62       45.806       -19.806       -46.451
 NODE            63       12.501       -23.499       -45.492
 NODE            64       11.556        -6.977       -54.000
 NODE            65       29.023       -24.444       -54.000
 NODE            66       20.105       -15.700       -54.000
 NODE            67       30.000       -24.510       -54.596
 NODE            68       30.977       -24.444       -54.000
 NODE            69       44.716       -23.513       -45.617
 NODE            70       39.896       -15.700       -54.000
 NODE            71       28.750       -15.700       -54.000
```

```
NODE          72        31.000       -15.700       -54.000
NODE          73        44.716       -21.713       -45.617
NODE          75        28.750       -14.500       -54.000
NODE          76        12.667        11.333       -44.000
NODE          77        47.333        11.333       -44.000
NODE          78        46.000         9.585       -42.194
NODE          79        47.100        11.100       -41.900
NODE          80        44.122         7.707       -25.294
NODE          81        45.222         9.222       -25.000
NODE          82        46.082        -6.000       -32.745
NODE          83        46.022        -5.165       -32.200
NODE          84        30.835        10.022       -32.200
NODE          85        30.000        10.082       -32.745
NODE          86        29.165        10.022       -32.200
NODE          87        13.978        -5.165       -32.200
NODE          89        13.918        -6.000       -32.745
NODE          90        31.000       -14.500       -54.000
NODE          91        28.750       -14.500       -43.100
NODE          95        42.947       -16.947       -20.721
NODE          96        31.000       -14.500       -43.100
NODE          97        15.000         9.000       -23.000
NODE         100        47.333       -23.333       -44.000
NODE         101        46.022        -6.835       -32.200
NODE         102        12.668       -23.332       -44.000
NODE         103        30.835       -22.022       -32.200
NODE         104        30.000       -22.082       -32.745
NODE         105        29.165       -22.022       -32.200
NODE         106        13.978        -6.835       -32.200
NODE         107        22.842       -15.698       -32.200
NODE         108        37.158       -15.698       -32.200
NODE         109        28.750       -15.699       -32.200
NODE         110        31.000       -15.699       -32.200
NODE         111        44.725       -16.901       -20.521
NODE         112        45.000         9.000       -23.000
NODE         114        30.000         7.992       -13.929
NODE         115        28.750       -14.500       -32.200
NODE         117        43.209         7.209       -14.381
NODE         118        44.022         8.022       -14.200
NODE         119        43.467         7.467        -9.200
NODE         120        42.367         5.952        -9.494
NODE         121        42.654         6.654        -9.381
NODE         122        40.567         4.152         6.706
NODE         123        31.000       -14.500       -32.200
NODE         124        45.000       -21.000       -23.000
NODE         125        42.081       -19.026       -21.438
NODE         126        42.086       -20.804       -21.238
NODE         127        15.000       -21.000       -23.000
NODE         128        15.438       -20.562       -19.061
NODE         129        44.562       -20.562       -19.061
NODE         130        40.566       -19.282        -7.539
NODE         131        40.566       -17.482        -7.539
NODE         132        43.349       -15.574        -8.139
NODE         133        41.574       -15.574        -8.367
NODE         134        43.992        -6.000       -13.929
NODE         135        34.292       -15.700       -13.929
NODE         136        30.000       -19.992       -13.929
NODE         137        25.708       -15.700       -13.929
NODE         138        28.750       -15.700       -13.929
NODE         139        31.000       -15.700       -13.929
NODE         140        16.008        -6.000       -13.929
NODE         143        39.456         3.041        16.706
NODE         144        38.900         2.485        21.706
NODE         145        42.098         6.098        -4.381
NODE         146        42.278         6.278         1.500
NODE         147        42.911         6.911        -4.200
NODE         148        41.465         5.465         1.319
NODE         149        40.854         4.854         6.819
```

```
NODE          150        41.667         5.667         7.000
NODE          151        41.111         5.111        12.000
NODE          152        40.298         4.298        11.819
NODE          153        40.556         4.556        17.000
NODE          154        39.743         3.743        16.819
NODE          155        39.187         3.187        21.819
NODE          157        41.444         5.444         9.000
NODE          158        32.500         5.444         9.000
NODE          160        43.111         7.111        -6.000
NODE          161        41.444        -3.400         9.000
NODE          163        27.399         5.444         9.000
NODE          165        18.556         5.444         9.000
NODE          168        16.889         7.111        -6.000
NODE          172        18.556        -3.500         9.000
NODE          173        30.000         5.444         9.000
NODE          175        20.000         4.000        22.000
NODE          176        28.750       -14.500       -13.929
NODE          177        40.000         4.000        22.000
NODE          179        39.666       -13.666         8.800
NODE          180        38.000        -4.000        22.000
NODE          181        41.444       -13.666         9.000
NODE          182        41.444        -8.601         9.000
NODE          183        41.444        -8.601         9.700
NODE          184        41.444       -17.440         9.700
NODE          185        38.744       -17.444         9.700
NODE          186        38.744       -17.444         9.000
NODE          187        38.744       -15.666         8.800
NODE          188        32.500       -17.444         9.000
NODE          189        16.889       -19.111        -6.000
NODE          190        18.556        -8.600         9.000
NODE          191        27.400       -17.444         9.000
NODE          192        31.000       -14.500       -13.929
NODE          194        42.333       -18.333         1.000
NODE          195        42.000       -18.000         4.000
NODE          196        42.667       -18.667        -2.000
NODE          197        43.111       -19.111        -6.000
NODE          198        38.000        -4.000        25.750
NODE          199        38.000       -10.000        22.000
NODE          200        28.750       -14.500        -4.250
NODE          201        27.903       -15.347         9.000
NODE          202        28.750       -14.500         9.000
NODE          203        18.556        -6.000         9.000
NODE          204        18.556       -17.444         9.000
NODE          205        20.000       -16.000        22.000
NODE          206        31.000       -14.500        -4.250
NODE          207        41.444       -17.444         9.000
NODE          209        38.000       -10.000        25.750
NODE          211        40.000         4.000        25.750
NODE          212        30.000        -6.000        25.750
NODE          213        20.000         4.000        25.750
NODE          214        31.972       -15.472         9.000
NODE          215        41.444        -6.000         9.000
NODE          216        30.000       -17.444         9.000
NODE          219        40.000       -16.000        22.000
NODE          221        40.867       -16.867        14.200
NODE          222        40.289       -16.289        19.400
NODE          223        40.000       -16.000        25.750
NODE          224        28.750       -14.500        25.750
NODE          225        31.000       -14.500         9.000
NODE          229        20.000       -16.000        25.750
NODE          230        30.000       -16.000        25.750
NODE          232        31.000       -14.500        25.750
NODE          244        10.000         4.000        25.750
NODE          245        10.000       -16.000        25.750
NODE          254        10.000         4.000        32.750
NODE          255        10.000       -16.000        32.750
'
```

```
'           Elem ID     np1      np2   material   geom    lcoor    ecc1    ecc2
 BEAM          1001      29       47         15      2        1
 BEAM          1002      47       49         15      2        1
 BEAM          1003      49       63         15      1        1
 BEAM          1004      63      102         15      3        1
 BEAM          1005     102      127         15      4        1
 BEAM          1006     127      128         15      3        1
 BEAM          1007     128      189         15      5        1
 BEAM          1008     189      204         15      5        1
 BEAM          1009     204      205         15      5        1
 BEAM          1010     205      229         15      5        1
 BEAM          1011      36       48         15      2        1
 BEAM          1012      48       50         15      2        1
 BEAM          1013      50       59         15      1        1
 BEAM          1014      59      100         15      3        1
 BEAM          1015     100      124         15      4        1
 BEAM          1016     124      129         15      3        1
 BEAM          1017     129      197         15      5        1
 BEAM          1018     197      196         15      5        1
 BEAM          1019     196      194         15      5        1
 BEAM          1020     194      195         15      5        1
 BEAM          1022     195      207         15      5        1
 BEAM          1024     207      221         15      5        1
 BEAM          1026     221      222         15      5        1
 BEAM          1027     222      219         15      5        1
 BEAM          1028     219      223         15      5        1
 BEAM          1029      30       45         15      2        1
 BEAM          1030      45       44         15      2        1
 BEAM          1031      44       46         15      1        1
 BEAM          1032      46       76         15      3        1
 BEAM          1033      76       97         15      4        1
 BEAM          1037      97      168         15      5        1
 BEAM          1039     168      165         15      5        1
 BEAM          1041     165      175         15      5        1
 BEAM          1042     175      213         15      5        1
 BEAM          1043      33       40         15      2        1
 BEAM          1044      40       38         15      2        1
 BEAM          1045      38       39         15      1        1
 BEAM          1046      39       77         15      3        1
 BEAM          1047      77       79         15      4        1
 BEAM          1048      79       81         15      4        1
 BEAM          1049      81      112         15      4        1
 BEAM          1051     112      118         15      5        1
 BEAM          1052     118      119         15      5        1
 BEAM          1053     119      160         15      5        1
 BEAM          1054     160      147         15      5        1
 BEAM          1055     147      146         15      5        1
 BEAM          1056     146      150         15      5        1
 BEAM          1057     150      157         15      5        1
 BEAM          1058     157      151         15      5        1
 BEAM          1059     151      153         15      5        1
 BEAM          1060     153      177         15      5        1
 BEAM          1061     177      211         15      5        1
 BEAM          1062      47       31          1     16        1
 BEAM          1063      31       48          1     10        1
 BEAM          1064      45       34          1     16        1
 BEAM          1065      34       35          1     10        1
 BEAM          1066      35       40          1     10        1
 BEAM          1067      27       22          1     23        1
 BEAM          1068      28       26          1     23        1
 BEAM          1069      47       27          1     16        1
 BEAM          1071      27       25          1     16        1
 BEAM          1073      25       28          1     16        1
 BEAM          1074      28       45          1     16        1
 BEAM          1075      48       32          1     16        1
 BEAM          1076      32       40          1     16        1
 BEAM          1077      22        8          1     25        1
```

```
BEAM        1078        8        9        1       25       1
BEAM        1079        9       26        1       25       1
BEAM        1080       25       22        1       18       1
BEAM        1081       25       26        1       18       1
BEAM        1082       22       31        1       18       1
BEAM        1083       26       34        1       18       1
BEAM        1084       31       32        1       18       1
BEAM        1085       34       32        1       18       1
BEAM        1086        8        4        1       28       1
BEAM        1087        9       13        1       28       1
BEAM        1088       56       55        1       25       1
BEAM        1089       64       66        1       25       1
BEAM        1090       65       66        1       25       1
BEAM        1091       52       53        1       25       1
BEAM        1092       68       70        1       25       1
BEAM        1093       70       61        1       25       1
BEAM        1094       66       71        1       27       1
BEAM        1095       71       72        1       27       1
BEAM        1096       72       70        1       27       1
BEAM        1097       71       75        1       33       1
BEAM        1098       72       90        1       37       1
BEAM        1099       87       86        1       27       1
BEAM        1100      106      107        1       27       1
BEAM        1101      105      107        1       27       1
BEAM        1102       84       83        1       27       1
BEAM        1103      103      108        1       27       1
BEAM        1104      108      101        1       27       1
BEAM        1105      107      109        1       29       1
BEAM        1106      109      110        1       29       1
BEAM        1107      110      108        1       29       1
BEAM        1108      109      115        1       33       1
BEAM        1109      110      123        1       37       1
BEAM        1110      140      114        1       27       1
BEAM        1111      140      137        1       27       1
BEAM        1112      137      136        1       27       1
BEAM        1113      136      135        1       27       1
BEAM        1114      135      134        1       27       1
BEAM        1115      114      134        1       27       1
BEAM        1116      137      138        1       30       1
BEAM        1117      138      139        1       30       1
BEAM        1118      139      135        1       30       1
BEAM        1119      138      176        1       33       1
BEAM        1120      139      192        1       37       1
BEAM        1121      204      191        1       20       1
BEAM        1122      191      216        1        6       1
BEAM        1123      216      188        1        6       1
BEAM        1124      188      186        1       21       1
BEAM        1125      186      207        1       21       1
BEAM        1126      165      163        1       20       1
BEAM        1127      163      173        1        6       1
BEAM        1128      173      158        1        6       1
BEAM        1130      158      157        1       21       1
BEAM        1131      204      190        1       20       1
BEAM        1132      190      203        1        6       1
BEAM        1134      203      172        1        6       1
BEAM        1137      172      165        1       20       1
BEAM        1138      207      181        1       20       1
BEAM        1139      181      182        1       20       1
BEAM        1140      182      215        1        6       1
BEAM        1141      215      161        1        6       1
BEAM        1142      161      157        1       20       1
BEAM        1143      203      173        1       26       1
BEAM        1144      203      201        1       26       1
BEAM        1145      201      216        1       26       1
BEAM        1146      173      215        1       26       1
BEAM        1147      216      214        1       26       1
BEAM        1148      214      215        1       26       1
```

```
BEAM        1149     201     202       1      33       1
BEAM        1150     214     225       1      32       1
BEAM        1152       1       4       9      12       1
BEAM        1154       4       5       9      12       1
BEAM        1157       5      21       9      12       1
BEAM        1159      21      43       9      12       1
BEAM        1160      43      73       9      12       1
BEAM        1161      73     125       9      12       1
BEAM        1162     125     131       9      12       1
BEAM        1163     131     187      10      11       1
BEAM        1164     187     199      10      11       1
BEAM        1165     199     209       9      12       1
BEAM        1166      47      67       1      17       1
BEAM        1167      48      67       1      16       1
BEAM        1168      65      67       1      13       1
BEAM        1169      65     102       1      17       1
BEAM        1170      67      68       1      13       1
BEAM        1171      68      69       1      17       1
BEAM        1172      69     100       1      17       1
BEAM        1173     102     104       1      22       1
BEAM        1174     100     104       1      22       1
BEAM        1175     105     104       1      19       1
BEAM        1176     105     127       1      22       1
BEAM        1177     104     103       1      19       1
BEAM        1178     103     124       1      22       1
BEAM        1179     127     136       1      22       1
BEAM        1180     124     126       1      22       1
BEAM        1181     126     136       1      22       1
BEAM        1182     136     189       1      20       1
BEAM        1183     136     130       1      20       1
BEAM        1184     130     197       1      20       1
BEAM        1185     189     216       1      20       1
BEAM        1186     197     216       1      20       1
BEAM        1187     216     205       1      20       1
BEAM        1188     216     219       1      20       1
BEAM        1189      45      51       1      17       1
BEAM        1190      40      41       1      16       1
BEAM        1191      41      51       1      16       1
BEAM        1192      51      55       1      13       1
BEAM        1193      55      76       1      17       1
BEAM        1194      52      51       1      13       1
BEAM        1195      52      77       1      17       1
BEAM        1196      77      85       1      22       1
BEAM        1197      76      85       1      22       1
BEAM        1198      84      85       1      19       1
BEAM        1199      84     112       1      22       1
BEAM        1200      85      86       1      19       1
BEAM        1201      86      97       1      22       1
BEAM        1202      97     114       1      22       1
BEAM        1203     112     114       1      22       1
BEAM        1205     114     168       1      20       1
BEAM        1206     114     160       1      20       1
BEAM        1208     168     173       1      20       1
BEAM        1209     160     173       1      20       1
BEAM        1211     173     175       1      20       1
BEAM        1212     173     177       1      20       1
BEAM        1213      47      58       1      17       1
BEAM        1214      45      58       1      17       1
BEAM        1215      58      64       1      13       1
BEAM        1216      64     102       1      17       1
BEAM        1217      56      58       1      13       1
BEAM        1219      56      76       1      17       1
BEAM        1220     102      89       1      22       1
BEAM        1222      76      89       1      22       1
BEAM        1223      89     106       1      19       1
BEAM        1224     106     127       1      22       1
BEAM        1225      87      89       1      19       1
```

```
BEAM        1227      87      97       1      22       1
BEAM        1228     127     140       1      22       1
BEAM        1230      97     140       1      22       1
BEAM        1231     140     189       1      20       1
BEAM        1233     140     168       1      20       1
BEAM        1235     189     203       1      20       1
BEAM        1237     168     203       1      20       1
BEAM        1239     203     205       1      20       1
BEAM        1241     203     175       1      20       1
BEAM        1242      48      54       1      17       1
BEAM        1243      40      54       1      17       1
BEAM        1244      61      54       1      13       1
BEAM        1245      61      60       1      17       1
BEAM        1246      60     100       1      17       1
BEAM        1247      54      53       1      13       1
BEAM        1248      53      77       1      17       1
BEAM        1249     100      82       1      22       1
BEAM        1250      77      82       1      22       1
BEAM        1251     101      82       1      19       1
BEAM        1252     101     124       1      22       1
BEAM        1253      82      83       1      19       1
BEAM        1254      83     112       1      22       1
BEAM        1255     124     111       1      22       1
BEAM        1256     111     134       1      22       1
BEAM        1257     112     134       1      22       1
BEAM        1258     134     132       1      20       1
BEAM        1259     132     197       1      20       1
BEAM        1260     134     160       1      20       1
BEAM        1261     197     215       1      20       1
BEAM        1262     160     215       1      20       1
BEAM        1263     215     219       1      20       1
BEAM        1264     215     177       1      20       1
BEAM        1265      69      73       1      24       1
BEAM        1266      60      62       1      24       1
BEAM        1267     126     125       1      24       1
BEAM        1268     111      95       1      24       1
BEAM        1269     130     131       1      24       1
BEAM        1270     132     133       1      24       1
BEAM        1271     186     187       1      24       1
BEAM        1272     181     179       1      24       1
BEAM        1274      11      13      11      11       1
BEAM        1276      13      14      11      11       1
BEAM        1277      14      15      11      11       1
BEAM        1278      15      16      11      11       1
BEAM        1281      16      20      11      11       1
BEAM        1282      20      62      11      11       1
BEAM        1283      62      95      11      11       1
BEAM        1284      95     133       1       9       1
BEAM        1285     133     179      12       9       1
BEAM        1286     179     180      13       8       1
BEAM        1287     180     198      11      11       1
BEAM        1288      90      96       2      35       1
BEAM        1289      96     123       2      35       1
BEAM        1290     123     192       4      36       1
BEAM        1291     192     206       4      36       1
BEAM        1292     206     225       4      36       1
BEAM        1294     225     232       1      36       1
BEAM        1295      75      91       3      14       1
BEAM        1296      91     115       3      14       1
BEAM        1297     115     176       5      15       1
BEAM        1298     176     200       5      15       1
BEAM        1299     200     202       5      15       1
BEAM        1301     202     224       1      15       1
BEAM        1302      96      91       1      40       1
BEAM        1303     206     200       1      40       1
BEAM        1304      37      42       1      34       1
BEAM        1305      78      42       1      34       1
```

```
 BEAM          1306       78       80        1       34        1
 BEAM          1307       80      120        1       34        1
 BEAM          1308      120      122        1       34        1
 BEAM          1309      122      143        1       34        1
 BEAM          1310      143      144        1       34        1
 BEAM          1311       35       37        1       38        1
 BEAM          1312       41       42        1       38        1
 BEAM          1313       79       78        1       38        1
 BEAM          1314       81       80        1       38        1
 BEAM          1315      119      120        1       38        1
 BEAM          1316      150      122        1       38        1
 BEAM          1317      153      143        1       38        1
 BEAM          1318      177      144        1       38        1
 BEAM          1319      117      121        1       41        1
 BEAM          1320      121      145        1       41        1
 BEAM          1321      145      148        1       41        1
 BEAM          1322      148      149        1       41        1
 BEAM          1323      149      152        1       41        1
 BEAM          1324      152      154        1       41        1
 BEAM          1325      154      155        1       41        1
 BEAM          1326      118      117        1       42        1
 BEAM          1327      119      121        1       42        1
 BEAM          1328      147      145        1       42        1
 BEAM          1329      146      148        1       42        1
 BEAM          1330      150      149        1       42        1
 BEAM          1331      151      152        1       42        1
 BEAM          1332      153      154        1       42        1
 BEAM          1333      177      155        1       42        1
 BEAM          1334      185      184        1        7        1
 BEAM          1335      184      183        1        7        1
 BEAM          1336      186      185        1       31        1
 BEAM          1337      207      184        1       31        1
 BEAM          1338      182      183        1       31        1
 BEAM          1339      197      194        1       39        1
 BEAM          1340      207      221        1       39        1
 BEAM          1341      196      195        1       39        1
 BEAM          1342      195      207        1       39        1
 BEAM          1343      221      222        1       39        1
 BEAM          1344      222      223        1       39        1
 BEAM          1346      229      213       14        5        1
 BEAM          1348      213      211       14        5        1
 BEAM          1350      211      223       14        5        1
 BEAM          1351      223      230       14        5        1
 BEAM          1352      230      229       14        5        1
 BEAM          1353      229      212       14        5        1
 BEAM          1354      213      212       14        5        1
 BEAM          1355      211      212       14        5        1
 BEAM          1356      223      212       14        5        1
 BEAM          1366      223      209       14        5        1
 BEAM          1367      209      198       14        5        1
 BEAM          1368      198      211       14        5        1
 BEAM          1369      230      232       14        5        1
 BEAM          1370      230      224       14        5        1
 BEAM          1404      213      244       14        5        1
 BEAM          1405      229      245       14        5        1
 BEAM          1414      244      254       14       14        1
 BEAM          1415      245      255       14       14        1
'
'            Elem ID     np1   material    lcoor   ecc1
 SPRNG2GR      1501       29       16
 SPRNG2GR      1502       30       16
 SPRNG2GR      1503       33       16
 SPRNG2GR      1504       36       16
'
'            Geom ID       Do         Thick    Shear_y   Shear_z
 PIPE             1      3.800       0.050
 PIPE             2      3.800       0.060
```

```
 PIPE             3       1.750       0.090
 PIPE             4       1.700       0.040
 PIPE             5       1.300       0.080
 PIPE             6       1.250       0.065
 PIPE             7       1.180       0.015
 PIPE             8       1.056       0.045
 PIPE             9       1.048       0.041
 PIPE            10       1.040       0.080
 PIPE            11       1.037       0.035
 PIPE            12       1.025       0.029
 PIPE            13       1.020       0.050
 PIPE            14       1.000       0.010
 PIPE            15       1.000       0.020
 PIPE            16       0.980       0.030
 PIPE            17       0.960       0.020
 PIPE            18       0.900       0.030
 PIPE            19       0.885       0.050
 PIPE            20       0.850       0.040
 PIPE            21       0.850       0.060
 PIPE            22       0.825       0.020
 PIPE            23       0.800       0.020
 PIPE            24       0.800       0.030
 PIPE            25       0.775       0.020
 PIPE            26       0.720       0.030
 PIPE            27       0.700       0.020
 PIPE            28       0.700       0.022
 PIPE            29       0.650       0.020
 PIPE            30       0.650       0.030
 PIPE            31       0.650       0.033
 PIPE            32       0.600       0.025
 PIPE            33       0.600       0.030
 PIPE            34       0.515       0.018
 PIPE            35       0.50000     0.00500
 PIPE            36       0.500       0.015
 PIPE            37       0.450       0.020
 PIPE            38       0.420       0.020
 PIPE            39       0.384       0.015
 PIPE            40       0.350       0.010
 PIPE            41       0.219       0.016
 PIPE            42       0.215       0.016
’
’            Loc-Coo           dx             dy             dz
 UNITVEC           1         0.000          1.000          1.000
’
’            Ecc-ID             Ex             Ey             Ez
’
’            Mat  ID     E-mod       Poiss     Yield      Density     ThermX
 MISOIEP          1   2.100E+11   3.000E-01   3.550E+08   7.850E+03   0.000E+00
 MISOIEP          2   2.100E+11   3.000E-01   3.550E+08   2.360E+04   0.000E+00
 MISOIEP          3   2.100E+11   3.000E-01   3.550E+08   1.570E+04   0.000E+00
 MISOIEP          4   2.100E+11   3.000E-01   3.550E+08   1.310E+04   0.000E+00
 MISOIEP          5   2.100E+11   3.000E-01   3.550E+08   1.180E+04   0.000E+00
 MISOIEP          9   2.100E+11   3.000E-01   3.550E+08   8.740E+03   0.000E+00
 MISOIEP         10   2.100E+11   3.000E-01   3.550E+08   9.110E+03   0.000E+00
 MISOIEP         11   2.100E+11   3.000E-01   3.550E+08   8.580E+03   0.000E+00
 MISOIEP         12   2.100E+11   3.000E-01   3.550E+08   8.930E+03   0.000E+00
 MISOIEP         13   2.100E+11   3.000E-01   3.550E+08   8.840E+03   0.000E+00
 MISOIEP         14   2.100E+11   3.000E-01   3.550E+08   0.000E+00   0.000E+00
 MISOIEP         15   2.100E+11   3.000E-01   3.550E+08   7.850E+03   0.000E+00
’
’            Mat  ID          S P R I N G    C H A R.
 SPRIDIAG        16    2.67000E+09    2.67000E+09    4.67000E+09
                       1.16000E+11    1.16000E+11    8.94000E+10
’
’            Node ID                            M A S S
 NODEMASS        29              1.50000E+06
 NODEMASS        30              1.50000E+06
```

```
 NODEMASS         33              1.50000E+06
 NODEMASS         36              1.50000E+06
 NODEMASS        211              7.61200E+05
 NODEMASS        212              7.61200E+05
 NODEMASS        213              7.61200E+05
 NODEMASS        223              7.61200E+05
 NODEMASS        229              9.59200E+05
'
'
'
 GroupDef          998 Elem          !  Element Group no 998

                          1346               1348               1350
                 1351     1352      1353     1354      1355     1356
                 1366     1367


 GroupDef          999 Elem          !  Element Group no 999

                 1404     1405      1414     1415
```

C.2.1 Load file load.fem

```
HEAD


'
' Dead weight of structural steel and masses on nodes
' ---------------------------------------------------
'
'            Load Case       Acc_X         Acc_Y          Acc_Z
 GRAVITY            1           0.             0.          -9.81
'
'
' Wind load positive x-direction, in total 3 MN
' (is not included in original NIRWANA file)
' ------------------------------------------
'
'          Load Case  Node ID     fx        fy        fz
' NODELOAD       5       211     6.0E+5      0.0       0.0
' NODELOAD       5       212     6.0E+5      0.0       0.0
' NODELOAD       5       213     6.0E+5      0.0       0.0
' NODELOAD       5       223     6.0E+5      0.0       0.0
' NODELOAD       5       229     6.0E+5      0.0       0.0
'
'
' Wind load positive y-direction, in total 3 MN
' (is not included in original NIRWANA file)
' ------------------------------------------
'
'          Load Case  Node ID     fx        fy        fz
' NODELOAD       6       211      0.0     6.0E+5       0.0
' NODELOAD       6       212      0.0     6.0E+5       0.0
' NODELOAD       6       213      0.0     6.0E+5       0.0
' NODELOAD       6       223      0.0     6.0E+5       0.0
' NODELOAD       6       229      0.0     6.0E+5       0.0
'
'
' Specify calculation of buoyancy
' (NB! If buoyancy is calculated, flooded members
' must be correctly given in the load file.)
' ----------------------------------------------
'
'          Ildcs  Option
```

```
 BUOYANCY     1    NoWrite
'
' Wave loads
' ----------
'
' Wave-in-deck load (for magnitude see file deckforce_values.xls) for deck width 47 m.
'
'           Load Case  Node ID     fx        fy        fz
 NODELOAD      9       211       FDECKX.     0.0       0.0
 NODELOAD      9       213       FDECKX.     0.0       0.0
 NODELOAD      9       223       FDECKX.     0.0       0.0
 NODELOAD      9       219       FDECKX.     0.0       0.0
'
'
'           Ildcs  <type>   H    Period   Direction Phase  Surf_Lev Depth
 WAVEDATA     10   Stoke  WAVEH  PERIOD     0.0    130.0   SURFACE  DEPTH
'
'
'
' Current profile according to original NIRWANA input file
' ------------------------------------------------------
'
'           Ildcs  Speed Direction Surf_Lev  Depth    [Profile]
 CURRENT      10     1.0     0.0   SURFACE   DEPTH     0.0  1.0
                                                     -50.0  0.3
                                                     -67.0  0.0
                                                     -70.0  0.0
'
'
' Hydrodynamic factors
' --------------------
' The dragfactor for (two at the time of) elements 1411 - 1418
' is calculated based on Cs = 3 and that they each cover 20 m
' of the deck wall width.
'
'           Cd    Cm
 Hyd_CdCm   0.85  2.0
 Hyd_CdCm   0.0   0.0    1346 1348 1350 1351 1352
                         1353 1354 1355 1356
                         1366 1367 1368 1369 1370
                         1404 1405 1414 1415
'                         1401 1402 1403 1404 1405 1406 1407 1408
'                         1411 1412 1413 1414 1415 1416 1417 1418
'Hyd_CdCm 0.0 0.0
'Hyd_CdCm  60.0   0.0   1411 1418    ! Forces -x direction
'Hyd_CdCm  60.0   0.0   1412 1413    ! Forces -y direction
'Hyd_CdCm  60.0   0.0   1414 1415    ! Forces +x direction
'Hyd_CdCm  60.0   0.0   1416 1417    ! Forces +y direction
'
'
' Marine growth (copied from Eko-file, modified 'randomly')
' ---------------------------------------------------------
'
'                Z          Add_Thick
 M_GROWTH       5.000       0.0
                2.000       0.0
                0.000       0.055
              -15.000       0.053
              -23.000       0.040
              -32.000       0.035
              -35.000       0.028
              -45.000       0.025
              -55.000       0.0
              -67.000       0.0
'
'
'
```

```
'
'FLOODED        1002    1003    1004    1005    1006    1007    1008    1009    1010
'               1012    1013    1014    1015    1016    1017    1018    1019    1020
'       1021    1022    1023    1024    1025    1026    1027    1028            1030
'       1031    1032    1033    1034    1035    1036    1037    1038    1039    1040
'       1041    1042            1044    1045    1046    1047    1048    1049    1050
'       1051    1052    1053    1054    1055    1056    1057    1058    1059    1060
'       1061    1062    1063    1064    1065    1066    1067    1068    1069    1070
'       1071    1072    1073    1074    1075    1076    1077    1078    1079    1080
'       1081    1082    1083    1084    1085    1086    1087    1088    1089    1090
'       1091    1092    1093    1094    1095    1096    1097    1098    1099    1100
'       1101    1102    1103    1104    1105    1106    1107    1108    1109    1110
'       1111    1112    1113    1114    1115    1116    1117    1118    1119    1120
'       1121    1122    1123    1124    1125    1126    1127    1128    1129    1130
'       1131    1132    1133    1134    1135    1136    1137    1138    1139    1140
'       1141    1142    1143    1144    1145    1146    1147    1148    1149    1150
'       1151    1152    1153    1154    1155    1156    1157    1158    1159    1160
'       1161    1162    1163    1164    1165    1166    1167    1168    1169    1170
'       1171    1172    1173    1174    1175    1176    1177    1178    1179    1180
'       1181    1182    1183    1184    1185    1186    1187    1188    1189    1190
'       1191    1192    1193    1194    1195    1196    1197    1198    1199    1200
'       1201    1202    1203    1204    1205    1206    1207    1208    1209    1210
'       1211    1212    1213    1214    1215    1216    1217    1218    1219    1220
'       1221    1222    1223    1224    1225    1226    1227    1228    1229    1230
'       1231    1232    1233    1234    1235    1236    1237    1238    1239    1240
'       1241    1242    1243    1244    1245    1246    1247    1248    1249    1250
'       1251    1252    1253    1254    1255    1256    1257    1258    1259    1260
'       1261    1262    1263    1264    1265    1266    1267    1268    1269    1270
'       1271    1272    1273    1274    1275    1276    1277    1278    1279    1280
'       1281    1282    1283    1284    1285    1286    1287    1288    1289    1290
'       1291    1292    1293    1294    1295    1296    1297    1298    1299    1300
'       1301    1302    1303    1304    1305    1306    1307    1308    1309    1310
'       1311    1312    1313    1314    1315    1316    1317    1318    1319    1320
'       1321    1322    1323    1324    1325    1326    1327    1328    1329    1330
'       1331    1332    1333    1334    1335    1336    1337    1338    1339    1340
'       1341    1342    1343    1344
'
```

C.2.2 Control file to static analysis

```
' ========================================================================
' ||           Ultimate load analysis for typical North Sea jacket      ||
' ||                                                                    ||
' ||           Control file to USFOS, file name: statctr.fem            ||
' ========================================================================
'
HEAD      Static pushover analysis of jacket model DE


'
'    Units:     Force         : Newton
'               Length        : Meters
'               Rotation      : Rad
'
'    Files:     Control file  : statctr.fem
'               Geometry file : stru.fem
'               Load file     : load.fem
'               Result file   : statres.fem
'
' ------------------------------------------------------------------
'
' Overview, basic load cases
' --------------------------
'
```

```
'     1.  Permanent loads (gravity- and live loads)
'     5.  Wind +X, in total 3 MN
'     6.  Wind +Y, in total 3 MN
'    10.  Wave (and current) +X direction
' ---------------------------------------
'
' Analysis control data
' ---------------------
'
 XFOSFULL                      ! All available data stored for RAF-file
 CSAVE    0   -1    1          ! Saving of data restart, xfos and out-file
 CPRINT   1    1    1          ! What to write on outfile
 CMAXSTEP  5000
'
'          epsol     gamstp  ifunc  pereul  ktrmax  dentsw  cmax  ifysw  deters
 CPROPAR    1.0E-20   0.05    2.0    0.05    10      1       999    0     1
'
'
'          cmin     cneg    itmax     isol   epsit    cmineg
 CITER     0.000    -2.0     20          1    0.00001   -0.0
'
'
' Displacement control nodes
' --------------------------
'
 CNODES     1
'          nodex     idof    dfact
            212       1       1.0
'
'
 CCOMB    1   1
 CCOMB    2   9    12
'
'
' Static pushover analysis specification
' --------------------------------------
'
'          nloads    npostp  mxpst  mxpis
 CUSFOS     2         1000     0.50   0.50
'          lcomb     lfact   mxld   nstep   minstp
            1        0.2     1.0     0      0.010
            2        0.10    0.3     0      0.005
            2        0.05    0.5     0      0.001
            2        0.01    0.7     0      0.001
            2        0.001   3.0     0      0.0001
'            11       0.05    0.25    0      0.010  ! For treghetslasten
'            11       0.005   0.50    0      0.001  ! For treghetslasten
'
'
' Rayleigh damping 1.5 %
' ----------------------
'
'           alpha1       alpha2
'RAYLDAMP   0.00997      0.00366
'
'
' Specify calculation of relative velocity
' ----------------------------------------
'
'REL_VELO
'
```

C.2.3 Control file to quasi-static analysis

```
' ======================================================================
```

```
' ||           Ultimate load analysis for typical North Sea jacket      ||
' ||                                                                    ||
' ||           Control file to USFOS, file name: kvasictr.fem           ||
' ======================================================================
'
HEAD      Quasistatic pushover analysis of jacket model DE


'
'    Units:     Force         : Newton
'               Length        : Meters
'               Rotation      : Rad
'
'    Files:     Control file  : kvasictr.fem
'               Geometry file : stru.fem
'               Load file     : load.fem
'               Result file   : kvasires.fem
'
' ---------------------------------------------------------------
'
' Overview, basic load cases
' --------------------------
'
'     1.  Permanent loads and live loads
'     5.  Wind +X
'     6.  Wind +Y
'    10.  Wave 28m and current +X direction
' ----------------------------------------
'
' Global results to be saved
' --------------------------
'
 DynRes_G  WaveLoad
 DynRes_G  WaveElev
 DynRes_G  WaveOVTM
 DynRes_G  ReacBSH
 DynRes_G  ReacOVTM
 Dynres_N  Disp  212   1
'
'
' Defining all elements elastic
' -----------------------------
'
 Lin_Elem   0    All
'
'
' Analysis control data
' ---------------------
'
XFOSFULL                      ! All available data stored for RAF-file
CSAVE    0    1    1          ! Saving of data restart, xfos and out-file
CPRINT   1    1    1          ! What to write on outfile
CMAXSTEP   2000
'
'          epsol     gamstp  ifunc  pereul  ktrmax  dentsw  cmax  ifysw  deters
CPROPAR    1.0E-20   0.05    2.0    0.05    10      1       999    0     1
'
'
' Displacement control nodes
' --------------------------
'
CNODES     1
'          nodex     idof    dfact
            212       1       1.0
'
'
' Dynamic analysis specification
```

```
' ------------------------------
'
'           End_Time   Delta_T   Dt_Res   Dt_Pri
 Static       17.0      0.05     0.05     1.0
'
 Ini_time      1.0
'
 WavCase1   31   1
'
'             ID   <type>    Time         Factor
 TIMEHIST     51   Points     0.0          .0
                              0.1         1.0
                             20.0         1.0
'
'             ID   <type>    Time         Factor
 TIMEHIST     52   Points     0.0          .0
                              5.4         0.0
                              5.9         1.0
                              6.4         0.4
                              8.5         0.0
                             20.0         0.0
'
'             ID   <type>  Dtime Factor   Start_time
 TIMEHIST     53   Switch    0     1.0       1.0

'
'
'           Ildcs   Tim Hist
 LOADHIST     1        51
 LOADHIST     9        52
 LOADHIST    10        53
'
'
' Rayleigh damping 1.5 %
' ---------------------
'
'           alpha1       alpha2
'RAYLDAMP   0.00997      0.00366
'
'
' Specify calculation of relative velocity and buoyancy
' (NB! If buoyancy is calculated, flooded members must
' be correctly given in the load file.)
' ------------------------------------------------------
'
'REL_VELO
'
```

C.2.4 Control file to dynamic analysis

```
' ========================================================================
' ||           Ultimate load analysis for typical North Sea jacket      ||
' ||                                                                    ||
' ||           Control file to USFOS, file name: dynctr.fem             ||
' ========================================================================
'
HEAD      Dynamic pushover analysis of jacket model DE


'
'    Units:     Force         : Newton
'               Length        : Meters
'               Rotation      : Rad
'
```

```
'    Files:     Control file  : dynctr.fem
'               Geometry file : stru.fem
'               Load file     : load.fem
'               Result file   : dynres.fem
'
' ---------------------------------------------------------------
'
' Overview, basic load cases
' --------------------------
'
'     1.  Permanent loads and live loads
'     5.  Wind +X
'     6.  Wind +Y
'    10.  Wave 28m and current +X direction
' ----------------------------------------
'
' Global results to be saved
' --------------------------
'
 DynRes_G  WaveLoad
 DynRes_G  WaveElev
 DynRes_G  WaveOVTM
 DynRes_G  ReacBSH
 DynRes_G  ReacOVTM
 Dynres_N  Disp  212   1
'
' Analysis control data
' ---------------------
'
XFOSFULL                      ! All available data stored for RAF-file
CPRINT   1    1    1          ! What to write on outfile
CMAXSTEP  10000
'
CDYNPAR    -0.3
PCOR_ON
'          cmin      cneg      itmax      isol      epsit      cminneg
CITER       0.0       -2         30        1        0.00001       -0.0
'
'          epsol     gamstp  ifunc  pereul  ktrmax  dentsw  cmax  ifysw  deters
CPROPAR    1.0E-20   0.05    2.0    0.05    10      1       999    0     1
'
'
' Displacement control nodes
' --------------------------
'
CNODES     1
'          nodex     idof    dfact
            212       1       1.0
'
'
' Dynamic analysis specification
' ------------------------------
'
'           End_Time   Delta_T   Dt_Res   Dt_Pri
 Static        1.0      0.05     0.05     1.0
 Dynamic       5.5      0.05     0.05     1.0
 Dynamic       6.0      0.025    0.001    1.0
 Dynamic      12.1      0.001    0.001    1.0
 Dynamic      17.0      0.005    0.005    1.0
 Eigenval      0.0
'
 Ini_time      1.0
'
'             ID   <type>    Time         Factor
 TIMEHIST     51   Points     0.0          .0
                              1.0         1.0
                             20.0         1.0
```

```
’
’             ID   <type>    Time         Factor
 TIMEHIST     52   Points     0.0          .0
                               5.4         0.0
                               5.9         1.0
                               6.4         0.4
                               8.5         0.0
                              20.0         0.0
’
’             ID   <type>  Dtime Factor   Start_time
 TIMEHIST     53   Switch    0     1.0       1.0

’
’
’           Ildcs   Tim Hist
 LOADHIST     1        51
 LOADHIST     9        52
 LOADHIST    10        53
’
’
’ Rayleigh damping 1.5 %
’ ----------------------
’
’           alpha1       alpha2
’RAYLDAMP   0.00997      0.00366
’
’
’ Specify calculation of relative velocity and buoyancy
’ (NB! If buoyancy is calculated, flooded members must
’ be correctly given in the load file.)
’ -------------------------------------------------------
’
’REL_VELO
’
```

C.2.5 Batch file for analysis run

```
#!/usr/bin/sh
#  ================================================
#  ||   Made by: Katrine Hansen 18 March 2005    ||
#  ||   File name: go.ksh                        ||
#  ||   Run file for jacket analysis             ||
#  ||   Usage: go.ksh  Wave_height Period  Depth ||
#  ================================================

SURFACE=$3-70;

FdX75=1
FdX76=1870206
FdX77=3698977
FdX78=6434033
FdX79=8457817
FdX795=9437982
FdX80=10418379
FdX81=12316448


case $3
in
  75)
    FDECKX=$FdX75
  ;;
  76)
    FDECKX=$FdX76
```

```
  ;;
  77)
    FDECKX=$FdX77
  ;;
  78)
    FDECKX=$FdX78
  ;;
  79)
    FDECKX=$FdX79
  ;;
  79.5)
    FDECKX=$FdX795
  ;;
  80)
    FDECKX=$FdX80
  ;;
  81)
    FDECKX=$FdX81
  ;;
  *)
    echo 'No deck load given for chosen water depth'

    exit
  ;;
esac

echo $FDECKX

# Lager resultatkatalog hvis denne ikke eksisterer
# ------------------------------------------------

if ! test -d /cygdrive/d/UsfosWork/deres/h$1t$2d$3
   then mkdir /cygdrive/d/UsfosWork/deres/h$1t$2d$3
fi

cd /cygdrive/d/UsfosWork/deres/h$1t$2d$3
cp /cygdrive/d/UsfosWork/draupnerE/load.fem load.fem

sed s/WAVEH/$1/g load.fem > l1.tmp
sed s/PERIOD/$2/g l1.tmp > l2.tmp
sed s/DEPTH/$3/g l2.tmp > l3.tmp
sed s/SURFACE/$SURFACE/g l3.tmp > l4.tmp
sed s/FDECKX/$FDECKX/g l4.tmp > l5.tmp

mv l5.tmp load.fem
rm l?.tmp

# Kjrer kvasistatisk usfos
# --------------------

usfos 25 << EOF5
d:/UsfosWork/draupnerE/kvasi/kvasictr
d:/UsfosWork/draupnerE/stru
load
kvasires
EOF5

echo 'Kvasistatic analysis finished'

# Kjrer dynamisk usfos
# ----------------------

usfos 25 << EOF7
d:/UsfosWork/draupnerE/dynamic/dynctr$3
d:/UsfosWork/draupnerE/stru
load
dynres
```

```
EOF7

echo ’Dynamic analysis finished’

# Lager tillegg til load.fem med pushover-lasten
# ----------------------------------------------

cp kvasires_wave_load.fem pushover.fem

vim "+/       129"  "+:1,.d"   "+/load case   time" "+:.,\$d" "+:x" pushover.fem

sed ’s/  129  /   12  /g’ pushover.fem > pushover1.fem

cat pushover1.fem >> load.fem
rm pushove*.fem

# Kjrer statisk usfos
# --------------------

usfos 25 << EOF1
d:/UsfosWork/draupnerE/static/statctr$3
d:/UsfosWork/draupnerE/stru
load
statres
EOF1

echo ’Static analysis finished’
```